UNIVERSIDADE ESTADUAL PAULISTA "JÚLIO DE MESQUITA FILHO"

Programa de Pós-Graduação em Ciência e Tecnologia de Materiais

DESENVOLVIMENTO E CARACTERIZAÇÃO DE NOVAS LIGAS DO SISTEMA Ti-Ta-Zr PARA APLICAÇÕES BIOMÉDICAS

Pedro Akira Bazaglia Kuroda

Orientador: Prof. Carlos Roberto Grandini, FBSE

Bauru (SP)

2019

UNIVERSIDADE ESTADUAL PAULISTA "JÚLIO DE MESQUITA FILHO"

Programa de Pós-Graduação em Ciência e Tecnologia de Materiais

DESENVOLVIMENTO E CARACTERIZAÇÃO DE NOVAS LIGAS DO SISTEMA Ti-Ta-Zr PARA APLICAÇÕES BIOMÉDICAS

Tese apresentado à Universidade Estadual Paulista, como um dos requisitos à obtenção do título de Doutor em Ciência e Tecnologia de Materiais, Área de Concentração Biomateriais, sob a orientação do Prof. Dr. Carlos Roberto Grandini

Bauru (SP)

2019

Kuroda, Pedro Akira Bazaglia
K96d Desenvolvimento e caracterização de novas ligas do sistema Ti-Ta-Zr para aplicações biomédicas / Pedro Akira Bazaglia Kuroda. -- Bauru, 2019
176 f. : il., tabs., fotos

Tese (doutorado) - Universidade Estadual Paulista (Unesp), Faculdade de Ciências, Bauru
Orientador: Carlos Roberto Grandini

1. Ligas de Ti. 2. Biomateriais. 3. Microestrutura. 4. Tratamentos Térmicos. 5. Biocompatibilidade. I. Título.

Sistema de geração automática de fichas catalográficas da Unesp. Biblioteca da Faculdade de Ciências, Bauru. Dados fornecidos pelo autor(a).

Essa ficha não pode ser modificada.

unesp

UNIVERSIDADE ESTADUAL PAULISTA

Câmpus de Bauru

Faculdade de Ciências

ATA DA DEFESA PÚBLICA DA TESE DE DOUTORADO DE PEDRO AKIRA BAZAGLIA KURODA, DISCENTE DO PROGRAMA DE PÓS-GRADUAÇÃO EM CIÊNCIA E TECNOLOGIA DE MATERIAIS, DA FACULDADE DE CIÊNCIAS - CÂMPUS DE BAURU.

Aos 09 dias do mês de dezembro do ano de 2019, às 09:00 horas, no(a) Anfiteatro da Seção Técnica de Pós-Graduação - FC/Bauru, reuniu-se a Comissão Examinadora da Defesa Pública, composta pelos seguintes membros: Prof. Dr. CARLOS ROBERTO GRANDINI - Orientador(a) do(a) Departamento de Física / Faculdade de Ciências - UNESP/Bauru, Prof. Dr. CONRADO RAMOS MOREIRA AFONSO do(a) Departamento de Engenharia de Materiais / Centro de Ciências Exatas e de Tecnologia / UFSCar, Prof. Titular RUBENS CARAM JUNIOR do(a) Departamento de Engenharia de Materiais / UNIVERSIDADE ESTADUAL DE CAMPINAS, Prof. Dr. AROLDO GERALDO MAGDALENA do(a) Departamento de Química / Faculdade de Ciências - UNESP - Bauru, Prof. Titular CARLOS ANGELO NUNES do(a) Departamento de Materiais / EEL-USP, sob a presidência do primeiro, a fim de proceder a arguição pública da TESE DE DOUTORADO de PEDRO AKIRA BAZAGLIA KURODA, intitulada **Desenvolvimento e Caracterização de novas Ligas do Sistema Ti-25Ta-Zr para Aplicações Biomédicas**. Após a exposição, o discente foi arguido oralmente pelos membros da Comissão Examinadora, tendo recebido o conceito final: APROVADO. Nada mais havendo, foi lavrada a presente ata, que após lida e aprovada, foi assinada pelos membros da Comissão Examinadora.

Prof. Dr. CARLOS ROBERTO GRANDINI

Prof. Dr. CONRADO RAMOS MOREIRA AFONSO

Prof. Titular RUBENS CARAM JUNIOR POR VIDEOCONFERÊNCIA

Prof. Dr. AROLDO GERALDO MAGDALENA PARECER CIRCUNSTANCIADO

Prof. Titular CARLOS ANGELO NUNES

AGRADECIMENTOS

Agradeço meus pais, Milton e Maria Diná, pelo amor e apoio ao longo dos estudos.

Aos meus irmãos Tiago, Paula, Lucas e Matheus pelo companheirismo e momento de descontração.

Ao meu orientador, Prof. Dr. Carlos Roberto Grandini, pela orientação deste trabalho e por todo incentivo e suporte dado desde a iniciação científica.

À Juliana pelo todo amor, incentivo, que segurou a barra nos momentos turbulentos e pelo todo companheirismo.

Aos meus amigos de graduação (Alex, Diego, Marcel e Caio). Aos colegas do Laboratórios de Analesticidade e Biomateriais.

Ao Prof. Dr. Conrado Ramos Moreira Afonso da Universidade Federal de São Carlos pelas medidas de microscopia eletrônica de transmissão.

À FAPESP (Proc. 2015/09.480-0) pela bolsa de doutorado concedida.

“A persistência é o menor caminho do êxito”.

Charles Chaplin

KURODA, P.A.B. **Desenvolvimento e caracterização de novas ligas do sistema Ti-Ta-Zr para aplicações biomédicas.** 2019. 176 p. Tese (Doutorado em Ciência e Tecnologia de Materiais) UNESP, Faculdade de Ciências, Bauru (SP), 2019**.**

RESUMO

Titânio e suas ligas, atualmente, são utilizados como implantes por possuírem excelente resistência à corrosão e propriedades mecânicas mais adequadas que os implantes de aço inoxidável e de Co-Cr. A liga de titânio mais utilizada para aplicações biomédicas é a liga Ti-6Al-4V, porém estudos mostraram que os elementos vanádio e alumínio são elementos nocivos à saúde humana. Assim, para contornar este problema, novas ligas de titânio sem a presença desses elementos estão sendo estudadas. O objetivo desse trabalho foi preparar ligas do sistema Ti-25Ta-Zr (onde o teor de zircônio foi variado de 0 a 75% em peso), e analisar a influência do soluto substitucional zircônio na estrutura cristalina, microestrutura, microdureza, módulo de elasticidade e biocompatibilidade das ligas. Paralelamente, diversos tratamentos de recozimento, laminação e solubilização foram realizados com o intuito de modificar as fases, microestrutura e módulo de elasticidade dos materiais. A caracterização química dos materiais foi realizada por espectroscopia de energia dispersiva, espectrometria de emissão óptica por plasma acoplado indutivamente, análise de gases e medidas de densidade. A análise estrutural foi efetuada por difração de raios X. A análise microestrutural foi realizada por microscopia ótica, microscopia eletrônica de varredura e de transmissão. Uma análise preliminar das propriedades mecânicas da liga foi obtida por intermédio de medidas de microdureza Vickers e módulo de elasticidade dinâmico. Testes de citotoxicidade foram realizados para uma análise inicial da biocompatibilidade das ligas. Os resultados de composição química mostraram que as amostras produzidas são de muito boa qualidade, respeitando a estequiometria proposta. Os resultados estruturais e microestruturais indicam a coexistência de fases α, α', α", β e ω, dependendo da concentração de zircônio e do tratamento termomecânico realizado e, que o zircônio atua como um elemento β estabilizador no sistema de ligas proposto. Os tratamentos de solubilização são capazes de modicar as fases presentes nas amostras, pois tratamentos realizados em baixas temperaturas, induzem a precipitação da fase α", tratamentos realizados em altas temperaturas induzem a retenção da fase β e tratamentos realizados com resfriamento lento promovem a difusão da fase α em ligas com a fase α". Os valores de dureza e o módulo de elasticidade das ligas foram alterados com o acréscimo no teor de zircônio. A dureza aumenta, devido ao endurecimento por solução sólida e o módulo de elasticidade diminui devido à estabilização da fase β. Não foram observados efeitos citotóxicos em nenhuma das ligas preparadas.

Palavras-chaves: Ligas de Ti; Biomateriais; Microestrutura; Tratamentos Térmicos.

KURODA, P.A.B. **Development and Characterization of new Alloys of the Ti-Ta-Zr system for Biomedical Applications.** 2019. 176 p. Thesis (PhD in Materials Science and Technology) UNESP, Faculdade de Ciências, Bauru (SP), 2019.

ABSTRACT

Titanium and alloys currently are used as implants possessing excellent corrosion resistance and mechanical properties more suited to stainless steel implants and Co-Cr. The titanium alloy used for most biomedical applications is Ti-6Al-4V, however studies showed that vanadium and aluminum are harmful to human health. The objective of this study was to prepare Ti-25Ta-Zr system alloys, where the zirconium content was varied from 0 to 75 % in weight, and to analyze the influence of zirconium substitutional solute in the structure, microstructure, hardness and elastic modulus. At the same time, several annealing, lamination and solubilization treatments were carried out to modify the phases, structures, microstructure and elastic modulus of the materials. The chemical characterization of materials was performed by energy-dispersion spectroscopy, inductively coupled plasma optical emission spectrometry, gas analysis, and density measurements. The structural analysis was performed by x-ray diffraction measurements. Microstructural analysis was performed by optical, scanning and transmission electron microscopy. To verify the initial biocompatibility of the alloys, cytotoxic tests were performed. A preliminary analysis of the mechanical properties of the alloy was obtained by means of microhardness and dynamic elastic modulus measurements. The chemical composition results showed that the samples produced are of good quality, close to proposed stoichiometry. The results showed the coexistence of α, α', α", β e ω phases, depending of zirconium content and thermomechanical treatment done and, that zirconium helped the β phase stabilization. Solubilization heat treatments are capable of modifying the phases present in the samples and, treatments performed at low temperatures, induced α" phase precipitation; treatments performed at high temperatures induced β phase retention and, slow cooling treatments promoted α phase diffusion. The hardness and elastic modulus values of the alloys are changed by increasing the zirconium content. Hardness increases due to solid solution hardening and the elastic modulus decreases due to β phase stabilization. No cytotoxic effects were observed in all produced alloys.

Keywords: Titanium alloys; Biomaterials; Microstructure; Thermomechanical treatments

Sumário

AGRADECIMENTOS..... vii
RESUMO..... xi
ABSTRACT..... xiii

Capítulo 1: 1
Estrutura da Tese..... 1
Capítulo 2: 5
Ligas de Titânio como Biomaterial..... 5
Sistema Ti-Ta..... 9
Sistema Ti-Zr..... 12
Referências..... 15
Capítulo 3: 19
Previsões Teóricas Para a Formação das Ligas..... 19
Teoria do Alumínio e Molibdênio Equivalente..... 20
Teoria do Orbital Molecular..... 21
Referências..... 24
Capítulo 4: 25
Preparation, Structural, Microstructural, Mechanical and Cytotoxic Characterization of as-cast Ti-25Ta-Zr Alloy..... 25
Abrstract..... 25
Introduction..... 26
Materials and Methods..... 27
Results..... 29
Discussion..... 33
Conclusions..... 40
References..... 40
Capítulo 5: 45
Preparação e caracterização de uma liga de titânio com a adição de tântalo e zircônio para aplicações biomédicas..... 45
Resumo..... 45

Abstract..... 46
Introdução..... 46
Materiais e Métodos..... 48
Resultados e Discussão..... 49
Conclusões..... 54
Referências..... 55
Capítulo 6: 59
Preparation, Structural and Microstructural Characterization of Ti-25Ta-10Zr Alloy for Biomedical Applications..... 59
Abstract..... 59
Introduction..... 59
Materials and Methods..... 61
Results and Discutions 63
Conclusions..... 68
References..... 69
Capítulo 7: 73
Desenvolvimento da liga Ti-25Ta-50Zr para aplicações biomédicas..... 73
Resumo..... 73
Abstract..... 73
Introdução..... 74
Materiais e Métodos..... 75
Resultados e Discussão..... 77
Conclusões..... 85
Reeferências..... 85
Capítulo 8: 89
Effect of Thermomechanical Treatments on the Phases, Microstructure, Microhardness and Young's Modulus of Ti-25Ta-Zr Alloys..... 89
Abrstract..... 89
Introduction..... 90
Materials and Methods..... 91
Results..... 92
Discussion..... 94
Conclusions..... 100

References..... 101
Capítulo 9: 105
The effect of solution heat treatment on phase transformations, microstructure and properties of Ti-25Ta-xZr alloys used as a biomaterial..... 105
Abrstract..... 105
Introduction..... 106
Experimental Procedure..... 107
Results and Discussions..... 108
Conclusions..... 115
References..... 115
Capítulo 10: 119
The effect of solution heat treatment time on the structure, microstructure, and selected mechanical properties of Ti-25Ta-Zr alloys used as biomaterials..... 119
Abrstract..... 119
Introduction..... 120
Experimental Procedure..... 121
Results and Discussions..... 122
Conclusions..... 129
References..... 130
Capítulo 11: 133
The Effect of Titanium on the Structure, Microstructure and Select Mechanical Properties of Zr-25Ta-Ti Alloys..... 133
Abrstract..... 133
Introduction..... 134
Materials and Methods..... 135
Results and Discussions..... 136
Conclusions..... 142
References..... 144
Capítulo 12: 147
Conclusões Gerais..... 147
Capítulo 13: 149
Trabalhos Futuros..... 149

Formação e Contribuição Científica..... 151

Publicações..... 153

Premiações Acadêmicas..... 155

Autorização dos Co-autores para incluir Artigos na Tese 157

Capítulo 1

Estrutura da Tese

Esta tese será apresentada na forma de artigos, fugindo um pouco da linha tradicional, com parte sendo escrita na língua pátria e parte na língua oficial do artigo publicado e/ou submetido. Para uma melhor compreensão e leitura deste documento, um esboço da organização da tese está detalhado neste capítulo, explicando o foco principal de cada seção. Sendo assim:

O **Capítulo 2** apresenta uma introdução sobre a importância em se desenvolver ligas de titânio na área biomédica, assim como a motivação para a realização deste trabalho. As características físicas e químicas dos elementos utilizados neste trabalho são fornecidas e uma revisão bibliográfica é apresentada para mostrar os resultados experimentais de ligas de titânio com a presença de tântalo e zircônio. De acordo com estas informações, os objetivos iniciais deste projeto são descritos.

O **Capítulo 3** apresenta as previsões teóricas para o desenvolvimento das ligas estudadas, envolvendo a estrutura e microestrutura de ligas de titânio. A teoria do orbital molecular é uma técnica que se utiliza de parâmetros eletrônicos e ligações atômicas para prever as fases de uma liga idealizada. Já a teoria do molibdênio e alumínio equivalente são duas equações empíricas que possibilitam identificar a estrutura cristalina da liga de titânio através do uso de elementos estabilizadores de fase α e β.

A parte experimental, resultados e discussão deste trabalho estão compilados na forma de artigos científicos (já publicados, aceitos, submetidos ou em submissão para publicação em periódicos científicos). Tais informações compreendem os Capítulos 4 ao 11.

No **Capítulo 4** é apresentada a preparação e caracterização das ligas do sistema Ti-25Ta-Zr (Zr = 0, 10, 20, 30 e 40% em peso) após a fusão, onde é analisada a composição química, para verificar a qualidade das amostras produzidas. Neste artigo, analisou-se também o efeito do zircônio substitucional na estrutura, microestrutura, algumas propriedades mecânicas selecionadas e a biocompatibilidade das ligas produzidas.

O **Capítulo 5** apresenta um artigo que mostra a preparação e a caracterização estrutural, microestrurural e mecânica da liga Ti-25Ta-5Zr, no qual o valor de zircônio é intermediário aos valores apresentados no Capítulo 5. Este trabalho foi realizado como projeto de iniciação científica, da qual o autor foi co-orientador.

O **Capítulo 6** mostra resultados da ligas Ti-25Ta-10Zr, onde após a fusão do lingote, é realizado um tratamento térmico de homogeneização durante 24 horas na temperatura de 1000 °C, com o objetivo de homogeneizar a microestrutura do material. O tratamento de homogeneização modifica as fases e propriedades mecânicas da liga, complementando os resultados apresentados no Capítulo 4. Este trabalho também foi realizado como projeto de iniciação científica, da qual o autor foi co-orientador.

O **Capítulo 7** é um artigo que mostra a preparação e resultados de caracterização estrutura, microestrurural e mecânica da liga Ti-25Ta-50Zr. No Capítulo 4 foi mostrado que o acréscimo de zircônio diminui o módulo de elasticidade nas ligas e em razão disso, foi proposto fundir mais uma composição, objetivando desenvolver uma liga com valor mais baixo de módulo de elasticidade. Este trabalho também foi realizado como projeto de iniciação científica, da qual o autor foi co-orientador.

Após a fusão, as ligas Ti-25Ta-Zr (Zr = 0, 10, 20, 30 e 40% em peso) passaram por processos termomecânicos distintos, como laminação e tratamentos térmicos de recozimento com resfriamento lento e rápido com água gelada. No **Capítulo 8** são apresentados os resultados da caracterização das amostras para verificar a influência de alguns destes tratamentos termomecânicos na estrutura, microestrutura e algumas propriedades mecânicas das ligas desenvolvidas.

No **Capítulo 9**, é apresentado em estudo que teve como objetivo avaliar como a temperatura de um tratamento térmico de solubilização, pode alterar a estrutura, microestrutura, dureza e módulo de elasticidade das ligas dos sistema Ti-25Ta-Zr. Os tratamentos realizados tiveram como objetivo induzir a precipitação da fase β nas ligas.

No **Capítulo 10** são apresentados os resultados que analisaram a influência do tempo de duração do tratamento térmico de solubilização a 1000 °C, na estrutura, microestrutura, dureza e módulo de elasticidade, das ligas Ti-25Ta-Zr.

Por fim, o **Capítulo 11** apresenta os resultados das ligas dos sistema Ti-25Ta-Zr com altos teores de zircônio, ou seja, são ligas de zircônio (Zr-25Ta, Zr-25Ta-15Ti e Zr-25Ta-25Ti). Após a fusão dos materiais foi verificada a composição química e a influência do titânio substitucional na estrutura, microestrutura e algumas propriedades mecânicas selecionadas das ligas.

Após a série de artigos, o **Capítulo 12** apresenta as conclusões e considerações finais do trabalho.

No **Capítulo 13**, algumas perspectivas de trabalhos futuros são apresentadas, como possibilidades de continuidade deste trabalho.

Para finalizar, é apresentada a formação e a contribuição científica do autor, além das premiações conquistadas ao longo do desenvolvimento deste trabalho.

Capítulo 2

Ligas de Titânio como Biomaterial

Nos dias atuais tem-se a necessidade de construir novos instrumentos medicinais que suprem com maior eficácia as necessidades físicas e biológicas humanas. Em virtude do aumento na longevidade, as doenças relacionadas a disfunções esqueléticas, como a osteoporose, chamam a atenção para a utilização de dispositivos biomédicos que ofereçam mais qualidade de vida aos que necessitam desse tipo de cuidado. Estima-se que aproximadamente 10 milhões de brasileiros sofrem com osteoporose no Brasil, sendo que 2,4 milhões sofrem fraturas anualmente e destes, cerca de 200 mil morreram em decorrência direta de suas fraturas [1].

Devido ao avanço da idade, e para melhorar a qualidade de vida, são estudados novos tipos de biomateriais que atendam às necessidades do corpo humano. Também temos os casos de acidentes automobilísticos e acidentes devido a prática esportiva, que podem provocar rompimentos de nervos de ligamento, fratura óssea e amputações. Cabe às pesquisas científicas analisar o desenvolvimento na área de caracterização e processamento de materiais para contribuir na área biomédica, com o objetivo de descobrir novos tipos de instrumentos medicinais que podem contribuir na melhora da qualidade de vida.

Uma série de materiais metálicos são utilizados em vários campos da medicina, sendo que esses materiais podem ser usados como substitutos de articulações, raízes dentárias, *stents* e suportes ortopédicos [2; 3; 4]. Estudar o desenvolvimento e a fabricação de novas ligas de titânio é necessário para a melhoria da qualidade de vida, pois sabe-se que os implantes metálicos falham quando aplicados ao corpo humano a longo prazo, exigindo que o paciente seja submetido a uma cirurgia de revisão. Esta falha é devida às diferenças das propriedades mecânicas entre metal e osso. É conhecido que o módulo de elasticidade do titânio é aproximadamente três a quatro vezes maior que o de um osso cortical humano e essa diferença limita a transferência de solicitação mecânica do implante aos ossos, causando perda de densidade óssea, gerando folga no implante e provocando dor local no paciente. É por isso que novas ligas de titânio estão sendo

desenvolvidas para melhorar a compatibilidade mecânica (implante/osso) e prolongar a vida útil do implante [5; 6; 7; 8; 9; 10; 11; 12].

Entre os materiais metálicos utilizados na ortopedia, o titânio e suas ligas se destacam por possuírem uma boa biocompatibilidade, uma boa resistência à corrosão em fluídos corpóreos e boa relação densidade/resistência mecânica. Na produção de ligas de titânio os elementos que mais se destacam como elementos de liga, de modo substitucional, são o nióbio, molibdênio, zircônio, tântalo, ferro, estanho, manganês e cromo [5; 6; 7; 8; 9; 10; 11; 12]. A liga de titânio mais utilizada em aplicações biomédicas ainda é o Ti-6Al-4V [12]. Porém, há relatos de que o vanádio causa efeitos citotóxicos e reações adversas em alguns tecidos [13; 14], enquanto o alumínio tem sido associado a distúrbios neurológicos [15; 16]. Para contornar esse problema, novas ligas de titânio sem a presença desses elementos estão sendo estudadas e estão em desenvolvimento. Além disso as ligas de titânio comerciais ainda possuem altos valores de módulo de elasticidade.

Produzir novas ligas de titânio sem a presença de elementos nocivos à saúde e com bons resultados de propriedade mecânica é o foco de muitos trabalhos atuais. Sabe-se pela literatura que ligas de titânio com a estrutura cristalina cúbica de corpo centrado (CCC), fase β, possuem um baixo valor de módulo de elasticidade. Por outro lado, para produzir ligas β de titânio é necessário acrescentar os elementos β estabilizadores na liga, e esses elementos possuem um alto valor de densidade. A fusão desses elementos geralmente resulta em uma liga com resultados satisfatórios de módulo de elasticidade e resultados insatisfatório de densidade. Um implante com alta densidade pode causar rejeição devido as diferenças de absorção das cargas durante um esforço mecânico e, além disso, altos valores de dureza dificulta a conformação mecânica do material para a manufatura de parafusos ou chapas implantáveis. Por outro lado, as ligas de titânio com a estrutura hexagonal compacta (HCP), fase α, tendem a possuir baixos valores de densidade e elevados valores de módulo de elasticidade.

Atualmente o grande foco da área é produzir ligas do tipo β, pois acredita-se que é melhor um implante possuir menores valores de módulo de elasticidade [12].

O titânio é um metal de transição que possui uma transformação alotrópica em torno de 883 ºC. Abaixo desta temperatura, sua estrutura cristalina é da forma hexagonal compacta (fase α). Acima desta temperatura sua estrutura é a cúbica de corpo centrado (fase β) (vide Figura 2.1) [17; 18; 19; 20]. Essa característica oferece a possibilidade de se obter ligas com microestruturas do tipo α, β ou α/β, dependendo de tratamentos térmicos e dos elementos ligantes que estabilizam as fases [21].

A Tabela 2.1 apresenta as características do titânio.

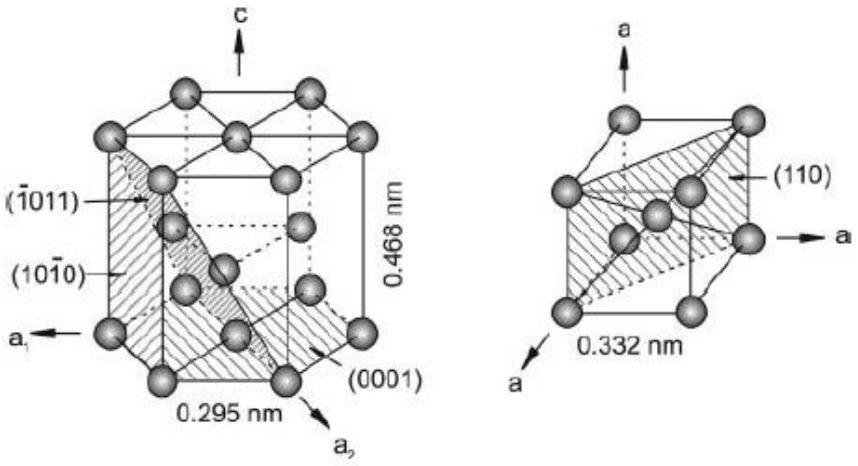


Figura 2.1 – Estruturas cristalinas do titânio [21].

Tabela 2.1 - Características físico-químicas do titânio [22].

Elemento	**Titânio**
Símbolo	Ti
Número Atômico	22
Densidade (g/cm³)	α = 4,51 a20°C β = 4,35 a885°C
Estrutura Cristalina	HCP, para T < 882°C CCC, para T > 882°C
Raio Atômico (nm)	0,145
Ponto de Fusão (°C)	1670
Massa atômica (u.m.a.)	47,90
Parâmetro de rede (nm)	α: *a* = 0,295; c = 0,468 β: *a* = 0,332 a 900 °C

O titânio é bastante utilizado na área biomédica devido às características favoráveis que possui, porém, essas características, principalmente as propriedades mecânicas, podem ser alteradas acrescentando um elemento para formar ligas com o titânio.

Os elementos de liga são divididos em neutros, α estabilizadores e β estabilizadores. Os elementos neutros são aqueles que não alteram a temperatura de transformação de fase, α estabilizadores aumentam a temperatura de transformação de fase e os β estabilizadores diminuem a temperatura de transformação de fase do titânio. Isoladamente, os elementos zircônio, estanho e háfnio são classificados como neutros. O alumínio, gálio, germânio, carbono, oxigênio e nitrogênio são classificados como α-estabilizadores. Os elementos β-estabilizadores são subdivididos em β-isomorfos ou β-eutetóides de acordo com a formação, ou não, de um composto intermetálico. Os elementos β-isomorfos são o molibdênio, vanádio, tântalo e nióbio, enquanto os β-eutetóides são o ferro, manganês, cromo, cobalto, níquel, cobre, silício e hidrogênio. [23; 24]. A Figura 2.2 apresenta as diferenças destes elementos na transformação de fase do titânio.

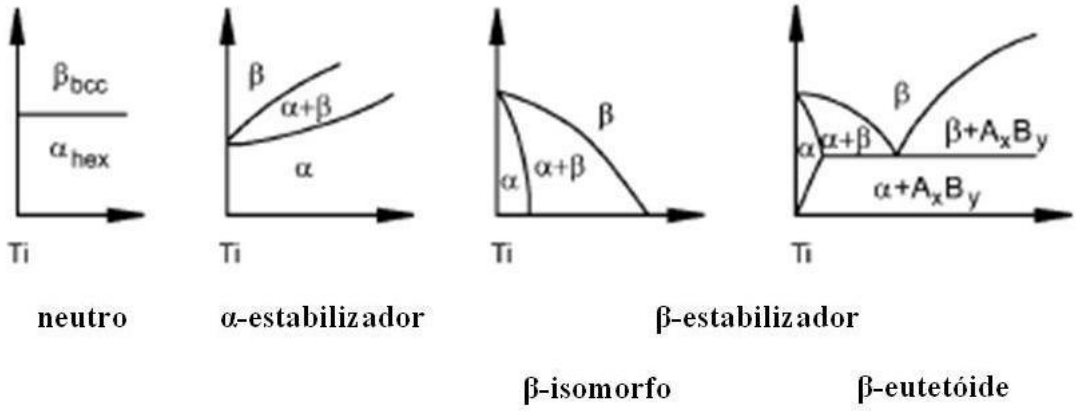


Figura 2.2 – Efeito de elementos de liga nas fases do titânio e suas ligas [23].

O titânio pode apresentar fases metaestáveis, isto é, aquelas que se formam fora do equilíbrio. A fase martensítica α' substitui a fase α devido a uma alta taxa de resfriamento a partir do campo de fase β. Possui estrutura cristalina hexagonal distorcida proveniente da transformação da fase β para a fase α por difusão atômica limitada, sendo caracterizada por uma formação acicular na microestrutura [25].

A fase martensítica α" possui estrutura ortorrômbica. É a fase intermediária que surge da transformação da estrutura cristalina cúbica de corpo centrado para a hexagonal compacta. Pode ser gerada por altas taxas de resfriamento ou pela deformação, devido à aplicação de forças externas [25].

A fase ω é uma fase sub-microscópica, pode ser classificada como atérmica, formada no resfriamento rápido da fase β ou isotérmica, que se origina no aquecimento em médias temperaturas da fase β metaestável. A fase ω atérmica surge durante a transformação da fase β para a fase α e possui uma estrutura trigonal ou hexagonal. Sua morfologia pode ser elipsoidal ou cuboidal [23].

Sistema Ti-Ta

O tântalo é um metal de transição do grupo 5 da Tabela Periódica, possuindo estrutura cristalina cúbica de corpo centrado (CCC). Possui um altíssimo ponto de fusão, pois sua ligação interatômica é extremamente forte, o que dificulta a sua fusão. Devido às ligações interatômicas fortes, possui alto módulo de elasticidade (200 GPa), alta resistência mecânica e alta dureza [26; 27]. A Tabela 2.2 apresenta as características físico-químicas do tântalo.

Em ligas de titânio, o tântalo é considerado um elemento β-estabilizador, ou seja, diminui a temperatura de transformação para a fase β. A Figura 2.3 apresenta o diagrama de fase para o sistema Ti-Ta [28].

Zhou e colaboradores (2004) estudaram as ligas do sistema Ti-Ta e observaram que a estrutura cristalina do sistema é sensível ao teor de tântalo. Quando resfriadas rapidamente a partir do campo β, ligas com o teor abaixo de 20% em peso de tântalo exibem a estrutura hexagonal (fases α e α'), com o teor entre 30 e 50% em peso de tântalo a estrutura é a ortorrômbica (fase α"), quando o teor de tântalo é até 60% em peso, uma grande quantidade da fase β metaestável é detectada juntamente com a fase α" e quando o conteúdo tântalo é superior a 60%, somente a fase β é observada [29].

Tabela 2.2: Características Físico-Químicas do tântalo [22].

Elemento	Tântalo
Símbolo	Ta
Número Atômico	73
Densidade (g/cm³)	16,6
Estrutura Cristalina	CCC
Raio Atômico (nm)	0,143
Ponto de Fusão (°C)	3017
Massa atômica (u.m.a.)	180,95
Parâmetro de rede (nm)	a = 0,330

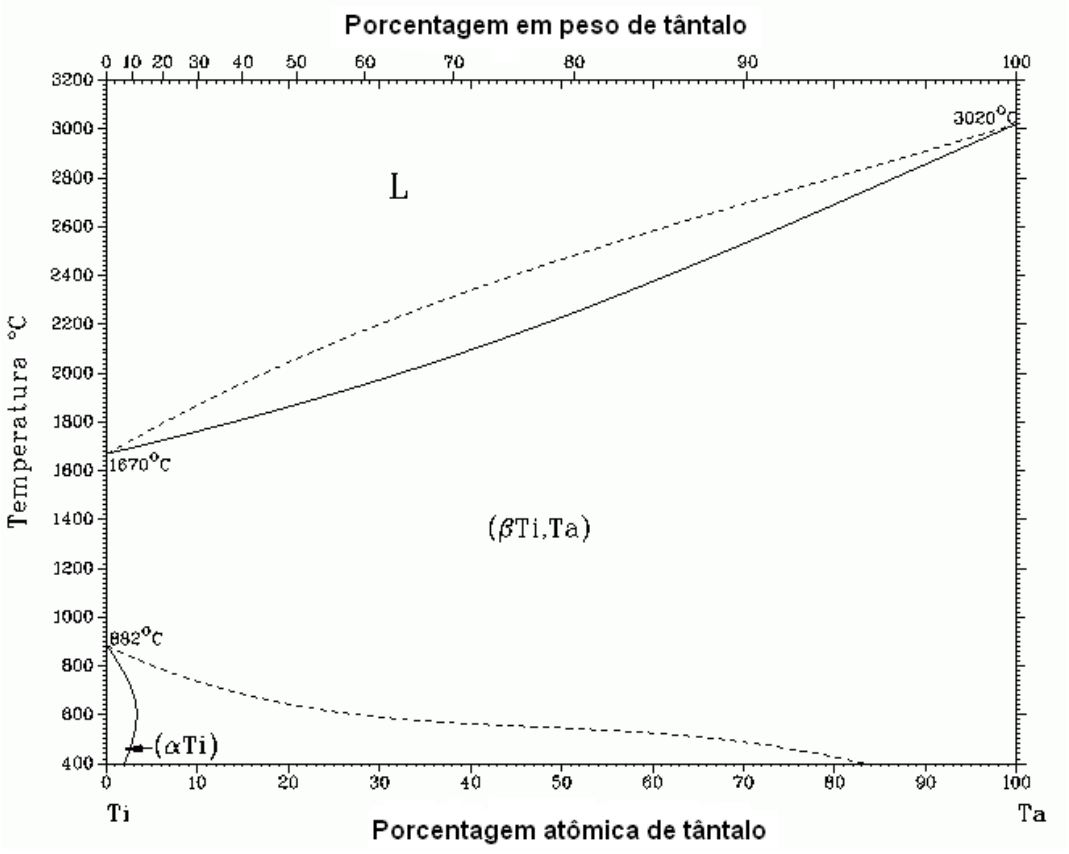


Figura 2.3 – Diagrama de fase para o sistema Ti-Ta [28].

Zhou e colaboradores, também em 2004, analisaram as transformações da fase martensita α" nas ligas Ti-Ta, com conteúdo de 30 até 50% de tântalo, e durante tratamentos de envelhecimento, o módulo de elasticidade foi avaliado nas ligas. No trabalho, foi observado que a microestrutura e o módulo de elasticidade são sensíveis ao acréscimo de tântalo e à temperatura de envelhecimento [30]. Na liga Ti-30Ta (com fase α”), o tratamento de envelhecimento realizado na temperatura de 723 K por 3 dias, não induziu nenhuma mudança de fase. O mesmo tratamento na temperatura de 773 K levou à formação da fase α, e o tratamento realizado nas temperaturas de 832 e 873 K induziu a formada das α+β. Para 40% em peso de tântalo, precipitados das fases α e β foram observados após o envelhecimento realizado na temperatura 723 K e 873 K. A fase martensita α" na liga Ti-50Ta se decompõe nas fases ω+β após a realização do tratamento de envelhecimento em temperaturas inferiores a 723K, e nas fases α+β para temperaturas superiores. Neste trabalho todos os tratamentos foram realizados em um período de três dias.

Passado um ano da publicação de 2004, Zhou e colaboradores investigaram a resistência à corrosão, resistência ao desgaste e citotoxicidade de ligas do sistema Ti-Ta com diferentes microestruturas. Neste trabalho foram produzidas quatro ligas com microestruturas distintas, a Ti-10Ta com a fase α’, Ti-30Ta com a fase α”, Ti-30Ta com a fase α (após tratamento térmico com baixa taxa de resfriamento) e a liga Ti-70Ta apenas com a fase β. Concluiu-se que a resistência à corrosão de ligas é melhorada com o acréscimo do elemento tântalo, pois os filmes passivos mais estáveis do tântalo, Ta_2O_5, reforçam os filmes passivos que envolvem a superfície do titânio, TiO_2. As ligas não são citotóxicas. Tanto a resistência à corrosão, quanto a citotoxicidade, não são influenciadas pela microestrutura do material [31].

Zhou e Niinomi, em 2009, publicaram resultados sobre a liga Ti-25Ta e o trabalho, mostrou que com 25% em peso de tântalo a liga possui a fase α” quando resfriada rapidamente do campo β até a temperatura ambiente. O volume da célula unitária da fase α” é superior às das demais fases do titânio, indicando que o módulo de elasticidade da liga é o mais baixo do sistema. A liga apresentou um módulo de elasticidade de 64 GPa [32]. A Figura 2.4 mostra o módulo de elasticidade do sistema Ti-Ta após um tratamento térmico a 1000°C, num patamar de uma hora e resfriamento rápido com água [29; 32].

Devido aos resultados citados do sistema Ti-Ta foi escolhida a liga com 25 %p de tântalo para ser a liga base deste trabalho, por possuir melhor compatibilidade mecânica para aplicações biomédicas.

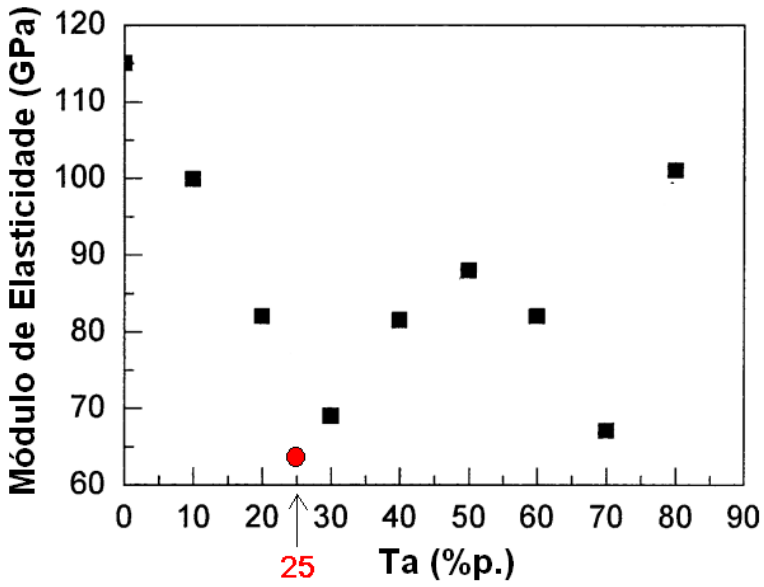


Figura 2.4 - Módulo de elasticidade de ligas do sistema Ti-Ta.

Sistema Ti-Zr

O zircônio pertence ao mesmo grupo do titânio na Tabela Periódica e possui propriedades químicas semelhantes a este elemento. O zircônio possui uma transformação alotrópica em torno de 862 ºC. Abaixo desta temperatura sua estrutura cristalina é da forma hexagonal compacta (fase α) e acima desta temperatura possui a estrutura cúbica de corpo centrado (fase β) [19; 33].

Em ligas de titânio, isoladamente o zircônio é considerado um elemento neutro, ou seja, não altera a temperatura de transformação de fase do titânio. A Figura 2.5 apresenta o diagrama de fase para o sistema Ti-Zr [28]. Pelo diagrama observa-se que o elemento possui influência na diminuição da temperatura de início da transformação martensitíca α' [22; 23; 34; 35].

A Tabela 2.3 apresenta algumas características físico-químicas do zircônio.

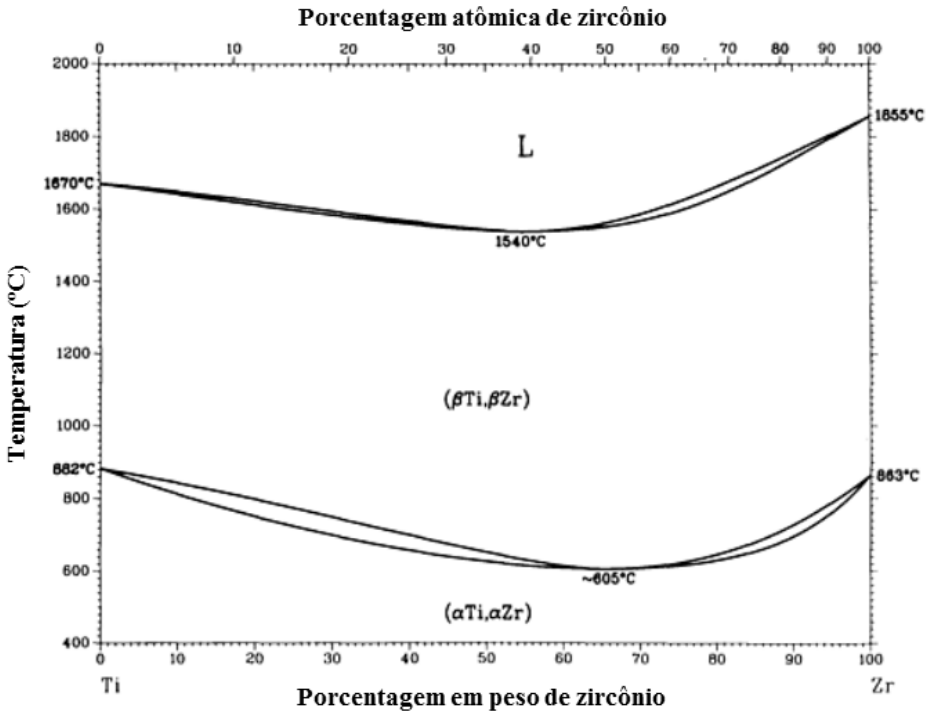


Figura 2.5 – Diagrama de fase do sistema Ti-Zr [28].

Tabela 2.3: Características do físico-químicas do zircônio [22].

Elemento	**Zircônio**
Símbolo	Zr
Número Atômico	40
Densidade (g/cm³)	6,51
Estrutura Cristalina	HCP, para T < 862°C CCC, para T > 862°C
Raio Atômico (nm)	0,159
Ponto de Fusão (°C)	1852
Massa atômica (u.m.a.)	91,22
Parâmetro de rede (nm)	α: *a* = 0,318; c = 0,468 β: *a* = 0,332 (900 °C)

Ho e colaboradores (2008), estudaram a estrutura, dureza e módulo de elasticidade de ligas do sistema Ti-xZr (x = 10, 20, 30 e 40 %p). Os resultados mostraram que o zircônio diminui a temperatura de início da transformação martensitíca α' conforme previsto pelo diagrama de fase. O zircônio aumentou a dureza e o módulo de elasticidade das ligas. Entre as ligas estudadas se destacou a Ti-40Zr por possuir os melhores resultados de propriedade mecânica [36].

Correa e colaboradores (2014) estudaram a estrutura, dureza, módulo de elasticidade e biocompatibilidade de ligas do sistema Ti-Zr, onde o zircônio foi variado de 5, 10 e 15% em peso. Os testes de dureza mostraram que a adição do zircônio aumentou a dureza do material, possivelmente devido ao efeito de solução sólida. Os valores de módulo de elasticidade permaneceram dentro da gama das ligas de titânio e os testes de biocompatibilidade não indicaram nenhuma reação adversa [35].

Han (2014) investigou a influência de zircônio (5, 10, 15 e 20% em peso) na microestrutura, propriedades físicas e corrosão. Com base nos resultados estruturais e microestruturais, todas as ligas de apresentaram a fase α' e possuem maior dureza que o titânio. Os ensaios de corrosão revelaram que a liga com 15% em peso de zircônio possui a maior resistência à corrosão dentre todas as ligas estudadas [37].

Medveded e colaboradores (2016) fizeram uma comparação da microestrutura e desempenho mecânico da liga Ti-15Zr com o titânio comercialmente puro grau 4. Os resultados globais indicaram que a Ti-15Zr é mais adequada para ser utilizado como implante dentário no quesito propriedades mecânicas [38].

Jing, Liang e Zhang (2012) analisaram a estrutura e propriedades mecânicas da liga Ti-6Al-4V após a adição de zircônio. Neste estudo o elemento titânio é substituído pelo zircônio, Ti-xZr-6Al-4V, onde x corresponde as concentrações de 5, 10, 15 e 20% em peso. Os resultados estruturais mostraram que o zircônio diminuiu a temperatura de transformação da fase β, aumentou a resistência à tração e o tipo de fratura muda gradualmente de dúctil para ruptura frágil com 20% em peso de zircônio [39].

Vicente e colaboradores (2014) estudaram o efeito do molibdênio na estrutura, microestrutura, dureza e módulo de elasticidade de ligas Ti-15Mo-xZr (x = 5, 10 e 15 %p). Foi observado que todas as ligas possuem predominância da fase β, com pequenas concentrações da fase martensítica α', após a realização de dopagem com oxigênio, mostrando que o oxigênio atuou como elemento α-estabilizador. Foi concluído que as

ligas desse sistema possuem valores de módulo de elasticidade menores em relação ao Ti-cp e a liga Ti-6Al-4V [40].

Levando-se em consideração as diversas condições favoráveis das ligas do sistema Ti-Ta e Ti-Zr para aplicação como biomateriais, a formação de ligas ternárias do sistema Ti-Ta-Zr pode apresentar propriedades mais interessantes para a área biomédica. Portanto, este trabalho possui como **objetivo,** desenvolver novas ligas de titânio contendo tântalo e zircônio (Ti-25Ta-Zr) e avaliar detalhadamente a estrutura, microestrutura, algumas propriedades mecânicas (microdureza e módulo de elasticidade) e a biocompatibilidade das ligas produzidas em períodos curtos de tempo. Este trabalho também objetivou analisar a influência de tratamentos termomecânicos e de solubilização nas ligas, visando a diminuição do módulo de elasticidade das ligas, potencializando sua característica para se candidatar como um biomaterial para aplicações ortopédicas.

Referências

1 FREIRE, F. M. Osteoporose: um artigo de atualização. 2004.
2 NIINOMI, M. Mechanical properties of biomedical titanium alloys. **Materials Science and Engineering: A,** v. 243, n. 1–2, p. 231-236, 1998.
3 LIPPARD, S. J. Metals in medicine. In: (Ed.). **Bioinorganic chemistry**: University Science Books, Mill Valley, California, 1994. p.505-584.
4 DABROWIAK, J. C. **Metals in medicine**. John Wiley & Sons, 2017.
5 GEETHA, M. et al. Ti based biomaterials, the ultimate choice for orthopaedic implants - A review. **Progress in Materials Science,** v. 54, n. 3, p. 397-425, 2009.
6 VASILESCU, M.; DOBRESCU, M. Titanium and Titanium Alloys as Biomaterials. Properties, Processing and Dental Applications. **Metalurgia International,** v. 15, n. 11, p. 69-73, 2010.
7 MOHAMMED, M.; KHAN, Z.; SIDDIQUEE, A. **Titanium and its Alloys, the Imperative Materials for Biomedical Applications**. International Conference on Recent Trends in Engineering & Technology (ICRTET2012) 2012. 91-95 p.
8 WANG, W.; POH, C. K. Titanium Alloys in Orthopaedics. In: (Ed.). **Titanium Alloys - Advances in Properties Control**. Rijeka: InTech, 2013. cap. 1, p.1-20.
9 LI, Y. et al. New Developments of Ti-Based Alloys for Biomedical Applications. **Materials,** v. 7, n. 3, p. 1709-1800, 2014.
10 KIRMANIDOU, Y. et al. New Ti-Alloys and Surface Modifications to Improve the Mechanical Properties and the Biological Response to Orthopedic and Dental Implants: A Review. **BioMed Research International,** v. 2016, p. 21, 2016.
11 KOLLI, R.; DEVARAJ, A. A Review of Metastable Beta Titanium Alloys. **Metals,** v. 8, n. 7, p. 506, 2018.
12 KAUR, M.; SINGH, K. Review on titanium and titanium based alloys as biomaterials for orthopaedic applications. **Materials Science and Engineering: C,** v. 102, p. 844-862, 2019.

13 MORETTI, B. et al. Peripheral neuropathy after hip replacement failure: is vanadium the culprit? **The Lancet,** v. 379, n. 9826, p. 1676, 2012.
14 ALRABEAH, G. O. et al. The effect of metal ions released from different dental implant-abutment couples on osteoblast function and secretion of bone resorbing mediators. **Journal of Dentistry,** v. 66, p. 91-101, 2017.
15 FERREIRA, P. C. et al. Aluminum as a risk factor for Alzheimer's disease. **Revista Latino-Americana de Enfermagem,** v. 16, p. 151-157, 2008.
16 CHAPPARD, D. et al. Aluminum and bone: Review of new clinical circumstances associated with Al3+ deposition in the calcified matrix of bone. **Morphologie,** v. 100, p. 95-105, 2016.
17 BANERJEE, S.; MUKHOPADHYAY, P. **Phase Transformations: Examples from Titanium and Zirconium Alloys**. Elsevier Science, 2010.
18 CORREA, D. R. N. et al. Tribocorrosion behavior of β-type Ti-15Zr-based alloys. **Materials Letters,** v. 179, p. 118-121, 2016.
19 KURODA, P. A. B.; BUZALAF, M. A. R.; GRANDINI, C. R. Effect of molybdenum on structure, microstructure and mechanical properties of biomedical Ti-20Zr-Mo alloys. **Materials Science and Engineering: C,** v. 67, p. 511-515, 2016.
20 KURODA, P. A. B. Preparation, Microstructural Characterization, and Selected Mechanical Properties of Ti-20Zr-2.5Mo and Ti-20Zr-7.5Mo Used as Biomaterial. v. 869, p. 946-951, 2016.
21 LEE, C. M.; JU, C. P.; CHERN LIN, J. H. Structure–property relationship of cast Ti–Nb alloys. **Journal of Oral Rehabilitation,** v. 29, n. 4, p. 314-322, 2002.
22 LIDE, D. R. Handbook of Chemistry and Physics. In: (Ed.). 87 ed. CRC Press: New York (USA), 2007.
23 PETERS, M. et al. Structure and Properties of Titanium and Titanium Alloys. In: (Ed.). **Titanium and Titanium Alloys**: Wiley-VCH Verlag GmbH & Co. KGaA, 2005. p.1-36.
24 LÜTJERING, G.; WILLIAMS, J. C. **Titanium**. Springer, 2003.
25 BANUMATHY, S.; MANDAL, R. K.; SINGH, A. K. Structure of orthorhombic martensitic phase in binary Ti–Nb alloys. **Journal of Applied Physics,** v. 106, n. 9, p. 093518, 2009.
26 ASKELAND, D. R.; PHULÉ, P. P. **Ciência e engenharia dos materiais**. Cengage Learning, 2008.
27 CALLISTER JR., W. D. **Fundamentos da Ciência e Engenharia de Materiais**. 2ª ed. Rio de Janeiro: LTC, 2006.
28 INTERNATIONAL, A.; COMMITTEE, A. I. A. P. D.; COMMITTEE, A. I. H. **ASM Handbook**. ASM International, 1992.
29 ZHOU, Y. L.; NIINOMI, M.; AKAHORI, T. Effects of Ta content on Young's modulus and tensile properties of binary Ti–Ta alloys for biomedical applications. **Materials Science and Engineering: A,** v. 371, n. 1, p. 283-290, 2004.
30 _____. Decomposition of martensite α″ during aging treatments and resulting mechanical properties of Ti−Ta alloys. **Materials Science and Engineering: A,** v. 384, n. 1, p. 92-101, 2004.
31 ZHOU, Y. L. et al. Corrosion resistance and biocompatibility of Ti–Ta alloys for biomedical applications. **Materials Science and Engineering: A,** v. 398, n. 1-2, p. 28-36, 2005.
32 ZHOU, Y.-L.; NIINOMI, M. Ti–25Ta alloy with the best mechanical compatibility in Ti–Ta alloys for biomedical applications. **Materials Science and Engineering: C,** v. 29, n. 3, p. 1061-1065, 2009.

33 CORREA, D. R. N.; KURODA, P. A. B.; GRANDINI, C. R. Structure, Microstructure, and Selected Mechanical Properties of Ti-Zr-Mo Alloys for Biomedical Applications. **Advanced Materials Research,** v. 922, p. 75-80, 2014.
34 HO, W.-F. et al. Evaluation of low-fusing porcelain bonded to dental cast Ti–Zr alloys. **Journal of Alloys and Compounds,** v. 471, n. 1–2, p. 185-189, 2009.
35 CORREA, D. R. N. et al. The effect of the solute on the structure, selected mechanical properties, and biocompatibility of Ti–Zr system alloys for dental applications. **Materials Science and Engineering: C,** v. 34, p. 354-359, 2014.
36 HO, W.-F. et al. Structure, mechanical properties, and grindability of dental Ti–Zr alloys. **Journal of Materials Science: Materials in Medicine,** v. 19, n. 10, p. 3179-3186, 2008.
37 HAN, M.-K. et al. Effect of zirconium content on the microstructure, physical properties and corrosion behavior of Ti alloys. **Materials Science and Engineering: A,** v. 616, p. 268-274, 2014.
38 MEDVEDEV, A. E. et al. Microstructure and mechanical properties of Ti–15Zr alloy used as dental implant material. **Journal of the mechanical behavior of biomedical materials,** v. 62, p. 384-398, 2016.
39 JING, R. et al. Structure and mechanical properties of Ti–6Al–4V alloy after zirconium addition. **Materials Science and Engineering: A,** v. 552, p. 295-300, 2012.
40 VICENTE, F. B. **Efeito do oxigênio intersticial no módulo de elasticidade de ligas Ti-15Mo-xZr (x= 5, 10, 15%p).** 2014. UNESP, Faculdade de Ciências, Bauru (SP).

Capítulo 3

Previsões Teóricas para a Formação das Ligas

O projeto de novas ligas de titânio para aplicações em implantes biomédicos, tem como objetivo encontrar materiais estruturais que são caracterizados por baixo módulo de elasticidade, alta resistência à fadiga, alta relação resistência mecânica/densidade, boa ductilidade, excelente resistência ao desgaste e boa resistência à corrosão em fluidos biológicos, além de baixa citotoxicidade e praticamente nenhuma tendência à provocar reações alérgicas [1].

Comumente, as ligas a base de titânio ocorrem com uma ou na mistura de duas estruturas cristalinas estáveis básicas, a fase α, com estrutura cristalina hexagonal compacta e a fase β, com estrutura cristalina cúbica de corpo centrado. Outras estruturas metaestáveis podem ocorrer, dependendo das condições de processamento das ligas.

Estudos recentes revelaram que os requisitos biomédicos mencionados acima podem ser obtidos a partir da concepção de ligas de titânio que utilizam os elementos mais biocompatíveis, ou seja, tântalo, molibdênio, nióbio e zircônio, como componentes da liga para estabilizar a fase β [2; 3]. Uma característica atraente das ligas de titânio do tipo β é seu baixo módulo de elasticidade, que está abaixo das ligas de titânio convencionais, do tipo α ou α-β, comumente usadas para aplicações biomédicas. Esta propriedade é de particular relevância, porque uma exigência importante de implantes para substituição óssea é uma baixa rigidez elástica que se aproxima, tanto quanto possível, do tecido ósseo circundante, evitando assim o indesejável efeito de "stress-shielding" [4].

Para ligas de titânio multicomponente, é difícil definir a relação entre componentes-propriedades-microestrutura, porque muitas vezes envolve as interações complicadas entre os elementos e as microestruturas. Existem diversos métodos para a previsão teórica de ligas de titânio para aplicações biomédicas e a maioria deles são baseados nos elétrons da camada d. Dentre estes métodos, destacamos o cálculo do alumínio e do molibdênio equivalente [5] e a teoria do orbital molecular [6; 7; 8].

Teoria do Alumínio e Molibdênio Equivalente

A partir de resultados empíricos, foram deduzidas duas equações que possibilitam escolher composições das ligas nas quais as quantidades de elementos podem estabilizar a fase β ou a fase α. As equações usam a porcentagem equivalente de molibdênio e de alumínio por serem os principais estabilizadores da fase β e α. A equação do alumínio equivalente [Al_{eq}] agrupa os elementos α-estabilizadores e a equação do molibdênio equivalente [Mo_{eq}] agrupa os elementos classificados como β estabilizadores [9; 10].

$$[Al]_{eq} = [Al] + \frac{[Zr]}{6} + \frac{[Sn]}{3} + 10[O] \quad (1)$$

$$[Mo]_{eq} = [Mo] + \frac{[Ta]}{5} + \frac{[Nb]}{3{,}6} + \frac{[W]}{2{,}5} + \frac{[V]}{1{,}5} + 1{,}25[Cr] + 1{,}25[Ni] + 1{,}7[Mn] + 1{,}7[Co] + 2{,}5[Fe] \quad (2)$$

onde: [ELEMENTO] indica a concentração em peso do elemento [11].

A Tabela 3.1 mostra os valores de [Al_{eq}] e [Mo_{eq}] para as ligas propostas neste trabalho.

Tabela 3.1 - Valores de alumínio e molibdênio equivalente para as ligas propostas neste trabalho.

Liga	**[Al_{eq}]**	**[Mo_{eq}]**
Ti-25Ta	0,00	5,00
Ti-25Ta-5Zr	0,83	5,00
Ti-25Ta-10Zr	1,67	5,00
Ti-25Ta-20Zr	3,33	5,00
Ti-25Ta-30Zr	5,00	5,00
Ti-25Ta-40Zr	6,67	5,00
Ti-25Ta-50Zr	8,33	5,00
Ti25Ta-60Zr	10,00	5,00
Ti25Ta-70Zr	11,67	5,00
Zr-25Ta	12,5	5,00

Atallah e colaboradores (2009) desenvolveram um diagrama de molibdênio e alumínio equivalente com a classificação das ligas de titânio, mostrado na Figura 3.1. No diagrama estão inseridos os valores das ligas estudadas neste trabalho [12].

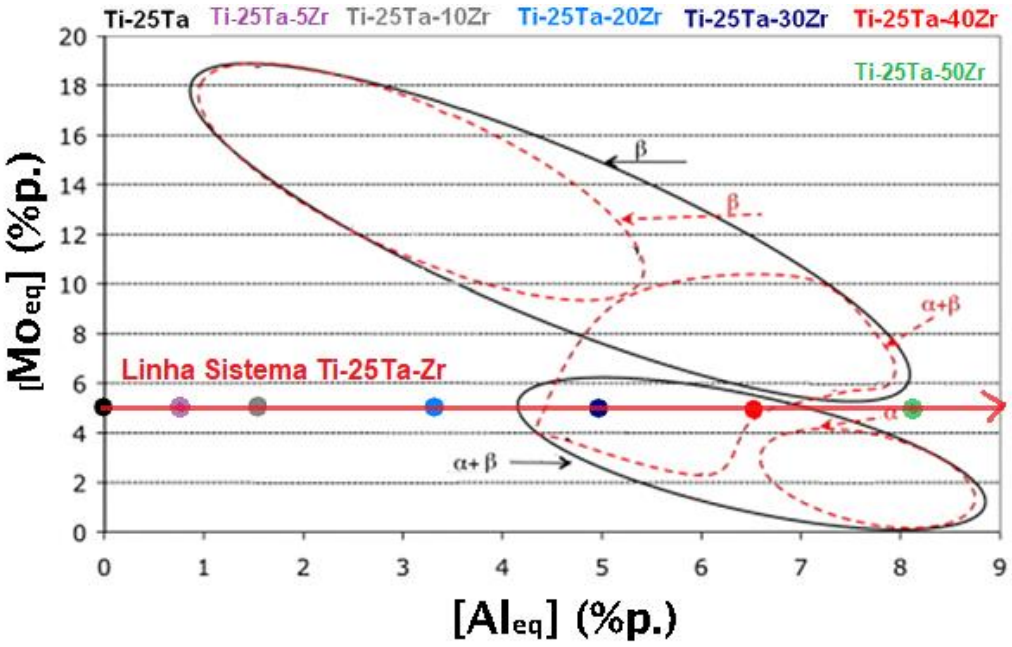


Figura 3.1 – Diagrama Al e Mo equivalente [12].

É possível observar que as ligas Ti-25Ta, Ti-25Ta-10Zr e Ti-25Ta-20Zr estão em uma região ainda não classificada pelo diagrama. As ligas Ti-25Ta-30Zr e Ti-25Ta-40Zr estão localizadas na região de ligas do tipo α+β.

Teoria do Orbital Molecular

Outra técnica utilizada para prever fases de ligas de titânio é a teoria do orbital molecular DV-Xα. O método é baseado na aproximação de Hartree-Fock-Slater usando o potencial Xα de Slater [6; 13]. O parâmetro de ordem de ligação *Bo* representa a intensidade da força de ligação entre o titânio e seus elementos de liga. O parâmetro de nível de energia *Md* é relacionado camada *d* do metal de transição que está sendo ligado. Este parâmetro está relacionado com a eletronegatividade e o raio metálico dos elementos adicionados ao titânio. Estes dois parâmetros são levados em consideração para prever a estrutura do material e seu módulo de elasticidade. Na Tabela 3.2 são apresentados os valores de Bo e Md do titânio, tântalo e zircônio [7].

Tabela 3.2 – Valores *Bo* e *Md* para os elementos de liga.

Elemento	***Bo***	***Md* (eV)**
Ti	2,790	2,447
Ta	3,144	2,531
Zr	3,086	2,934

Para obter os valores de *Bo* e *Md* das ligas propostas, foi realizado um cálculo utilizando a porcentagem atômica de cada elemento em cada liga e os valores de Bo e Md do titânio, tântalo e zircônio[7].

$$\overline{Md} = \sum_i x_i Md_i \quad (1)$$

$$\overline{Bo} = \sum_i x_i Bo_i \quad (2)$$

onde: x é a porcentagem atômica do elemento de liga.

Os valores dos parâmetros médios *Bo* e *Md* para as ligas propostas neste estudo são apresentados na Tabela 3.3. Em seguida, os valores são foram inseridos em um diagrama *Bo-Md*, de acordo com a Figura 3.2.

Tabela 3.3 – Média dos parâmetros Bo-Md.

Liga	$\overline{Md}$	$\overline{Bo}$
Ti-25Ta	2,408	2,812
Ti-25Ta-5Zr	2,423	2,823
Ti-25Ta-10Zr	2.438	2.834
Ti-25Ta-20Zr	2.473	2.858
Ti-25Ta-30Zr	2.513	2.886
Ti-25Ta-40Zr	2.559	2.918
Ti-25Ta-50Zr	2,612	2,955
Ti-25Ta-60Zr	2,675	3,000
Ti-25Ta-70Zr	2,715	3,052
Zr-25Ta	2,794	3,083

A liga Ti-25Ta se encontram na região de α". Trabalhos da literatura mostram que a liga Ti-25Ta realmente possui a predominância da fase martensita α" [14]. As demais ligas estão em uma região ainda não classificada pelo diagrama, porém é possível observar que o acréscimo de zircônio, em alta quantidade, pode ajudar a estabilizar a fase β e diminuir o módulo de elasticidade, devido ao aumento da distância interatômica, potencializando as características para o uso biomédico.

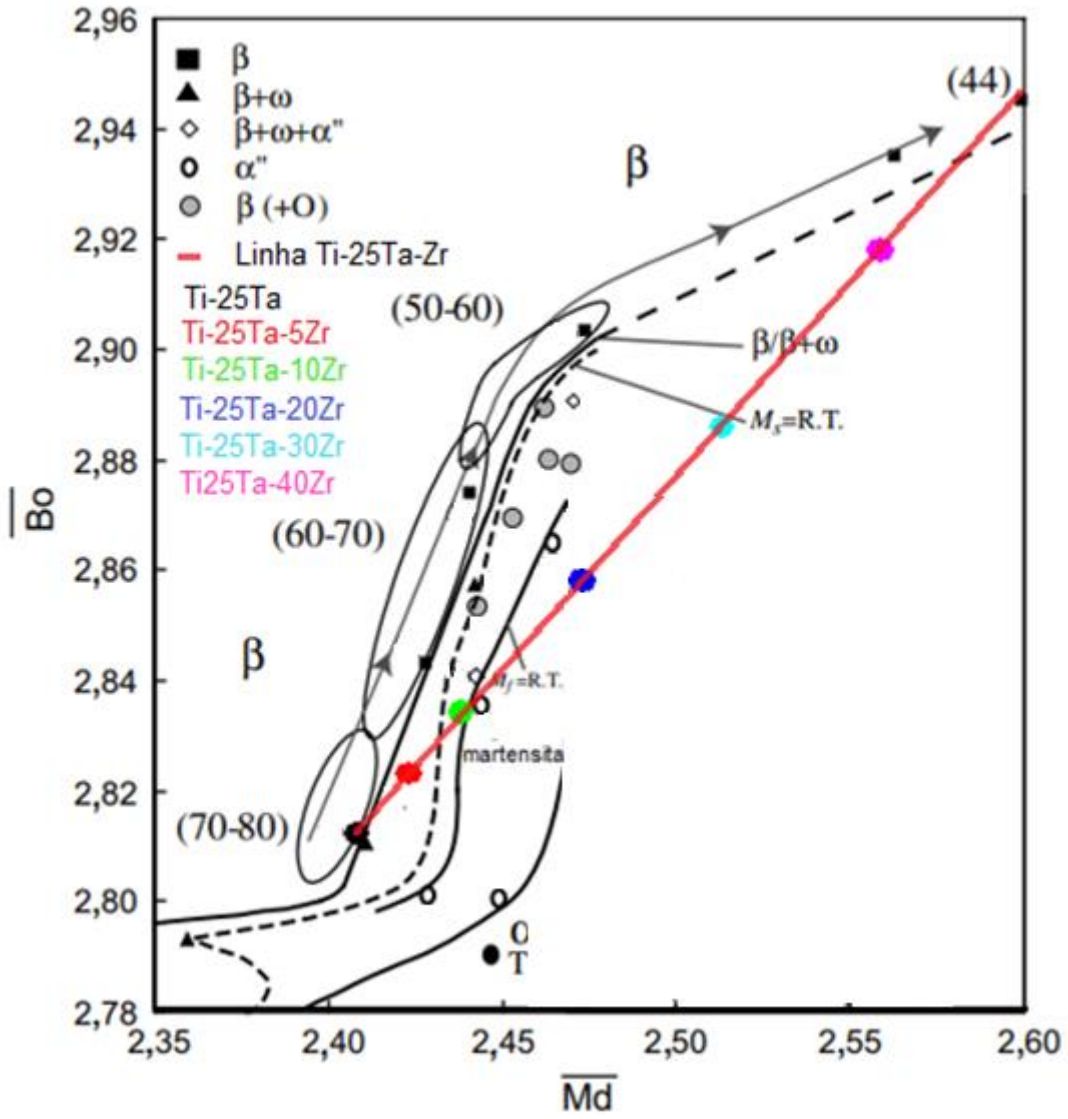


Figura 3.2 – Diagrama Bo-Md [7].

Referências

1 RAABE, D. et al. Theory-guided bottom-up design of β-titanium alloys as biomaterials based on first principles calculations: Theory and experiments. **Acta Materialia,** v. 55, n. 13, p. 4475-4487, 2007.
2 LI, Y. et al. New Developments of Ti-Based Alloys for Biomedical Applications. **Materials,** v. 7, n. 3, p. 1709-1800, 2014.
3 KAUR, M.; SINGH, K. Review on titanium and titanium based alloys as biomaterials for orthopaedic applications. **Materials Science and Engineering: C,** v. 102, p. 844-862, 2019.
4 NAGELS, J.; STOKDIJK, M.; ROZING, P. M. Stress shielding and bone resorption in shoulder arthroplasty. **Journal of Shoulder and Elbow Surgery,** v. 12, n. 1, p. 35-39, 2003.
5 LEYENS, C.; PETERS, M. **Titanium and Titanium Alloys: Fundamentals and Applications**. New York: Wiley-VCH, 2005.
6 MORINAGA, M.; YUKAWA, H. Alloy design with the aid of molecular orbital method. **Bulletin of Materials Science,** v. 20, n. 6, p. 805-815, 1997.
7 ABDEL-HADY, M.; HINOSHITA, K.; MORINAGA, M. General approach to phase stability and elastic properties of β-type Ti-alloys using electronic parameters. **Scripta Materialia,** v. 55, n. 5, p. 477-480, 2006.
8 MORINAGA, M. **Electronic Approach to Alloy Design**. Toyota Physical & Chemical Research Institute. Japan, p.1-6, 2011.
9 DONACHIE, M. J. **Titanium: a technical guide**. ASM international, 2000.
10 LÜTJERING, G.; WILLIAMS, J. C. **Titanium**. Springer, 2003.
11 BOYER, R.; WELSCH, G.; COLLINGS, E. W. **Materials properties handbook: titanium alloys, ASM International**. Materials Park, OH, USA: 1994.
12 ATTALLAH, M. et al. Comparative determination of the α/β phase fraction in α+ β-titanium alloys using X-ray diffraction and electron microscopy. **Materials Characterization,** v. 60, n. 11, p. 1248-1256, 2009.
13 ABDEL-HADY, M. et al. Phase stability change with Zr content in β-type Ti–Nb alloys. **Scripta Materialia,** v. 57, n. 11, p. 1000-1003, 2007.
14 ZHOU, Y.-L.; NIINOMI, M. Ti–25Ta alloy with the best mechanical compatibility in Ti–Ta alloys for biomedical applications. **Materials Science and Engineering: C,** v. 29, n. 3, p. 1061-1065, 2009.

Capítulo 4

Published in Journal of Materials Science: Materials in Medicine, 31, article 19 (2020). https://doi.org/10.1007/s10856-019-6350-7.

Preparation, Structural, Microstructural, Mechanical and Cytotoxic Characterization of as-cast Ti-25Ta-Zr Alloys

Pedro Akira Bazaglia Kuroda[1,2], Fernanda de Freitas Quadros[1,2], Karolyne dos Santos Jorge Sousa[1,2], Tatiani Ayako Goto Donato[1,2], Raul Oliveira de Araújo[1,2,3], and Carlos Roberto Grandini[1,2*]

[1] UNESP – Univ. Estadual Paulista, Laboratório de Anelasticidade e Biomateriais, 17.033-360, Bauru, SP, Brazil

[2] IBTN/Br – Institute of Biomaterials, Tribocorrosion and Nanomedicine – Brazilian Branch, 17.033-360, Bauru, SP, Brazil

[3] IFSP – São Paulo Federal Institute of Education, Science and Technology, 14,781-502, Barretos, SP, Brazil

Abstract

Titanium alloys have been widely used as biomaterials, especially for orthopedic prostheses and dental implants, but these materials have Young's modulus almost three times greater than human cortical bones. Because of this, new alloys are being produced for the propose of decreasing Young's modulus to achieve a more balanced mechanical compatibility with the bone. In this paper, it is reported the development of Ti-25Ta alloys as a base material, in which was introduced zirconium, with concentration varying between 0 and 40wt%, with the aim of biomedical applications. The alloys were prepared in an arc-melting furnace. The microstructural analysis was performed by x-ray diffraction as well as optical and scanning electron microscopy. The mechanical properties were analyzed by microhardness and Young's modulus measurements, and cytotoxicity analysis by indirect test. X-ray measurements revealed the presence of α"

phase in the alloy without zirconium; α”+β phases for alloys with 10, 20, and 30 wt% of zirconium, and β phase only for the alloy with 40 wt% of zirconium. These results were corroborated by the microscopy results. The hardness of the alloy was higher than that of cp-Ti due to the actions of zirconium and tantalum as hardening agents. The Young’s modulus decreases with high levels of zirconium due to the stabilization of the β phase. The cytotoxicity test showed that the extracts of studied alloys are not cytotoxic for osteoblast cells in short periods of culture.

Introduction

The study of the development and manufacture of new titanium alloys is necessary for improvements in quality of life. It is known that metal implants fail when applied to the human body in the long term, requiring the patient to undergo repair surgery. This failure is mainly due to the differences in the mechanical properties between metal and bone. The elastic modulus of titanium is approximately three times greater than that of human cortical bone. This difference causes the patient bone lose density causing the implant to loosen, and local pain in the patient. This is why new titanium alloys are being developed to improve mechanical bone compatibility to extend implant life [1; 2].

Intense research and development of metallic alloys are being carried out across the biomedical field; the major part based on titanium as the metallic matrix. The elements that stand out as the alloy’s elements are niobium, molybdenum, zirconium, tantalum, iron, tin, manganese and chromium [3; 4].

The most-used titanium alloy in biomedical applications still is Ti-6Al-4V [5]. But, there are reports that vanadium causes cytotoxic effects and adverse reactions in some tissues [6], while aluminum has been associated with neurological disorders [7].To work around this issue, new titanium alloys without the presence of these elements are being studied and are in development.

Zhou et al. [8; 9] studied alloys of the Ti-Ta system (Ta = 10, 20, 30, 40, 50, 60, 70 and 80 wt%) and observed that the crystalline structure of the system is sensitive to tantalum content. Alloys with tantalum content less than 20 wt% exhibit the hexagonal structure (α and α’); with the content between 30 and 50 wt% of tantalum, the structure is orthorhombic (α”); when the tantalum content is up to 60 wt%, a large amount of metastable β-phase, with body centered cubic crystalline structure is detected, together with the α-phase and when the tantalum content is higher than 60 wt%, the alloys are of the β-type. Their results indicated that Young's modulus values first decrease almost

linearly with the increase of the tantalum content until reaching a minimum of 69 GPa with 30 wt% of tantalum and from this point, the elastic modulus tends to increase with the tantalum addition. Therefore, binary alloys with tantalum content between 20 to 30 wt% may have more satisfactory values of elastic modulus for biomedical applications.

In another paper, Zhou and Niinomi [10] studied in more details Ti-25Ta alloy. The authors proposed this composition as the alloy with the best mechanical compatibility in Ti–Ta alloys for biomedical applications. The results showed that with 25 wt% of tantalum, the alloy presents the α" phase when rapidly cooled from the β field to room temperature. The unit cell volume of the α" phase is higher than other titanium phases, indicating that the alloy's elastic modulus is the lowest in the studied system. The alloy presented an elastic modulus of 64 GPa. Due to the good mentioned results of Ti-Ta system, the alloy with 25% of tantalum was chosen to be the base alloy of this study, because of its better mechanical compatibility for biomedical applications.

Ho et al. [11] and Correa et al. [12] studied the structure, hardness and Young's modulus of Ti-Zr system alloys. The results showed that the zirconium decreases the starting temperature of the martensitic transformation α'. The hardness and elastic modulus of the alloys showed an increase with the addition of zirconium. Analyzing these results, it was concluded that the Ti-40Zr alloy presented the best properties to be applied for dental applications. Due to the good properties of the system, the zirconium content used in this study ranged up to 40 wt%. Considering the diverse favorable properties of the Ti-Ta and Ti-Zr systems for application as biomaterials, the formation of Ti-Ta-Zr ternary alloys may present more interesting properties for orthopaedical or dental applications. Information about the structure, microstructure and mechanical properties of Ti-Ta-Zr system alloys are scarce. The developed alloys of this system have elastic modulus similar to cp-Ti (109-130 GPa), good biocompatibility and are β-type alloys [13]. With respect to corrosion, Ti-15Ta-5Zr alloy was studied and its surface has the TiO_2, Ta_2O_5 and ZrO_2 passive oxides films, which protect the alloy from corrosion [14].

In this paper, the development and chemical, structural, microstructural, mechanical and cytotoxic characterization of Ti-25Ta-Zr system alloys that contain various levels of zirconium is presented, aiming biomedical applications

Materials and Methods

The ingots were produced through arc-melting furnace with a non-consumable tungsten electrode, where the raw materials were melted in a water-cooled copper crucible in an

argon atmosphere to avoid possible contamination [15; 16]. Due to the large difference in the melting points of precursor metals, the melting process was carried out ten times to improve its chemical homogeneity.

After melting, to verify the chemical composition (i.e. the stoichiometry and homogeneity) of the samples, a qualitative and quantitative chemical analysis were conducted by inductively coupled plasma - optical emission spectrometry (ICP-OES), using a Varian Vista equipment; energy dispersive spectroscopy (EDS), using an Oxford, INCA model equipment, and density measurements based on the Archimedes' principle, using an Ohaus, Explorer model analytical balance. Also, the concentration of interstitial elements present in the sample was obtained with a gas analyzer LECO, TC-400 model. These measurements were based on ASTM specific standards [17; 18; 19].

The structure was analyzed by x-ray diffraction measurements, with quantitative analysis of phases using the Rietveld's method. For structural analyses, x-ray diffraction measurements were performed using a Rigaku, D/Max-2100PC model. The selected method to obtain the diffractograms was the powder method, with Cu-Kα radiation (λ = 1.544 Å), 20 mA current, a potential of 40 kV, a time of 3.2 s, and ranging from 20° to 100°, with 0.02° of step size and fixed time. For the analysis of diffractograms by Rietveld's method, it was used the GSAS® software and the EXPIGUI interface, with crystallographic database records of the ICSD (Inorganic Crystal Structure Database) [20; 21]. Due to the difficulty of differentiating x-ray patterns from α, α' and α" phases, the Rietveld's structural refinement is able to differentiate patterns and make a volumetric percentage calculation of each phase the alloys [22].

Before the microstructural analysis, samples were submitted to a standard metallographic preparation [18]. Images were obtained using an optical microscope Olympus, BX51M model, and a scanning electron microscope Carl Zeiss, EVO-015 model. For hardness measurements a microhardness Shimadzu, HMV-2 model tester was used, with 250 g load during a time of 60 s [23]. Elastic (Young's) modulus measurements were made by the impulse excitation method using Sonelastic® equipment (ATCP Physical Engineering, Brazil)), following standard procedures [24].

The cytotoxicity tests were made using MC3T3-E1 osteoblast cells[25], which were maintained in the alpha-minimum essential medium (α-MEM, Invitrogen, Carlsbad, CA) and supplemented with 10% FBS. The cells were incubated under standard cell culture conditions (37ºC, 95% humidity and 5% CO_2) and the medium was changed every 2-3 days. The alloys' extracts were prepared from 1 g of alloy/ 1 mL of α-MEM at 37°C for

48 hours. The indirect cytotoxicity of the Ti-25Ta-Zr system alloys, containing various levels of zirconium for biomedical applications (Zr = 0, 10, 20, 30, 40 and 50 wt%),was determined using the MTT assay for 48 hours, as previously described elsewhere [26; 27].The cells were cultivated in 96 well microplates and incubated at a density of 110 cells/mm². The medium base was used as the negative control (no cytotoxicity) and was substituted by the obtained extracts from the alloys, while a solution of α-MEM, 10% of FBS and 1% of phenol was a positive control (cytotoxicity). The optical density of the wells was determined using a plate reader at a test wavelength of 640 nm in a Molecular Devices microplate reader SpectraMax Plus model. In the scanning electron microscopy (SEM) analysis, osteoblast cells were cultivated on a glass coverslip and the culture medium was substituted by the obtained extracts of the alloys. After 48 hours, the cells were fixed and were then routinely processed for SEM [27]. Specimens were mounted onto aluminum substrates, sputtered with gold, and examined in a Carl Zeiss EVO LS-15 scanning electron microscopy. The polystyrene was used as the negative control (no cytotoxicity), while a solution of α-MEM, 10% of FBS and 1% of phenol served as the positive control (cytotoxicity).

Results

Table 4.1 shows the results of the chemical composition analysis of all studied samples. The alloys presented compositions close to the nominal values with the presence of metallic impurities in non-significant concentrations. Table 4.2 presents a quantitative EDS analysis that corroborates the results obtained through the ICP-OES technique, where only small changes in results can be visualized. Figure 4.1 shows the mappings of the distribution of elements that compose the alloys. Titanium is represented by a red color, zirconium by a blue, and tantalum by a green. In Table 4.3, results from the gas analysis are presented for the samples of Ti-25Ta-Zr system. Figure 4.2 shows the density values for the samples of Ti-25Ta-Zr system alloys.

The x-ray diffractograms are presented in Figure 4.3. It can be observed that the crystalline structure of the alloys was sensitive to the zirconium concentration in solid solution. By the Rietveld method, it is possible to detect the crystalline phases, lattice parameters, and phase quantity [28]. Figure 4.4 shows the quantitative results of the phases by the analysis of the diffractograms using Rietveld's method.

Table 4.1 – Chemical composition for as-cast Ti-25Ta-Zr alloys, obtained by ICP-OES.

Element (wt%)	0Zr	10Zr	20Zr	30Zr	40Zr
Al	0.014	0.047	0.083	0.130	0.160
Cr	0.007	0.022	0.007	0.007	0.006
Cu	0.650	0.640	0.640	0.630	0.660
Fe	0.071	0.035	0.029	0.046	0.048
Hf	0.035	0.042	0.080	0.128	0.204
Mo	0.013	0.011	0.011	0.012	0.012
Ni	0.11	0.12	0.11	0.10	0.08
Si	0.068	0.082	0.079	0.083	0.065
Ta	25.1	23.9	24.9	23.6	23.5
Zr	0.1	11.3	20.2	29.5	37.2
Ti	Balance	Balance	Balance	Balance	Balance

Table 4.2 – Quantitative chemical analysis for as-cast Ti-25Ta-Zr by EDS.

Alloy	Ti (wt%)	Ta (wt%)	Zr (wt%)
Ti-25Ta	62.3 ± 0.3	28.2 ± 0.2	-
Ti-25Ta-10Zr	51.1 ± 0.2	29.1 ± 0.2	9.8 ± 0.2
Ti-25Ta-20Zr	45.1 ± 0.2	26.0 ± 0.2	17.6 ± 0.2
Ti-25Ta-30Zr	39.3 ± 0.2	25.8 ± 0.2	29.8 ± 0.2
Ti-25Ta-40Zr	30.9 ± 0.2	25.2 ± 0.2	39.4 ± 0.2

Table 4.3 – Results obtained from gas analysis for as-cast Ti-25Ta-Zr alloys.

	Oxygen (wt%)	Nitrogen (wt%)
Ti-25Ta	0.137 ± 0.004	0.007 ± 0.001
Ti-25Ta-10Zr	0.072 ± 0.005	0.009 ± 0.002
Ti-25Ta-20Zr	0.081 ± 0.007	0.008 ± 0.001
Ti-25Ta-30Zr	0.111 ± 0.001	0.013 ± 0.001
Ti-25Ta-40Zr	0.144 ± 0.003	0.012 ± 0.001

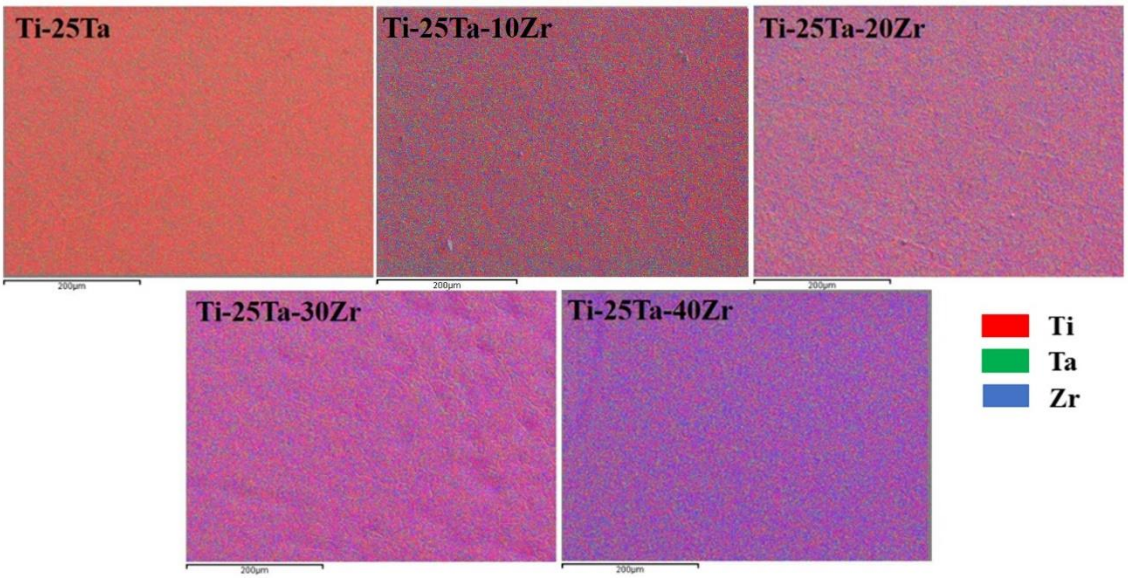


Figure 4.1 – EDS mapping for as-cast Ti-25Ta-Zr alloys, where red points represent titanium, green points represent tantalum and blue points represent zirconium.

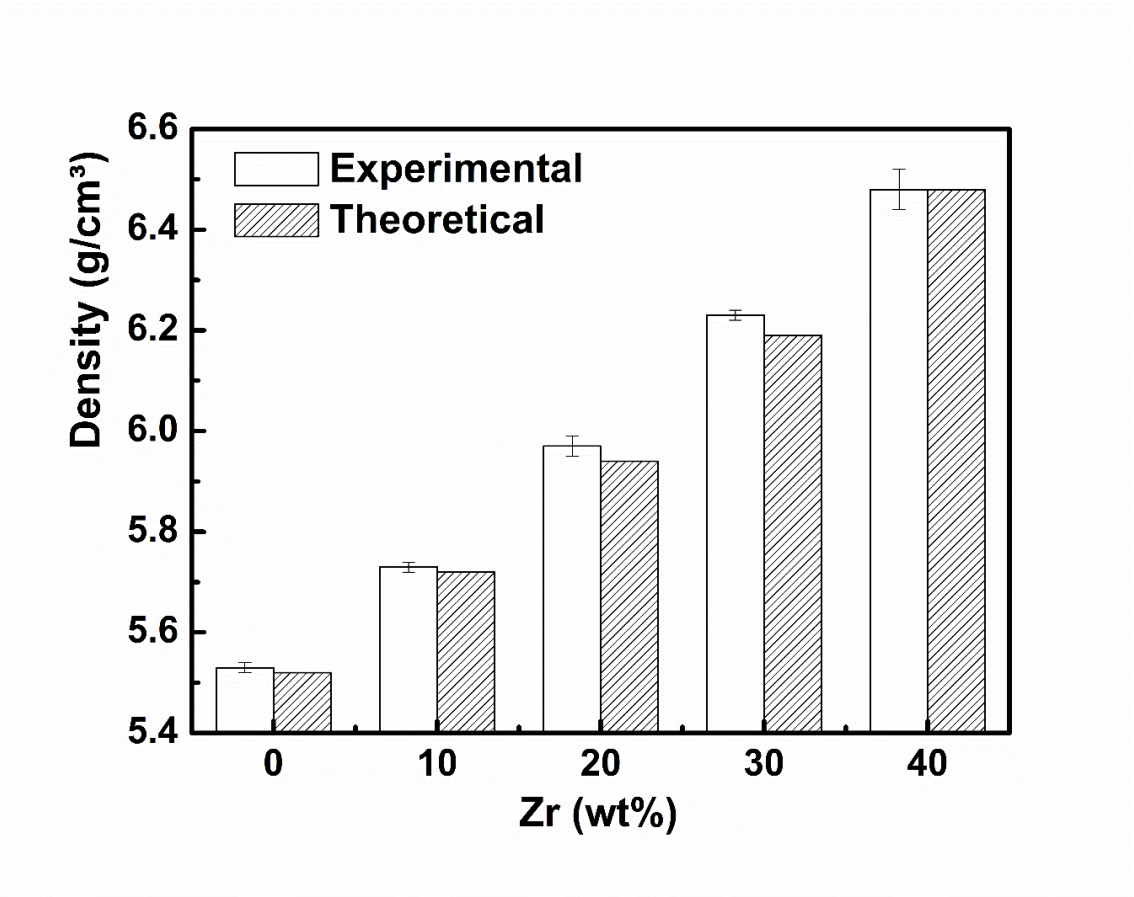


Figure 4.2 – Density as a function of zirconium concentration, for as-castTi-25Ta-Zr alloys.

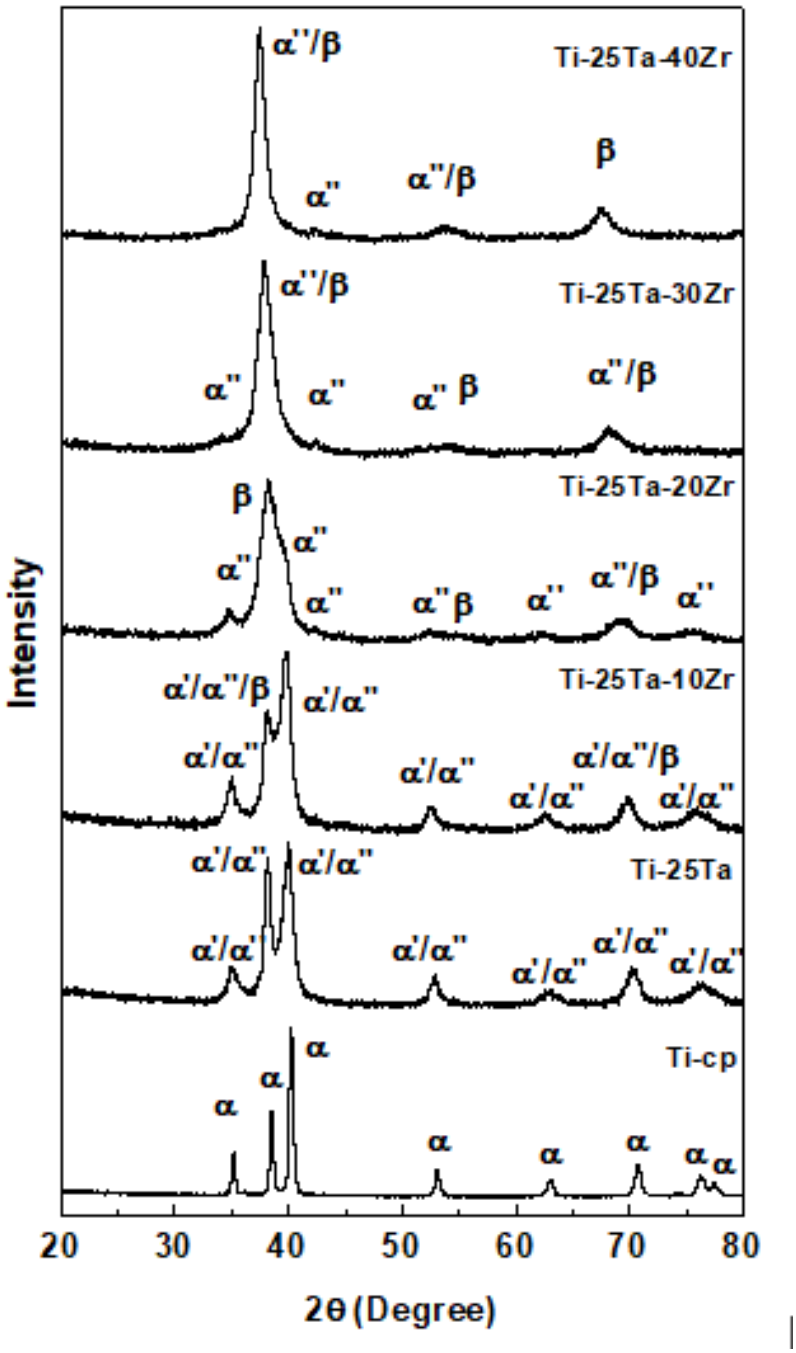


Figure 4.3 – XRD diffractograms for as-cast Ti-25Ta-Zr alloys.

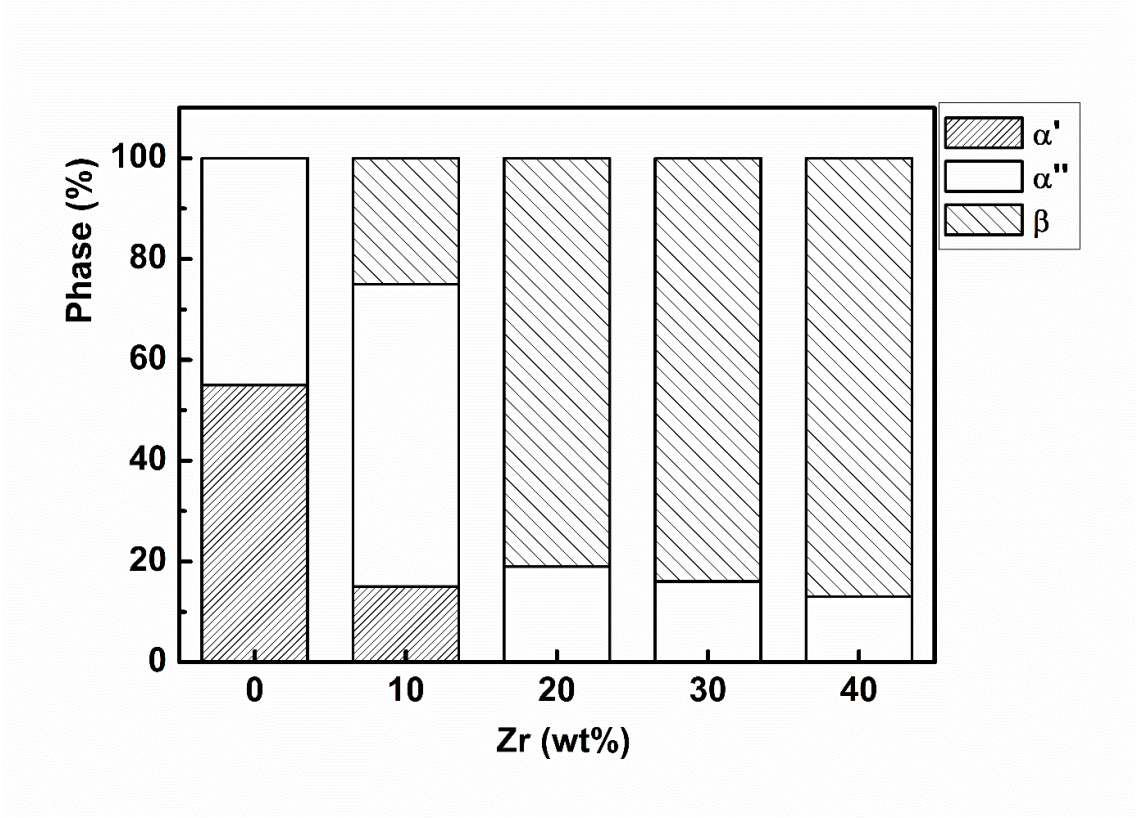


Figure 4.4 - Percentage of phases of as-cast Ti-25Ta-Zr alloys, as a function of zirconium.

Figure 4.5 shows the micrographs obtained by optical and scanning electron microscopy for the Ti-25Ta-Zr alloys. It can be observed that the microstructure of Ti-25Ta is composed of acicular structures (Widmanstätten pattern), typical of martensitic α' and α'' phases [29].

Figure 4.6 shows the results of the Vickers microhardness measurements for Ti-25Ta-Zr alloys and the results of the elastic modulus can be observed in Figure 4.7.

The results of the indirect cytotoxicity test and SEM analysis of cellular proliferation obtained by SEM are presented in Figure 4.8 and Figure 4.9, respectively.

Discussion

The results of chemical analysis show a good agreement with the stoichiometric purposes of the alloys. There is a good distribution, indicating that the procedure produced a truly homogeneous sample without the presence of aggregates or segregates. The samples of the Ti-25Ta-Zr system have oxygen and nitrogen dissolved in small quantities from the melting process. The results show a low content of oxygen and nitrogen in the produced samples. By ASTM F 2066 – 08 standard [30], for Ti-15Mo alloy it is tolerate a maximum

content of (0.20 ± 0.02) wt% and of (0.05 ± 0.02) wt%, for oxygen and nitrogen, respectively. Thus, the interstitials present in the samples are in small quantities e certainly, from the melting process, not compromising the continuation of the study. The results present a small difference between experimental and theoretical values, indicating that the composition of the alloys is close to stoichiometric values. It was observed that the value of the alloy's density increased when compared with pure titanium, because the density of tantalum and zirconium are higher than titanium [31], thus providing the observed increase. Experimental density is slightly higher than theoretical due to the presence of metallic impurities in alloys, such as copper and nickel, from the melting process and precursor materials. These highlighted impurities have higher density than titanium, resulting in a small increase in experimental density value. In general, the results of the chemical analysis indicate that the produced alloys have chemical compositions close to the nominal values, presenting a good quality to be used in the study.

The crystalline structure of the alloys was sensitive to the zirconium concentration in solid solution, as can be seen in Figure 4.3. For the alloy without zirconium, the presence of peaks that are characteristic of α'/α" phases were observed [8], while in the alloy with 10 wt% of zirconium, a small peak that is characteristic of β phase was observed, together with peaks of the α'/α" phases [15; 32]. The alloys with 20 wt% and 30 wt% of zirconium presented a diffraction pattern formed only by peaks that characterize the α"/β phases. For the alloy with 40 wt% zirconium, a small peak characteristic of α" phase was observed. The other peaks are representative of β phase [4]. It can be observed that zirconium acted as a β-stabilizer element, in the presence of another β-stabilizing element, in the case, tantalum [33; 34]. Using the Rietveld's method, the Ti-25Ta alloy showed the formation of α' phase (with around 54%) and α" phase (with around 46%). Ti-25Ta-10Zr alloy showed the coexistence of three crystalline phases, α' (with approximately 15%), α" (with around 60%) and β (with around 25%). Ti-25Ta-20Zr, Ti-25Ta-30Zr, and Ti-25Ta-40Zr alloys presented only two phases, α" and β, with respectively, 19% and 81% for the alloy with 20wt% of zirconium;16% and 84%, for the alloy with 30wt% of zirconium, and 13% and 87% for the alloy with 40wt% of zirconium. Therefore, the inclusion of zirconium in the alloys of the Ti-25Ta system decreased the percentages of the α' phase and increased the percentage of the β phase.

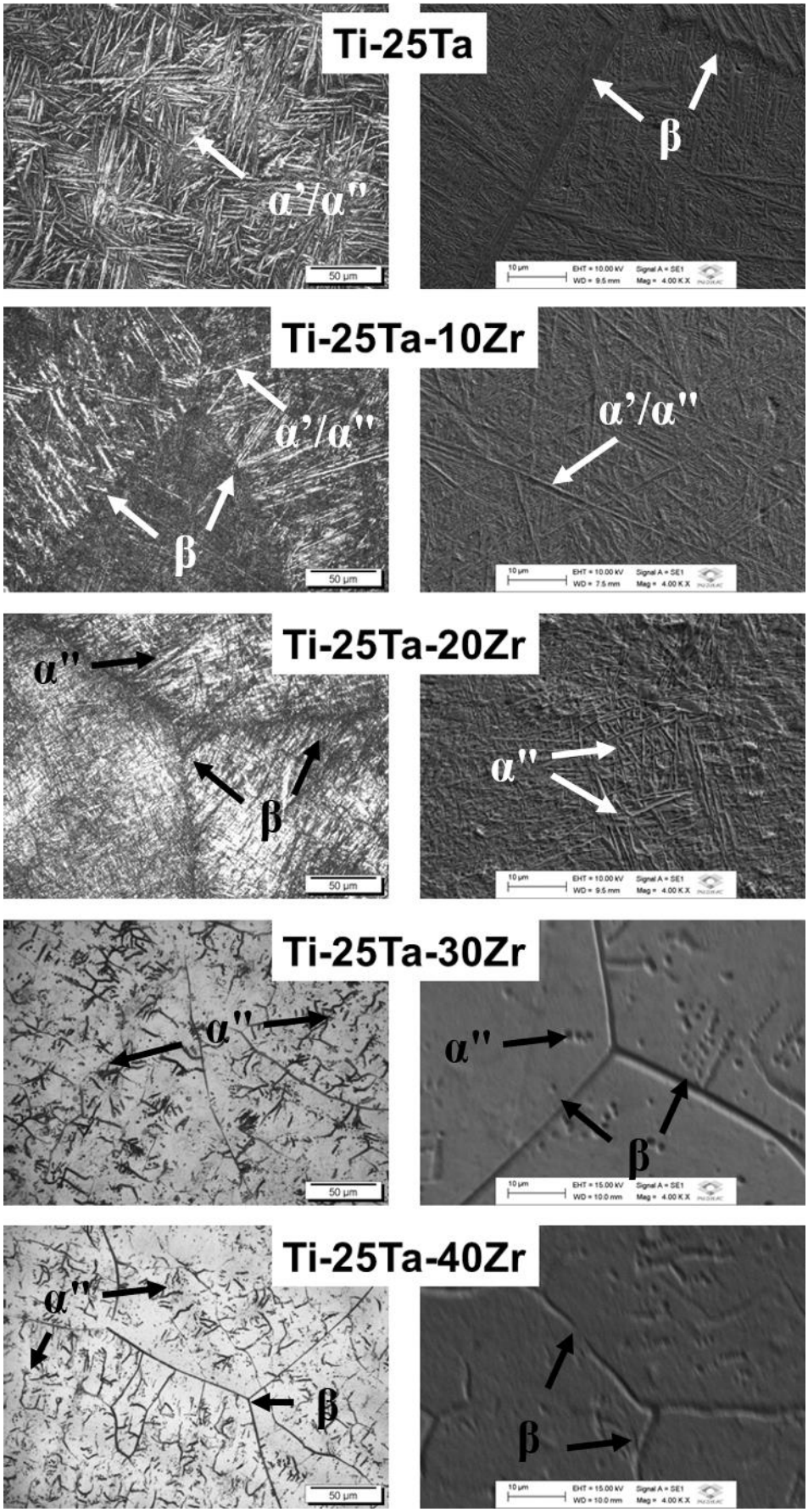


Figure 4.5 – Optical (left) and SEM (right) micrographs for as-cast Ti-25Ta-Zr alloys.

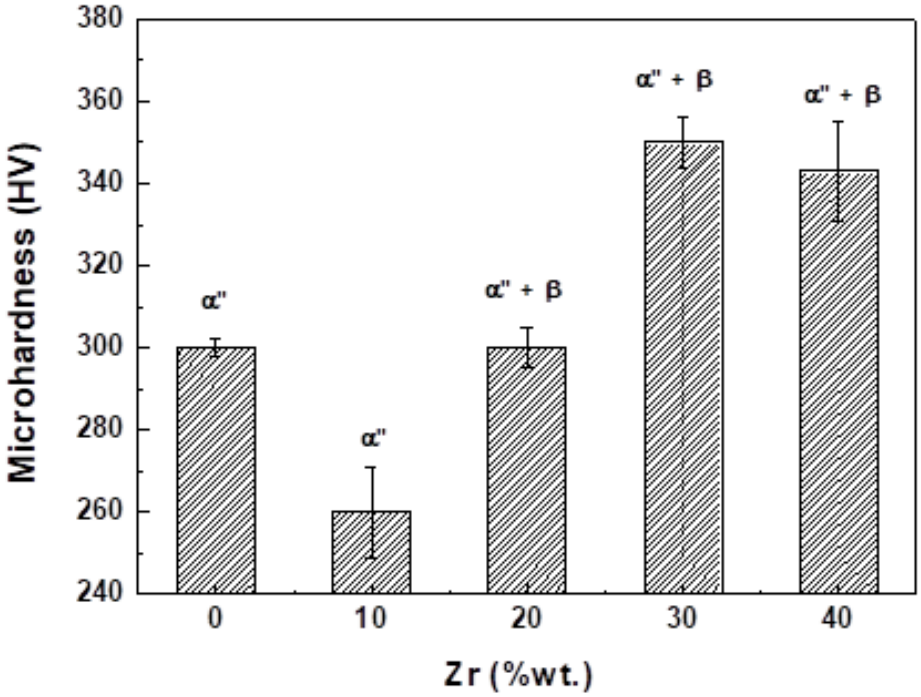


Figure 4.6 – Vickers Microhardness of as-cast Ti-25Ta-Zr alloys, as a function of zirconium.

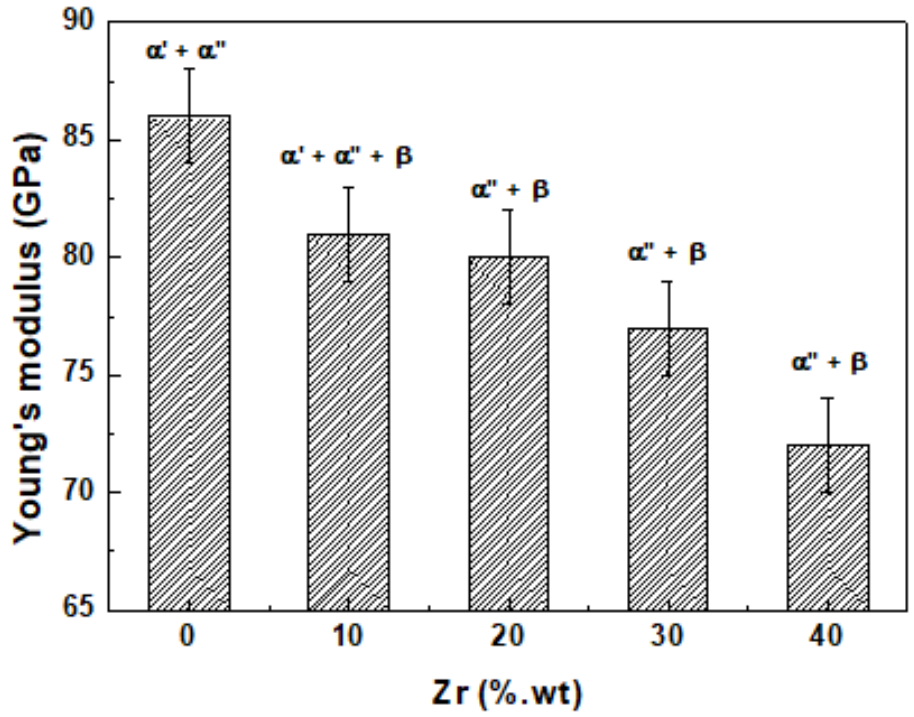


Figure 4.7 – Elastic modulus of Ti-25Ta-Zr alloys, as a function of zirconium.

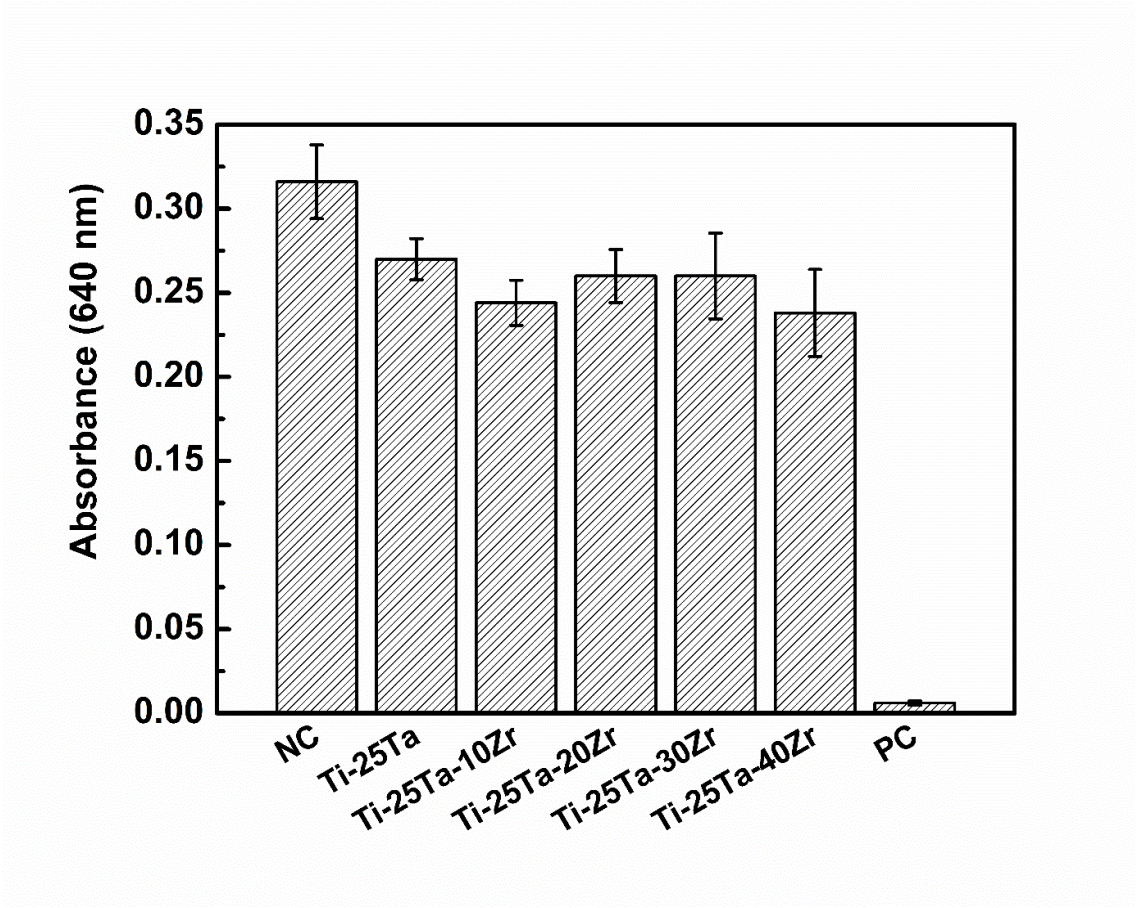


Figure 4.8 – Indirect cytotoxicity test of as-cast Ti-25Ta-Zr alloysin MC3T3-E1 cells cultured for 48 hours. **NC:** Negative control; **PC:** Positive control.

In the case of Ti-25Ta-10Zr, it is observed in the Figure 4.5, that the microstructure consists of the lamellas, which are typical of α' phase, thinner needles that are typical of α" phase, in a β phase matrix [35]. For Ti-25Ta-20Zr, Ti-25Ta-30Zr, and Ti-25Ta-40Zr alloys, the micrographs showed small needles characteristics of martensitic α" phase and β phase matrix [36]. All the images corroborate the experimental results of x-ray diffraction. Also, the microstructure was sensitive to the zirconium content. It was possible to observe a decrease in the size and quantities of needles of the martensitic phases with the increase of zirconium.

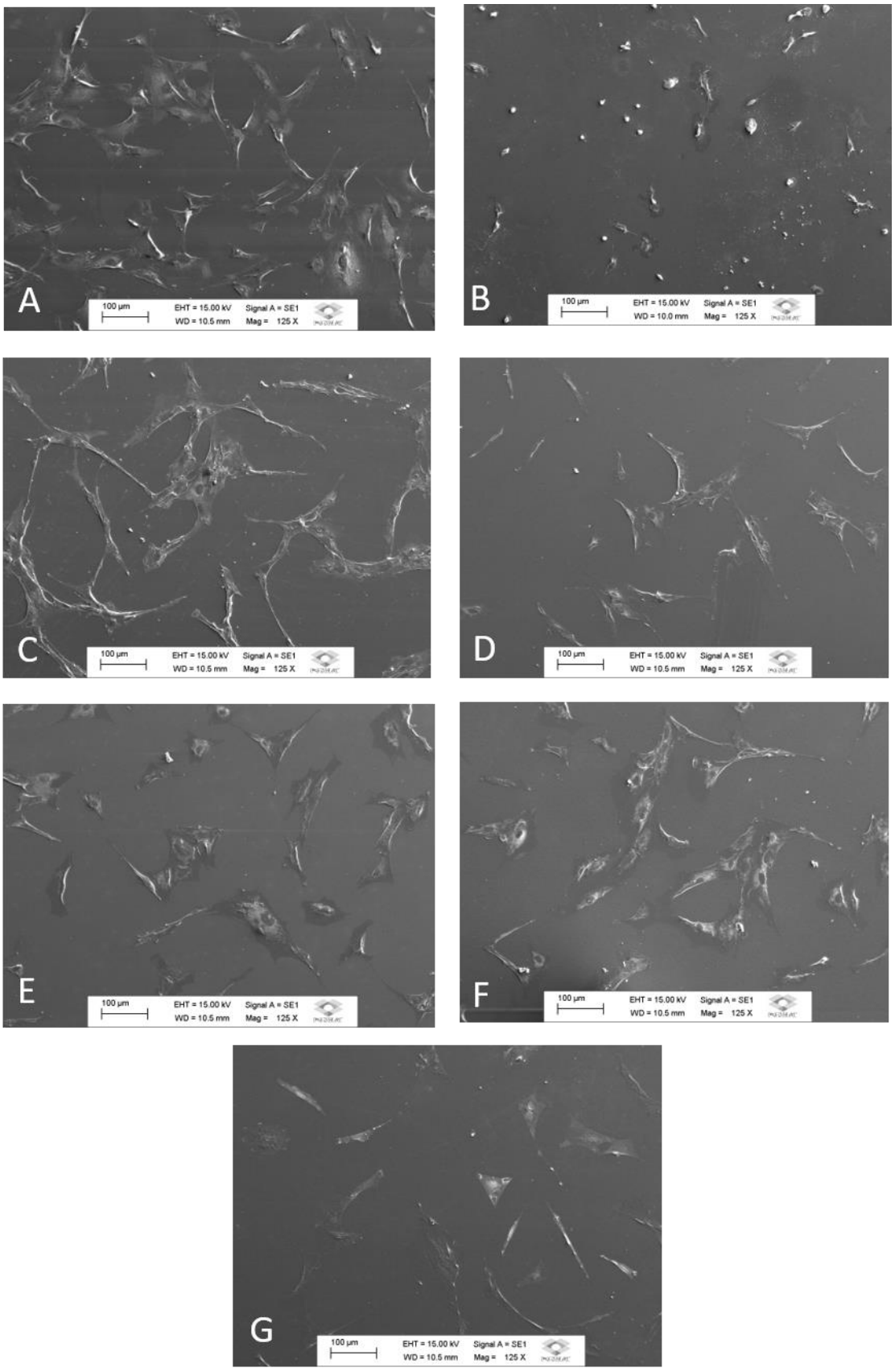


Figure 4.9 –SEM images for MC3T3-E1 cells cultured for 48 hours in as-cast Ti-25Ta-Zr alloys. Negative Control (A); Positive Control (B); Ti-25Ta (C); Ti-25Ta-10Zr (D); Ti-25Ta-20Zr (E); Ti-25Ta-30Zr (F) and Ti-25Ta-40Zr (G).

It was observed, in Figure 4.6, that the alloys have hardness values significantly higher than pure titanium (164 HV), giving an indication of greater mechanical resistance as a result of the hardening by solid solution [37]. This effect was caused by the addition of tantalum and zirconium, which have higher atomic masses than titanium [38]. According to Davis et al. [39], the phase transition from β to α" involves lower stresses than in the transition to hexagonal α'. Due to the low stresses in this transition, the α"-structure had a lower hardness, so the Ti-25Ta and Ti-25Ta-10Zr alloys have lower Vickers microhardness results due to their higher α"-phase volumetric concentration than the other studied alloys. The β-type alloys generally have a higher level of hardness than those of the martensitic phases because they have a stronger solid solution due to phase stability [4]. It is possible to observe that, for the alloys Ti-25Ta-20Zr, Ti-25Ta-30Zr and Ti-25Ta-40Zr, there was an increase in the hardness due to the appearance of the β phase. This increase can also be explained by the presence of the α-phase which may become an obstacle to the movement of the dislocations [40].

In the results of the elastic modulus showed in Figure 4.7, it can be observed that Young's modulus of the alloys studied varied approximately from 86 GPa for the alloy without zirconium and reached a minimum value of 72 GPa for the alloy with the highest zirconium content (40 wt%). With increase zirconium there is an increase in the percentage of the β phase, which decreases the elastic modulus [41] since the β phase has the smallest modulus of elasticity between the phases in titanium alloys. All Ti-25Ta-Zr system alloys have lower modulus values compared to cp-Ti (100 GPa). In Ti-25Ta alloy, the elastic modulus (approximately 86 GPa) is higher than the alloy studied by Zhou et al [10]. In this work the elastic modulus is superior, since the authors performed a fast cooling annealing heat treatment, and this type of treatment retains the beta phase and decreases the modulus of β-metastable alloys. The Ti-25Ta-40Zr alloy has the best modulus of elasticity to be used as a biomedical material because its value is more close to human cortical bone (30 GPa) [5].

The results of the indirect cytotoxicity test, presented in Figure 4.8, showed that none of the extracts from the studied alloys had a cytotoxic effect in contact with MC3T3-E1 cells [26]. The number of viable cells is higher than the negative control (non-cytotoxic - life) and higher than the positive (cytotoxic - death) control in all extracts [42]. Thus, it can be inferred that the studied alloys did not release cytotoxic elements into the culture medium within 48 hours. The results of the indirect cytotoxicity test were corroborated by SEM analysis, as shown in Figure 4.9. The cell morphology was preserved, as well as

in the negative control (non-cytotoxicity) [43]. Also, the cells have adhered to the substrate as can be seen by its cytoplasmic extensions, as well as cells in the process of cell division [44]. The same effect cannot be seen by the cells from the positive control (cytotoxicity – phenol solution) they did not spread, rather they maintained a rounded morphology without evidence of mitotic processes [45].

Conclusions

From the results presented in this paper it is possible to conclude:

- The alloys were successfully melted, producing good quality materials, as shown by the chemical composition analysis;
- The results of the structural and microstructural analyses of the alloys showed that the microstructure of Ti-25Ta alloy is formed by martensitic α' and α" phases. The Ti-25Ta-10Zr alloys are formed by α', α" and β phase. In Ti-25Ta-20Zr, Ti-25Ta-30Zr, and Ti-25Ta-40Zr alloys, the phases α" and β are present, with a predominance of β phase in the alloys;
- The zirconium element acts in the stabilization of the β phase, together with tantalum;
- The hardness of the alloys was higher than the commercially pure titanium, caused by solid solution hardening of the alloy;
- The elastic modulus decreases with high levels of zirconium due to the stabilization of β phase;
- The cytotoxicity test showed that the extracts of studied alloys are not cytotoxic for osteoblast cells in a short period of culture.

References

1 GEETHA, M. et al. Ti based biomaterials, the ultimate choice for orthopaedic implants - A review. **Progress in Materials Science,** v. 54, n. 3, p. 397-425, 2009.
2 KIRMANIDOU, Y. et al. New Ti-Alloys and Surface Modifications to Improve the Mechanical Properties and the Biological Response to Orthopedic and Dental Implants: A Review. **BioMed Research International,** v. 2016, p. 21, 2016.
3 LI, Y. et al. New Developments of Ti-Based Alloys for Biomedical Applications. **Materials,** v. 7, n. 3, p. 1709-1800, 2014.
4 KOLLI, R.; DEVARAJ, A. A Review of Metastable Beta Titanium Alloys. **Metals,** v. 8, n. 7, p. 506, 2018.
5 KAUR, M.; SINGH, K. Review on titanium and titanium based alloys as biomaterials for orthopaedic applications. **Materials Science and Engineering: C,** v. 102, p. 844-862, 2019.

6 ALRABEAH, G. O. et al. The effect of metal ions released from different dental implant-abutment couples on osteoblast function and secretion of bone resorbing mediators. **Journal of Dentistry,** v. 66, p. 91-101, 2017.
7 CHAPPARD, D. et al. Aluminum and bone: Review of new clinical circumstances associated with Al3+ deposition in the calcified matrix of bone. **Morphologie,** v. 100, p. 95-105, 2016.
8 ZHOU, Y. L. et al. Corrosion resistance and biocompatibility of Ti-Ta alloys for biomedical applications. **Materials Science and Engineering A,** v. 398, n. 1-2, p. 28-36, 2005.
9 ZHOU, Y. L.; NIINOMI, M.; AKAHORI, T. Effects of Ta content on Young's modulus and tensile properties of binary Ti–Ta alloys for biomedical applications. **Materials Science and Engineering: A,** v. 371, n. 1, p. 283-290, 2004.
10 ZHOU, Y.-L.; NIINOMI, M. Ti–25Ta alloy with the best mechanical compatibility in Ti–Ta alloys for biomedical applications. **Materials Science and Engineering: C,** v. 29, n. 3, p. 1061-1065, 2009.
11 HO, W. F. et al. Structure, mechanical properties, and grindability of dental Ti-Zr alloys. **J Mater Sci Mater Med,** v. 19, n. 10, p. 3179-86, 2008.
12 CORREA, D. R. N. et al. The effect of the solute on the structure, selected mechanical properties, and biocompatibility of Ti–Zr system alloys for dental applications. **Materials Science and Engineering: C,** v. 34, p. 354-359, 2014.
13 BIESIEKIERSKI, A. et al. Extraordinary high strength Ti-Zr-Ta alloys through nanoscaled, dual-cubic spinodal reinforcement. **Acta Biomaterialia,** v. 53, p. 549-558, 2017.
14 VASILESCU, C. et al. Long-term corrosion resistance of new Ti–Ta–Zr alloy in simulated physiological fluids by electrochemical and surface analysis methods. **Corrosion Science,** v. 93, p. 310-323, 2015.
15 KURODA, P. A. B.; BUZALAF, M. A. R.; GRANDINI, C. R. Effect of molybdenum on structure, microstructure and mechanical properties of biomedical Ti-20Zr-Mo alloys. **Materials Science and Engineering: C,** v. 67, p. 511-515, 2016.
16 QUADROS, F. D. F. et al. Preparation, structural and microstructural characterization of Ti-25Ta-10Zr alloy for biomedical applications. **Journal of Materials Research and Technology**, v. 8, p. 4108-4114, 2019.
17 ASTM. **E2371 – 04 - Standard Test Method for Analysis of Titanium and Titanium Alloys by Atomic Emission Plasma Spectrometry**. E2371 – 04 - Standard Test Method for Analysis of Titanium and Titanium Alloys by Atomic Emission Plasma Spectrometry. West Conshohocken: ASTM International. E2371 – 04 2004.
18 _____. **E407-07 - Standard Practice for Microetching Metals and Alloys**. E407-07 - Stanard Practice for Microetching Metals and Alloys. West Conshohocken: ASTM International. ASTM E-407-07 2007.
19 _____. **E1409 – 08 - Standard Test Method for Determination of Oxygen and Nitrogen in Titanium and Titanium Alloys by the Inert Gas Fusion Technique**. E1409 – 08 - Standard Test Method for Determination of Oxygen and Nitrogen in Titanium and Titanium Alloys by the Inert Gas Fusion Technique. West Conshohocken: ASTM International. ASTM E1409 – 08 2008.
20 TOBY, B. H. EXPGUI, a Graphical User Interface for GSAS. **Journal of Applied Crystallography,** v. 34, p. 210-213, 2001.
21 RIETVELD, H. M. Profile Refinement Method for Nuclear and Magnetic Structure. **Journal of Applied Crystallography,** v. 2, p. 65-71, 1969.

22 SEVERINO MARTINS, J. R.; GRANDINI, C. R. Structural characterization of Ti-15Mo alloy used as biomaterial by Rietveld method. **Journal of Applied Physics,** v. 111, n. 8, p. 083535, 2012.
23 ASTM. **E92-82 - Standard Test Method for Vickers Hardness of Metallic Materials**. E92-82 - Standard Test Method for Vickers Hardness of Metallic Materials. West Conshohocken, PA: ASTM International. E92-82 2003.
24 _____. **E1876–01 - Standard Test Method for Dynamic Young's Modulus, Shear Modulus, and Poisson's Ratio by Impulse Excitation of Vibration**. E1876–01 - Standard Test Method for Dynamic Young's Modulus, Shear Modulus, and Poisson's Ratio by Impulse Excitation of Vibration. Philadelphia (USA): ASTM International. E1876–01 2002.
25 ISO. **10993-5 - Biological evaluation of medical devices - Part 5: Tests for in vitro cytotoxicity**. 10993-5 - Biological evaluation of medical devices - Part 5: Tests for in vitro cytotoxicity. Geneva: International Organization for Standardization 2009.
26 DONATO, T. A. G. et al. Cytotoxicity study of some Ti alloys used as biomaterial. **Materials Science & Engineering C-Biomimetic and Supramolecular Systems,** v. 29, n. 4, p. 1365-1369, 2009.
27 DONATO, T. et al. In Vitro Cytotoxicity of a Ti-35Nb-7Zr-5Ta Alloy Doped with Different Oxygen Contents. **Materials,** v. 7, n. 3, p. 2183-2193, 2014.
28 MARTINS JR, J. R. S.; GRANDINI, C. R. Structural characterization of Ti-15Mo alloy used as biomaterial by Rietveld method. **Journal of Applied Physics,** v. 111, n. 8, p. 083535-8, 2012.
29 COLLINGS, E. W. **The Physical Metallurgy of Titanium Alloys**. Ohio: ASM International, 1989.
30 ASTM. **F2066-08 - Standard specification for wrought titanium-15 molybdenum alloy for surgical implant application**. F2066-08 - Standard specification for wrought titanium-15 molybdenum alloy for surgical implant application. Philadelphia (USA): ASTM International. F 2066-08 2008.
31 LIDE, D. **CRC handbook of chemistry and physics: a ready-reference book of chemical and physical data**. 85th. Boca Raton, USA: CRC Press, 2004.
32 CORREA, D. R. N. et al. Development of Ti-15Zr-Mo alloys for applying as implantable biomedical devices. **Journal of Alloys and Compounds,** v. 749, p. 163-171, 2018.
33 HO, W.-F. et al. Effects of molybdenum content on the structure and mechanical properties of as-cast Ti–10Zr-based alloys for biomedical applications. **Materials Science and Engineering: C,** v. 32, n. 3, p. 517-522, 2012.
34 CORREA, D. R. N. et al. Effect of the substitutional elements on the microstructure of the Ti-15Mo-Zr and Ti-15Zr-Mo systems alloys. **Journal of Materials Research and Technology,** v. 4, n. 2, p. 180-185,
35 LÜTJERING, G.; WILLIAMS, J. C.; GYSLER, A. Microstructure and Mechanical Properties of Titanium Alloys. In: (Ed.). **Microstructure and Properties of Materials**, 1998. p.1-77.
36 FREESE, H. L. et al. Titanium and its Alloys in Biomedical Engineering. In: EDITORS-IN-CHIEF: , K. H. J. B.;ROBERT, W. C., *et al* (Ed.). **Encyclopedia of Materials: Science and Technology (Second Edition)**. Oxford: Elsevier, 2001. p. 9374-9380.
37 BANERJEE, R. et al. Strengthening mechanisms in Ti–Nb–Zr–Ta and Ti–Mo–Zr–Fe orthopaedic alloys. **Biomaterials,** v. 25, n. 17, p. 3413-3419, 2004.
38 HO, W.-F. et al. Structure, mechanical properties and grindability of dental Ti-10Zr-X alloys. **Materials Science and Engineering: C,** v. 29, n. 1, p. 36-43, 2009.

39 DAVIS, R.; FLOWER, H. M.; WEST, D. R. F. The decomposition of Ti-Mo alloy martensites by nucleation and growth and spinodal mechanisms. **Acta Metallurgica,** v. 27, n. 6, p. 1041-1052, 1979.
40 DEY, G. K. et al. Metastability of the [beta]-phase in Zr-rich Zr-Nb alloys. **Journal of Nuclear Materials,** v. 224, n. 2, p. 146-157, 1995.
41 MOHAMMED, M. T.; KHAN, Z. A.; SIDDIQUEE, A. N. Beta Titanium Alloys: The Lowest Elastic Modulus for Biomedical Applications: A Review. **International Journal of Chemical, Molecular, Nuclear, Materials and Metallurgical Engineering,** v. 8, p. 821-827, 2014.
42 CHEN, Q.; THOUAS, G. A. Metallic implant biomaterials. **Materials Science and Engineering: R: Reports,** v. 87, p. 1-57, 2015/01/01/ 2015.
43 LI, Y. et al. Cytotoxicity of titanium and titanium alloying elements. **Journal of Dental Research,** v. 89, n. 5, p. 493-497, 2010.
44 PARK, Y.-J. et al. Cytocompatibility of pure metals and experimental binary titanium alloys for implant materials. **Journal of Dentistry,** v. 41, n. 12, p. 1251-1258, 2013.
45 SEVCIKOVA, J.; PAVKOVA GOLDBERGOVA, M. Biocompatibility of NiTi alloys in the cell behaviour. **BioMetals,** v. 30, n. 2, p. 163-169, 2017.

Capítulo 5

Aceito para publicação na Revista Matéria, 2020.

Preparação e caracterização de uma liga de titânio com a adição de tântalo e zircônio para aplicações biomédicas

Preparation and characterization of a titanium alloy with the addition of tantalum and zirconium for biomedical applications

Pedro Akira Bazaglia Kuroda, Mycaella Vieira do Nascimento, Carlos Roberto Grandini
UNESP – Univ. Estadual Paulista, Laboratório de Anelasticidade e Biomateriais, 17.033.360, Bauru (SP), e
IBTN-Br, Braço Brasileiro do Institute of Biomaterials, Tribocorrosion and Nanomedicine, 17.033.360, Bauru (SP)

Resumo

Ligas de titânio são amplamente utilizadas na área biomédica devido à sua excelente resistência à corrosão em fluídos corpóreos, elevada razão resistência mecânica/densidade, baixo módulo de elasticidade e comprovada biocompatibilidade. As ligas mais promissoras para serem utilizadas na área biomédica possuem elementos em solução sólida que diminuem a temperatura de transformação de fase do titânio. Tais elementos são denominados beta-estabilizadores e obtêm-se como resultado a diminuição do módulo de elasticidade e uma excelente resistência à corrosão. Os elementos tântalo e zircônio, quando acrescentados ao titânio, melhoram a resistência à corrosão e diminuem o módulo de elasticidade, pois o tântalo é considerado um elemento β-estabilizador e o zircônio atua como elemento estabilizador desta fase, na presença de outro elemento β-estabilizador. Neste trabalho, a liga Ti-25Ta-5Zr foi preparada por fusão à arco, visando aplicações biomédicas. As caracterizações química, estrutural, microestrutural e mecânica foram realizadas por intermédio de medidas da composição química, análise de gases, espectrometria por dispersão de energia (EDS), difração de raios X, microscopias

óptica e eletrônica de varredura, microdureza Vickers e módulo de elasticidade. Os resultados obtidos mostraram uma boa estequiometria e homogeneidade da amostra. As análises estrutural e microestrutural corroboraram entre si e indicaram que a liga possui a coexistência de duas fases, α" (com estrutura cristalina ortorrômbica) e β (com estrutura cristalina cúbica de corpo centrado). A microdureza elevou-se com a adição de tais elementos e o módulo de elasticidade possui valores abaixo das ligas utilizadas comercialmente, satisfatório para aplicação como implante ortopédico.

Abstract

Titanium alloys are widely used in the biomedical field due to its excellent corrosion resistance in bodily fluids, high mechanical strength/density ratio, low elastic modulus and good biocompatibility. The most promising alloys to be used in the biomedical field have solid solution elements that decrease the phase transformation temperature of titanium. Such elements are called beta-stabilizers and are obtained as a result of their introduction in the alloy, the decrease of the elastic modulus and an excellent corrosion resistance. Tantalum and zirconium elements, when added to the titanium, improve the corrosion resistance and diminish the elastic modulus, because tantalum is considered a β-stabilizer element and the zirconium acts as a stabilizing element of this phase, in presence of another β-stabilizer element. In this paper, Ti-25Ta-5Zr alloy was prepared by arc-melting, aiming biomedical applications. The chemical, structural, microstructural and mechanical characterizations were performed by means of chemical composition measurements, gas analysis, energy dispersive spectrometry (EDS), X-ray diffraction, optical and scanning electron microscopies, Vickers microhardness and elastic modulus. The obtained results showed a good stoichiometry and homogeneity of the samples. Structural and microstructural analyses corroborated each other and indicated that the alloy has the coexistence of two phases, α" (with orthorhombic crystalline structure) and β (with body-centered cubic structure). The microhardness increased with the addition of such elements and the elastic modulus has values below the commercially used alloys, satisfactory for application as orthopedic implant.

Introdução

Ligas de titânio tem sido muito utilizadas com sucesso na área biomédica desde os anos 40 do século passado [1; 2]. Porém, estudos recentes mostram alguns efeitos citotóxicos de alguns elementos em longo prazo, em especial o alumínio e o vanádio, que tem sido

associados com desordens neurológicas [3; 4]. Outro problema está associado com a grande diferença entre os módulos de elasticidade das ligas utilizadas comercialmente (em torno de 100 GPa) e do osso cortical (em torno de 30 GPa) [5]. Este diferença faz com que todos os esforços mecânicos sejam absorvidos pelo material implantado, causando efeitos de reabsorção óssea [6]. Assim, intensa investigação e desenvolvimento de ligas metálicas estão sendo realizadas em todo o campo biomédico, com o objetivo de encontrar novas ligas de titânio que possuam módulo de elasticidade cada vez mais próximo do osso, ótima resistência à corrosão e excelente biocompatibilidade [7; 8].

Na linha de ligas binárias vantajosas para aplicação biomédica, destacam-se as ligas do sistema Ti-Ta, com o teor de tântalo variando de 20 a 30 %p [9]. A microestrutura das ligas Ti-Ta é influenciada pela quantidade de tântalo presente na sua composição. Para concentrações abaixo de 20 %p tântalo, a liga apresenta uma microestrutura composta apenas pela fase α, com estrutura cristalina hexagonal compacta. Para concentração de tântalo variando entre 30 a 50%, coexistem as fases martensíticas α' e α'', com estrutura cristalina hexagonal distorcida e ortorrômbica, respectivamente. Quando a concentração aumenta para até 60% em peso de tântalo, as fases α'' e β coexistem e apenas para ligas com concentração de tântalo acima de 60% há a predominância da fase β, com estrutura cristalina cúbica de corpo centrado, sem a formação de fases martensíticas [10]. Tais ligas possuem boas propriedades mecânicas e baixo módulo de elasticidade, onde se destaca a liga Ti-25Ta, com módulo de elasticidade abaixo de 70 GPa [11]. Estas características fazem a liga Ti-25Ta bastante promissora para ser utilizada em aplicações ortopédicas e odontológicas.

Outra possibilidade bastante interessante é o caso de ligas do sistema Ti-Zr [9; 12; 13; 14]. Sabe-se que o zircônio possui propriedades químicas semelhantes às do titânio, podendo formar soluções sólidas com certa facilidade [15], além da concentração de zircônio reduzir o ponto de fusão da liga facilitando o manuseio do material nos processos de conformação mecânica [16]. Embora o zircônio seja considerado um elemento neutro em ligas binárias de titânio, na presença de um outro elemento beta estabilizador (como tântalo, por exemplo), ele pode ajudar na retenção desta fase e diminuir a temperatura da transição matensítica α' [17; 18; 19; 20; 21].

Levando-se em consideração as diversas condições favoráveis das ligas dos sistemas Ti-Ta e Ti-Zr para aplicação como biomateriais, a formação de ligas ternárias do sistema Ti-Ta-Zr pode apresentar propriedades mais interessantes ainda para a área biomédica. A liga Ti-25Ta com o acréscimo de cinco por cento de zircônio pode mostrar

propriedades mecânicas e eletroquímicas favoráveis para a fabricação de implantes, além dos elementos constituintes apresentarem excelente biocompatibilidade com o organismo [22].

Neste sentido, este trabalho mostra o desenvolvimento de uma nova liga a base de titânio, a liga Ti-25Ta-5Zr, visando aplicações ortopédicas e dentárias. Também são apresentados os resultados da caracterização química, estrutural, microestrutural e de algumas propriedades mecânicas selecionadas da liga.

Materiais e Métodos

A fusão foi realizada utilizando um forno arco-voltaico, com cadinho de cobre refrigerado a água, eletrodo não-consumível de tungstênio e atmosfera controlada de argônio [18; 23; 24; 25; 26; 27; 28].

A composição química das amostras produzidas foi verificada utilizando a técnica da solubilização em meio ácido, seguido da detecção dos elementos em um espectrômetro de emissão ótica com plasma induzido (ICP-OES) [29]; pela técnica de espectrometria por dispersão de energia (EDS), utilizando um microscópio eletrônico de varredura da Carls Zeiss, modelo EVO-015, com a sonda INCA e a quantidades dos gases oxigênio e nitrogênio foram verificados utilizando um equipamento LECO, modelo TC-400 pela fusão direta das amostras em cadinhos de grafite que combina o carbono com o oxigênio liberado pela amostra [30].

As medidas de difração de raios X foram realizadas por intermédio de um difratômetro Rigaku D/Max 2100PC, utilizando a radiação Kα do cobre (λ=1,506 Å), corrente de 20 mA, potencial de 40 kV, tempo de permanência de 1,6 s e passo de 0,02 graus, de 20° à 100°, no modo de tempo fixo.

Para a obtenção das imagens de microscopia óptica, foi utilizado um microscópio Olympus modelo BX51M e para as imagens de microscopia eletrônica de varredura, foi utilizado um microscópio eletrônico da Carls Zeiss, modelo EVO-015. Os materiais passaram por um preparo metalográfico prévio no qual as amostras foram lixadas com lixas com 360, 400, 500, 600, 800, 1200 e 1500 mesh de granulometria [31]. Após o lixamento, as amostras foram polidas em suspensão de alumina de 1 μm. Para revelar a microestrutura das amostras, foi realizado um ataque químico com o reagente Kroll [32], utilizando uma solução de 15% de HNO3, 5% de HF e 80% de H2O.

Para a caracterização mecânica inicial das amostras, foram selecionadas duas propriedades extremamente importantes para a utilização como biomaterial, a dureza e o

módulo de elasticidade [33]. As medidas de microdureza Vickers foram obtidas por intermédio de um microdurômetro Shimadzu HMV-2, com carga de 200 g (1,961 N) e tempo de 60s [34]. Para as medidas do módulo de elasticidade, foi utilizado método dinâmico, baseado na técnica de excitação por impulso [35], por intermédio de um equipamento Sonelastic®, da ATCP.

Resultados e Discussão

A Tabela 5.1 mostra os valores obtidos para os elementos que compõem a liga, utilizando a técnica de ICP-EOS e análise de gases. Observa-se que a composição química da liga é próxima ao valor nominal e as impurezas metálicas apresentam concentrações não significativas. Com relação à análise de gases, pode ser visto que a liga possui oxigênio e nitrogênio dissolvidos intersticialmente em pequenas quantidades, oriundos do processo de fusão. Os resultados mostram um baixo teor de oxigênio e nitrogênio nas amostras produzidas. A Tabela 5.2 mostra uma análise dos elementos da liga utilizando EDS. Os valores encontrados são próximos da estequiometria proposta e corrobora os resultados obtidos por ICP-EOS. Segundo a norma ASTM 2066 [36], uma liga binária Ti-15%pMo deve possuir uma quantidade de molibdênio entre 14 e 16 %p. Como a liga produzida é nova e não possui uma norma específica, analisando os resultados à luz da norma ASTM 2066, observa-se que a liga é obtida de forma satisfatória. Por esta norma, na liga Ti-15%pMo, o teor máximo de gases tolerado é (0,20 ± 0,02) %p e (0,05 ± 0,02) %p, para o oxigênio e nitrogênio, respectivamente. Assim, conclui-se que o teor de oxigênio e nitrogênio para os lingotes produzidos estão de acordo com o estabelecido pela norma.

Tabela 5.1: Composição química das amostras da liga Ti-25Ta-5Zr

Elemento	Al	Cr	Cu	Fe	Hf	Mo	Ni	Si	Ta	Zr	O	N	Ti
%p	0,07	0,01	0,01	0,07	0,01	0,02	0,01	0,01	25,07	5,35	0,17	0,01	Balanço

Tabela 5.2: Análise química quantitativa por EDS das amostras da liga Ti-25Ta-5Zr

Elemento	Ti	Ta	Zr
%p	Balanço	(29,1 ± 0,2)	(5,6 ± 0,2)

A Figura 5.1 mostra imagens do mapeamento por EDS, dos elementos que compõem uma amostra de liga de Ti-25Ta-5Zr, onde os pontos de coloração vermelha representam o titânio, os pontos verde representam o tântalo e os azuis, representam o

zircônio. Observa-se uma distribuição homogênea, sem a presença de aglomerados ou segregados.

A partir de resultados empíricos, foi desenvolvida uma equação que possibilita escolher composições das ligas nas quais as quantidades de elementos substitucionais podem estabilizar a fase β. A equação usa a porcentagem equivalente de molibdênio por ser um dos principais estabilizadores da fase β [37]:

$$[Mo] = Mo + \frac{Ta}{5} + \frac{Nb}{3{,}6} + \frac{W}{2{,}5} + \frac{V}{1{,}5} + 1{,}25Cr + 1{,}25Ni + 1{,}7Mn + 1{,}7Co + 2{,}5Fe \quad (1)$$

Para as ligas produzidas neste trabalho, o molibdênio equivalente é igual a 5,23. Assim, segundo a teoria a liga Ti-25Ta-5Zr deve possui uma estrutura semelhante a liga binária Ti-5Mo. Ho e colaboradores [38] estudaram as ligas do sistema Ti-Mo para aplicações como biomaterial e observaram que com 5 %p de molibdênio, uma pequena quantidade de fase α" está presente na liga. Logo espera-se que a liga Ti-25Ta-5Zr possua, além da fase b, a fase α" em sua microestrutura.

Outra técnica utilizada para prever fases de ligas de titânio é a teoria do orbital molecular DV-Xα [39]. O método é baseado na aproximação de Hartree-Fock-Slater usando o potencial Xα de Slater [40; 41; 42]. O parâmetro de ordem de ligação Bo representa a intensidade da força de ligação entre o titânio e seus elementos de liga. O parâmetro de nível de energia Md é relacionado à camada d do metal de transição que está sendo ligado. Estes dois parâmetros são levados em consideração para prever a estrutura do material e seu módulo de elasticidade [40]. O cálculo dos parâmetros médios Bo e Md para as ligas de estudo é apresentado na em um diagrama Bo-Md, mostrado na Figura 5.2. Em ambas as teorias, a previsão é que a liga Ti-25Ta-5Zr possua a fase ortorrômbica α", coexistindo com a fase b.

A Figura 5.3 mostra um gráfico comparativo dos difratogramas de raios X para as amostras da liga Ti-25Ta-5Zr na condição bruta de fusão. Observando os difratogramas, verifica-se que as amostras da liga em questão, apresentaram picos da fase martensítica α" e β, com estrutura cristalina ortorrômbica e cúbica de corpo centrado, respectivamente [38]. O tântalo é um elemento β-estabilizador [10], e a presença do mesmo faz com que o zircônio deixe de ser neutro e passe a atuar na estabilização da fase β na liga [21; 23], devido a isso é possível detectar a presença de picos que são associados à fase β.

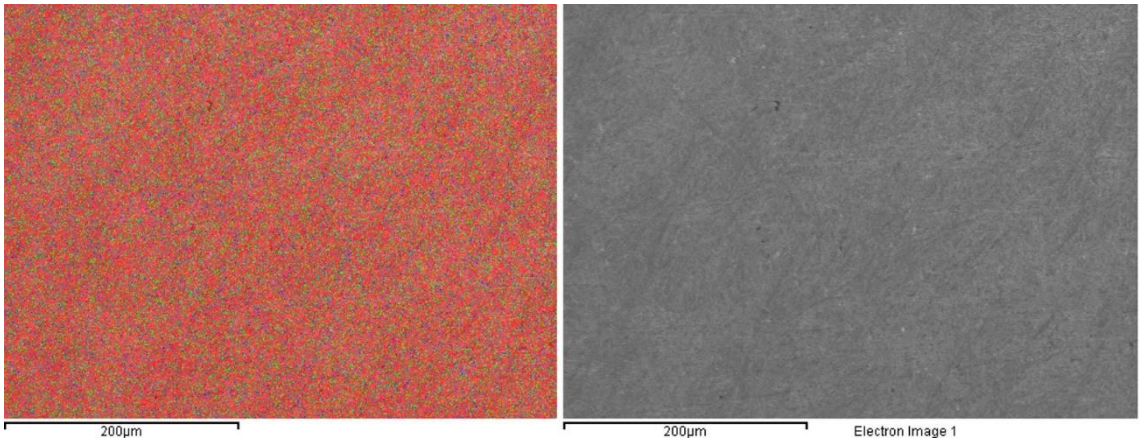


Figura 5.1: Mapeamento da distribuição dos elementos titânio (em verde), tântalo (em azul) e zircônio (em verde), nas amostras da liga Ti-25Ta-5Zr

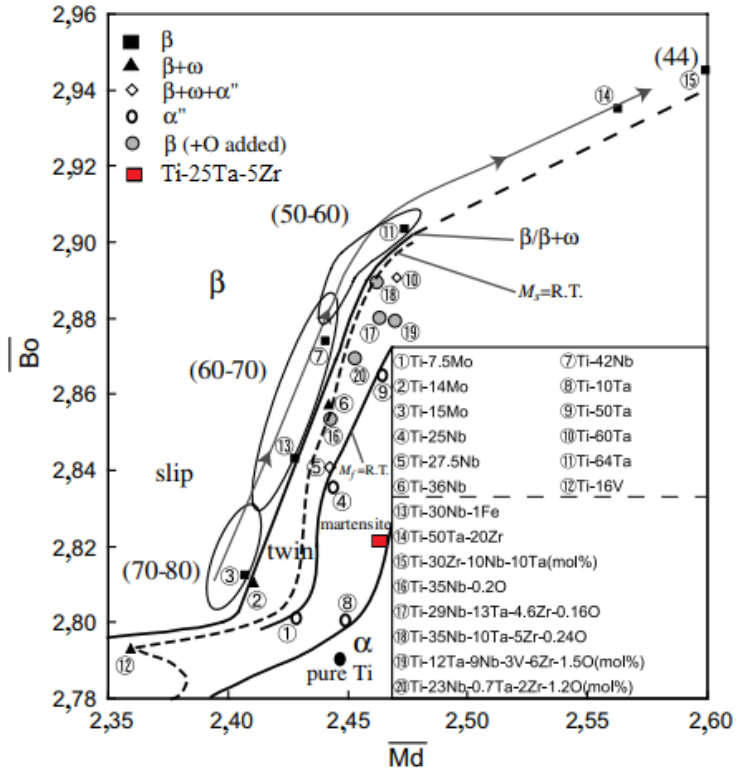


Figura 5.2: Diagrama Bo-Md (adaptado de Abdel-Hady e colaboradores [41].

Segundo Zhou e Niinomi [11] a liga binária Ti-25Ta, possui a estrutura cristalina ortorrômbica (fase α"), quando resfriada rapidamente do campo β até a temperatura ambiente. Neste estudo, foi observado que a fase α" possui uma célula unitária maior que as demais fases do titânio, e como o módulo de elasticidade depende da força de ligação entre os átomos, este resultado indica ligas do tipo α" do sistema Ti-Ta possuem os

menores valores para o módulo de elasticidade do sistema. Logo, a liga Ti-25Ta-5Zr pode possuir um menor módulo de elasticidade que a liga Ti-25Ta, pois a liga proposta possui fração volumétrica de fase β, que reduz mais ainda o módulo da liga [32].

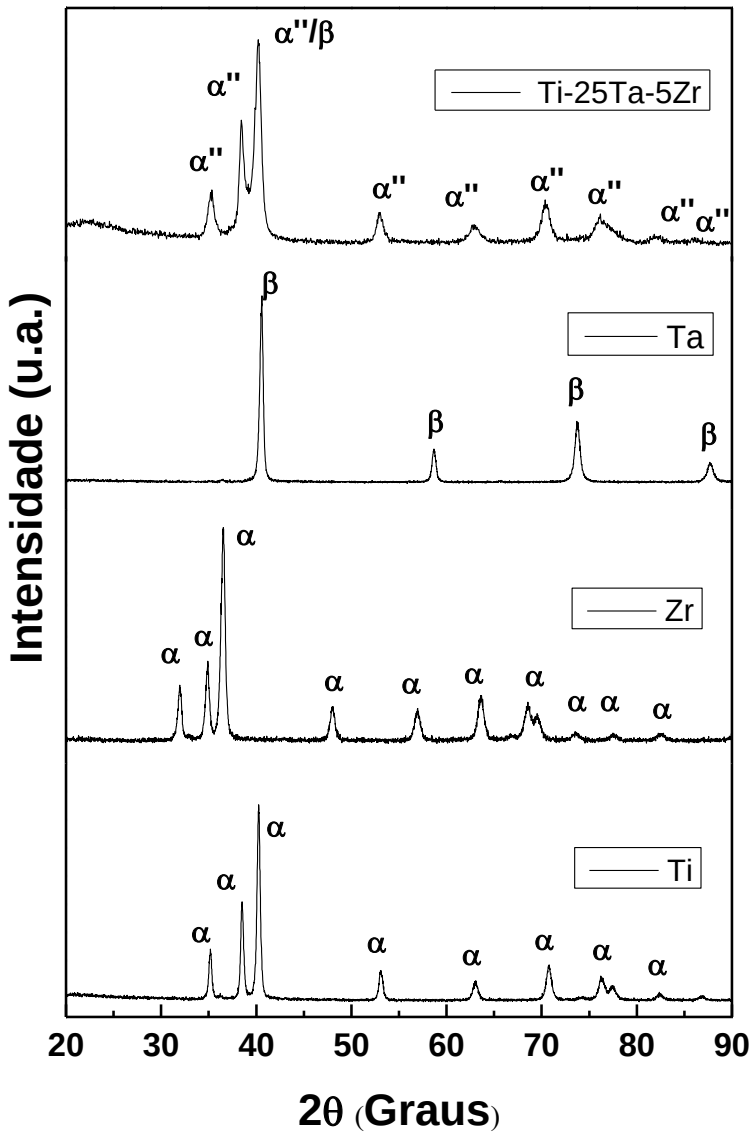
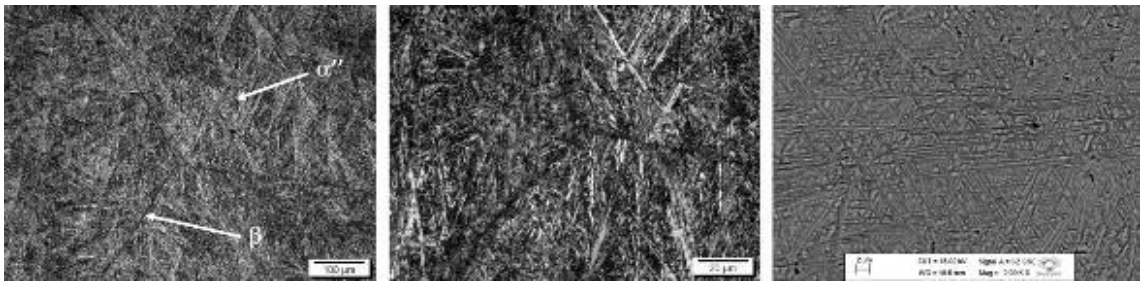


Figura 5.3: Difratogramas de raios X para os elementos constituintes e para a liga Ti-25Ta-5Zr, após a fusão.

A Figura 5.4 apresenta as micrografias ópticas e a eletrônicas de varredura. As micrografias corroboraram os resultados obtidos nos difratogramas de raios X. A liga Ti-25Ta-5Zr apresentou uma microestrutura composta por agulhas que são típicas de estruturas das fases α" e contorno de grãos característicos da fase β [43], conforme esperado a partir dos resultados da difração de raios X. Os resultados das caracterizações estrutural

e microestrutural mostraram que as teorias do molibdênio equivalente e do orbital molecular funcionaram bem no caso da liga Ti-25Ta-5Zr. Ambas as teorias indicaram que a liga deveria possuir a coexistência das fases α" b.



(a) **(b)** **(c)**

Figura 5.4: Micrografias das amostras da liga Ti-25Ta-5Zr após a fusão, obtidas por microscopia óptica (a) e (b) e por microscopia eletrônica de varredura (c).

Com relação aos resultados de dureza da liga Ti-25Ta-5Zr, obteve-se o valor de (264 ± 11) HV, significativamente maior que o titânio puro (167 HV) e menor que a liga Ti-25Ta (300 ± 2) HV. A liga produzida possui dureza maior que o Ti-cp devido a um processo de endurecimento por solução solida causada pela adição de tântalo e zircônio que possuem massa atômica superiores a do titânio [44]. Com o acréscimo de 5 %p de zircônio, houve um aumento de dureza da liga pois ele é bifásica e isso aumenta a barreira para o movimento das discordâncias, acarretando uma maior dureza quando comparado com a liga Ti-25Ta, que é monofásica [45].

A Figura 5.5 mostra uma comparação do módulo de elasticidade de alguns biomateriais metálicos comumente encontrados no mercado, juntamente com a liga Ti-25Ta-5Zr, desenvolvida neste trabalho [8]. A liga produzida neste trabalho possui módulo de elasticidade de aproximadamente 80GPa. Pode ser observado que apenas a liga TNTZ (Ti-35Nb-5Ta-7Zr), o nitinol (55Ni-45Ti equiatômico) e a liga Ti25Ta possuem resultados mais satisfatórios para serem implantados em um osso cortical. As ligas Ti-1313 (Ti-13Nb-13Zr), Ti-15Mo e TMZF (Ti-13Mo-6Zr-2Fe), possuem valores de módulo de elasticidade próximos ao da liga Ti-25Ta-5Zr, dentro da margem experimental. As demais ligas possuem valores de módulo de elasticidade bem maiores. A liga Ti-25Ta-5Zr possui melhores resultados de módulo de elasticidade comparado com o titânio comercialmente puro, pois a liga possui uma fração da fase ortorrômbica

α”, e essa fase tem um fator de empacotamento atômico menor que a fase hexagonal compacta (α) do titânio.

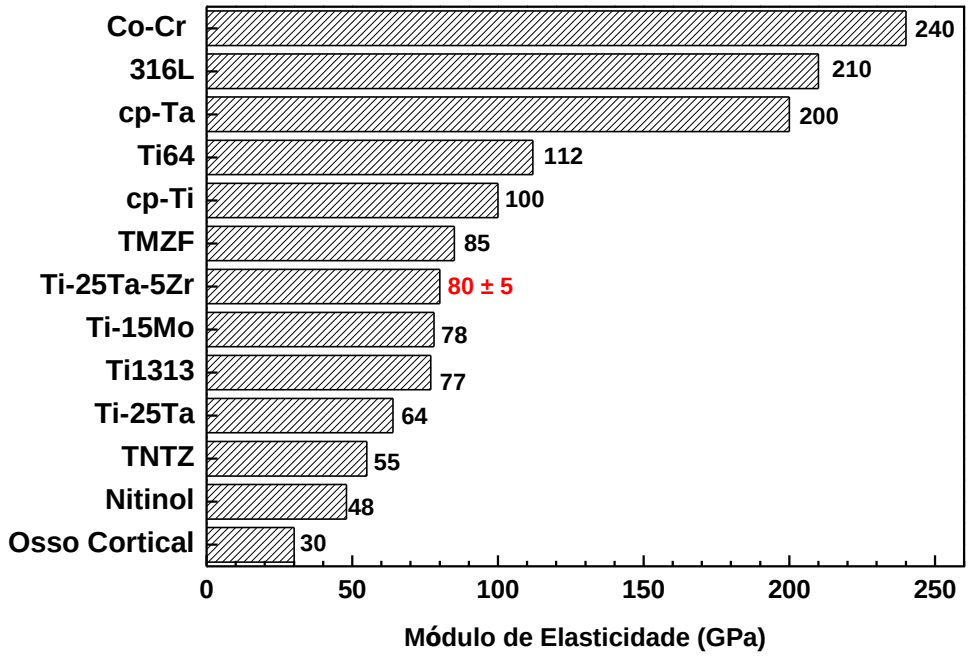


Figura 5.5: Módulo de elasticidade da liga Ti-25Ta-5Zr, comparado com valores de materiais metálicos usados comumente na área biomédica [8].

Conclusões

A liga Ti-25Ta-5Zr foi preparada por fusão à arco e as medidas de composição química, EDS e mapeamento indicam que a liga foi fundida de maneira homogênea, preservando a estequiometria proposta. A análise estrutural mostra uma coexistência de fase β e α”, o que foi corroborado pela análise microsestrutural. Os valores de dureza obtidos estiverem acima do titânio comercialmente puro, causado pelo endurecimento por solução sólida da liga. O módulo de elasticidade da liga é mais baixo comparada com a titânio comercialmente puro, pois a liga possui a coexistência das fases β e da ortorrômbica α”, que tendem a possuir um valor de módulo de elasticidade menor, quando comparado com as ligas do tipo α (Hexagonal compacta). Tais características fazem desta liga uma boa alternativa para aplicações ortopédicas.

Referências

1 LI, Y. et al. New Developments of Ti-Based Alloys for Biomedical Applications. **Materials,** v. 7, n. 3, p. 1709-1800, 2014.
2 IBRAHIM, M. Z. et al. Biomedical materials and techniques to improve the tribological, mechanical and biomedical properties of orthopedic implants – A review article. **Journal of Alloys and Compounds,** v. 714, p. 636-667, 2017.
3 MANAM, N. S. et al. Study of corrosion in biocompatible metals for implants: A review. **Journal of Alloys and Compounds,** v. 701, p. 698-715, 2017.
4 MARKHOFF, J. et al. Biocompatibility and Inflammatory Potential of Titanium Alloys Cultivated with Human Osteoblasts, Fibroblasts and Macrophages. **Materials,** v. 10, n. 1, p. 52, 2017.
5 KOLLI, R.; DEVARAJ, A. A Review of Metastable Beta Titanium Alloys. **Metals,** v. 8, n. 7, p. 506, 2018.
6 NIINOMI, M.; NAKAI, M. Titanium-Based Biomaterials for Preventing Stress Shielding between Implant Devices and Bone. **International Journal of Biomaterials,** v. 2011, p. 836587, 10 pages, 2011.
7 LEI, Z. et al. Development of advanced materials via entropy engineering. **Scripta Materialia,** v. 165, p. 164-169, 2019. ISSN 1359-6462.
8 KAUR, M.; SINGH, K. Review on titanium and titanium based alloys as biomaterials for orthopaedic applications. **Materials Science and Engineering: C**, v. 102, p. 844-862, 2019.
9 CORDEIRO, J. M. et al. Development of binary and ternary titanium alloys for dental implants. **Dental Materials,** v. 33, n. 11, p. 1244-1257, 2017.
10 ZHOU, Y.-L. et al. Comparison of Various Properties between Titanium-Tantalum Alloy and Pure Titanium for Biomedical Applications. **Materials Transactions,** v. 48, n. 3, p. 380-384, 2007.
11 ZHOU, Y.-L.; NIINOMI, M. Ti–25Ta alloy with the best mechanical compatibility in Ti–Ta alloys for biomedical applications. **Materials Science and Engineering: C,** v. 29, n. 3, p. 1061-1065, 2009.
12 CORDEIRO, J. M. et al. Characterization of chemically treated Ti-Zr system alloys for dental implant application. **Materials Science and Engineering: C,** v. 92, p. 849-861, 2018.
13 CORREA, D. R. N. et al. The effect of the solute on the structure, selected mechanical properties, and biocompatibility of Ti-Zr system alloys for dental applications. **Materials Science & Engineering C-Materials For Biological Applications,** v. 34, p. 354-359, 2014.
14 VICENTE, F. B. et al. The Influence of Small Quantities of Oxygen in the Structure, Microstructure, Hardness, Elasticity Modulus and Cytocompatibility of Ti-Zr Alloys for Dental Applications. **Materials,** v. 7, n. 1, p. 542-553, 2014.
15 LIU, X. et al. Binary titanium alloys as dental implant materials—a review. **Regenerative Biomaterials,** v. 4, n. 5, p. 315-323, 2017.
16 BANERJEE, D.; WILLIAMS, J. C. Perspectives on Titanium Science and Technology. **Acta Materialia,** v. 61, n. 3, p. 844-879, 2013.
17 CORREA, D. R. N. et al. Adjustment of the microstructure and selected mechanical properties of biomedical Ti-15Zr-Mo alloys through oxygen doping. **Journal of Alloys and Compounds,** v. 775, p. 158-167, 2019.

18 CORREA, D. R. N. et al. Microstructure and selected mechanical properties of aged Ti-15Zr-based alloys for biomedical applications. **Materials Science and Engineering: C,** v. 91, p. 762-771, 2018.
19 CORREA, D. R. N. et al. Effect of the substitutional elements on the microstructure of the Ti-15Mo-Zr and Ti-15Zr-Mo systems alloys. **Journal of Materials Research and Technology,** v. 4, n. 2, p. 180-185, 2015.
20 CORREA, D. R. N. et al. Effect of Heat Treatment in the Structure and Microstructure of Ti-15Zr-XMo Alloys. **Defect and Diffusion Forum,** v. 365, p. 305-310, 2015.
21 CORREA, D. R. N.; KURODA, P. A. B.; GRANDINI, C. R. Structure, Microstructure, and Selected Mechanical Properties of Ti-Zr-Mo Alloys for Biomedical Applications. **Advanced Materials Research,** v. 922, p. 75-80, 2014.
22 HO, W.-F. et al. Evaluation of low-fusing porcelain bonded to dental cast Ti–Zr alloys. **Journal of Alloys and Compounds,** v. 471, n. 1–2, p. 185-189, 2009.
23 KURODA, P. A. B.; BUZALAF, M. A. R.; GRANDINI, C. R. Effect of molybdenum on structure, microstructure and mechanical properties of biomedical Ti-20Zr-Mo alloys. **Materials Science and Engineering: C,** v. 67, p. 511-515, 2016.
24 KURODA, P. A. B.; BUZALAF, M. A. R.; GRANDINI, C. R. Preparation, microstructural characterization, and selected mechanical properties of Ti-20Zr-2.5Mo and Ti-20Zr-7.5Mo used as biomaterial. **Materials Science Forum,** v. 869, p. 946-951, 2016.
25 KURODA, P. A. B. et al. Thermomechanical treatments influence on the phase composition, microstructure, and selected mechanical properties of Ti–20Zr–Mo alloys system for biomedical applications. **Journal of Alloys and Compounds**, p. 152108, 2019.
26 QUADROS, F. D. F. et al. Preparation, structural and microstructural characterization of Ti-25Ta-10Zr alloy for biomedical applications. **Journal of Materials Research and Technology**, v. 8, p. 4108-4114, 2019.
27 LUZ, A. R. et al. Characterization of the morphology, structure and wettability of phase dependent lamellar and nanotube oxides on anodized Ti-10Nb alloy. **Applied Surface Science,** v. 448, p. 30-40, 2018.
28 CORREA, D. R. N. et al. Development of Ti-15Zr-Mo alloys for applying as implantable biomedical devices. **Journal of Alloys and Compounds,** v. 749, p. 163-171, 2018.
29 ASTM. **E2371 – 04 - Standard Test Method for Analysis of Titanium and Titanium Alloys by Atomic Emission Plasma Spectrometry**. E2371 – 04 - Standard Test Method for Analysis of Titanium and Titanium Alloys by Atomic Emission Plasma Spectrometry. West Conshohocken: ASTM International. E2371 – 04 2004.
30 _____. **E1409 – 08 - Standard Test Method for Determination of Oxygen and Nitrogen in Titanium and Titanium Alloys by the Inert Gas Fusion Technique**. E1409 – 08 - Standard Test Method for Determination of Oxygen and Nitrogen in Titanium and Titanium Alloys by the Inert Gas Fusion Technique. West Conshohocken: ASTM International. ASTM E1409 – 08 2008.
31 _____. **E407-07 - Standard Practice for Microetching Metals and Alloys**. E407-07 - Stanard Practice for Microetching Metals and Alloys
West Conshohocken: ASTM International. ASTM E-407-07 2007.
32 COLLINGS, E. W. **The Physical Metallurgy of Titanium Alloys**. Ohio: ASM International, 1989.

33 WANG, W.; POH, C. K. Titanium Alloys in Orthopaedics. In: (Ed.). **Titanium Alloys - Advances in Properties Control**. Rijeka: InTech, 2013. cap. 1, p.1-20.
34 ASTM. **E92-82 - Standard Test Method for Vickers Hardness of Metallic Materials**. E92-82 - Standard Test Method for Vickers Hardness of Metallic Materials. West Conshohocken, PA: ASTM International. E92-82 2003.
35 _____. **E1876–01 - Standard Test Method for Dynamic Young's Modulus, Shear Modulus, and Poisson's Ratio by Impulse Excitation of Vibration**. E1876–01 - Standard Test Method for Dynamic Young's Modulus, Shear Modulus, and Poisson's Ratio by Impulse Excitation of Vibration. Philadelphia (USA): ASTM International. E1876–01 2002.
36 _____. **F2066-08 - Standard specification for wrought titanium-15 molybdenum alloy for surgical implant application**. F2066-08 - Standard specification for wrought titanium-15 molybdenum alloy for surgical implant application. Philadelphia (USA): ASTM International. F 2066-08 2008.
37 LÜTJERING, G.; WILLIAMS, J. C. **Titanium**. Springer, 2003.
38 HO, W. F.; JU, C. P.; CHERN LIN, J. H. Structure and properties of cast binary Ti-Mo alloys. **Biomaterials,** v. 20, n. 22, p. 2115-2122, 1999.
39 MORINAGA, M.; YUKAWA, H. Alloy design with the aid of molecular orbital method. **Bulletin of Materials Science,** v. 20, n. 6, p. 805-815, 1997.
40 MORINAGA, M.; MURATA, Y.; YUKAWA, H. Molecular orbital approach to alloy design. In: BOZZOLO, G.;NOEBE, R. D., *et al* (Ed.). **Applied Computational Materials Modeling: Theory, Simulation and Experiment**. Boston, MA: Springer US, 2007. p.255-306.
41 ABDEL-HADY, M.; HINOSHITA, K.; MORINAGA, M. General approach to phase stability and elastic properties of β-type Ti-alloys using electronic parameters. **Scripta Materialia,** v. 55, n. 5, p. 477-480, 2006.
42 KURODA, D. et al. Design and mechanical properties of new β type titanium alloys for implant materials. **Materials Science and Engineering: A,** v. 243, n. 1–2, p. 244-249, 1998.
43 LEYENS, C.; PETERS, M. **Titanium and Titanium Alloys: Fundamentals and Applications**. New York: Wiley-VCH, 2005.
44 BOYER, R.; WELSCH, G.; COLLINGS, E. W. **Materials Properties Handbook: Titanium Alloys**. Materials Park: ASM International, 1994.
45 MANDA, P.; CHAKKINGAL, U.; SINGH, A. K. Hardness characteristic and shear band formation in metastable β-titanium alloys. **Materials Characterization,** v. 96, n. 0, p. 151-157, 2014.

Capítulo 6

Published in Journal of Materials Research and Technology, 8 (5): 4108-4114. 2019. Doi: 10.1016/j.jmrt.2019.07.020.

Preparation, Structural and Microstructural Characterization of Ti-25Ta-10Zr Alloy for Biomedical Applications

Fernanda de Freitas Quadros[1,2]; **Pedro Akira Bazaglia Kuroda**[1,2]; Karolyne dos Santos Jorge Sousa[1,2], Tatiani Ayako Goto Donato[1,2]; Carlos Roberto Grandini[1,2]

[1] UNESP - Univ Estadual Paulista, Laboratório de Anelasticidade e Biomateriais, 17.033-360, Bauru, SP, Brazil

[2] IBTN-Br – Institute of Biomaterials, Tribocorrosion and Nanomedicine – Brazilian Branch, 17.033-360, Bauru, SP, Brazil

Abstract:

Titanium alloys are widely used in the biomedical field due to their good corrosion resistance, high mechanical strength/density ratio, low elastic modulus, and good biocompatibility. With the addition of β-stabilizers elements (such as tantalum), the decrease of the elastic modulus and excellent corrosion resistance are obtained. Zirconium despite being a neutral element appends a good corrosion resistance to titanium alloys. In this paper, Ti-25Ta-10Zr alloy was prepared and characterized aiming biomedical applications. Structural and microstructural analysis corroborated each other and showed the presence of characteristic peaks of three crystalline structures, hexagonal (α phase) and orthorhombic (α'' phase), dissolved in a matrix with body-centered cubic crystalline structure (β phase). In the indirect cytotoxicity test, no cytotoxic effects were observed on the produced alloy.

1. Introduction

Titanium uses in medicine started after the mid-20th century when titanium alloys began

to replace stainless steel and Co-Cr alloys in biomedical applications [1; 2]. Below 882° C, titanium has a hexagonal compact (hcp) crystalline structure, also known as α phase and, above such temperature has body-centered cubic (bcc) crystalline structure, also known as β phase [3]. The α phase is characterized by having a good mechanical resistance and β phase by presenting low elastic modulus and high resistance to corrosion and wear [4].

The first titanium alloys produced were characterized as being of α-type, developed for the aerospace industry [5]. Then α + β type alloys have gained prominence due to its properties [6] and, it can be cited as an example, the Ti-6Al-4V alloy widely used as biomaterial [7], however, research reports that aluminum and vanadium ions when present in the bloodstream can cause toxic reactions and neurological problems to the patient as the Alzheimer's disease [8].

Tantalum is a β-stabilizer element and has a high elastic modulus, high mechanical strength and high hardness due to its extremely strong chemical bonds, resulting in a high melting temperature [9]. Mainly due to good corrosion resistance and its biocompatibility, tantalum can be used in the biomedical field [10], but its production cost is very high [11].
Zirconium belongs to the same family of titanium on the Periodic Table and can assist in corrosion resistance, mechanical strength, biocompatibility [12]. Although zirconium is considered a neutral element in binary Ti-alloys, however, in the presence of another beta stabilizer element (as tantalum, for example), it improves the retention of this phase and decreases the temperature of the α' martensitic transformation [13; 14; 15; 16; 17]. The allotropic transformation of zirconium occurs at 862° C [18]. Below this temperature, its crystalline structure is hexagonal compact (α phase) and above such temperature, the crystalline structure is body-centered cubic (β phase).

Currently, β-type titanium alloys have been produced, by presenting good biocompatibility, good mechanical strength/density ratio, and high corrosion resistance, besides low elastic modulus [19]. Such alloys have been produced mainly with the addition of molybdenum, zirconium, tantalum, and niobium, which are elements that do not exhibit cytotoxic effects in the human body [20; 21; 22; 23].

The alloys developed with these elements have advantageous properties to be used in the orthopedic area, such as the Ti-20Nb-20Ta-20Zr-20Mo and Ti-29Nb-13Ta-4.6Zr alloys. The high entropy Ti-20Nb-20Ta-20Zr-20Mo alloy, which constitutes a new class of structural materials, presents high biocompatibility when compared to commercially pure titanium, in addition to the hardness and yield stresses superior to the Ti-6Al-4V alloy [24]. Likewise, the Ti-29Nb-13Ta-4.6Zr alloy also has excellent properties, but its

mechanical durability is unsatisfactory to be used as a biomedical implant. To reverse this result, the fatigue of the material is improved by the modification of the surface through the formation of a nanostructured gradient under the sample [25].

The objective of this paper is to presents the preparation and the structural and microstructural characterization of the Ti-25Ta-10Zr alloy, as well as verify the feasibility of this sample in the biomedical area.

2. Materials and Methods

After the separation of the precursors, commercially pure titanium (99.8% purity, Sandinox); zirconium (99.8% purity Aldrich) and tantalum (99.9% purity, Goodfellow), the melting of alloy Ti-25Ta-10Zr was held in an arc-furnace, with water-cooled copper crucible, non-consumable tungsten electrode and argon controlled atmosphere [13; 14; 26; 27]. To ensure a good homogeneity and eliminate the possibility of containing tantalum aggregated or segregated in the sample, the melting was held by ten times. Then, the sample was subjected to homogenization heat treatment with a heating rate of 10 °C/min up to 1000 °C, in which remained at this temperature for 24 hours and then cooled slowly in the furnace [16; 27]

Chemical characterization was obtained by dissolution in acidic medium, followed by the detection of elements in an inductively coupled plasma optical emission spectrometry (ICP-OES) equipment (Varian, Vista model) and energy dispersive spectroscopy (EDS) technique using a scanning electron microscopy (SEM) equipment (Carls Zeiss, EVO-015 model, with Oxford INCA probe). To confirm the stoichiometry of the material, density measurements were carried out following the Archimedes' Principle. In this method, the samples were weighed in water and in the air, and then the density of the material was obtained [28].

The alloy structure was analyzed by X-ray diffraction measurements, with the diffractograms submitted to the Rietveld's structural refinement. Diffraction patterns were obtained on a Rigaku D/Max-2100 PC model diffractometer, using the powder method, Cu-K_α radiation (λ = 1.544 Å), 20 mA current and potential of 40 kV, the scan rate of 0.02 degrees/min, 10° to 100°, in the fixed time mode. From the GSAS [29]software, with EXPEGUI interface [30] and crystallographic database sheets of the International Centre for Diffraction Data (ICDD), it was made the refinement of the diffractograms, obtaining the lattice parameters and the quantification of the phases. The crystallographic data of the α'' phase have been entered manually based on the results suggested by

Banumathy et al. [31].

The crystalline microstructure was obtained by optical and electronic microscopy. To obtain the images, it was used an Olympus optical microscope, BX51M model and a Carl Zeiss SEM, model EVO-015.

Cells were obtained according to research protocols approved by the Ethical Committee for Animal Research of the University of São Paulo of Bauru, Brazil (Protocol #004/2016). Osteogenic cells were isolated by sequential trypsin/collagenase digestion of calvaria bone from newborn (2-day-old) Wistar rats, as previously described by Donato et al. [32].

The obtained cells were cultured in α-minimum essential medium (α-MEM) (FBS, Cultilab, Campinas, Brazil) containing 10% fetal bovine serum (FBS, Cultilab) and 1% penicillin (Cultilab), plated in 60-mm diameter plastic culture dishes and incubated at a density of 110cells/mm². 24 hours after plating, the cell cultures were supplemented with 50 µg/mL ascorbic acid (Sigma, St. Louis, MO, USA) and 10 mM β-glycerophosphate (Sigma). The cells were incubated under standard cell culture conditions (37ºC, 95% humidity and 5% CO_2) and the medium was changed every 2-3 days [33; 34; 35].

A standard colorimetric assay – 3-(4,5-dimethyl-2-thiazolyl)-2,5-diphenyl-2H-tetrazolium bromide (MTT assay, Sigma) was used to estimate cell viability and proliferation [36; 37]. The evaluation of indirect cell viability of the Ti-25Ta-10Zr alloy was done by MTT assay at 48 hours. For indirect cytotoxicity test, the extracts of the alloy were obtained – 1 g of alloy/10 mL medium at 48 hours –, rat calvaria derived osteogenic cells were grown on the microplates and the culture medium was substituted by the obtained extracts. The tests were made using 96 wells microplates (Corning). The polystyrene from the microplate was used as the negative control (no cytotoxicity), while a solution of α-MEM, 10% of FBS, and 1% of phenol was the positive control (cytotoxicity). After this time, then routinely processed for MTT assay [35]. The optical density (OD) of the wells was determined using a plate reader at a test wavelength of 640 nm in a SpectraMax Plus microplate reader (Molecular Devices).

The osteogenic cells were on the glass coverslip and the culture medium was substituted by the obtained extracts of the alloy. After 48 hours, the cells were fixed and were then routinely processed for SEM [34]. Specimens were mounted onto aluminum substrates, sputtered with gold, and examined in a Carl Zeiss EVO LS-15 model microscopy. The polystyrene was used as the negative control (no cytotoxicity), while a solution of α-MEM, 10% of FBS, and 1% of phenol was the positive control

(cytotoxicity).

3. Results and Discussion

Table 6.1 shows the chemical composition of the alloy using the ICP-OES technique. The values found are near the proposed composition, which shows that the stoichiometry of the alloy was respected [38].

Table 6.1: Chemical composition of Ti-25Ta-10Zr alloy

	Al	Cr	Cu	Fe	Hf	Mn	Mo	Ni	Si	Ta	Zr	Ti
wt%	0.05	0.02	0.64	0.03	0.04	0.01	0.01	0.01	0.08	23.9	11.3	Balance

Figure 6.1 shows an image of the EDS mapping of the elements present in a sample of Ti-25Ta-10Zr alloy, where the red points represent titanium, the green points represent tantalum and the blue points represent zirconium. A homogeneous distribution, without the presence of agglomerates or segregates, can be observed. The experimental value of density, obtained by Archimedes' Principle, was (5.72 ± 0.01) g/cm^3. Comparing with the theoretical value, 5.73 g/cm^3, it can be observed an excellent agreement, reinforcing that the stoichiometry was respected.

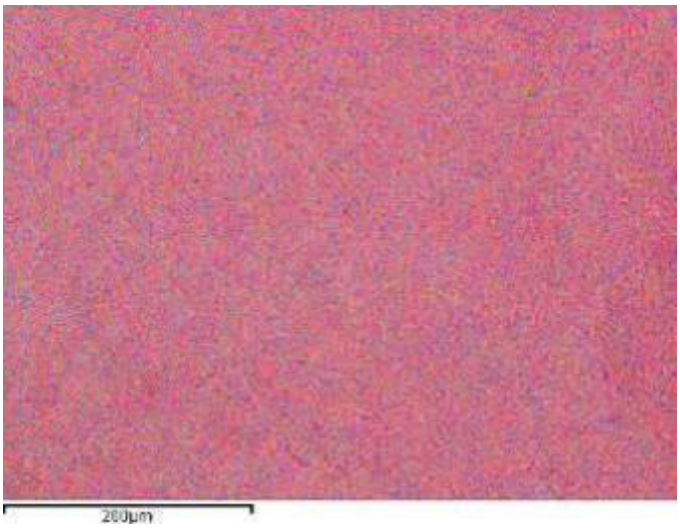


Figure 6.1: EDS mapping for Ti-25Ta-10Zr alloy.

Figure 6.2 shows a comparison of X-ray diffractograms from the alloy after melting and after homogenization heat treatment. It can be observed that the alloy presented the α'/α'' martensitic phases, with a hexagonal and orthorhombic crystalline structure, respectively, plus a few peaks of β phase, with a body-centered cubic crystalline

structure. Tantalum is a strongly β-stabilizer, and its presence makes zirconium no neutral and passes the acts also in the stabilizing of the β phase [39; 40]. The homogenization heat treatment causes changes in intensity and in the width of the peaks, which may be a result of changes in lattice parameters, crystallite size, microstrain and phase percentage [41].

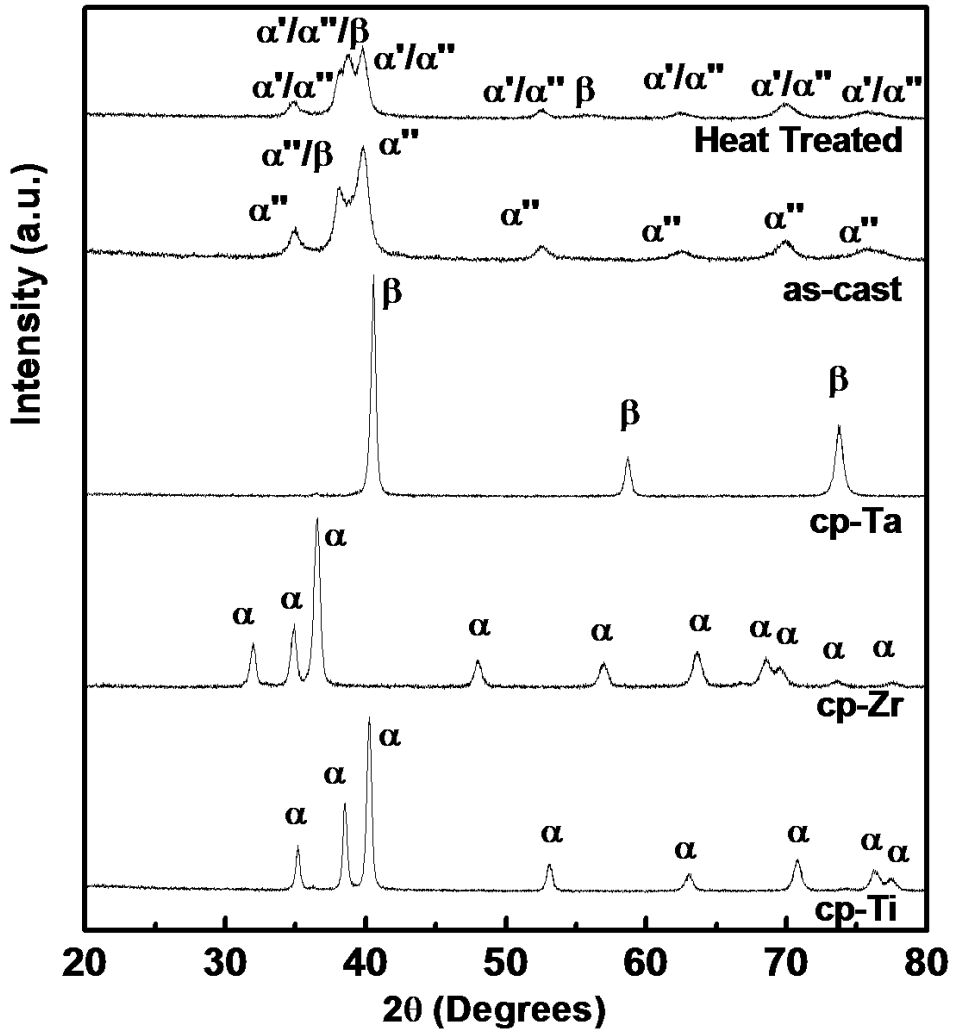


Figure 6.2: X-ray diffraction patterns for Ti-25Ta-10Zr alloy, as cast and after homogenization heat treatment, compared with cp-Ti, cp-Ta, and cp-Zr.

Figure 6.3 shows the x-ray diffractograms, analyzed by Rietveld's method, for each of the studied conditions. The black line indicates the experimental data of the diffractogram; the red line indicates the intensity calculated by refinement; the green line shows the background, and the blue line shows the residue, which is the difference

between the experimental and calculated intensity. The graph shows a good agreement between experimental and calculated intensities, which indicates a good refinement of the data. The merit parameters of the refinement are chi-squared (χ^2) equal to 1.090 for the as-cast condition and 1.107 for sample after homogenization heat treatment; R-factor (RF^2) is equal to 7.67% and 11.02%, respectively, for the same conditions mentioned above. The results show low χ^2 values, which indicates a good refinement of the data. The χ^2 must be equal to 1 for a perfect refinement, but values below 5 already reflect an optimized refinement. For RF^2, the accepted values are around 10% [42; 43].

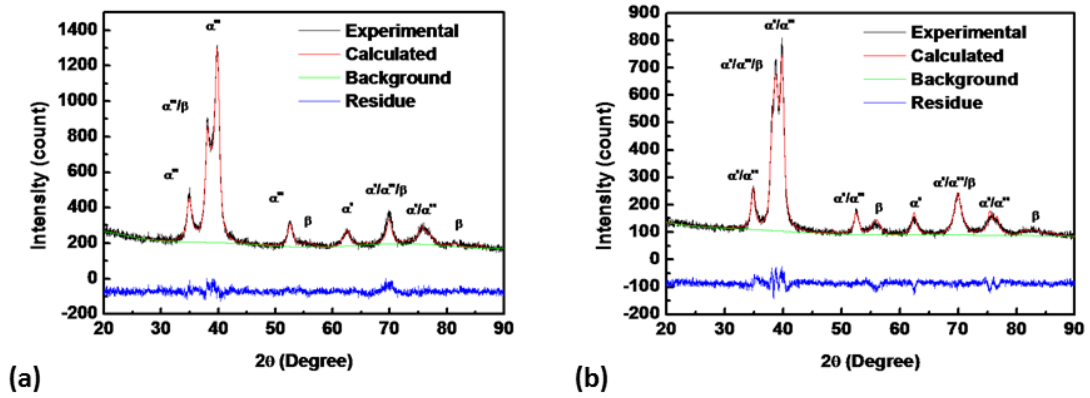


Figure 6.3: X-ray diffractograms of Ti-25Ta-10Zr alloys analyzed by Rietveld's Method in the (a) as-cast and (b) after homogenization heat treatment conditions.

In Table 6.2 are presented the phases quantities and the lattice parameters, for Ti-25Ta-10Zr alloys, obtained by Rietveld's Method, after each processing condition. The lattice parameters (a, b and c) of α' phase are dilated compared to titanium due to the addition of tantalum and zirconium, due to these elements have larger atomic radius than titanium, and zirconium has the same hexagonal structure [9]. Homogenization heat treatment promoted the transformation of α'' phase for the α phase; the treatment was carried out at a temperature above the titanium β-transus and cooled slowly giving the necessary conditions for the metastable phase α'' turn to less energy phase α [44]. With respect to lattice parameters of α' phase, the homogenization heat treatment promoted an increase in the unit cell due to thermal expansion [45; 46].

Figure 6.4 shows the optical and the scanning electronic micrographs, both for as-cast and after homogenization heat treatment conditions, for the Ti-25Ta-10Zr alloy. Such results corroborate x-ray diffractograms results. The alloy presented a structure composed of needles that are typical of structures of phases α' (thicker needles), α'' (finer needles)

and grain boundary characteristic of β-type alloys [2]. Homogenization heat treatment promoted the growth of acicular structures and of the grains.

Table 6.2: Phases percentage and lattice parameters, for the samples of Ti-25Ta-10Zr alloy, obtained by Rietveld's Method, after each processing condition

	Phase (%)			**Lattice parameter (Å)**		
	α'	**α''**	**β**	**a**	**b**	**c**
As cast	4	-	-	2.883 (4)	2.883 (4)	4.733 (1)
	-	64	-	2.996 (1)	5.126 (2)	4.738 (1)
	-	-	32	3.309 (1)	3.309 (1)	3.309 (1)
Heat Treated	65	-	-	2.976 (1)	2.976 (1)	4.729 (1)
	-	0	-	-	-	-
	-	-	35	3.303 (1)	3.303 (1)	3.303 (1)
cp – Ti [28]	-	-	-	2.951	2.951	4.684

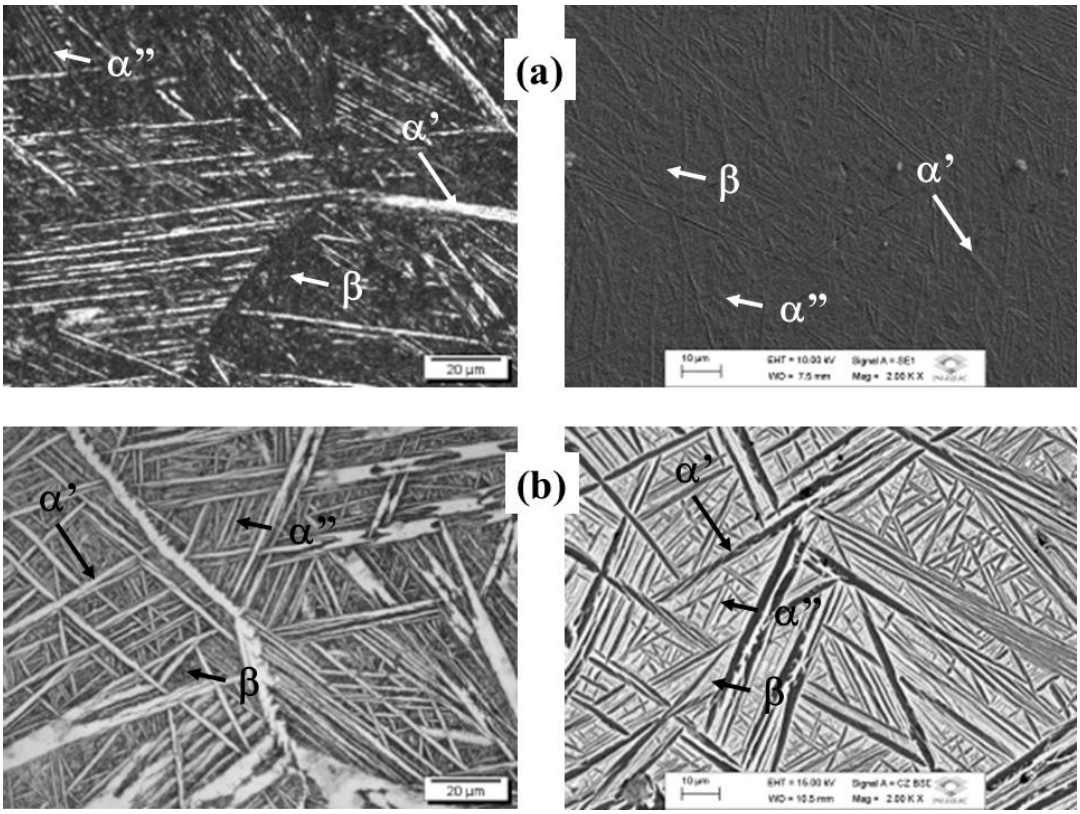


Figure 6.4: Optical (left) and SEM (right) micrographs of Ti-25Ta-10Zr alloy in the (a) as cast and (b) after homogenization heat treatment conditions.

Figure 6.5 shows the hardness values of the alloy and makes a comparison with

cp-Ti and Ti-6Al-4V alloy [47]. It was observed that the Ti-25Ta-10Zr alloy presents values of hardness significantly higher than cp-Ti and Ti-6Al-4V alloy. This occurs due to the presence of the α'' phase and solid solution hardening caused by the addition of tantalum and zirconium elements that hinder the dislocations motion and, consequently, the microstructure of the alloy is influenced from the deformation of the crystalline lattice.
It was observed that the alloy presents values of hardness significantly higher than the pure titanium, being a result of the hardening in solid solution caused by the addition of tantalum and zirconium that possess atomic mass superior to the titanium.

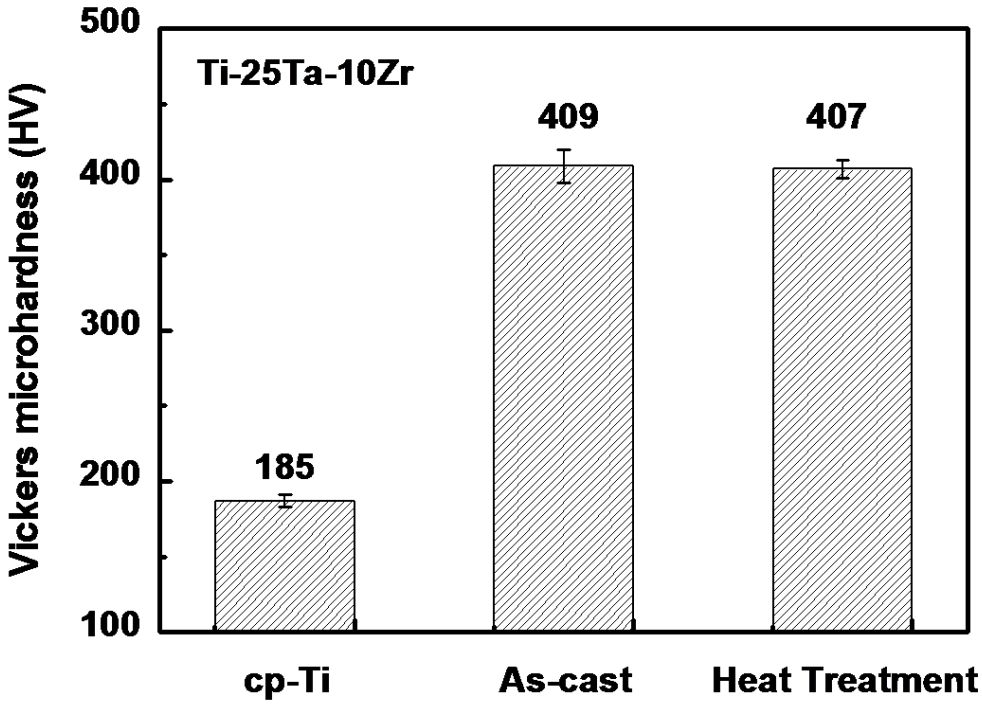


Figure 6.5: Vickers microhardness for Ti-25Ta-10Zr, compared with cp-Ti and Ti-6Al-4V.

The results of the indirect cytotoxicity test are presented in Figure 6.6 and showed that the extracts of Ti-25Ta-10Zr no inhibit the proliferation of osteogenic cells and the number of viable cells was similar to the negative control (no cytotoxicity) and higher to the positive control (cytotoxicity).

The date observed by SEM (Figure 6.7) corroborate the indirect MTT test. The cell morphology was preserved even after being in contact with the extract of Ti-25Ta-10Zr, showing the same of the negative control (no cytotoxicity), contrasting with the

positive control (cytotoxicity – phenol solution) cell morphology. The extract of alloy did not interfere in the cellular adhesion, that was being well adhered and numerous and, long cellular processes on the glass, as well as cell mitosis process. These characteristics were not seen in positive control [34; 36]. This information suggests that Ti-25Ta-10Zr alloy may be interesting material to an application as biomaterials.

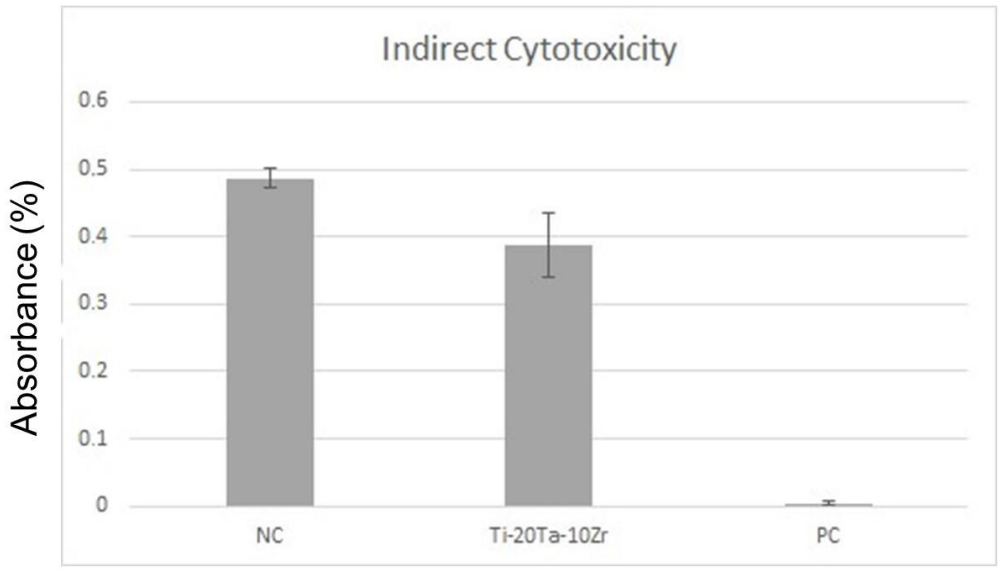


Figure 6.6: Indirect cytotoxicity test in primary culture of osteogenic cells cultured for 48 hours on Ti-25Ta-10Zr alloy.

4. Conclusions

As the obtained results of chemical composition, density measurements, EDS and mapping indicated, the Ti-25Ta-10Zr alloy was melted in a homogeneous way, preserving the proposed stoichiometry.

Structural analysis showed a coexistence of α' phase (hexagonal compact), α'' (orthorhombic) and β (body-centered cubic). By means of the Rietveld's method, it was possible to quantify the fraction of these phases in the alloy and observed the variations in the lattice parameters caused by the addition of zirconium and tantalum.

In the microstructural analysis, the presence of intra-grain needles was observed, characteristic of martensític phases α' and α'', in agreement with the x-ray diffractogram.

The hardness values were above the commercially pure titanium and Ti-6Al-4V alloy, whereby the continuous solution hardening of the alloy.

In Ti-25Ta-10Zr alloy were not present any indirect cytotoxic for primary culture of osteogenic cells. To the contrary, the alloy presented perfectly cellular division,

maintaining the morphology, indicating good integration between materials – cells, characteristics desirable to a biomaterial.

The present study showed that Ti-25Ta-10Zr alloy becomes attractive material for use as a biomaterial.

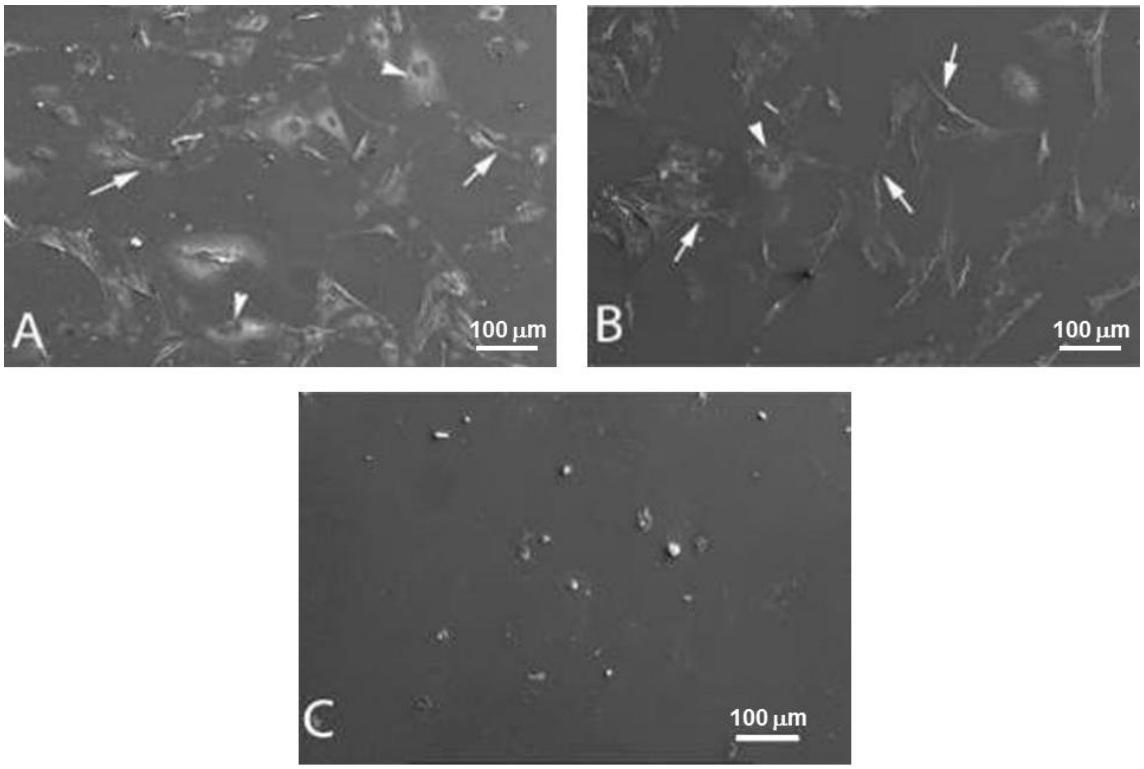


Figure 6.7: SEM in primary culture of osteogenic cells cultured for 48 hours with extract of Ti-25Ta-10Zr alloy. A) Negative Control (NC) – glass; B) Extract of Ti-25Ta-10Zr; C) Positive Control (PC) – 1% phenol solution. Arrowhead: cells in mitosis process and cytoplasmatic processes.

References

1 LONG, M.; RACK, H. J. Titanium alloys in total joint replacement--a materials science perspective. **Biomaterials,** v. 19, n. 18, p. 1621-1639, 1998.

2 LEYENS, C.; PETERS, M. **Titanium and Titanium Alloys: Fundamentals and Applications**. New York: Wiley-VCH, 2005.

3 COLLINGS, E. W. **The Physical Metallurgy of Titanium Alloys**. Ohio: ASM International, 1989.

4 RACK, H. J.; QAZI, J. I. Titanium alloys for biomedical applications. **Materials Science and Engineering: C,** v. 26, n. 8, p. 1269-1277, 2006.

5 BOYER, R. R. An overview on the use of titanium in the aerospace industry. **Materials Science and Engineering: A,** v. 213, n. 1–2, p. 103-114, 1996.

6 GEETHA, M. et al. Ti based biomaterials, the ultimate choice for orthopaedic implants - A review. **Progress in Materials Science,** v. 54, n. 3, p. 397-425, 2009.

7 FREESE, H. L. et al. Titanium and its Alloys in Biomedical Engineering. In: EDITORS-IN-CHIEF: , K. H. J. B.;ROBERT, W. C., *et al* (Ed.). **Encyclopedia of Materials: Science and Technology (Second Edition)**. Oxford: Elsevier, 2001. p.9374-9380.
8 BRUNETTE, D. M. et al. **Titanium in Medicine: Material Science, Surface Science, Engineering, Biological Responses and Medical Applications**. Berlim: Springer-Verlag, 2001.
9 EISENBARTH, E. et al. Biocompatibility of β-stabilizing elements of titanium alloys. **Biomaterials,** v. 25, n. 26, p. 5705-5713, 2004.
10 LEVINE, B. R. et al. Experimental and clinical performance of porous tantalum in orthopedic surgery. **Biomaterials,** v. 27, n. 27, p. 4671-4681, 2006.
11 ZHOU, Y.-L. et al. Comparison of Various Properties between Titanium-Tantalum Alloy and Pure Titanium for Biomedical Applications. **Materials Transactions,** v. 48, n. 3, p. 380-384, 2007.
12 GRANDIN, H. M.; BERNER, S.; DARD, M. A Review of Titanium Zirconium (TiZr) Alloys for Use in Endosseous Dental Implants. **Materials,** v. 5, n. 8, p. 1348, 2012.
13 CORREA, D. R. N. et al. Adjustment of the microstructure and selected mechanical properties of biomedical Ti-15Zr-Mo alloys through oxygen doping. **Journal of Alloys and Compounds,** v. 775, p. 158-167, 2019.
14 CORREA, D. R. N. et al. Microstructure and selected mechanical properties of aged Ti-15Zr-based alloys for biomedical applications. **Materials Science and Engineering: C,** v. 91, p. 762-771, 2018.
15 CORREA, D. R. N. et al. Effect of the substitutional elements on the microstructure of the Ti-15Mo-Zr and Ti-15Zr-Mo systems alloys. **Journal of Materials Research and Technology,** v. 4, n. 2, p. 180-185, 2015.
16 CORREA, D. R. N. et al. Effect of Heat Treatment in the Structure and Microstructure of Ti-15Zr-XMo Alloys. **Defect and Diffusion Forum,** v. 365, p. 305-310, 2015.
17 CORREA, D. R. N.; KURODA, P. A. B.; GRANDINI, C. R. Structure, Microstructure, and Selected Mechanical Properties of Ti-Zr-Mo Alloys for Biomedical Applications. **Advanced Materials Research,** v. 922, p. 75-80, 2014.
18 ZHOU, F. Y. et al. Microstructure, mechanical property, corrosion behavior, and in vitro biocompatibility of Zr–Mo alloys. **Journal of Biomedical Materials Research Part B: Applied Biomaterials,** v. 101B, n. 2, p. 237-246, 2013.
19 KAUR, M.; SINGH, K. Review on titanium and titanium based alloys as biomaterials for orthopaedic applications. **Materials Science and Engineering: C**, v. 102, p. 844-862. 2019.
20 LI, Y. et al. New Developments of Ti-Based Alloys for Biomedical Applications. **Materials,** v. 7, n. 3, p. 1709-1800, 2014.
21 LEI, Z. et al. Development of advanced materials via entropy engineering. **Scripta Materialia,** v. 165, p. 164-169, 2019.
22 CHEN, J. et al. A review on fundamental of high entropy alloys with promising high–temperature properties. **Journal of Alloys and Compounds,** v. 760, p. 15-30, 2018.
23 KOLLI, R.; DEVARAJ, A. A Review of Metastable Beta Titanium Alloys. **Metals,** v. 8, n. 7, p. 506, 2018.
24 NAGASE, T. et al. Microstructure of equiatomic and non-equiatomic Ti-Nb-Ta-Zr-Mo high-entropy alloys for metallic biomaterials. **Journal of Alloys and Compounds,** v. 753, p. 412-421, 2018.

25 KHERADMANDFARD, M. et al. Simultaneous grain refinement and nanoscale spinodal decomposition of β phase in Ti-Nb-Ta-Zr alloy induced by ultrasonic mechanical impacts. **Journal of Alloys and Compounds,** v. 738, p. 540-549, 2018.
26 MARTINS JR, J. R. S. et al. Preparation and characterization of alloys of the Ti–15Mo–Nb system for biomedical applications. **Journal of Biomedical Materials Research Part B: Applied Biomaterials,** v. 106, n. 2, p. 639-648, 2018..
27 XAVIER, C. C. et al. Low temperature heat treatments on Ti-15Zr-xMo alloys. **Journal of Alloys and Compounds,** v. 727, n. Supplement C, p. 246-253, 2017.
28 LIDE, D. **CRC handbook of chemistry and physics: a ready-reference book of chemical and physical data**. 85th. Boca Raton, USA: CRC Press, 2004.
29 LARSON, A. C.; DREELE, R. B. V. **GSAS - General Structure Analysis System**. p.223. 2000. (LANSCE, MS-H805)
30 TOBY, B. EXPGUI, a graphical user interface for GSAS. **Journal of Applied Crystallography,** v. 34, n. 2, p. 210-213, 2001.
31 BANUMATHY, S.; MANDAL, R. K.; SINGH, A. K. Structure of orthorhombic martensitic phase in binary Ti-Nb alloys. **Journal of Applied Physics,** v. 106, n. 9, p. 093518-6, 2009.
32 DONATO, T. A. G.; MARTINEZ, E. F.; ARANA-CHAVEZ, V. E. Effects of TGF-β1 on mineralization mediated by rat calvaria-derived osteogenic cells. **Microscopy Research and Technique,** v. 79, n. 12, p. 1139-1146, 2016.
33 ISO. **10993-5 - Biological evaluation of medical devices - Part 5: Tests for in vitro cytotoxicity**. 10993-5 - Biological evaluation of medical devices - Part 5: Tests for in vitro cytotoxicity. Geneva: International Organization for Standardization 2009.
34 DONATO, T. et al. In Vitro Cytotoxicity of a Ti-35Nb-7Zr-5Ta Alloy Doped with Different Oxygen Contents. **Materials,** v. 7, n. 3, p. 2183-2193, 2014.
35 DONATO, T. A. G. et al. Cytotoxicity study of some Ti alloys used as biomaterial. **Materials Science & Engineering C-Biomimetic and Supramolecular Systems,** v. 29, n. 4, p. 1365-1369, 2009.
36 PARK, Y.-J. et al. Cytocompatibility of pure metals and experimental binary titanium alloys for implant materials. **Journal of Dentistry,** v. 41, n. 12, p. 1251-1258, 2013.
37 VELASCO-ORTEGA, E. et al. In vitro evaluation of cytotoxicity and genotoxicity of a commercial titanium alloy for dental implantology. **Mutation Research/Genetic Toxicology and Environmental Mutagenesis,** v. 702, n. 1, p. 17-23, 2010.
38 ASTM. **F2066-08 - Standard specification for wrought titanium-15 molybdenum alloy for surgical implant application**. F2066-08 - Standard specification for wrought titanium-15 molybdenum alloy for surgical implant application. Philadelphia (USA): ASTM International. F 2066-08 2008.
39 KURODA, P. A. B.; BUZALAF, M. A. R.; GRANDINI, C. R. Effect of molybdenum on structure, microstructure and mechanical properties of biomedical Ti-20Zr-Mo alloys. **Materials Science and Engineering: C,** v. 67, p. 511-515, 2016.
40 NAG, S.; BANERJEE, R.; FRASER, H. L. Microstructural evolution and strengthening mechanisms in Ti-Nb-Zr-Ta, Ti-Mo-Zr-Fe and Ti-15Mo biocompatible alloys. **Materials Science and Engineering: C,** v. 25, n. 3, p. 357-362, 2005.
41 SEVERINO MARTINS, J. R., JR.; GRANDINI, C. R. Structural characterization of Ti-15Mo alloy used as biomaterial by Rietveld method. **Journal of Applied Physics,** v. 111, n. 8, 083535-8, 2012.

42 RIETVELD, H. M. A profile refinement method for nuclear and magnetic structures. **Journal of Applied Crystallography,** v. 2, p. 65-71, 1969.
43 TOBY, B. H. R factors in Rietveld analysis: How good is good enough? **Powder Diffraction,** v. 21, n. 1, p. 67-70, 2012.
44 FROES, F. H. Titanium Alloys: Thermal Treatment and Thermomechanical Processing. In: EDITORS-IN-CHIEF: , K. H. J. B.;ROBERT, W. C., *et al* (Ed.). **Encyclopedia of Materials: Science and Technology (Second Edition)**. Oxford: Elsevier, 2001. p.9369-9373.
45 BANERJEE, D.; WILLIAMS, J. C. Perspectives on Titanium Science and Technology. **Acta Materialia,** v. 61, n. 3, p. 844-879, 2013.
46 BANERJEE, S.; VIJAYAKAR, S. J.; KRISHNAN, R. Strength of zirconium-titanium martensites and deformation behaviour. **Acta Metallurgica,** v. 26, n. 12, p. 1815-1831, 1978.
47 HO, W. F.; JU, C. P.; CHERN LIN, J. H. Structure and properties of cast binary Ti-Mo alloys. **Biomaterials,** v. 20, n. 22, p. 2115-2122, 1999.

Capítulo 7

Submetido para publicação na Revista Matéria, 2019.

Desenvolvimento da liga Ti-25Ta-50Zr para aplicações biomédicas

Development of the Ti25Ta-50Zr alloys for biomedical applications

Pedro Akira Bazaglia Kuroda, Barbara Letícia Tomaz Pedroso, Carlos Roberto Grandini
UNESP – Univ. Estadual Paulista, Laboratório de Anelasticidade e Biomateriais, 17.033.360, Bauru (SP), e
IBTN-Br, Braço Brasileiro do Institute of Biomaterials, Tribocorrosion and Nanomedicine, 17.033.360, Bauru (SP)

Resumo

Este artigo trata do estudo do desenvolvimento e caracterização estrutural, microestrutural e propriedades mecânicas selecionadas da liga Ti-25Ta-50Zr destinada a aplicações biomédicas. As ligas foram fundidas em um forno a arco-voltaico e laminadas. A liga após a fusão apresentou uma estrutura do tipo β e uma pequena quantidade de fase α" ortorrômbica. Após a laminação a fase α" é suprimida devido a aplicação de deformação plástica. Com relação a dureza, a liga laminada possuiu um alto valor de dureza pois as deformações externas nas ligas ao passar pelo processo de laminação, aumentam as tensões internas na liga. O módulo de elasticidade do titânio comercialmente puro é três vezes maior que o osso cortical humano, já a Ti-25Ta-50Zr possui ótimos resultados de módulo de elasticidade, onde a diferença do valor do módulo material/osso cai para apenas duas vezes, indicando que o material pode ser utilizado na área biomédica.

Abstract

This paper deals with the study of the development and structural characterization, microstructural and selected mechanical properties of Ti-25Ta-50Zr alloy for biomedical applications. The alloys were melted in an arc-volt furnace and hot-rolled. The alloy after melting has a β-type structure and a small amount of orthorhombic α" phase. After rolling,

the α" phase is suppressed due to the application of plastic deformation. Regarding the hardness, the rolled alloy had a high hardness value because the external deformations in the alloys through the rolling process increase the internal tensions in the alloy. The modulus of elasticity of commercially pure titanium is three times larger than human cortical bone, whereas Ti-25Ta-50Zr has excellent modulus of elasticity results, where the difference in modulus value, material/bone, falls to only twice, indicating that the material can be used in the biomedical area.

Introdução

O titânio e suas ligas são utilizados como dispositivos médicos e implantes por possuírem uma boa resistência à corrosão e ao desgaste, elevada resistência mecânica, boa ductilidade, trabalhabilidade e biocompatibilidade. Porém a liga de titânio mais utilizada na ortopedia possui o alumínio e vanádio na sua composição química e estudos mostram que o vanádio e o alumínio geram óxidos nocivos ao corpo humano, dessa forma há uma grande preocupação devido a toxicidade dos materiais [1; 2; 3]. Outro problema está associado com a grande diferença entre os módulos de elasticidade das ligas de titânio e do osso humano, quando existe uma grande diferença de propriedade mecânica do implante com o osso, ocorre o fenômeno chamado "stress shielding" onde há a perda densidade óssea no local onde foi implantado o biomaterial [4; 5]. O implante absorve a carga que o osso deveria suportar para manter sua estrutura. Esse fenômeno pode causar folga no implante, dor local e necessitando que seja realizado uma cirurgia de revisão no paciente [6]. Assim, intensa investigação e desenvolvimento de ligas metálicas estão sendo realizadas em todo o campo biomédico, com o objetivo de encontrar novas ligas de titânio que possuam módulo de elasticidade cada vez mais próximo do osso e sem a presença de elementos nocivos a saúde [7; 8].

O titânio é um elemento que possui dimorfismo, sua estrutura cristalina se modificar na temperatura de 883 ºC. Abaixo desta temperatura sua estrutura cristalina é da forma hexagonal compacta (fase α) e acima desta temperatura sua estrutura cristalina é da forma cúbica de corpo centrado (fase β). O zircônio possui uma transformação alotrópica semelhante ao titânio na temperatura de 862°C. No sistema binário Ti-Zr, sabe-se que o zircônio atua como elemento neutro, ou seja, não modifica a temperatura de transformação de fase, assim as ligas do sistema binário possuem apenas a estrutura α ou α' na temperatura ambiente [9; 10; 11; 12]. O tântalo é um metal refratário com estrutura cúbica de corpo centrado, sendo um elemento β-estabilizador para formação de ligas de titânio,

ou seja, o acréscimo de tântalo na liga diminui a temperatura de transformação de fase[5; 13; 14; 15]. Estudos mostram que a fração de 25% em peso de tântalo na liga de titânio possui excelentes resultados de propriedade mecânica comparado com o titânio puro. Esta liga possui apenas a fase ortorrômbica α" como estrutura cristalina [12].

Conhecendo que as ligas binárias do sistema Ti-Zr e Ti-Ta são promissoras e com potencial biomédico, ligas ternárias estão vendo desenvolvidas utilizando o titânio, zircônio e tântalo para potencializar suas as características como biomaterial. A liga Ti-25Ta, que possui melhores resultados do sistema Ti-Ta, com o acréscimo de cinquenta por cento em peso de zircônio pode possuir melhores valores propriedade mecânica, pois embora o zircônio seja considerado um elemento neutro em ligas binárias de titânio, na presença de um outro elemento β estabilizador (como tântalo), ele pode ajudar na retenção desta fase, e ligas do tipo β tendem a possuir baixo valor de módulo de elasticidade [3].

Recentemente resultados da liga Ti-25Ta-10Zr foram publicados [13]. O estudo mostrou que o acréscimo de 10% em peso de zircônio induziu a formação da fase β, ou seja, o zircônio atuou como elemento β-estabilizador. Porém a liga ainda possui as fases martensíticas α' e α", o que faz com que liga possua alta dureza (409 HV), o que é indesejável quando queremos forjar uma placa ou parafusos. Neste sentido, a liga Ti-25Ta-50Zr pode ser uma liga com bons resultados de propriedade mecânica, pois teoricamente deverá possuir uma porcentagem maior de fase β comparado com a Ti-25Ta-10Zr.

Neste sentido, este trabalho mostra o desenvolvimento de uma nova liga a base de titânio, a liga Ti-25Ta-50Zr, visando aplicações ortopédicas e dentárias.

Materiais e Métodos

Titânio comercialmente puro (grau 2) em formato de cilíndrico, folhas de tântalo com 99,9% de pureza e fios de zircônio com 99,8% em peso foram separados na composição nominal para a fusão do lingote Ti-25Ta-50Zr. A fusão foi realizada utilizando um forno arco-voltáico, com cadinho de cobre refrigerado a água, eletrodo não-consumível de tungstênio e atmosfera controlada de argônio [3; 13; 16; 17; 18; 19; 20; 21; 22; 23; 24; 25; 26].

Após a fusão, o material foi submetido a laminado à quente para a obtenção de lâminas. A laminação foi realizada em uma máquina FENN, no Departamento de Engenharia de Materiais (DEMa) da Universidade Federal de São Carlos (UFSCar), consistindo no aquecimento da amostra até a temperatura de 1000 ºC, aproximadamente, e em seguida a redução de suas dimensões iniciais e resfriamento ao ar. A amostra foi

finalizada com aproximadamente 4 mm de espessura. A parte (a) da Figura 7.1 mostra uma fotografia do lingote após fusão e a parte (b) é a liga após a laminação. Após a laminação, o material passou por um processo de decapagem química com ácido nítrico e fluorídrico (fração volumétrica de 3:1, respectivamente) para a retirada a camada de óxido formada na superfície do material [27].



(a) **(b)**

Figura 7.1: Fotografia do da liga Ti-25Ta-50Zr após a fusão (a) e laminação (b).

A composição química das amostras produzidas foi verificada utilizando a técnica da solubilização em meio ácido, seguido da detecção dos elementos em um espectrômetro de emissão ótica com plasma induzido (ICP-OES) [28]; pela técnica de espectrometria por dispersão de energia, para fazer o mapeamento dos elementos presente na superfície do material, utilizando uma sonda INCA acoplada em um microscópio eletrônico de varredura da Carls Zeiss, modelo EVO-015 e a quantidades dos gases oxigênio e nitrogênio foram verificados utilizando um equipamento LECO, modelo TC-400 pela fusão direta das amostras em cadinhos de grafite que combina o carbono com o oxigênio liberado pela amostra [29]. Medidas de densidade foram realizadas para verificar a estequiometria do material, para tal medida utilizou-se uma balança analítica da OHAUS, modelo Explorer.

A caracterização estrutural foi realizada por intermédio de medidas de difração de raios-X, realizadas em um difratômetro da marca Rigaku, modelo MiniFlex 600, com radiação Cu-Kα (λ = 1,54056 Å), corrente de 20 mA e potencial de 40 kV. As medidas foram efetuadas no modo de tempo fixo, com 0,02º de passo, na faixa de 20º e 80º, e taxa de 10º por minuto.

Para a obtenção das imagens de microscopia óptica, foi utilizado um microscópio Olympus modelo BX51M e para as imagens de microscopia eletrônica de varredura, foi

utilizado um microscópio eletrônico da Carl Zeiss, modelo EVO-015. Os materiais passaram por um preparo metalográfico prévio no qual as amostras foram lixadas com lixas com várias granulometria [30]. Após o lixamento, as amostras foram polidas em suspensão de alumina de 1 µm por 20 minutos. Para revelar a microestrutura das amostras, foi realizado um ataque químico com o reagente Kroll [31], utilizando uma solução de 15% de HNO3, 5% de HF e 80% de H2O.

Para a caracterização mecânica inicial das amostras, foram selecionadas duas propriedades extremamente importantes para a utilização como biomaterial, a dureza e o módulo de elasticidade [32]. Um biomaterial biomédico deve possuir boa ductibilidade/trabalhabilidade para a produção de parafusos e placas para implante. Já o módulo de elasticidade deve possui um módulo de elasticidade semelhante ao do osso humano, pois se um material implantado no corpo humano possuir um alto valor de módulo, pode ocorrer a rejeição do implante, assim como o afrouxamento do mesmo, causando dor ao paciente e necessitando fazer uma cirurgia de revisão. As medidas de microdureza Vickers foram obtidas por intermédio de um microdurômetro Shimadzu HMV-2, com carga de 200 g (1,961 N) e tempo de 60s [33]. Para as medidas do módulo de elasticidade, foi utilizado método dinâmico, baseado na técnica de excitação por impulso [34], por intermédio de um equipamento Sonelastic®, da ATCP.

Resultados e Discussão

A Tabela 7.1 mostra os valores obtidos para os elementos que compõem a liga, utilizando a técnica de ICP-EOS e análise de gases. Em seguida são apresentadas as imagens de mapeamento químico dos elementos que compõem a amostra, onde os pontos de coloração vermelha representam o titânio, os pontos verdes representam o tântalo e os azuis, representam o zircônio.

Os resultados mostram que a composição química da liga é próxima ao valor nominal e baixo teor de gases. As impurezas metálicas apresentam concentrações não significativas e os gases, oxigênio e nitrogênio, estão dissolvidos em pequenas quantidades. Segundo a norma ASTM 2066 [35], uma liga binária Ti-15%Mo (onde 15% é a porcentagem em peso) deve possuir uma erro de aproximadamente ± 1% na quantidade de molibdênio para se dizer a fusão desta liga é considerada satisfatório, ou seja, as ligas Ti-16Mo e Ti-14Mo podem ser denominadas como Ti-15Mo. Como a liga produzida é nova e não possui uma norma específica, analisando os resultados à luz da norma ASTM 2066, observa-se que a liga é obtida de forma satisfatória. Por esta norma, na liga Ti-

15%pMo, o teor máximo de gases tolerado é (0,20 ± 0,02) %p e (0,05 ± 0,02) %p, para o oxigênio e nitrogênio, respectivamente. Assim, conclui-se que o teor de oxigênio e nitrogênio para os lingotes produzidos estão de acordo com o estabelecido pela norma. Com relação ao mapeamento químico (Figura 7.2), observa-se uma distribuição homogênea, sem a presença de aglomerados ou segregados indicando que a fusão foi bem-sucedida.

Tabela 7.1: Composição química das amostras da liga Ti-25Ta-5Zr

Elemento	Al	Cr	Cu	Fe	Hf	Mo	Ni	Si	Ta	Zr	O	N	Ti
%p	0,07	0,01	0,01	0,01	0,01	0,01	0,01	0,01	23,5	45,1	0,18	0,01	Balanço

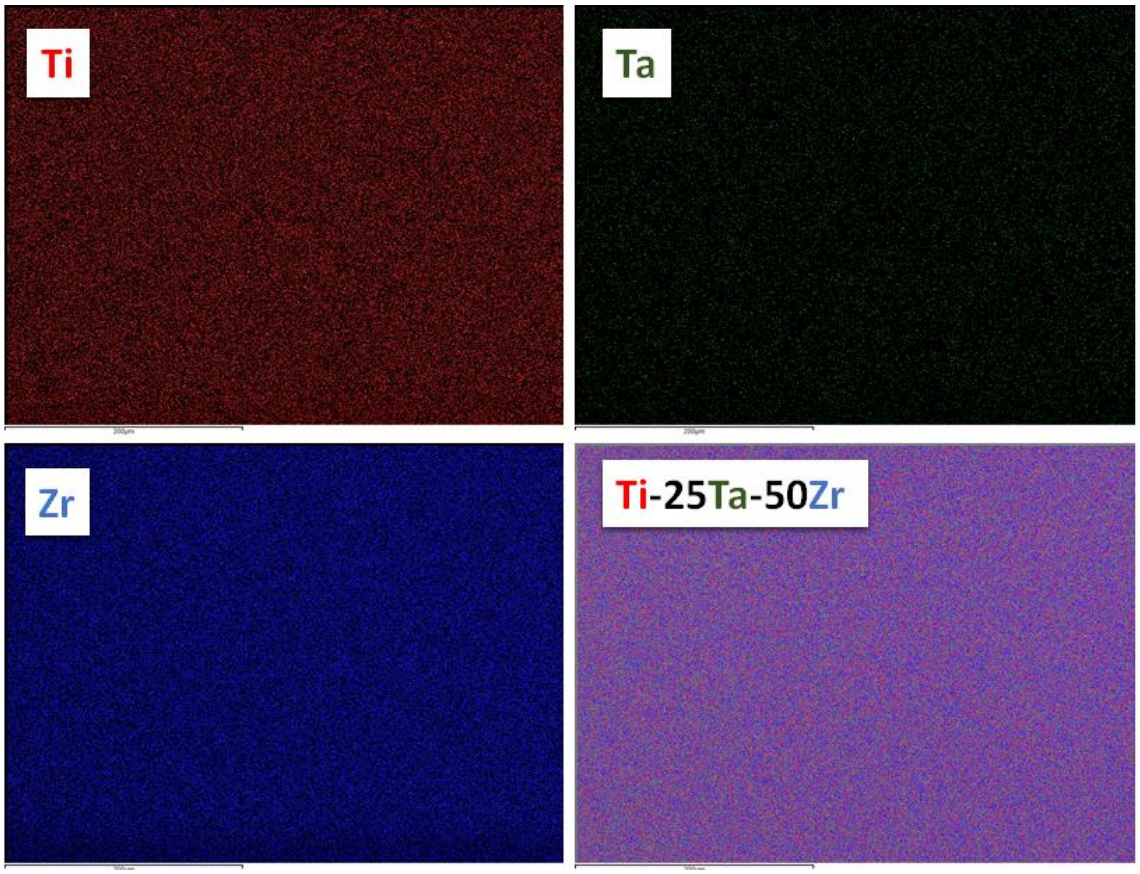


Figura 7.2: Mapeamento da distribuição dos elementos titânio (em verde), tântalo (em verde) e zircônio (em azul), nas amostras da liga Ti-25Ta-50Zr

Os resultados de medidas de densidade, calculados para avaliar a homogeneizada e estequiométrica do material produzido, são apresentados na Figura 7.3. Observa-se que a densidade experimental (6,78 g/cm^3) possui um valor próximo do valor teórico da liga (6,82 g/cm^3), uma diferença percentual inferior a 1%. A medida de densidade é realizada

em pequenos pedaços do lingote, para verificar a estequiometria. Nota-se que a densidade da liga é superior a do titânio e zircônio comercialmente puro, pois o tântalo possui a densidade elevada.

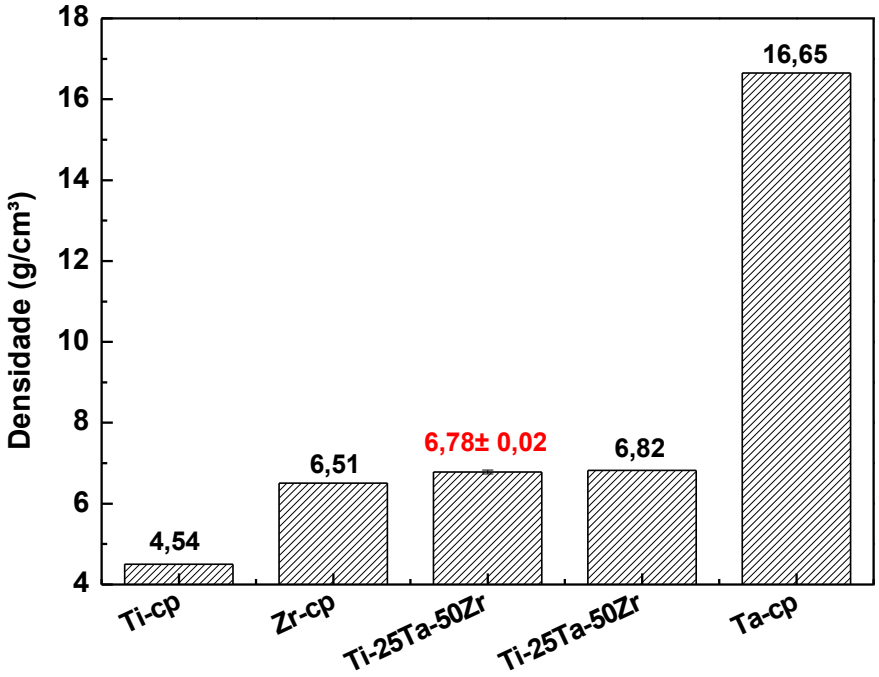


Figura 7.3: Valores de densidade da Ti-25Ta-50Zr.

A partir de resultados empíricos, foi desenvolvida uma equação que possibilita escolher composições das ligas nas quais as quantidades de elementos substitucionais podem estabilizar as fases α e β. A equação (1) usa a porcentagem equivalente de molibdênio por ser um dos principais estabilizadores da fase β e a equação (2) usa o alumínio por ser um dos principais estabilizadores da fase α [36] :

$$[Mo] = Mo + \frac{Ta}{5} + \frac{Nb}{3{,}6} + \frac{W}{2{,}5} + \frac{V}{1{,}5} + 1{,}25Cr + 1{,}25Ni + 1{,}7Mn + 1{,}7Co + 2{,}5Fe \qquad (1)$$

$$[Al] = Al + \frac{Zr}{6} + \frac{Sn}{3{,}6} + \frac{W}{2{,}5} + 10.O \qquad (2)$$

Para as ligas produzidas neste trabalho, o molibdênio equivalente é igual a 5. Assim, segundo a primeira equação a liga Ti-25Ta-50Zr deve possui uma estrutura semelhante a liga binária Ti-5Mo. Ho e colaboradores [37] estudaram as ligas do sistema

Ti-Mo para aplicações como biomaterial e observaram que com 5 %p de molibdênio, esta liga possui a fase ortorrômbica α". Pela equação 2 a liga deste trabalho possui o valor de alumínio equivalente igual a 8,33, então a liga deve possuir uma estrutura semelhante a Ti-8Al que possui apenas a fase α. Logo espera-se que a liga Ti-25Ta-50Zr possua as fases α e α" em sua microestrutura.

A Figura 7.4 mostra um diagrama de molibdênio e alumínio equivalentes, com a classificação das ligas de titânio [36]. No diagrama estão inseridos os valores Al e Mo da liga. No diagrama é possível observar que a liga Ti-25TaZr-50Zr está localizada próxima da região α+β.

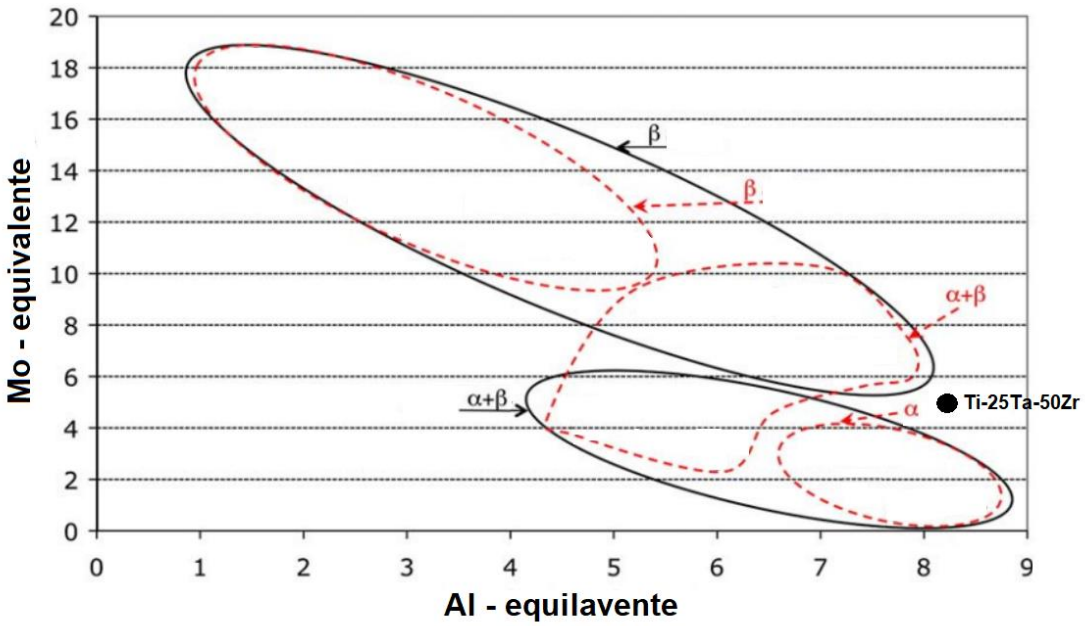


Figura 7.4: Diagrama Al e Mo equivalente [36].

A Figura 7.5 mostra um gráfico comparativo dos difratogramas de raios X para as amostras da liga Ti-25Ta-50Zr na condição bruta de fusão e laminada. Observando os difratogramas, verifica-se que a amostra após a fusão, apresenta picos da fase martensítica α e β, com estrutura cristalina hexagonal compacta e cúbica de corpo centrado, respectivamente [37]. Após a laminação apenas picos da fase β foram observados, indicando que o tratamento termomecânico forneceu as condições termodinâmicas favoráveis para a supressão da fase ortorrômbica α", uma vez que a conformação plástica induz a formação da fase α". Segundo Zhou e Niinomi [14] a liga binária Ti-25Ta submetida a uma solubilização com resfriamento rápido, possui a estrutura cristalina ortorrômbica (fase α") e segundo Willians [38] a liga Ti-50Zr possui a estrutura hexagonal compacta (fase

α). Trabalhos na literatura mostram que o tântalo é um elemento β-estabilizador [39], e o zircônio auxilia na estabilização da fase β devido a presença do tântalo [3; 40]. No trabalho atual, foi observado que a presença do tântalo e do zircônio ajudou na formação da fase β do titânio, pois nos sistemas binários nas concentrações utilizadas (Ti-25Ta e Ti-50Zr) não é detectado fração de fase β nas ligas.

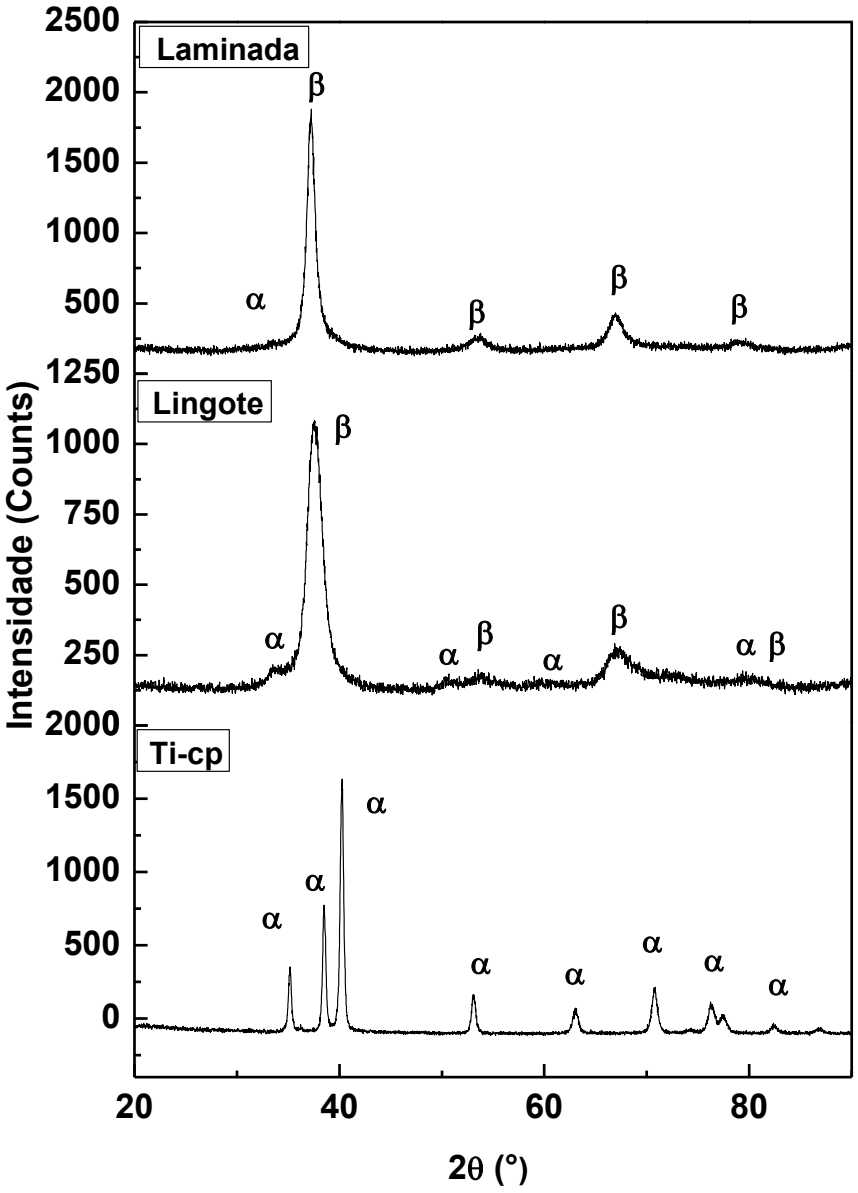
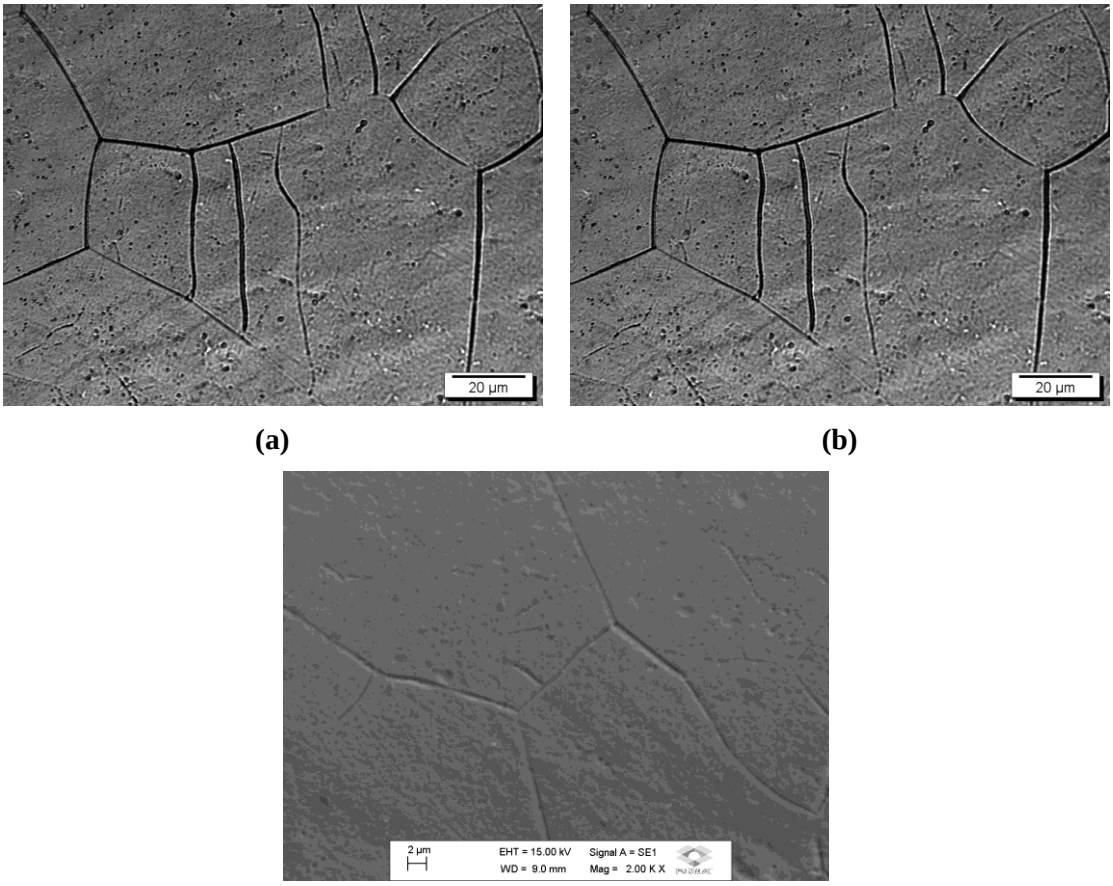


Figura 7.5: Difratogramas de raios X para a liga Ti-25Ta-50Zr.

As Figuras 7.6 e 7.7 apresentam as micrografias ópticas e a eletrônicas de varredura da liga bruta de fusão e após laminação, respectivamente. As micrografias

corroboraram os resultados obtidos nos difratogramas de raios X. A liga Ti-25Ta-50Zr, em ambas as condições, apresentaram uma microestrutura composta por contorno de grãos característicos da fase β, conforme esperado a partir dos resultados da difração de raios X, porém estruturas aciculares características da fase α não foram observadas nas micrografias da liga bruta de fusão, indicando que a fração da fase α deve ser pequena na amostra. Também pode ser observado que a laminação diminuiu o tamanho dos grãos da amostra.

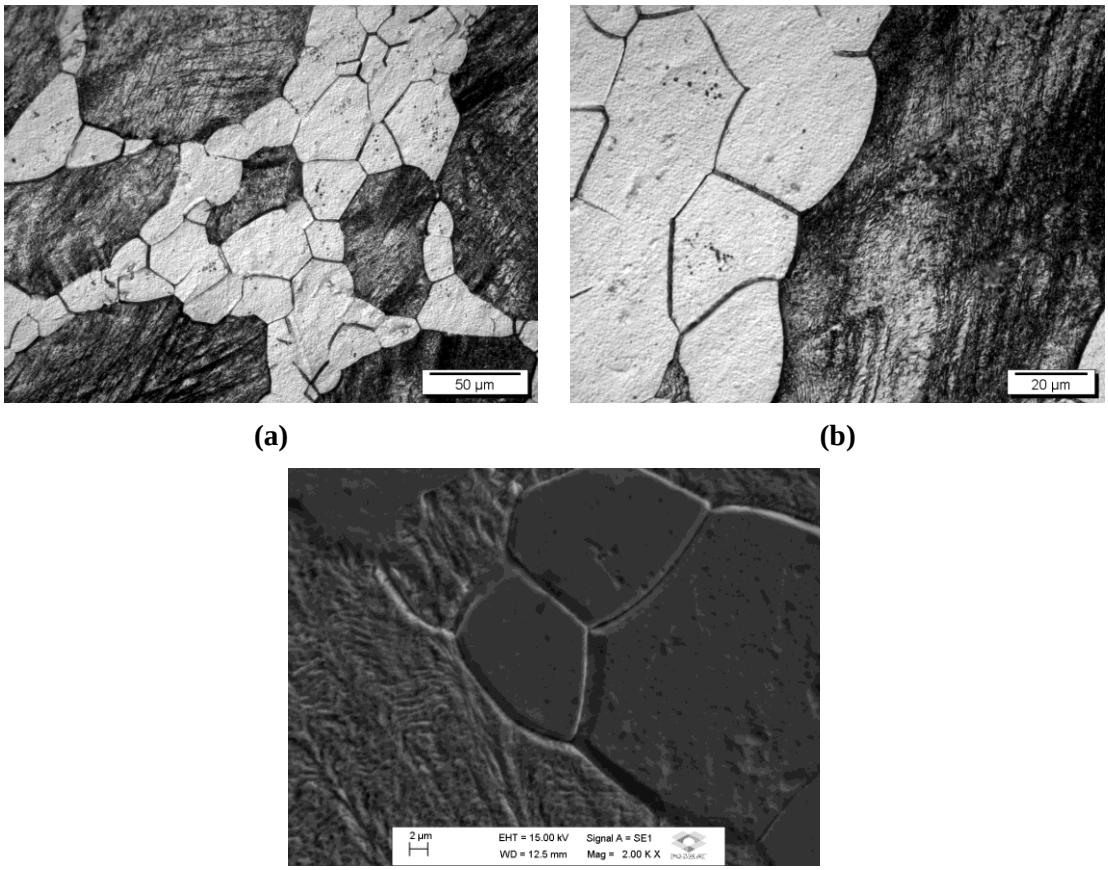
Os resultados das caracterizações estrutural e microestrutural mostraram que a teoria do molibdênio e alumínio equivalente funcionou bem no caso da liga Ti-25Ta-50Zr.



(a) **(b)**

(c)

Figura 7.6: Micrografias da liga Ti-25Ta-50Zr após a fusão, obtidas por microscopia óptica (a) e (b) e por microscopia eletrônica de varredura (c).



(a) **(b)**

(c)

Figura 7.7: Micrografias da liga Ti-25Ta-50Zr após a laminação, obtidas por microscopia óptica (a) e (b) e por microscopia eletrônica de varredura (c).

Com relação aos resultados de dureza da liga Ti-25Ta-50Zr, apresentados na Figura 7.8, obteve-se o valor de dureza da liga após fusão é de 337 HV e houve um acréscimo deste valor quando a liga foi submetida ao processo de laminação, 361 HV. A laminação gera altas taxas de resfriamento e deformações externas nas ligas, aumentando as tensões internas e a dureza do material. A liga, em ambas as condições, possui valores significativamente maior que o titânio puro (167 HV). A liga produzida possui dureza maior que o Ti-cp devido a um processo de endurecimento por solução solida causada pela adição de tântalo e zircônio que possuem massa atômica superiores a do titânio [41].

Figura 7.9 mostra uma comparação do módulo de elasticidade de alguns biomateriais metálicos comumente encontrados no mercado, juntamente com a liga Ti-25Ta-50Zr [8]. A liga produzida neste trabalho possui módulo de elasticidade de aproximadamente 60 GPa. Pode ser observado que apenas a liga Ti-35Nb-5Ta-7Zr e o nitinol (55Ni-45Ti equiatômico) possuem resultados mais satisfatórios para serem

implantados em um osso cortical. As demais ligas, inclusive o Ti-25Ta, possuem o valor de módulo de elasticidade superior.

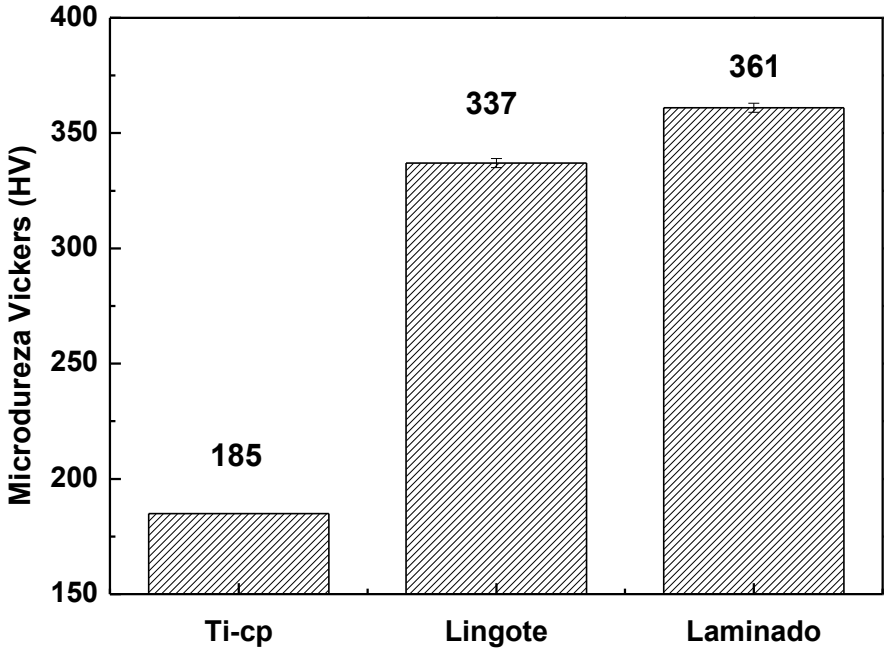


Figura 7.8: Microdureza Vickers da liga Ti-25Ta-50Zr.

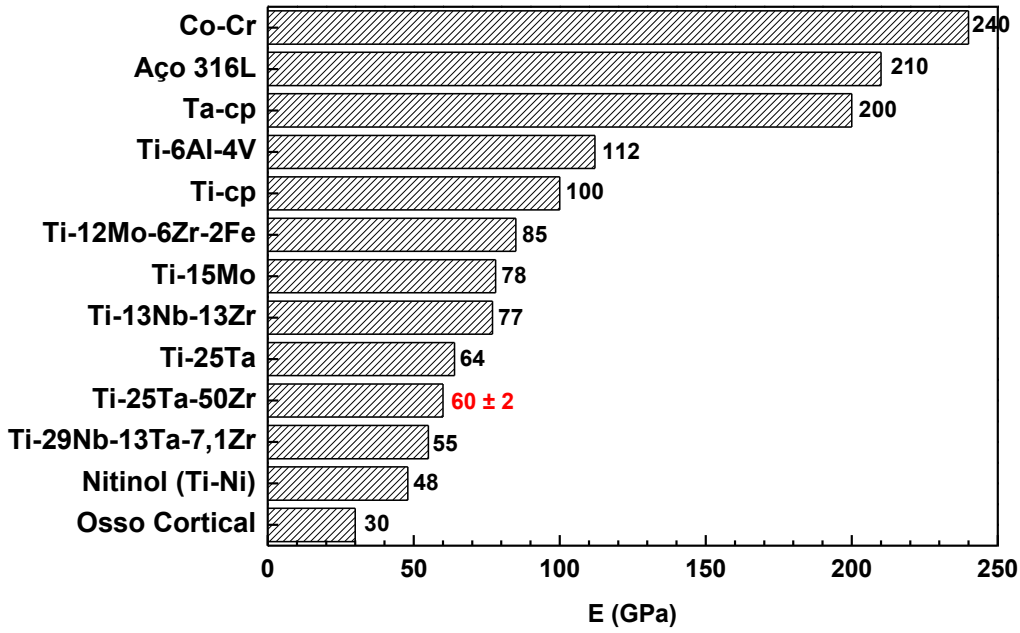


Figura 7.9: Módulo de elasticidade da liga Ti-25Ta-50Zr, comparado com valores de materiais metálicos usados comumente na área biomédica [4].

Os resultados de caracterização estrutural, microestrutural, microdureza de Vickers e módulo de elasticidade são satisfatórios para candidatar a liga Ti-25Ta-50Zr como um possível biomaterial, porém mais teste mecânicos, eletroquímicos e uma análise da biocompatibilidade são requeridos para uma caracterização completa do material.

Conclusões

As medidas de composição química e mapeamento indicam que a liga foi fundida de maneira homogênea, preservando a estequiometria proposta. A análise estrutural mostra que a liga é β metaestável, pois na condição bruta de fusão uma pequena fração da fase α" é detectada na difração de raio X, porém na condição laminada a liga possui apenas a fase β. Os valores de dureza obtidos estiverem acima do titânio comercialmente puro, causado pelo endurecimento por solução sólida. A laminação aumentou a dureza da liga devido ao aumento das tensões. O módulo de elasticidade da liga é mais baixo comparada com a titânio comercialmente puro e da Ti25Ta, pois a liga possui a predominância da fase β. Tais características fazem desta liga uma boa alternativa para aplicações ortopédicas.

Referências

1 MANAM, N. S. et al. Study of corrosion in biocompatible metals for implants: A review. **Journal of Alloys and Compounds,** v. 701, p. 698-715, 2017.
2 MARKHOFF, J. et al. Biocompatibility and Inflammatory Potential of Titanium Alloys Cultivated with Human Osteoblasts, Fibroblasts and Macrophages. **Materials,** v. 10, n. 1, p. 52, 2017.
3 KURODA, P. A. B.; BUZALAF, M. A. R.; GRANDINI, C. R. Effect of molybdenum on structure, microstructure and mechanical properties of biomedical Ti-20Zr-Mo alloys. **Materials Science and Engineering: C,** v. 67, p. 511-515, 2016.
4 GEETHA, M. et al. Ti based biomaterials, the ultimate choice for orthopaedic implants – A review. **Progress in Materials Science,** v. 54, n. 3, p. 397-425, 2009.
5 ZHOU, Y. L.; NIINOMI, M.; AKAHORI, T. Decomposition of martensite α″ during aging treatments and resulting mechanical properties of Ti−Ta alloys. **Materials Science and Engineering: A,** v. 384, n. 1, p. 92-101, 2004.
6 NIINOMI, M.; NAKAI, M. Titanium-Based Biomaterials for Preventing Stress Shielding between Implant Devices and Bone. **International Journal of Biomaterials,** v. 2011, p. 836587, 10 pages, 2011.
7 LEI, Z. et al. Development of advanced materials via entropy engineering. **Scripta Materialia,** v. 165, p. 164-169, 2019.
8 KAUR, M.; SINGH, K. Review on titanium and titanium based alloys as biomaterials for orthopaedic applications. **Materials Science and Engineering: C**, v. 102, p. 844-862, 2019.

9 CORDEIRO, J. M. et al. Characterization of chemically treated Ti-Zr system alloys for dental implant application. **Materials Science and Engineering: C,** v. 92, p. 849-861, 2018.
10 CORREA, D. R. N. et al. The effect of the solute on the structure, selected mechanical properties, and biocompatibility of Ti-Zr system alloys for dental applications. **Materials Science & Engineering C-Materials For Biological Applications,** v. 34, p. 354-359, 2014.
11 VICENTE, F. B. et al. The Influence of Small Quantities of Oxygen in the Structure, Microstructure, Hardness, Elasticity Modulus and Cytocompatibility of Ti-Zr Alloys for Dental Applications. **Materials,** v. 7, n. 1, p. 542-553, 2014.
12 CORDEIRO, J. M. et al. Development of binary and ternary titanium alloys for dental implants. **Dental Materials,** v. 33, n. 11, p. 1244-1257, 2017.
13 QUADROS, F. D. F. et al. Preparation, structural and microstructural characterization of Ti-25Ta-10Zr alloy for biomedical applications. **Journal of Materials Research and Technology**, v. 8, p. 4108-4114, 2019.
14 ZHOU, Y.-L.; NIINOMI, M. Ti–25Ta alloy with the best mechanical compatibility in Ti–Ta alloys for biomedical applications. **Materials Science and Engineering: C,** v. 29, n. 3, p. 1061-1065, 2009.
15 _____. Microstructures and mechanical properties of Ti–50mass% Ta alloy for biomedical applications. **Journal of Alloys and Compounds,** v. 466, n. 1, p. 535-542, 2008.
16 CORREA, D. R. N. et al. **Effect of Heat Treatment in the Structure and Microstructure of Ti-15Zr-XMo Alloys**. Defect & Diffusion Forum, v. 365, p. 305-310, 2015.
17 CORREA, D. R. N. et al. Effect of the substitutional elements on the microstructure of the Ti-15Mo-Zr and Ti-15Zr-Mo systems alloys. **Journal of Materials Research and Technology,** v. 4, n. 2, p. 180-185, 2015.
18 CORREA, D. R. N. et al. Tribocorrosion behavior of β-type Ti-15Zr-based alloys. **Materials Letters,** v. 179, p. 118-121, 2016.
19 CORREA, D. R. N. et al. Effect of Some Heat Treatments on Anelastic Properties of Ti-15Zr-xMo Alloys. **Materials Science Forum,** v. 869, p. 907-912, 2016.
20 KURODA, P. A. B.; BUZALAF, M. A. R.; GRANDINI, C. R. Preparation, microstructural characterization, and selected mechanical properties of Ti-20Zr-2.5Mo and Ti-20Zr-7.5Mo used as biomaterial. **Materials Science Forum,** v. 869, p. 946-951, 2016.
21 KURODA, P. A. B. et al. Thermomechanical treatments influence on the phase composition, microstructure, and selected mechanical properties of Ti–20Zr–Mo alloys system for biomedical applications. **Journal of Alloys and Compounds**, p. 152108, 2019.
22 LUZ, A. R. et al. Characterization of the morphology, structure and wettability of phase dependent lamellar and nanotube oxides on anodized Ti-10Nb alloy. **Applied Surface Science,** v. 448, p. 30-40, 2018.
23 CORREA, D. R. N. et al. Development of Ti-15Zr-Mo alloys for applying as implantable biomedical devices. **Journal of Alloys and Compounds,** v. 749, p. 163-171, 2018.
24 CORREA, D. R. N. et al. Microstructure and selected mechanical properties of aged Ti-15Zr-based alloys for biomedical applications. **Materials Science and Engineering: C,** v. 91, p. 762-771, 2018.

25 CORREA, D. R. N.; KURODA, P. A. B.; GRANDINI, C. R. Structure, Microstructure, and Selected Mechanical Properties of Ti-Zr-Mo Alloys for Biomedical Applications. **Advanced Materials Research,** v. 922, p. 75-80, 2014.
26 CORREA, D. R. N. et al. Adjustment of the microstructure and selected mechanical properties of biomedical Ti-15Zr-Mo alloys through oxygen doping. **Journal of Alloys and Compounds,** v. 775, p. 158-167, 2019.
27 KURODA, P. A. B. **Efeito do molibdênio substitucional na estrutura, microestrutura e algumas propriedades mecânicas de ligas do sistema Ti-20Zr-Mo**. 2016.
28 ASTM. **E2371 – 04 - Standard Test Method for Analysis of Titanium and Titanium Alloys by Atomic Emission Plasma Spectrometry**. E2371 – 04 - Standard Test Method for Analysis of Titanium and Titanium Alloys by Atomic Emission Plasma Spectrometry. West Conshohocken: ASTM International. E2371 – 04 2004.
29 _____. **E1409 – 08 - Standard Test Method for Determination of Oxygen and Nitrogen in Titanium and Titanium Alloys by the Inert Gas Fusion Technique**. E1409 – 08 - Standard Test Method for Determination of Oxygen and Nitrogen in Titanium and Titanium Alloys by the Inert Gas Fusion Technique. West Conshohocken: ASTM International. ASTM E1409 – 08 2008.
30 _____. **E407-07 - Standard Practice for Microetching Metals and Alloys**. E407-07 - Stanard Practice for Microetching Metals and Alloys
West Conshohocken: ASTM International. ASTM E-407-07 2007.
31 COLLINGS, E. W. **The Physical Metallurgy of Titanium Alloys**. Ohio: ASM International, 1989.
32 WANG, W.; POH, C. K. Titanium Alloys in Orthopaedics. In: (Ed.). **Titanium Alloys - Advances in Properties Control**. Rijeka: InTech, 2013. cap. 1, p.1-20.
33 ASTM. **E92-82 - Standard Test Method for Vickers Hardness of Metallic Materials**. E92-82 - Standard Test Method for Vickers Hardness of Metallic Materials. West Conshohocken, PA: ASTM International. E92-82 2003.
34 _____. **E1876–01 - Standard Test Method for Dynamic Young's Modulus, Shear Modulus, and Poisson's Ratio by Impulse Excitation of Vibration**. E1876–01 - Standard Test Method for Dynamic Young's Modulus, Shear Modulus, and Poisson's Ratio by Impulse Excitation of Vibration. Philadelphia (USA): ASTM International. E1876–01 2002.
35 _____. **F2066-08 - Standard specification for wrought titanium-15 molybdenum alloy for surgical implant application**. F2066-08 - Standard specification for wrought titanium-15 molybdenum alloy for surgical implant application. Philadelphia (USA): ASTM International. F 2066-08 2008.
36 ATTALLAH, M. M. et al. Comparative determination of the α/β phase fraction in α+β-titanium alloys using X-ray diffraction and electron microscopy. **Materials Characterization,** v. 60, n. 11, p. 1248-1256, 2009.
37 HO, W. F.; JU, C. P.; CHERN LIN, J. H. Structure and properties of cast binary Ti-Mo alloys. **Biomaterials,** v. 20, n. 22, p. 2115-2122, 1999.
38 WILLIAMS, D. N. et al. The effects of zirconium in titanium-base alloys. **Journal of the Less Common Metals,** v. 6, n. 3, p. 219-225, 1964.
39 ZHOU, Y.-L. et al. Comparison of Various Properties between Titanium-Tantalum Alloy and Pure Titanium for Biomedical Applications. **Materials Transactions,** v. 48, n. 3, p. 380-384, 2007.

40 CORREA, D. R. N.; KURODA, P. A. B.; GRANDINI, C. R. Structure, Microstructure, and Selected Mechanical Properties of Ti-Zr-Mo Alloys for Biomedical Applications. **Advanced Materials Research,** v. 922, p. 75-80, 2014.
41 BOYER, R.; WELSCH, G.; COLLINGS, E. W. **Materials Properties Handbook: Titanium Alloys**. Materials Park: ASM International, 1994.

Capítulo 8

Published in Materials, 12: 3210. 2019. doi:10.3390/ma12193210.

Effect of Thermomechanical Treatments on the Phases, Microstructure, Microhardness and Young's Modulus of Ti-25Ta-Zr Alloys

Pedro Akira Bazaglia Kuroda[1,2], Fernanda de Freitas Quadros[1,2], Raul Oliveira de Araújo[2,3], Conrado Ramos Moreira Afonso[4] and, Carlos Roberto Grandini [1,2]

[1] UNESP – Univ. Estadual Paulista, Laboratório de Anelasticidade e Biomateriais, Bauru, SP, Brazil

[2] IBTN/BR –Institute of Biomaterials, Tribocorrosion and Nanomedicine - Brazilian Branch, Bauru, SP, Brazil

[3] IFSP – São Paulo Federal Institute of Education, Science and Technology, Barretos, SP, Brazil

[4] UFSCar – Univ. Federal de São Carlos, MaterialsEngineeringDepartment (DEMa), São Carlos, SP, Brazil

Abstract:

Titanium and its alloys currently are used as implants, possessing excellent mechanical properties (more suited than stainless steel and Co-Cr alloys), good corrosion resistance and good biocompatibility. The titanium alloy used for most biomedical applications is Ti-6Al-4V, however, studies showed that vanadium and aluminum cause allergic reactions in human tissues and neurological disorders. New titanium alloys without the presence of these elements are being studied. The objective of this study was to analyze the influence of thermomechanical treatments, as hot-rolling, annealing, and solution treatment in the structure, microstructure and mechanical properties of Ti-25Ta-Zr ternary alloy system. The structural and microstructural analyses were performed by x-ray diffraction as well as optical, scanning and transmission electron microscopy. The mechanical properties were analyzed by microhardness and Young's modulus

measurements. The results showed that the structure of the materials and the mechanical properties are influenced by the different thermal treatments: rapid cooling treatments (hot-rolling and solubilization) induced the formation of α" and β phases, while the treatments with slow cooling (annealing) induced the formation of martensite phases. Alloys in the hot-rolled and solubilized conditions have better mechanical properties results, as low elastic modulus, due to retention of the β phase in these alloys.

Introduction

The first alloy developed specifically for use in humans is known as "vanadium steel (1900)", a biomaterial produced for repairing bone fractures and for fixation screws used in orthopedics[1]. Currently, elements such as chromium, tantalum, zirconium, cobalt, titanium, niobium, tungsten, iron and nickel are also used as biomaterials, although the human body tolerates these elements only in small quantities[2]. Materials developed for use as biomaterials must possess certain favorable physical and chemical characteristics and must not induce inflammation, toxic reactions or allergenic symptoms in the host. They must be biocompatible, biofunctional, bioactive, bioinert and sterilizable[3].

Unfortunately, metal implants have been known to fail after prolonged use due to their high elasticity modulus compared to bone, and to their poor resistance to wear and corrosion in body fluids[4; 5]. The bonding force between atoms determines Young's modulus. This bond strength is related to the crystalline structure of the material and to the distances between atoms[6; 7]. It is possible to change the bond strength between atoms by thermomechanical treatment[8]. Plastic deformations are another treatment that can alter the structure of titanium, thus changing the atomic bond strength and Young's modulus [9]. The ω phase of titanium is known to have the highest modulus of elasticity, followed by the α and the α" phases; the β phase has the lowest modulus, due to its low atomic bond strength[10]. New alloys are being developed and investigated whose microstructure and mechanical properties can be altered with the addition of various elements, usually β-stabilizers [11; 12; 13; 14; 15; 16].

Ti-Ta-Zr alloys are being developed for biomedical applications. Zhou et al. [17]indicate that the most promising of the Ti-Ta binary system alloys for use as a biomaterial is Ti-25Ta. Some authors assert that zirconium is a neutral element in titanium alloys, that is, its addition does not modify the structure of the material[18]. Recently, new research has shown that zirconium helps stabilize the β phase in α + β-type alloys, acting as a β-stabilizer[19; 20; 21; 22; 23; 24]. Therefore, alloys of the Ti-25Ta-Zr system may be more

promising as biomaterials, hence the addition of zirconium facilitates the β phase stabilization, in reason of the fact that β-type alloys tend to have a lower modulus of elasticity than alpha-type alloys. Besides aiding in the stabilization of the β phase, zirconium contributes to cost savings in the manufacture and commercialization of these alloys[25], because tantalum has a high market value and a high melting point, making production in high ladder more difficult.

The literature does not have great information about the structure, microstructure, phases and mechanical properties of Ti-Ta-Zr alloys. Yan at al [26] developed Ti-15Ta-xZr system alloys (x = 1.5, 5.5, 10.5, and 15.5 wt.%) manufactured by selective laser melting. Structural and microstructural analyses show that the alloys have the α and β phases and excellent elastic modulus values, highlighting the Ti-15Ta-10.5Zr alloy with a value of approximately 43 GPa. Biesiekierski et al. [27] developed new Ti-Ta-Zr system alloys with high tantalum and zirconium contents (Ti-45Zr-10Ta, Ti40Zr-14Ta, Ti-35Zr-18Ta, and Ti-30Zr -22Ta). The results showed that the alloys produced are of β-type, have elastic modulus like commercially pure titanium and Ti-6Al-4V (109-130 GPa). All alloys have good biocompatibility.

Ti-25Ta-10Zr alloy is the only alloy of type α'+ α" + β reported in the literature. Hardness values are above commercially pure titanium, being hardening by the solid solution. Cytotoxicity assays showed that the alloy does not have a cytotoxic character; on the contrary, the alloy showed perfect cell division, maintaining morphology, indicating good integration between material-cell [28].

The objective of this work was to analyze the influence of thermomechanical treatments, such as hot-rolling and annealing heat treatments, on the structure, microstructure, microhardness and elastic modulus of ternary alloys of the Ti-25Ta-Zr system, with zirconium content varying from 0 to 40% in weight.

Materials and Methods

The alloys were melted in an arc-melting furnace[22; 28; 29; 30; 31; 32]. After melting, the ingots were submitted to a mechanical hot-rolling process at 1,273 K, followed by air-cooling.

Because the microstructure of the metal undergoes changes during rolling, an annealing heat treatment was used to reduce the internal stress caused by the mechanical rolling process. The purpose of the annealing treatment was to eliminate residual internal stress and most of the imperfections present in the material and to promote the growth of the grains[33].

Two types of heat treatments were performed. After thermomechanical processing, the samples were submitted to recrystallization heat treatments at 1,273 K, remaining at this temperature for 21.6 Ks, followed by slow cooling (–5 K/min), and another similar treatment was followed by water quenching (~273 K).

For structural analysis, x-ray diffraction (XRD) analysis (Rigaku model D/Max-2100PC) was used to obtain the diffractograms adopting the powder method, with Cu-Kα radiation, 20 mA current, potential 40 kV, for 3.2 s, range from 20° to 100°, and step of 0.02°, in the fixed time mode.

Before microstructural analysis, samples were submitted to a standard metallographic preparation. Images were obtained using an optical microscope (Olympus model BX51M), a scanning electron microscope (SEM) (Carl Zeiss model EVO-015) and a transmission electron microscope (TEM) (FEI Tecnai G² F20). TEM analysis were performed using a FEI Tecnai G2 F20 200 kV microscope with energy-dispersiveX-ray spectroscopy (EDS).

Hardness measurements were performed in a microhardness tester (Shimadzu, model HMV-2). In each sample, 20 indentations were made with a 25-g load for 60 s[34]. For dynamic elastic modulus, E (GPa) measurements, the impulse excitation technique (ATCP, Sonelastic®) was used [35].

Results

Phase Identification

The x-ray diffractograms, optical and SEM micrographs for Ti-25Ta-Zr system alloys after hot-rolling are shown in Figure 8.1; after annealing and with slow cooling are shown in Figure 8.2; and in Figure 8.3, the results for samples subjected to annealing with fast cooling, are presented. As shown, in some alloys the crystalline structure was sensitive to thermomechanical treatments.

Mechanical Characterization

Figure 8.4 shows the hardness values for Ti-25Ta-Zr system alloys, performed in the samples after each processing condition included in this study. It can be observed, an anomaly for the hardness of Ti-25Ta-30Zr alloy after annealing with rapid cooling. This anomaly can be associated with the retention of w phase [36; 37].

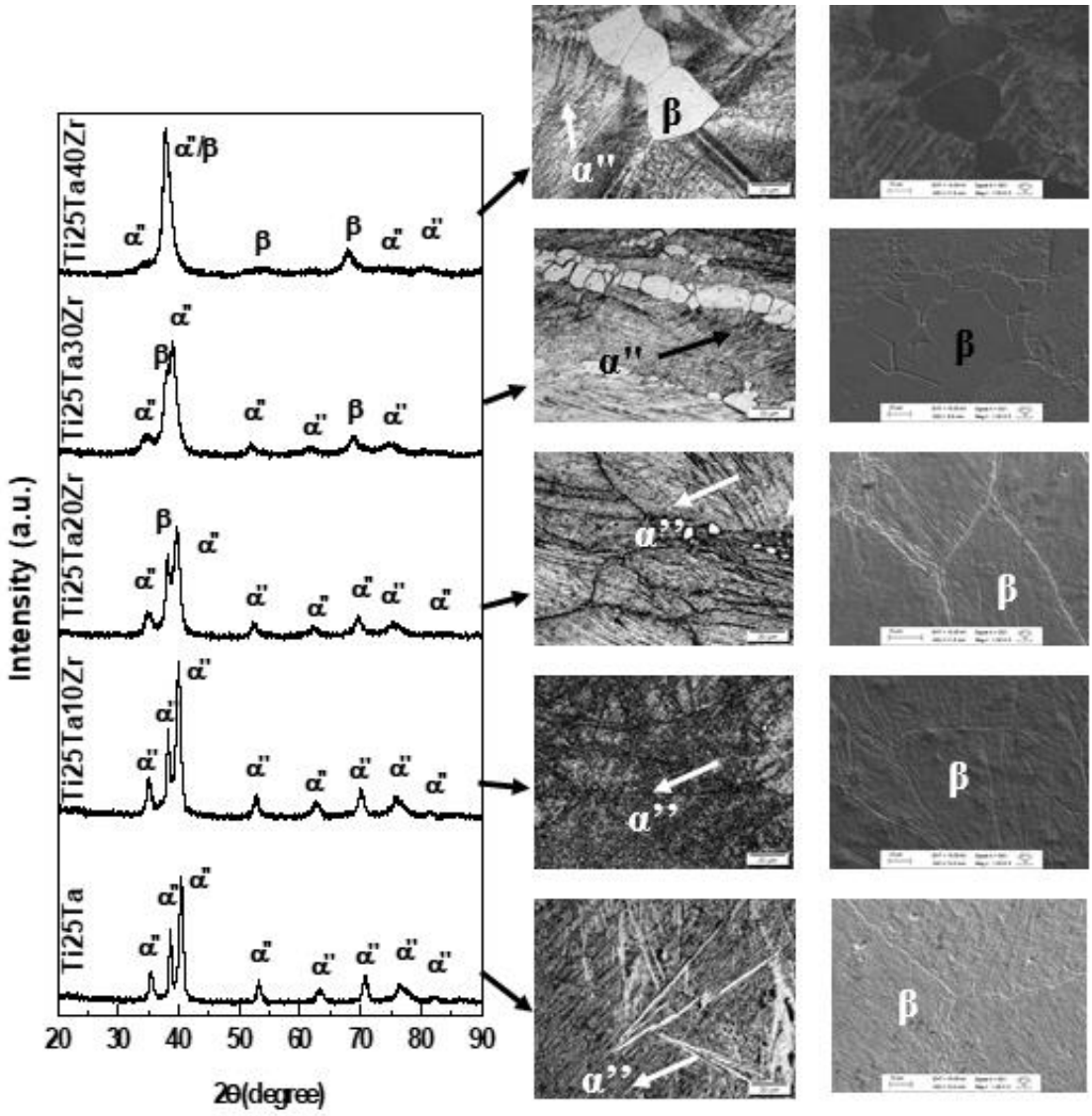


Figure 8.1. X-ray diffraction patterns, optical and SEM micrographs, for Ti-25Ta-xZr system alloys, after hot-rolling.

To verify the presence of w phase, TEM measurements were made in the Ti-25Ta-30Zr alloy after annealing with rapid cooling, and the results are presented in Figure 8.5, that shows the bright (part (a)) and dark (part (b)) field images, the diffraction pattern (part (c)) and a high-resolution image of the selected area (part (d)). It can be observed, clearly, the presence of w phase [33].

Figure 8.6 shows the values of Young's modulus for Ti-25Ta-Zr system alloys, under all conditions investigated in this study. It can be observed that the values of elastic modulus decrease with the zirconium amount for the hot-tolled and annealed with rapid cooling samples. For the annealed with slow cooling, it was observed an increase of elastic modulus with the zirconium amount.

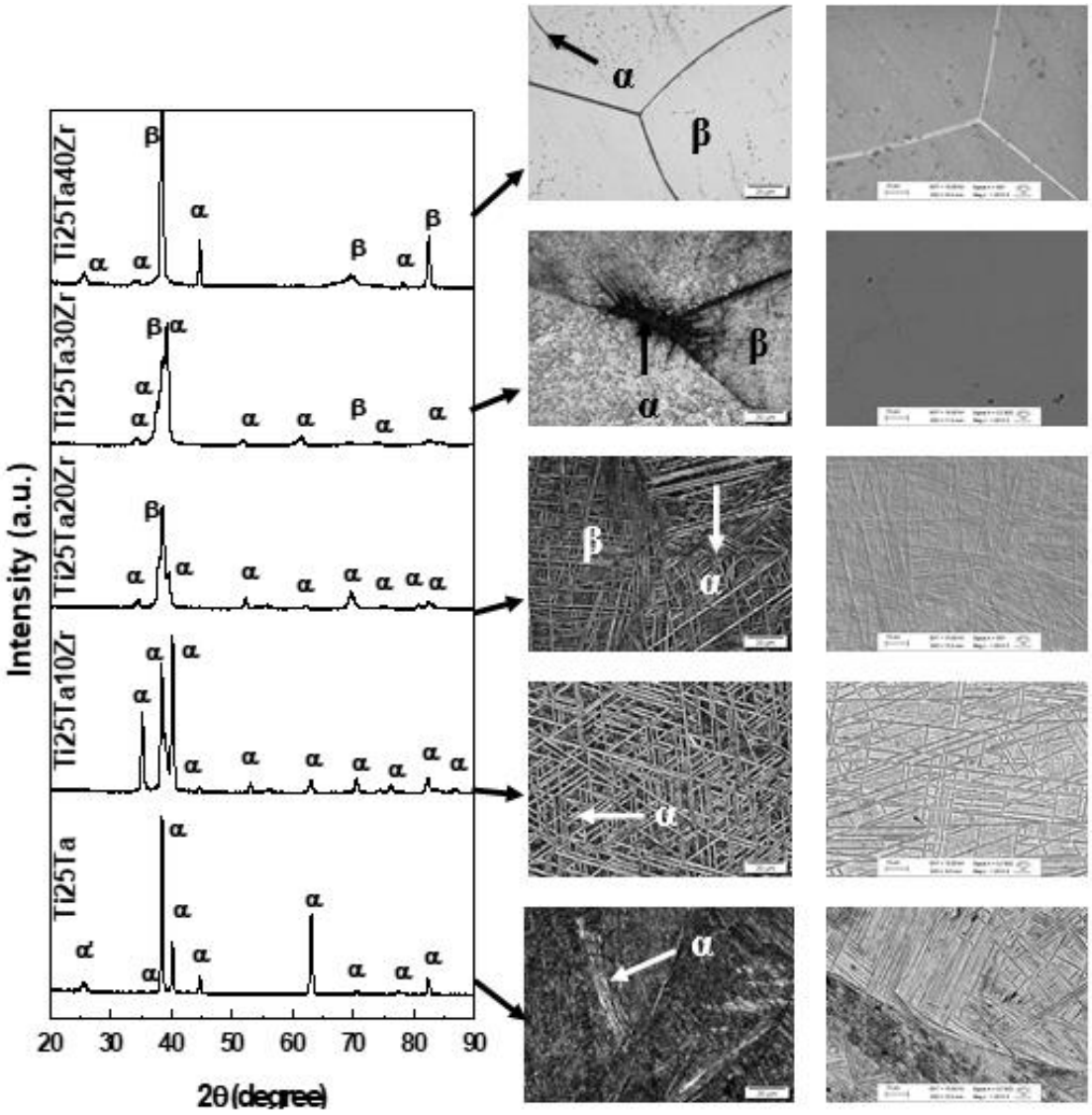


Figure 8.2. X-ray diffraction patterns, optical and SEM micrographs, for Ti-25Ta-xZr system alloys, after annealing heat treatment, with slow cooling.

Discussion

It can be observed, in Fig. 1, that Ti-25Ta and Ti-25aTa-10Zr alloys show only peaks of α" phase in the hot-rolled condition. For the Ti-25Ta-20Zr alloy, the diffractograms show the coexistence of peaks associated with α" and β phases, but those of β phase have lower intensity. Ti-25Ta-30Zr and Ti-25Ta-40Zr alloys have peaks that are associated with α" and β phases, too. It is evident that the zirconium acted as a β-stabilizing element, hence its presence increases the of the β phase retention.

After the annealing heat treatment with slow cooling, the orthorhombic α" phase changed to the hexagonal close-packed structure, α phase, and the β phase remained in the structure of the material. It can be clearly observed that heat treatment modified the

phases of the alloys. Since the annealing was carried out at a temperature above β-transus and cooled slowly, it was provided the necessary thermodynamic conditions for the stabilization of the phases at high temperatures, if they change to stable phases at room temperature, in case α "→ α [38].

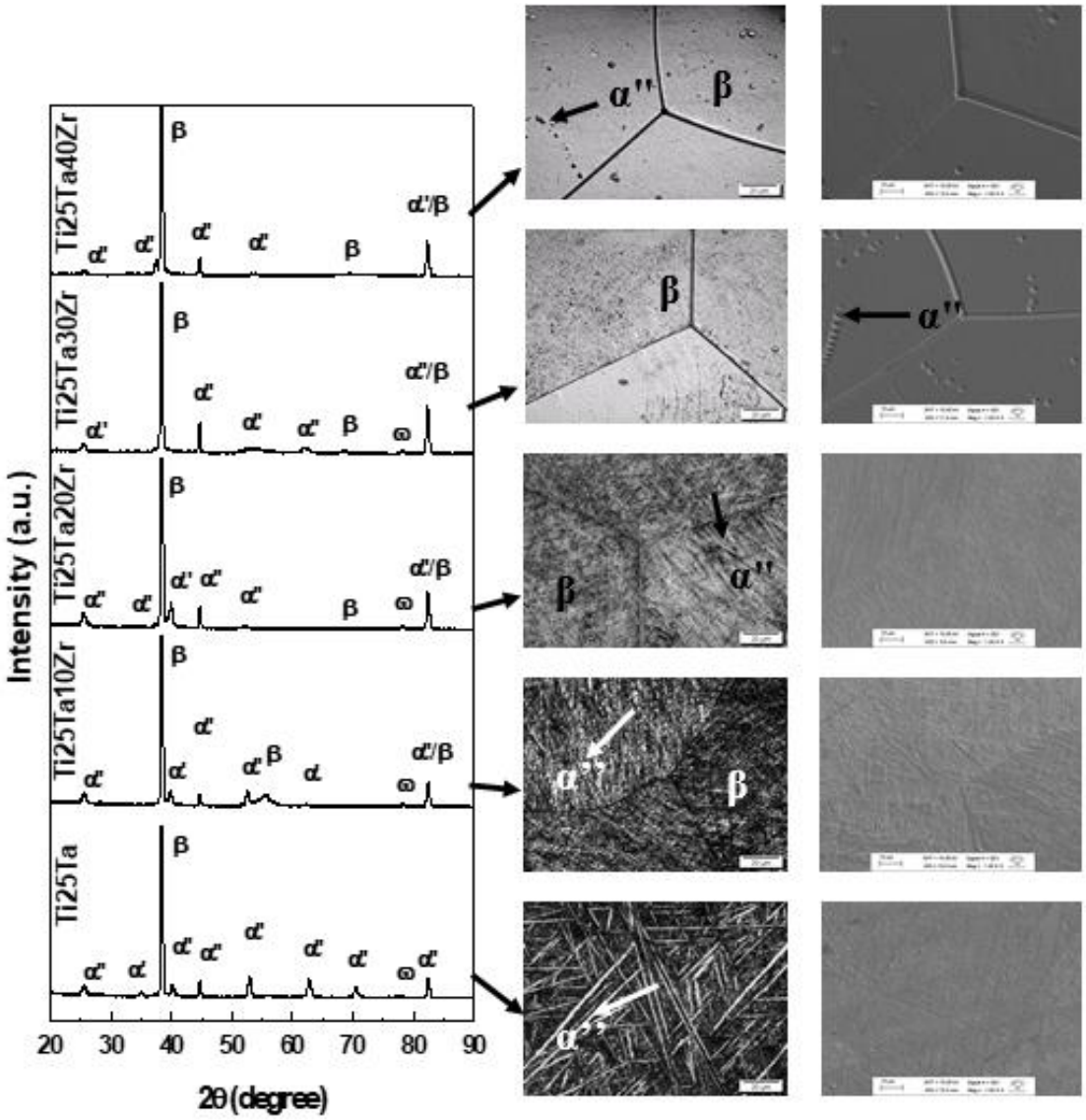


Figure 8.3. X-ray diffraction patterns, optical and SEM micrographs, for Ti-25Ta-xZr system alloys, after annealing heat treatment, with rapid cooling.

The alloys submitted to the annealing treatment with rapid cooling presented the metastable orthorhombic α" phase. In addition, alloys with a zirconium content above 20wt%, showed more intense β phase peak at θ ~ 68°, indicating higher fraction and greater stabilization of bcc structure. It is stated in the literature that rapid cooling of titanium alloys from the β field can induce the formation of the metastable α" martensite

since the fast cooling hinders the atomic rearrangement (retaining the β phase) and produces distortions in the crystalline structure [33]. In addition to detection of α" and β phases, in alloys with 0, 10, 20 and 30 weight percent zirconium, an ω phase peak can be visualized at θ ~ 78°. In the Ti-25Ta-40Zr alloy it was not possible to observe ω phase peaks, showing that zirconium acted as an omega phase suppressor.

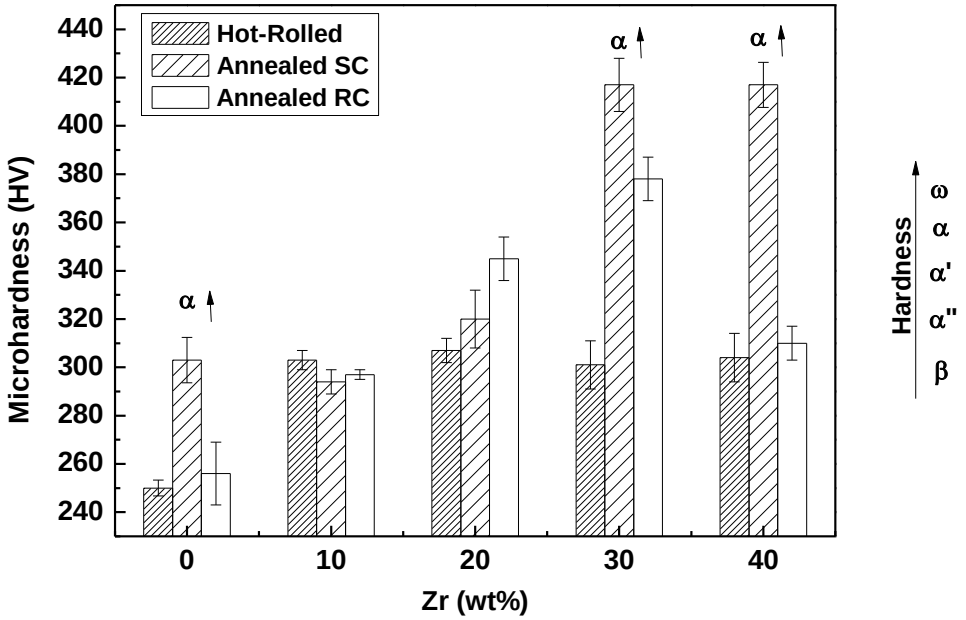


Figure 8.4. Vickers microhardness values of Ti-25Ta-Zr system alloys, after hot-rolling and heat treatments (annealing with slow and rapid cooling).

Combining the results of XRD, it can be seen in Figures 8.1 to 8.3 a typical martensitic structure, α" phase, and grains deformed due to plastic deformation in the Ti-25Ta, Ti-25Ta-10Zr and Ti-25Ta-20Zr alloys, in the condition after hot-rolling. After the annealing, there was recrystallization of the material leading homogenization of the structure and grain size. In these alloys, after recrystallization with slow cooling, an α-type lamellar structure can be seen, with needles emerging from the grain boundaries and thinner needles parallel to the thick needles. In the annealed condition with rapid cooling, there was an increase in grain size, but the martensites phases are more refined, that is, the intra-grain needles are finer with this type of treatment. The images indicate that the cooling rate influences the microstructure in the material—slow cooling induces the formation of the α phase, and rapid cooling promotes the formation of the orthorhombic α" phase.

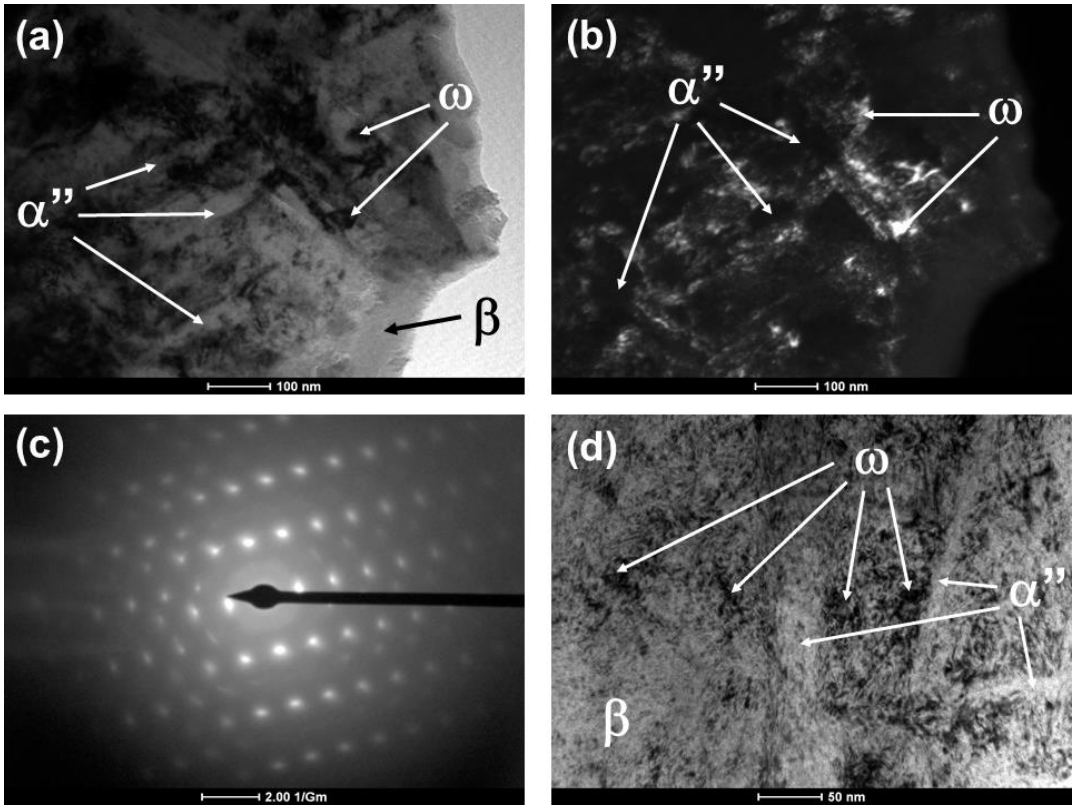


Figure 8.5. TEM images for Ti-25Ta-30Zr alloy after annealing with rapid cooling: bright-field (a), dark-field (b), diffraction of the selected area(c) and high-resolution image (d).

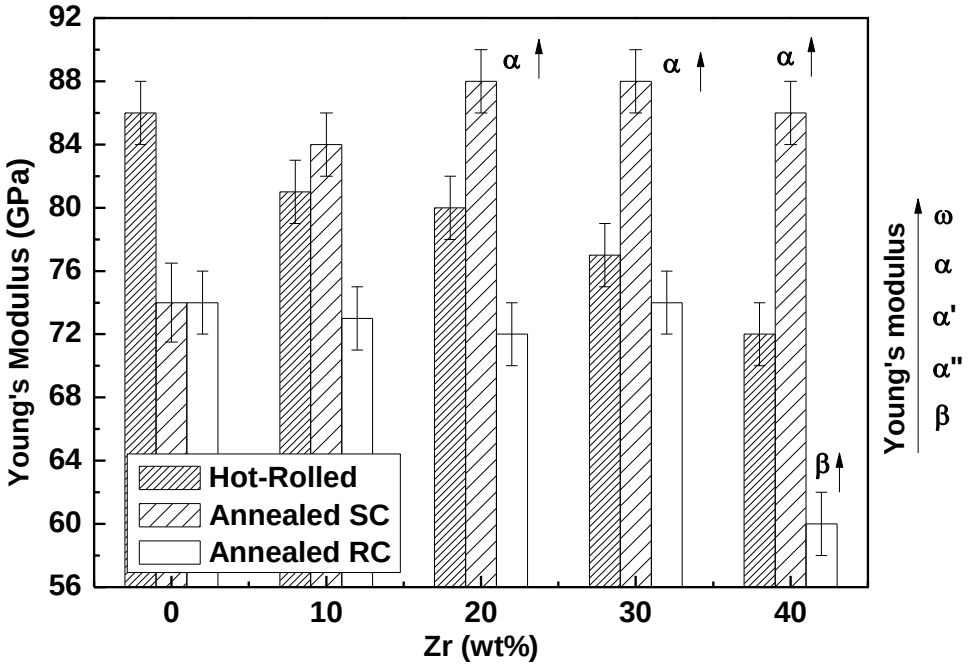


Figure 8.6. Young's modulus for Ti-25Ta-Zr system alloys, in all studied conditions.

In Ti-25Ta-30Zr alloy after hot-rolling, the α" and β phases coexist; the micrographs exhibit an equiaxial structure of very fine needles distributed in some β-type distorted grains. After annealing with slow cooling, there was an increase in grain size and the α phase needles could be in grain boundaries. In annealing with water cooling, grains of the β-matrix can be observed, with small α" phase precipitates.

In the alloy with 40wt% of zirconium, it is possible to observe small grains of the material, with morphology characteristic of the β phase, in the after hot-rolling condition. The annealing treatments promoted the growth of these grains. Typical structures of the martensites are difficult to see in micrographs, although the x-ray diffractograms showed peaks of the α 'and α" phases.

A major problem in the manufacture of titanium prostheses is the mechanical conformation. A biomedical material must be easily shaped to facilitate its handling to produce screws, plates, and other shapes. The microhardness of a material indicates whether it conforms easily (low hardness value) or is a hard, brittle material. Further, biocompatible alloys must have a hardness appropriate to their specific application, because if they have very high hardness in relation to the implanted tissue, it can result in rapid tissue wear. Thus, many studies evaluate the microhardness in titanium alloys, with respect to heat treatments, processing and the microstructure [39; 40; 41; 42; 43].

Figure 8.4 shows the hardness values for each process performed in the samples of Ti-25Ta-Zr alloys included in this study. According to the literature, among the phases formed in titanium alloys, the ω phase presents the greatest hardness value, followed by the α, α', α" and β [44; 45; 46]. Other studies report that β-type alloys may have a greater hardness level than mastensitic phases α' and α", because they have a stronger solid solution due to phase stability (ω > α' > α" > β > α) [47].

As can be observed, after the hot-rolling process the alloys have an equal or lower hardness value, compared to the values of annealed alloys with slow cooling. From the x-ray diffractograms, it is possible to visualize the effect of hot-rolling, heat treatment and zirconium substitution in the structure of the material. After the hot rolling, there is a formation of the α" phase for the alloys with zirconium up to 20%, and in those above 30% of zirconium, the β phase coexists with the α" phase. The annealing alleviated the internal stress from the mechanical process and modified the α" to the α phase in the alloys undergoing slow cooling. As mentioned above, α type titanium alloys have greater hardness compared to α" alloys. Consequently, the alloys in the hot-rolled condition tend

to have a lower hardness value compared to the annealed alloys with a slow cooling rate [47].

Ti-25Ta-30Zr and Ti-25Ta-40Zr alloys annealed with slow cooling have high hardness values (~ 425 HV). This increase can also be explained by the presence of the α and β phases which may be an obstacle to the dislocations motion.

From hardness measurements, it can be seen that for the lower (SC) cooling rate (5 K/s) condition, there is the formation of β + α phases for all the compositions. For water quenched (RC) condition after heat treatment, it might form precipitates of athermal ω phase due to higher hardness values (from 10 to 30%Zr) reached, but in a lower fraction than SC samples. For rapid cooling condition (RC) resulted in a greater stabilization of β phase for higher zirconium content (40%Zr) suppressing as well ω phase and decreasing hardness value.

It was observed that the hardness of the hot-rolled alloys and the alloys subjected to the annealing treatment with fast cooling have similar values. The alloys in these two conditions have the same crystalline structure (α" and β), and therefore their mechanical characteristics are similar. Only in the Ti-25Ta-30Zr alloy (with α" and β phases), there is an "anomaly" with reference to the hardness value. This high hardness value can be an indication of the formation and highest precipitation of the ω phase in this alloy, as the fast cooling can retain the ω phase, which has the characteristic of hardening and weakening the material.

Due to the high hardness of the Ti-25Ta-30Zr alloy subjected to rapid cooling, a more detailed analysis of the microstructure of the material was performed to see the ω phase as the enhancer. Figure 8.5 shows the bright and dark field images of TEM, a bright field (BF) image and the selected area diffraction pattern (SAD) showing fine martensite α" phase needles with a width of approximately 50 nm dispersed in a β phase (bcc) matrix. Nanoscale precipitates of athermal ω phase from 5 to 20 nm are visualized in the TEM micrographs; their nucleation and precipitation are located close to the α" phase structures. Such athermal ω phase formation occurs in α + β type alloys and when such alloys are subjected to rapid cooling from high temperatures. Due to the precipitation of w phase, Ti-25Ta-30Zr alloy submitted to rapid cooling, showed a high value of hardness, as indicated in Figure 8.4 [48; 49].

Figure 8.6 shows the values of the dynamic elastic modulus of the samples of all Ti-25Ta-Zr alloys used in this study, under all investigated conditions. In this figure, it can

be observed that Young's modulus of the alloys studied after hot-rolled condition was approximately 86 GPa for the non-zirconium alloy and reached a minimum value of 72 GPa for the alloy with the highest zirconium content (40 wt%). After hot-rolling, there is an increase in the percentage of the β phase, which decreases the elastic modulus, since the β phase has the smallest modulus value among the phases in titanium alloys. The hot-rolling process generates a high cooling rate when the sample is passed through the mill roller, retaining the β phase.

Annealing with slow cooling, by contrast, increased the value of Young's modulus with the addition of zirconium. The treatment decreased the percentage of the β phase and modified the α" to α phase due to the recrystallization of the sample. The alloys with the α phase have higher elastic modulus values than α" alloys. Annealing with rapid cooling decreased the modulus of these alloys, as this type of treatment at high temperatures and rapid cooling induces the formation of the β phase, which has the lowest modulus value in titanium alloys. The Ti-25Ta-40Zr alloy has the lowest modulus of the studied alloys of E = 60 GPa.

It can be noted by the hot-rolled condition, that increasing zirconium fraction leads to decreasing of elastic modulus 86 down to 72 (GPa), due to a combination of stress-induced martensite formation and β phase stabilization with suppression of ω formation. Evaluating the elastic modulus E (GPa), for lower cooling rate, lead to a tendency like hardness measurements, where the appearance of the alpha phase in high zirconium alloys leads to an increase in mechanical property values, increasing modulus from 74 to 88 GPa. Comparing with rapid cooling condition the modulus just decreased significantly from 74 down to around 60 GPa for higher zirconium content (40%) due greater stabilization of β phase suppressing as well ω phase precipitation.

The Ti-25Ta-xZr alloys produced in the annealed condition with fast cooling have a better modulus compared to Ti-cp and other commercial biomedical metals, such as Ti-6Al-4V, 316L and Co-Cr [12]. Among the produced alloys in this study, the Ti-25Ta-40Zr has the lowest elastic modulus value (60 ± 2) GPa, which represents twice the modulus of elasticity of human cortical bone [50].

Conclusions

The results detailed above lead to the following conclusions:

- X-ray diffraction and microscopy reveal that the crystalline structure of the alloys was sensitive to the addition of zirconium and sensitive to thermomechanical treatments;
- The zirconium acted as a β-stabilizing element combined with tantalum in Ti-25Ta-xZr alloys;
- Alloys subjected to a slow-cooling annealing heat treatment have the α phase in the crystalline structure.
- The alloys subjected to a fast-cooling annealing heat treatment have the α" phase, can retain the β phase with high zirconium content and rapid cooling precipitates the omega phase, but high levels of zirconium suppress this phase;
- Hardness increased due to solid solution hardening and due to α-phase precipitation in alloys subjected to slow-cooling annealing heat treatment; athermal ω phase precipitates harden materials;
- The Young's modulus decreases with high levels of zirconium due to the stabilization of the β phase;
- The thermomechanical process and heat treatment with rapid cooling retain the β phase, improving mechanical biocompatibility with the decreasing of elastic modulus values of the materials down to E = 60 GPa for Ti-25Ta-40Zr alloy.

References

1 MEYERS, M. A. et al. Biological materials: Structure and mechanical properties. **Progress in Materials Science,** v. 53, n. 1, p. 1-206, 2008.
2 NOUMBISSI, S.; SCARANO, A.; GUPTA, S. A Literature Review Study on Atomic Ions Dissolution of Titanium and Its Alloys in Implant Dentistry. **Materials,** v. 12, n. 3, p. 368, 2019.
3 RATNER, B. D.; BRYANT, S. J. Biomaterials: Where We Have Been and Where We Are Going. **Annual Review of Biomedical Engineering,** v. 6, n. 1, p. 41-75, 2004.
4 NIINOMI, M. Biologically and Mechanically Biocompatible Titanium Alloys. **Materials Transactions,** v. 49, n. 10, p. 2170-2178, 2008.
5 GEETHA, M. et al. Ti based biomaterials, the ultimate choice for orthopaedic implants - A review. **Progress in Materials Science,** v. 54, n. 3, p. 397-425, 2009.
6 ZHOU, Y. L.; NIINOMI, M.; AKAHORI, T. Effects of Ta content on Young's modulus and tensile properties of binary Ti–Ta alloys for biomedical applications. **Materials Science and Engineering: A,** v. 371, n. 1, p. 283-290, 2004.
7 LEE, Y. T.; WELSCH, G. Young's modulus and damping of Ti□6Al□4V alloy as a function of heat treatment and oxygen concentration. **Materials Science and Engineering: A,** v. 128, n. 1, p. 77-89, 1990.
8 FROES, F. H. Titanium Alloys: Thermal Treatment and Thermomechanical Processing. In: EDITORS-IN-CHIEF: , K. H. J. B.;ROBERT, W. C., *et al* (Ed.).

Encyclopedia of Materials: Science and Technology (Second Edition). Oxford: Elsevier, 2001. p. 9369-9373.

9 WEISS, I.; SEMIATIN, S. L. Thermomechanical processing of beta titanium alloys—an overview. **Materials Science and Engineering: A,** v. 243, n. 1, p. 46-65, 1998.

10 LÜTJERING, G.; WILLIAMS, J. C.; GYSLER, A. Microstructure and Mechanical Properties of Titanium Alloys. In: (Ed.). **Microstructure and Properties of Materials**, 1998. p.1-77.

11 OLDANI, C.; DOMINGUEZ, A. Titanium as a Biomaterial for Implants. In: FOKTER, S. K. (Ed.). **Recent Advances in Arthroplasty**. Croatia: IntechOpen, 2012. cap. 9, p.149-162.

12 KAUR, M.; SINGH, K. Review on titanium and titanium based alloys as biomaterials for orthopaedic applications. **Materials Science and Engineering: C,** v. 102, p. 844-862, 2019.

13 KOLLI, R.; DEVARAJ, A. A Review of Metastable Beta Titanium Alloys. **Metals,** v. 8, n. 7, p. 506, 2018.

14 KIRMANIDOU, Y. et al. New Ti-Alloys and Surface Modifications to Improve the Mechanical Properties and the Biological Response to Orthopedic and Dental Implants: A Review. **BioMed Research International,** v. 2016, p. 21, 2016.

15 LI, Y. et al. New Developments of Ti-Based Alloys for Biomedical Applications. **Materials,** v. 7, n. 3, p. 1709-1800, 2014.

16 WANG, W.; POH, C. K. Titanium Alloys in Orthopaedics. In: (Ed.). **Titanium Alloys - Advances in Properties Control**. Rijeka: InTech, 2013. cap. 1, p.1-20.

17 ZHOU, Y.-L.; NIINOMI, M. Ti–25Ta alloy with the best mechanical compatibility in Ti–Ta alloys for biomedical applications. **Materials Science and Engineering: C,** v. 29, n. 3, p. 1061-1065, 2009.

18 WANG, K. The use of titanium for medical applications in the USA. **Materials Science and Engineering: A,** v. 213, n. 1-2, p. 134-137, 1996.

19 CORREA, D. R. N.; KURODA, P. A. B.; GRANDINI, C. R. Structure, Microstructure, and Selected Mechanical Properties of Ti-Zr-Mo Alloys for Biomedical Applications. **Advanced Materials Research,** v. 922, p. 75-80, 2014.

20 CORREA, D. R. N. et al. Effect of the substitutional elements on the microstructure of the Ti-15Mo-Zr and Ti-15Zr-Mo systems alloys. **Journal of Materials Research and Technology,** v. 4, n. 2, p. 180-185, 2015.

21 ARAÚJO, R. O. D.; BUZALAF, M. A. R.; GRANDINI, C. R. Preparation and Characterization of Ti-10Mo-xZr Alloys for Biomedical Applications. **Materials Science Forum,** v. 869, p. 940-945, 2016.

22 KURODA, P. A. B.; BUZALAF, M. A. R.; GRANDINI, C. R. Effect of molybdenum on structure, microstructure and mechanical properties of biomedical Ti-20Zr-Mo alloys. **Materials Science and Engineering: C,** v. 67, p. 511-515, 2016.

23 CORREA, D. R. N. et al. Development of Ti-15Zr-Mo alloys for applying as implantable biomedical devices. **Journal of Alloys and Compounds,** v. 749, p. 163-171, 2018.

24 CORREA, D. R. N. et al. Microstructure and selected mechanical properties of aged Ti-15Zr-based alloys for biomedical applications. **Materials Science and Engineering: C,** v. 91, p. 762-771, 2018

25 CUI, C. et al. Titanium alloy production technology, market prospects and industry development. **Materials & Design,** v. 32, n. 3, p. 1684-1691, 2011.

26 YAN, L. et al. Improved mechanical properties of the new Ti-15Ta-xZr alloys fabricated by selective laser melting for biomedical application. **Journal of Alloys and Compounds,** v. 688, p. 156-162, 2016.
27 BIESIEKIERSKI, A. et al. Extraordinary high strength Ti-Zr-Ta alloys through nanoscaled, dual-cubic spinodal reinforcement. **Acta Biomaterialia,** v. 53, p. 549-558, 2017.
28 QUADROS, F. D. F. et al. Preparation, structural and microstructural characterization of Ti-25Ta-10Zr alloy for biomedical applications. **Journal of Materials Research and Technology**, v. 8, p. 4108-4114, 2019.
29 KURODA, P. A. B.; BUZALAF, M. A. R.; GRANDINI, C. R. Preparation, microstructural characterization, and selected mechanical properties of Ti-20Zr-2.5Mo and Ti-20Zr-7.5Mo used as biomaterial. **Materials Science Forum,** v. 869, p. 946-951, 2016.
30 KURODA, P. A. B. et al. Preparation, Structural, Microstructural, Mechanical and Cytotoxic Characterization of As-Cast Ti-25Ta-Zr Alloys. **Journal of Materials Science: Materials in Medicine**, v. 31, article 19, 2020.
31 KURODA, P. A. B. et al. Thermomechanical treatments influence on the phase composition, microstructure, and selected mechanical properties of Ti–20Zr–Mo alloys system for biomedical applications. **Journal of Alloys and Compounds**, p. 152108, 2019.
32 LUZ, A. R. et al. Characterization of the morphology, structure and wettability of phase dependent lamellar and nanotube oxides on anodized Ti-10Nb alloy. **Applied Surface Science,** v. 448, p. 30-40, 2018.
33 COLLINGS, E. W. **The Physical Metallurgy of Titanium Alloys**. Ohio: ASM International, 1989.
34 ASTM. **E92-82 - Standard Test Method for Vickers Hardness of Metallic Materials**. E92-82 - Standard Test Method for Vickers Hardness of Metallic Materials. West Conshohocken, PA: ASTM International. E92-82 2003.
35 _____. **E1876–01 - Standard Test Method for Dynamic Young's Modulus, Shear Modulus, and Poisson's Ratio by Impulse Excitation of Vibration**. E1876–01 - Standard Test Method for Dynamic Young's Modulus, Shear Modulus, and Poisson's Ratio by Impulse Excitation of Vibration. Philadelphia (USA): ASTM International. E1876–01 2002.
36 GRAY, G. T.; MORRIS, C. E.; LAWSON, A. C. **Omega Phase Formation in Titanium and Titanium Alloys**. Los Alamos National Laboratory, p. 1-9, 1992.
37 TANE, M. et al. ω Transformation in cold-worked Ti–Nb–Ta–Zr–O alloys with low body-centered cubic phase stability and its correlation with their elastic properties. **Acta Materialia,** v. 61, n. 1, p. 139-150, 2013.
38 DAVIS, R.; FLOWER, H. M.; WEST, D. R. F. The decomposition of Ti-Mo alloy martensites by nucleation and growth and spinodal mechanisms. **Acta Metallurgica,** v. 27, n. 6, p. 1041-1052, 1979.
39 CALLISTER JR., W. D. **Fundamentos da Ciência e Engenharia de Materiais**. 2ª ed. Rio de Janeiro: LTC, 2006.
40 HO, W. F.; JU, C. P.; CHERN LIN, J. H. Structure and properties of cast binary Ti–Mo alloys. **Biomaterials,** v. 20, n. 22, p. 2115-2122, 1999.
41 DELVAT, E. et al. Microstructure, mechanical properties and cytocompatibility of stable beta Ti-Mo-Ta sintered alloys. **J Mech Behav Biomed Mater,** v. 1, n. 4, p. 345-51, 2008.

42 KAO, Y. L. et al. A study on the hardness variation of α- and β-pure titanium with different grain sizes. **Materials Science and Engineering: A,** v. 398, n. 1, p. 93-98, 2005.
43 SUKEDAI, E. et al. Aging behavior of Ti–Mo alloys heavily compressed in ultra-high strain rate mode. **Materials Science and Engineering: A,** v. 387, n. Supplement C, p. 249-253, 2004.
44 LEYENS, C.; PETERS, M. **Titanium and Titanium Alloys: Fundamentals and Applications**. New York: Wiley-VCH, 2005.
45 ZHOU, Y.-L.; NIINOMI, M. Microstructures and mechanical properties of Ti–50 mass% Ta alloy for biomedical applications. **Journal of Alloys and Compounds,** v. 466, n. 1–2, p. 535-542, 2008.
46 GABRIEL, S. B. et al. Maximisation of the ratio of microhardness to the Young's modulus of Ti–12Mo–13Nb alloy through microstructure changes. **Materials Science and Engineering: C,** v. 33, n. 6, p. 3319-3324, 2013.
47 LEE, C. M.; JU, C. P.; CHERN LIN, J. H. Structure–property relationship of cast Ti–Nb alloys. **Journal of Oral Rehabilitation,** v. 29, n. 4, p. 314-322, 2002.
48 ALEIXO, G. T. et al. Effects of Cooling Rate and Sn Addition on the Microstructure of Ti-Nb-Sn Alloys. **Solid State Phenomena,** v. 172-174, p. 190-195, 2011.
49 AFONSO, C. R. M.; CHAVES, J. M.; FLORÊNCIO, O. Effect of Rapid Solidification on Microstructure and Elastic Modulus of β Ti–xNb–3Fe Alloys for Implant Applications. **Advanced Engineering Materials,** v. 19, n. 6, p. 1600370, 2017
50 WU, D. et al. Young's modulus of trabecular bone at the tissue level: A review. **Acta Biomaterialia,** v. 78, p. 1-12, 2018.

Capítulo 9

Submitted to Journal of Materials Engineering and Performance, 2019.

The effect of solution heat treatment on phase transformations, microstructure and properties of Ti-25Ta-xZr alloys used as a biomaterial

Pedro Akira Bazaglia Kuroda [1,2], Fernanda de Freitas Quadros [1,2], Conrado Ramos Moreira Afonso [3] and Carlos Roberto Grandini [1,2]

[1] UNESP – Univ. Estadual Paulista, Laboratório de Anelasticidade e Biomateriais, 17.033-360, Bauru, SP, Brazil

[2] IBTN/BR – Brazilian Branch Institute of Biomaterials, Tribocorrosion and Nanomedicine, 17.033-360, Bauru, SP, Brazil

[3] UFSCar – Universidade Federal de São Carlos, Department of Materials Engineering (DEMa), 13.565-905, São Carlos, SP, Brazil

Abstract

This paper describes a study of the effect of solution heat treatment temperature (500, 750 and 1000 °C) on the phase transformations, microstructure, microhardness and Young's modulus of Ti-25Ta-*x*Zr alloys, aimed at biomedical applications. The Ti-25Ta-*x*Zr alloys ingots were melted in an arc-furnace with five different compositions (*x* = 0, 10, 20 30 and 40wt.%) in order to produce samples with α", α"+β and β phase. The results showed that both the microstructure and mechanical properties of the studied alloys can be tailored according to the temperatures used for solution in the Ti-25Ta-*x*Zr system. Usually, higher solution heat treatment temperatures increase hardness due to the higher phase stabilization in single phase alloys, while in the α”+ β alloys or predominantly β, hardness decreases due to the suppression of phase α”. However, the elastic modulus of

the alloys decreases when solution heat treatment is performed at 1000 °C. In general, solution heat treatment performed at higher temperatures stabilize more the β phase, improving to lower modulus of the alloys.

Introduction

Due to advanced technological development coupled with increased life expectancy, diseases related to skeletal dysfunctions are increasingly common in the medical setting. To work around this problem and improve quality of life, new biomedical materials need to be developed to meet humans' physical and biological needs. In orthopedics, metals are the most suitable materials for use in bone repair treatments when mechanical stresses are required at the injured site. Among the metallic materials, three groups of alloys stand out: stainless steel, cobalt and chrome alloys, and titanium and its alloys. From these three groups, titanium and its alloys exhibit greater biocompatibility, higher corrosion resistance and good tensile strength ratio. Co-Cr alloys have the highest wear resistance compared to stainless steel and titanium alloys, while stainless steels generally have higher ductility and torsional strength [1; 2; 3].

Unfortunately, metal implants have been shown to fail after long-term use due to their high modulus of elasticity compared to bone[4]. If there is a big difference in the elastic modulus between the bone and the implant, a phenomenon called stress shielding can occur. When the implant has higher elastic modulus than the bone, the material possesses a greater load absorption capacity, reducing the load that is applied directly to the bone. This is because, according to Wolff's Law, human bone models itself according to the loads that are applied to it. If the load value decreases, the loading on a bone decreases, and the bone becomes more fragile and less dense[5].

Ti-Ta and Ti-Zr alloys have high potential to be used as biomaterials; several studies in the literature report that tantalum and zirconium are elements that, in a solid solution, enhance the characteristics of titanium as a biomedical material[6; 7; 8; 9; 10; 11; 12]. Tantalum and zirconium are not known to be toxic elements in the human body[13; 14], and they improve mechanical properties and increase the corrosion resistance in body fluids[15; 16]; however, little is known about the Ti-Ta-Zr ternary system. Tantalum is expected to aid in the β phase stabilization [8]and zirconium is considered a neutral element in the Ti-Zr binary system[17], but it helps in the β phase stabilization in ternary alloys, when this alloy has an element with a body-centered cubic structure[18].

Several studies have sought to improve the mechanical properties of titanium alloys through heat treatments[19; 20; 21; 22; 23; 24; 25]. In this paper, several alloys were subjected to heat treatments of solution, aging and mechanical conformation. The results of these experiments indicate that slow cooling treatments generally provide favorable thermodynamic conditions for precipitation of the α' and α" phases; that rapid cooling from the β field promotes greater stability of the β phase and, that rapid cooling from the α + β field induces metastable martensitic phases precipitation (α', α" and ω).

The objective of this paper was to analyze the influence of temperature of solution heat treatments on the crystalline phases, microstructure, microhardness and elastic modulus of the Ti-25Ta-*x*Zr alloys system, with varied zirconium content (*x* =0, 10, 20, 30 and 40wt.%) for applications as metallic biomaterials.

Experimental Procedure

The melting of the ingots was performed in an arc-furnace[26; 27; 28; 29], and the processing of the samples was performed by hot-rolling at 1000 °C. After these steps, 6h thermal solution treatments were performed at temperatures of 500, 750 and 1000 °C, followed by water cooling.

The x-ray diffraction (XRD) measurements were performed on a Malvern Panalytical X'Pert PRO. The following parameters were used: Cu-K_α radiation (λ = 1.544 Å), 40 mA current, 45 kV potential and continuous time mode. To analyze the diffraction results, we used the crystallographic data sheets from the Inorganic Crystal Structure Database (ICSD).

An Olympus BX51M model optical microscope was used for optical micrographs and, the scanning electron microscopy (SEM) measurements were performed with a Carl Zeiss microscope, EVO-015 model, and transmission electron microscopy (TEM) analysis were performed on a FEI Tecnai G^2 F20 200 kV equipped with a field emission gun (FEG), coupled to energy dispersive spectroscopy (EDS) microanalysis detector EDAX DX-4.

For hardness measurements, a Shimadzu HMV-2 model microdurometer was used. In the samples, 5 indentations were performed with a force of 0.245 N and load of 25 g with duration of 60 s[30]. For the elastic modulus measurements, a Sonelastic® equipment was used, with the measurements based on the impulse excitation technique[31].

Results and Discussion

The x-ray diffractograms, together with the micrographs of the Ti-25Ta sample, are shown in Fig. 1. In the XRD diffractograms, it can be observed that only peaks corresponding to the α" phase have been identified, only for the alloy subjected to 500 °C has the α phase. The increase in the heat treatments temperature promoted changes in the x-ray diffraction patterns, such as differences in intensity; as seen from the angle of 38°, α" peak disappears with increasing temperature. For the 500°C condition, this temperature is probably below the Ti-25Ta alloy β-transus temperature, because of this in this solubilization condition the alloy has only the α phase. In the micrographs, the needle-like structures associated with α and α" phase increase in width when the alloy is subjected to high temperatures. Such changes in structure and microstructure are related to changes in phase, lattice parameters of α" phases and the crystallite size of samples, as high temperatures tend to increase crystallite size due to diffusion [32].

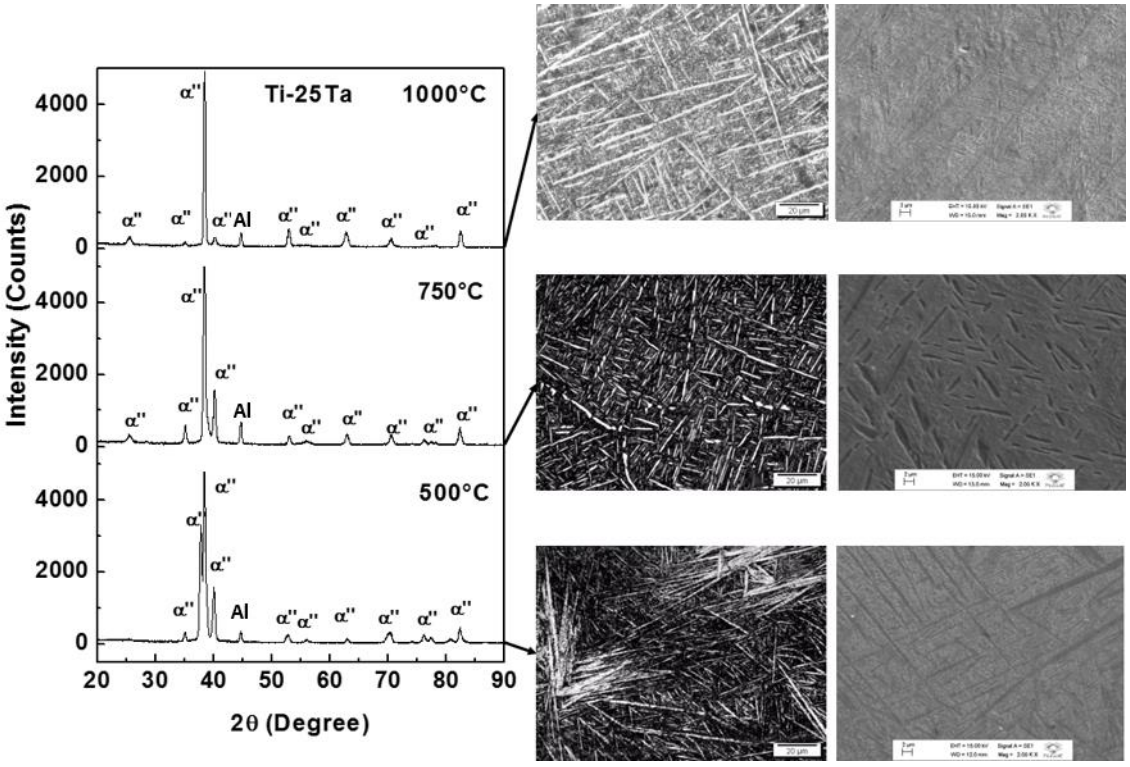


Figure 9.1. X-ray diffraction patterns and, optical and SEM micrographs for Ti-25Ta alloys.

In the Ti-25Ta-10Zr alloy, only peaks corresponding to α" phase were identified, too, as shown in Figure 9.2. It is again observed that the temperature was able to change the diffraction pattern of the alloys, like the Ti-25Ta alloy. With an increase in temperature, it was observed that the intensity of the peaks, referring to the α" phase, increased in intensity and that there was a decrease in the width of these peaks. From the

microscopic images, a typical α" martensitic structure, composed by small intra-grain located needles, can be seen.

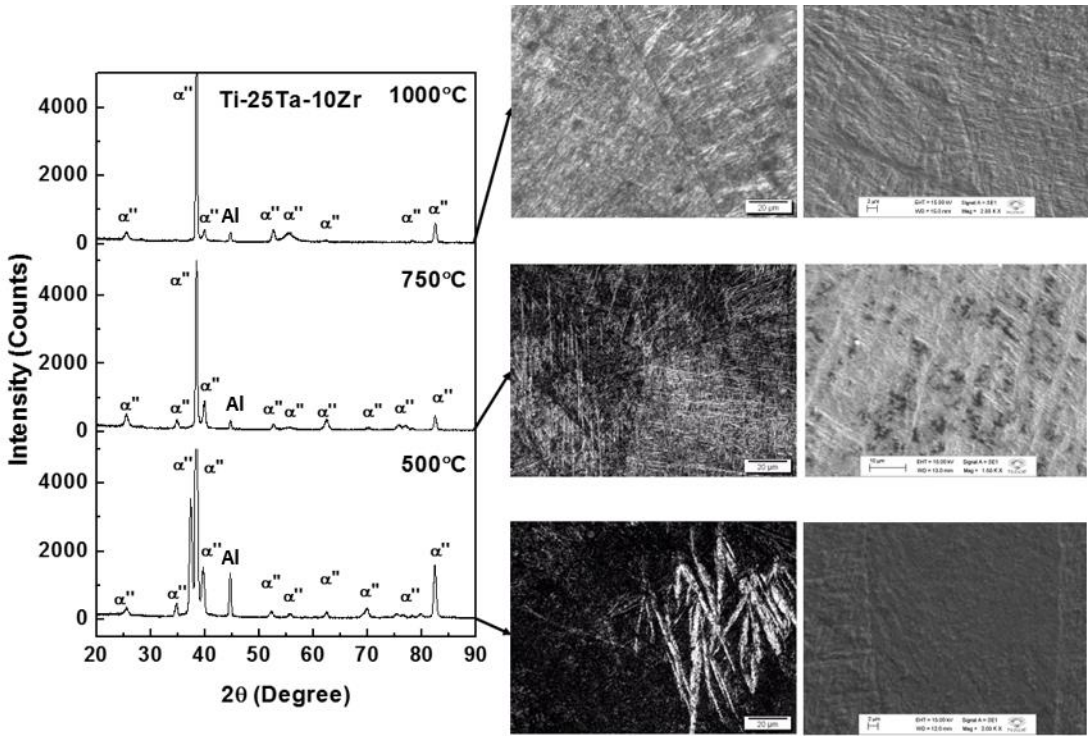


Figure 9.2. X-ray diffraction patterns and, optical and SEM micrographs of the Ti-25Ta-10Zr alloys.

The structural and microstructural results for the Ti-25Ta-20Zr alloy are shown in Figure 9.3. In this case, were identified the peaks associated with α" and β phases. The x-ray patterns were modified with the heat treatments, and the peaks of the α" phase decrease in intensity or disappear at higher temperatures. From the microscopic images, a typical martensitic structure associated with α" and grain boundariesof β phase matrix can be seen. The micrographs were not changed due to the different solution heat treatments performed in the Ti-25Ta-20Zr alloy.

In the XRD diffractograms showed in Figures 9.4 and 9.5, it is possible to observe that the α" and β phases were identified in the Ti-25Ta-30Zr and Ti-25Ta-40Zr alloys. The x-ray patterns were modified with the heat treatments that the samples were submitted, and it is possible to observe that the peaks related to the β phase become more refined and intense when the alloys were subjected to high temperature heat treatments. The micrographs of Ti-25Ta-30Zr show that there was a decrease in the martensitic α" phase structures present in the middle of the grain with the increase of the solution heat treatment temperature and that the alloys of the α+β phase type, submitted to high solution

heat treatment temperatures tend to have a larger β phase volume fraction. Microscopy images show only grain boundaries from the β phase matrix for the alloy with 40 wt% of zirconium.

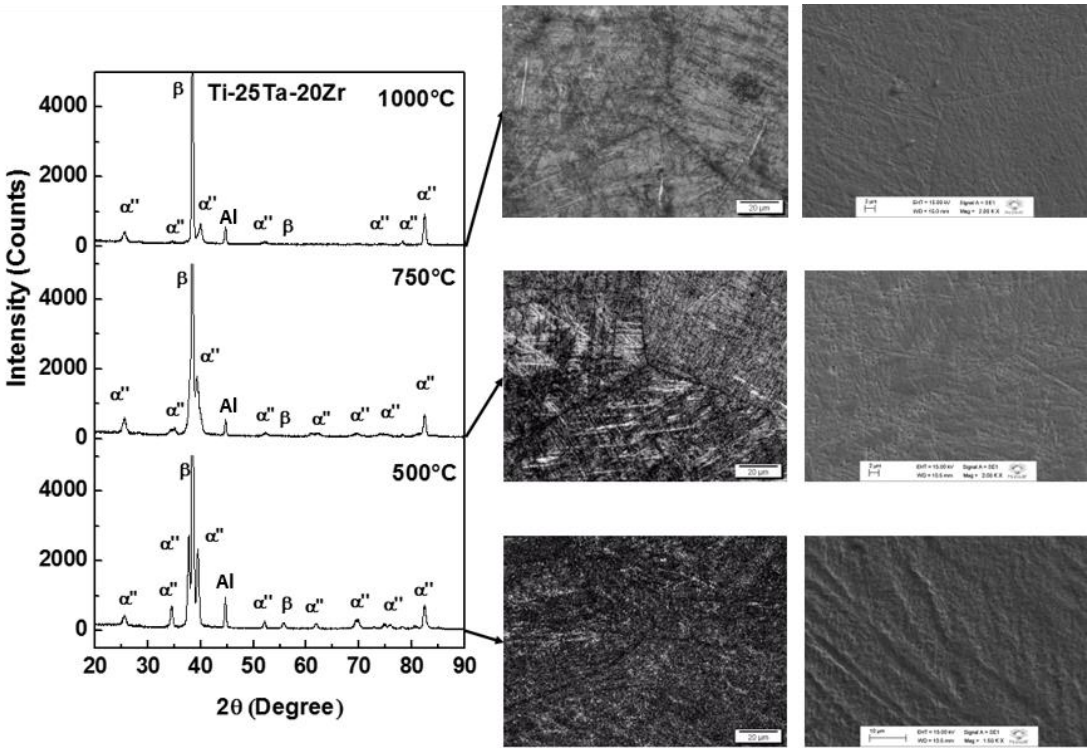


Figure 9.3. X-ray diffraction patterns and, optical and SEM micrographs of the Ti-25Ta-20Zr alloys.

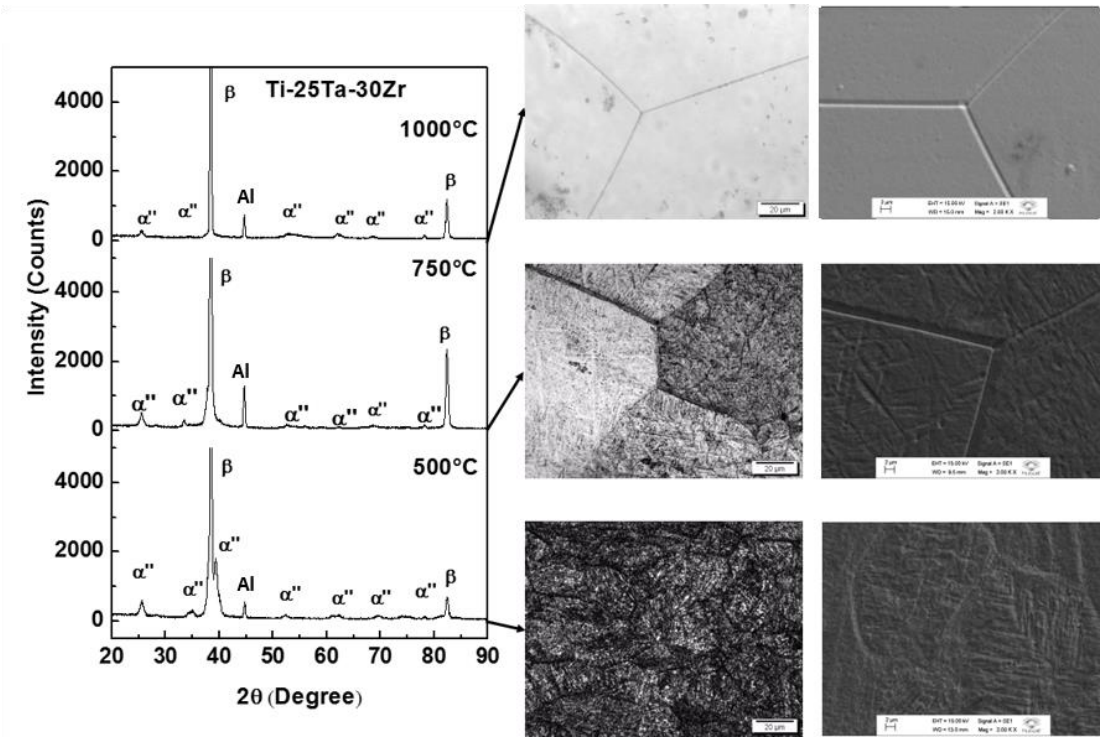


Figure 9.4. X-ray diffraction patterns and, optical and SEM micrographs of the Ti-25Ta-30Zr alloys.

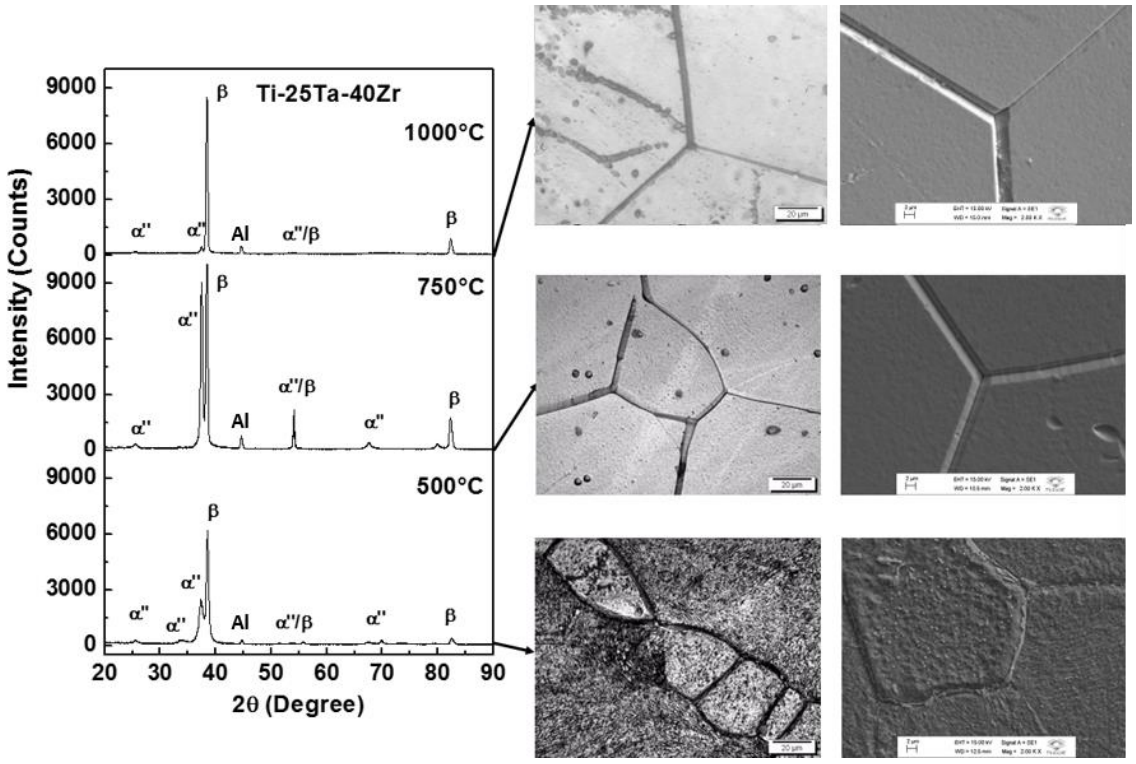


Figure 9.5. X-ray diffraction patterns and, optical and SEM micrographs of the Ti-25Ta-40Zr alloys.

Figure 9.6 shows the hardness values for each processing condition performed on the samples of each alloy used in this study. Among the phases formed in titanium alloys, the ω phase has the highest hardness value followed by the phases α, α ', α" and β[33].Ti-25Ta binary alloys have the lowest hardness value of the studied Ti-25Ta-Zr system alloys. This alloy has only the α" phase in its volume, and, according to Zhou et al. [34], the chemical composition of this alloy is close to the limit of the composition between the α' and α" phases. In this range, the crystalline lattice has a lower atomic density, decreasing the bond strength between the atoms and thus generating low hardness values. Two other factors that lead to the Ti-25Ta alloy having a lower hardness is that zirconium acts as a hardening element in the ternary system[35].Its absence eliminates this problem, and the Ti-25Ta alloy is a single-phase alloy with its low stability crystalline structure. The other alloys in the system are biphasic, and the distinct phases are barriers to dislocations motion [8].Only the Ti-25Ta-10Zr is single phase alloy, but the α" phase is more stable since zirconium helps stabilize the β phase.

In Ti-25Ta-10Zr alloy, the hardness value increased with the solution heat treatment temperature. It was observed that a higher treatment temperature may have

increased the stabilization of the α” phase. This can be seen in the x-ray diffraction with increased peaks relative to the α” phase and a decreased width of these peaks.

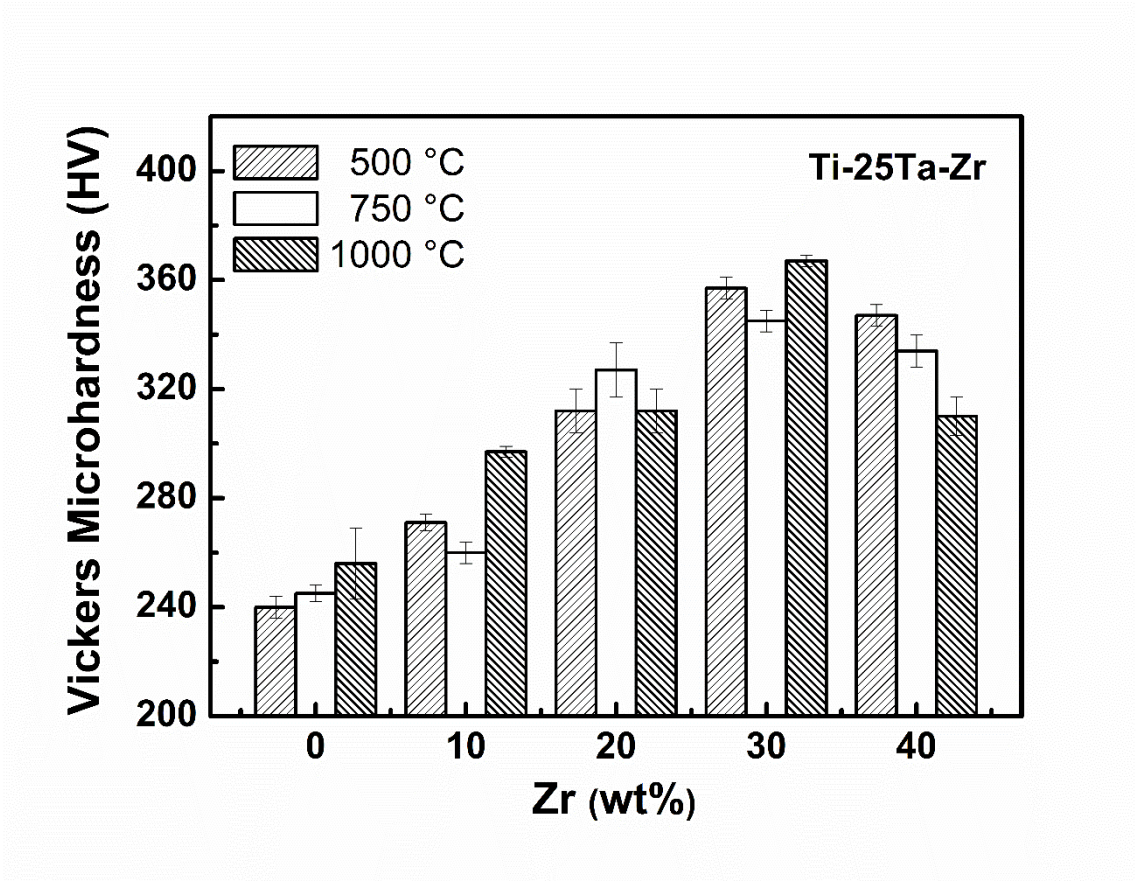


Figure 9.6. Microhardness values for Ti-25Ta-Zr alloys, after solution heat treatments.

The Ti-25Ta-20Zr, Ti-25Ta-30Zr and Ti-25Ta-40Zr alloys are biphasic and have high hardness values, as the addition of zirconium increases the volumetric fraction of the β phase and the barrier to atomic movement. The hardness value decreases with a 40 wt% of zirconium alloy due to the α” phase decreases [18; 36]. The temperature variation in the solution heat treatment did not change the hardness values of the alloys in a linear way; this can only be observed in the α” phase alloys, where the high solution heat treatment temperatures increase the hardness due to the higher phase stabilization. In the α”+β alloys, with β phase predominance, the hardness decreases due to the suppression of the α” phase.

Figure 9.7 shows that the elastic modulus of the studied alloys varied from 60 GPa up to 95 GPa, reaching the a minimum value for the alloy with the highest Zr content (Ti-25Ta-40Zr). A relation of the elastic modulus values with the increase of the solution heat treatment temperature was observed. The alloys subjected to high temperatures heat

treatment have better results (lower values) of elastic modulus for the biomedical area. On the other hand, alloys subjected to lower temperatures heat treatments showed highest elastic modulus values, in particular, Ti-25Ta-10Zr and Ti-25Ta-20Zr alloys. In the figure, it is possible to observe that Ti-25Ta-40Zr alloy stands out for having the best results of lowest modulus for all the temperatures (500, 750 and 1000ºC), reaching E = 76, 63 and 60 GPa, respectively. This alloy has the highest zirconium concentration, which stabilizes the β phase, and through this study, the high temperature solution heat treatment also induced β phase formation. This alloy demonstrated good mechanical property results for the use as biomaterial.

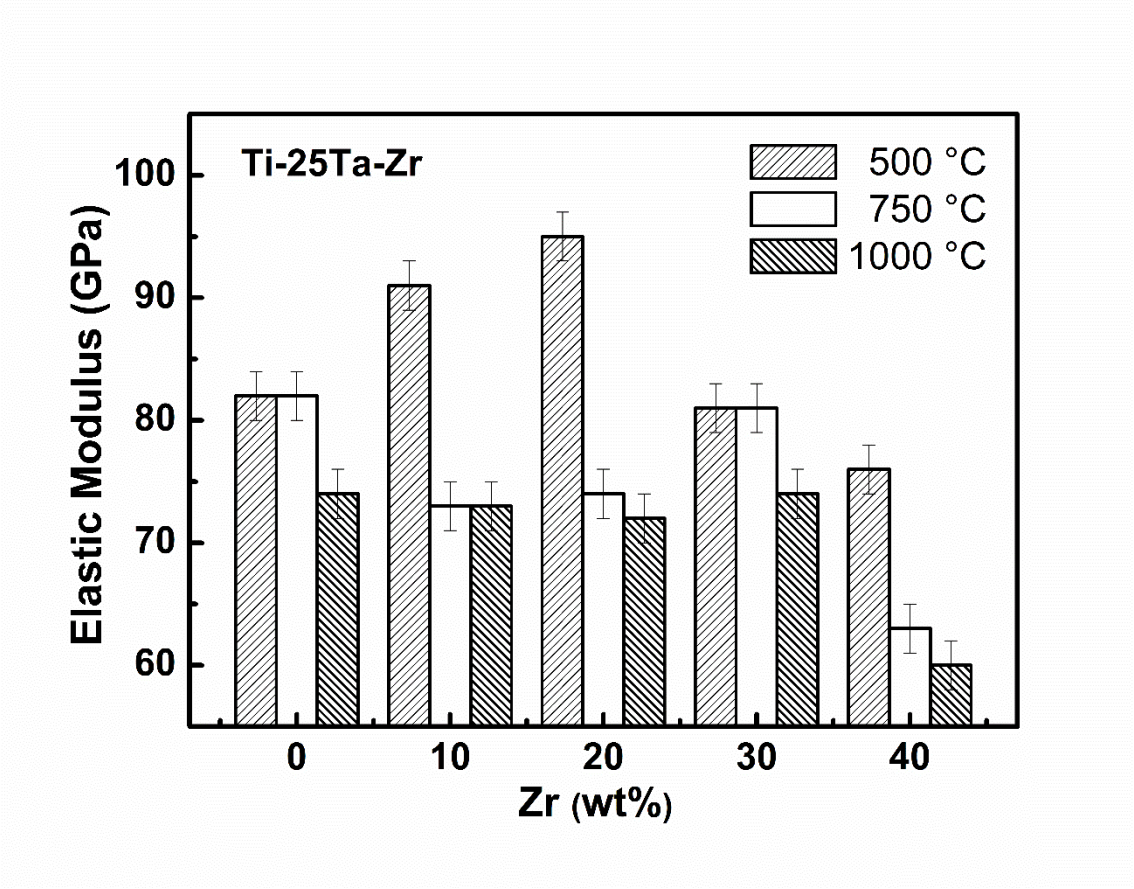


Figure 9.7. Elastic modulus values for Ti-25Ta-Zr alloys, after solution heat treatments.

Ti-25Ta-10Zr and Ti-25Ta-20Zr alloys submitted to solution at 500°C show high elastic modulus values (92 and 95 GPa, respectively) compared to other alloys and system conditions. This high elastic modulus should not be related only to the effect of the substitutive elements, but due to the phase precipitation as well. The precipitation of metastable nanoscale ω (omega) phase, which increases the elastic modulus, should be formed in these compositions (Zr = 10 and 20wt.%) and not in the others alloys. To

eliminate any question regarding that fact, a nanoscale analysis of the phases and structure of these alloys (Ti-25Ta-10Zr and Ti-25Ta-20Zr after solution heat treatment at 500°C was performed). Figure 9.8 shows TEM images of the bright field (BF), dark field (DF) and selected area electron diffraction (SAD) patterns, obtained by TEM analysis.

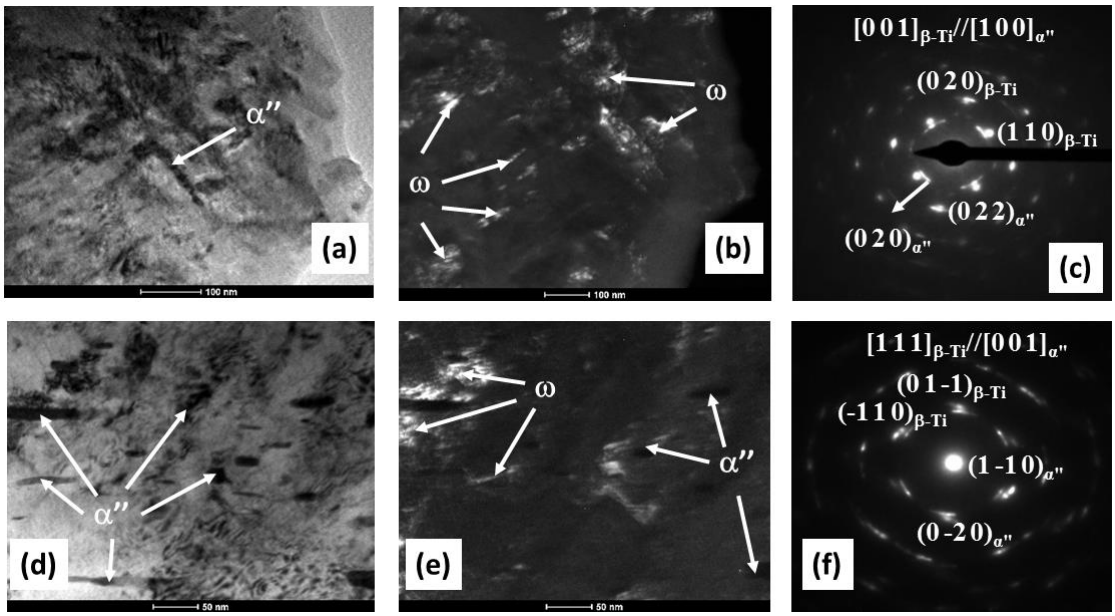


Figure 9.8. TEM images: a) bright field (BF), b) dark field (DF) and c) selected area electron diffraction (SAD) for Ti-25Ta-10Zr; and d) bright field (BF), e) dark field (DF) and f) SAD for Ti-25Ta-20Zr after solution heat treatment performed at 500 °C.

The results show the existence of the ω phase in the two alloys, represented as white scattered spots in the dark field (DF) images (b) and (e) [37; 38]. In the bright field images (a) and (d), it is possible to observe small needle-like structures of phase α" [39]. The ω phase is a nanometric phase that optical and scanning electron microscopy techniques are unable to detect[40]. This phase typically occurs during rapid quenching after solution heat treatment and/or aging at low temperatures and is termed athermal omega (ω_{ath}), which is characterized by the absence of atomic diffusion[41]. The detection of this ω phase in the Ti-25Ta-10Zr and Ti-25Ta-20Zr alloys after solution heat treatment performed at 500°C explains the high elastic modulus values in this condition, since the ω phase decreases the dislocations motion and increases internal stresses on the material, leading the material to a brittle and rigid behavior [42; 43].

Conclusions

- X-ray diffraction and microscopy results showed that the crystalline structure of the alloys was sensitive to zirconium addition and to solution heat treatment, confirming that Zr addition combined with other alloying elements can act as a β-stabilizing element;
- In the low content zirconium alloys, the presence of fine needles inside the β-Ti grains was verified. These structures are related to the α" phase; with the increase of the solution heat treatment temperature, there was a decrease in the quantity of these structures;
- Higher solution heat treatment temperatures lead to a greater β phase stabilization and the lower values of elastic modulus in the studied alloys;
- The temperature variation in the solution heat treatment did not change the hardness values of the alloys in a linear way; this can only be observed in α"type alloys. High solution heat treatment temperatures increase the hardness due to the higher phase stabilization, and in the α"+ β alloys, with β-Ti phase predominance, hardness decreases due to the suppression of α" phase;
- Hardness increases with the addition of zirconium due to solid solution hardening;
- The elastic modulus of Ti-25Ta-*x*Zr alloys decreases with increasing of zirconium contents due to β phase stabilization;
- The Ti-25Ta-*x*Zr alloy's elastic modulus decreases when the solution heat treatment is performed at 1000 °C;
- Treatment at lower treatment of 500 °C for 6 h followed by water quenching precipitates the nanoscale ω phase in the Ti-25Ta-10Zr and Ti-25Ta-20Zr alloys;
- The Ti-25Ta-40Zr alloy showed better mechanical compatibility with cortical bone.

References

1 NIINOMI, M.; NAKAI, M.; HIEDA, J. Development of new metallic alloys for biomedical applications. **Acta Biomaterialia,** v. 8, n. 11, p. 3888-3903, 2012.
2 LI, Y. et al. New Developments of Ti-Based Alloys for Biomedical Applications. **Materials,** v. 7, n. 3, p. 1709-1800, 2014.
3 KAUR, M.; SINGH, K. Review on titanium and titanium based alloys as biomaterials for orthopaedic applications. **Materials Science and Engineering: C,** v. 102, p. 844-862, 2019.
4 GEETHA, M. et al. Ti based biomaterials, the ultimate choice for orthopaedic implants – A review. **Progress in Materials Science,** v. 54, n. 3, p. 397-425, 2009.

5 NAGELS, J.; STOKDIJK, M.; ROZING, P. M. Stress shielding and bone resorption in shoulder arthroplasty. **Journal of Shoulder and Elbow Surgery,** v. 12, n. 1, p. 35-39, 2003.
6 ZHOU, Y. L.; NIINOMI, M.; AKAHORI, T. Effects of Ta content on Young's modulus and tensile properties of binary Ti–Ta alloys for biomedical applications. **Materials Science and Engineering: A,** v. 371, n. 1, p. 283-290, 2004.
7 MARECI, D. et al. Comparative corrosion study of Ti–Ta alloys for dental applications. **Acta Biomaterialia,** v. 5, n. 9, p. 3625-3639, 2009.
8 WU, C. Y. et al. Effects of Ta content on the phase stability and elastic properties of [beta] Ti-Ta alloys from first-principles calculations. **Solid State Sciences,** v. 12, n. 12, p. 2120-2124, 2010.
9 CORREA, D. R. N. et al. The effect of the solute on the structure, selected mechanical properties, and biocompatibility of Ti-Zr system alloys for dental applications. **Materials Science & Engineering C-Materials For Biological Applications,** v. 34, p. 354-359, 2014.
10 HAN, M.-K. et al. Effect of zirconium content on the microstructure, physical properties and corrosion behavior of Ti alloys. **Materials Science and Engineering: A,** v. 616, p. 268-274, 2014.
11 CORDEIRO, J. M. et al. Development of binary and ternary titanium alloys for dental implants. **Dental Materials,** v. 33, n. 11, p. 1244-1257, 2017.
12 LIU, X. et al. Binary titanium alloys as dental implant materials—a review. **Regenerative Biomaterials,** v. 4, n. 5, p. 315-323, 2017.
13 PARK, Y.-J. et al. Cytocompatibility of pure metals and experimental binary titanium alloys for implant materials. **Journal of Dentistry,** v. 41, n. 12, p. 1251-1258, 2013.
14 MARKHOFF, J. et al. Biocompatibility and Inflammatory Potential of Titanium Alloys Cultivated with Human Osteoblasts, Fibroblasts and Macrophages. **Materials,** v. 10, n. 1, p. 52, 2017.
15 ZHOU, Y. L. et al. Corrosion resistance and biocompatibility of Ti-Ta alloys for biomedical applications. **Materials Science and Engineering A,** v. 398, n. 1-2, p. 28-36, 2005.
16 GRANDIN, H. M.; BERNER, S.; DARD, M. A Review of Titanium Zirconium (TiZr) Alloys for Use in Endosseous Dental Implants. **Materials,** v. 5, n. 8, p. 1348, 2012.
17 CORDEIRO, J. M. et al. Characterization of chemically treated Ti-Zr system alloys for dental implant application. **Materials Science and Engineering: C,** v. 92, p. 849-861, 2018.
18 CORREA, D. R. N. et al. Effect of the substitutional elements on the microstructure of the Ti-15Mo-Zr and Ti-15Zr-Mo systems alloys. **Journal of Materials Research and Technology,** v. 4, n. 2, p. 180-185, 2015.
19 ZHOU, Y. L.; NIINOMI, M.; AKAHORI, T. Decomposition of martensite α″ during aging treatments and resulting mechanical properties of Ti−Ta alloys. **Materials Science and Engineering: A,** v. 384, n. 1, p. 92-101, 2004.
20 MARTINS, J. R. S.; GRANDINI, C. R. The Influence of Heat Treatment on the Structure and Microstructure of Ti-15Mo-xNb System Alloys for Biomedical Applications. **Materials Science Forum,** v. 783-786, p. 1255-1260, 2014.
21 CARDOSO, F. F. et al. Ti-Mo alloys employed as biomaterials: effects of composition and aging heat treatment on microstructure and mechanical behavior. **J Mech Behav Biomed Mater,** v. 32, p. 31-8, 2014.

22 WANG, K.; LI, M. Effects of heat treatment and hot deformation on the secondary α phase evolution of TC8 titanium alloy. **Materials Science and Engineering: A,** v. 613, p. 209-216, 2014.
23 CORREA, D. R. N. et al. Effect of Heat Treatment in the Structure and Microstructure of Ti-15Zr-XMo Alloys. **Defect and Diffusion Forum,** v. 365, p. 305-310, 2015.
24 LI, C. et al. Effect of solution heat treatment on the stress-induced martensite transformation in two new titanium alloys. **Journal of Alloys and Compounds,** v. 641, p. 192-200, 2015.
25 XAVIER, C. C. et al. Low temperature heat treatments on Ti-15Zr-xMo alloys. **Journal of Alloys and Compounds,** v. 727, p. 246-253, 2017.
26 KURODA, P. A. B. et al. Preparation, Structural, Microstructural, Mechanical and Cytotoxic Characterization of As-Cast Ti-25Ta-Zr Alloys. **Submitted to Journal of Materials Science: Materials in Medicine**, v. 31, article 19, 2020.
27 QUADROS, F. D. F. et al. Preparation, structural and microstructural characterization of Ti-25Ta-10Zr alloy for biomedical applications. **Journal of Materials Research and Technology,** v. 8, n. 5, p. 4108-4114, 2019.
28 KURODA, P. A. B. et al. Thermomechanical treatments influence on the phase composition, microstructure, and selected mechanical properties of Ti–20Zr–Mo alloys system for biomedical applications. **Journal of Alloys and Compounds**, p. 152108, 2019.
29 KURODA, P. A. B. et al. Effect of Thermomechanical Treatments on the Phases, Microstructure, Microhardness and Young's Modulus of Ti-25Ta-Zr Alloys. **Materials,** v. 12, n. 19, p. 3210, 2019.
30 ASTM. **E92-82 - Standard Test Method for Vickers Hardness of Metallic Materials**. E92-82 - Standard Test Method for Vickers Hardness of Metallic Materials. West Conshohocken, PA: ASTM International. E92-82 2003.
31 _____. **E1876–01 - Standard Test Method for Dynamic Young's Modulus, Shear Modulus, and Poisson's Ratio by Impulse Excitation of Vibration**. E1876–01 - Standard Test Method for Dynamic Young's Modulus, Shear Modulus, and Poisson's Ratio by Impulse Excitation of Vibration. Philadelphia (USA): ASTM International. E1876–01 2002.
32 PETERS, M. et al. Structure and Properties of Titanium and Titanium Alloys. In: (Ed.). **Titanium and Titanium Alloys**: Wiley-VCH Verlag GmbH & Co. KGaA, 2005. p.1-36. ISBN 9783527602117.
33 COLLINGS, E. W. **The Physical Metallurgy of Titanium Alloys**. Ohio: ASM International, 1989.
34 ZHOU, Y.-L.; NIINOMI, M. Ti–25Ta alloy with the best mechanical compatibility in Ti–Ta alloys for biomedical applications. **Materials Science and Engineering: C,** v. 29, n. 3, p. 1061-1065, 2009.
35 _____. Microstructures and mechanical properties of Ti–50mass% Ta alloy for biomedical applications. **Journal of Alloys and Compounds,** v. 466, n. 1, p. 535-542, 2008.
36 QU, W. et al. Microstructures and phase transformations of Ti-30Zr-xNb (x = 5, 7, 9, 13 at.%) shape memory alloys. **Materials Characterization,** v. 122, p. 1-5, 2016.
37 GRAY, G. T.; MORRIS, C. E.; LAWSON, A. C. **Omega Phase Formation in Titanium and Titanium Alloys**. Los Alamos National Laboratory, p.1-9. 1992.
38 HO, W.-F. Effect of Omega Phase on Mechanical Properties of Ti-Mo Alloys for Biomedical Applications. **Journal of Medical and Biological Engineering,** v. 28, n. 1, p. 47-51, 2008.

39 LÜTJERING, G.; WILLIAMS, J. C.; GYSLER, A. Microstructure and Mechanical Properties of Titanium Alloys. In: (Ed.). **Microstructure and Properties of Materials**, 1998. p.1-77.

40 DEY, G. K. et al. Formation of a shock deformation induced [omega] phase in Zr 20 Nb alloy. **Acta Materialia,** v. 52, n. 18, p. 5243-5254, 2004.

41 SUKEDAI, E.; MATSUMOTO, H.; HASHIMOTO, H. Electron microscopy study on Mo content dependence of β to ω phase transformation due to cooling in Ti–Mo alloys. **Microscopy,** v. 51, n. suppl_1, p. S143-S147, 2002.

42 OZAKI, T. et al. Beta Ti Alloys with Low Young's Modulus. **Materials Transactions,** v. 45, n. 8, p. 2776-2779, 2004.

43 NIINOMI, M. Low Modulus Titanium Alloys for Inhibiting Bone Atrophy. In: PIGNATELLO, R. (Ed.). **Biomaterials Science and Engineering**. Croatia: Intechopen, 2011. cap. 12, p.249-268.

Capítulo 10

For publication in Journal of Alloys and Compounds.

The effect of solution heat treatment time on the structure, microstructure, and selected mechanical properties of Ti-25Ta-Zr alloys used as biomaterials

Pedro Akira Bazaglia Kuroda [1,2], Fernanda de Freitas Quadros [1,2], Raul Oliveira de Araújo [2,3], Conrado Ramos Moreira Afonso [4] and Carlos Roberto Grandini [1,2]

[1] UNESP – Univ. Estadual Paulista, Laboratório de Anelasticidade e Biomateriais, Bauru, SP, Brazil

[2] IBTN/BR – Brazilian Branch Institute of Biomaterials, Tribocorrosion and Nanomedicine, Bauru, SP, Brazil

[3] IFSP – Federal Institute of Education, Science and Technology, Barretos, SP, Brazil

[4] UFSCar – Univ. Federal de São Carlos, Materials Engineering Department (DEMa), São Carlos, SP, Brazil

Abstract

Titanium alloys are the most used metallic materials in the biomedical field due to their excellent biocompatibility coupled with good corrosion resistance in body fluids. However, the alloys used in the orthopedic area have an elastic modulus that is two to four times greater than that of human cortical bone. New alloys are being studied with the objective of using alloys with elastic modulus closer to that of bone; titanium alloys

containing zirconium and tantalum are being studied in this regard. This study analyzed the influence of solution heat treatment on the structure, microstructure, hardness, and elastic modulus of a ternary alloy Ti-25Ta-Zr system, where the zirconium content was varied to 0, 10, 20, 30, and 40 % in weight. The solution heat treatments performed in this work were conducted at 1,273 K for 0, 3, and 6 h. Structural and microstructural analyses were performed using X-ray diffraction, optical microscopy, and scanning and transmission electron microscopy. An analysis of the mechanical properties of the alloy was carried out by means of microhardness and dynamic elastic modulus measurements. The results showed that zirconium helped stabilize the β phase, since by adding zirconium to the alloy, the tantalum volume fraction increased. Solution heat treatment with longer duration induced precipitation of the alloyed β phase of the Ti-25Ta-Zr system. With higher zirconium concentrations, the alloy had better mechanical compatibility with human bone and a low elastic modulus but high hardness, making the mechanical conformation of the alloy more difficult. The Ti-25Ta-30Zr alloy had high hardness and elastic modulus after being subjected to solution heat treatment for 3 and 6 h, indicating ω phase precipitation.

Keywords: Metallic biomaterial; Ti alloys; microstructure; mechanical properties.

Introduction

Metallic materials are used as structural materials in various medical devices in orthopedic surgery. It is estimated that 70% of the structural materials used in this area of expertise are metallic materials, and titanium and its alloys are the materials that stand out in this application [1]. The first generation of biomedical titanium alloys was the α-type, such as commercially pure titanium (cp-Ti). Subsequently, in the second generation, the α + β types of alloys received special attention because thermomechanical treatments could change the volumetric fraction of the phases, thereby modifying the mechanical properties of the material [2]. In this generation, the Ti-6Al-4V alloy showed good mechanical and corrosion resistance [3]. The third generation is focusing on β-type alloys, as they have a low modulus of elasticity, implying better mechanical compatibility with human bone [4; 5].

To improve some of the characteristics of titanium, several types of heat treatments are performed to modify the structure and microstructure of the material [6]. Since mechanical properties depend on the bond strength of atoms of materials, modifying their structure and microstructure can change the hardness and elastic modulus [7]. As the proposed material is developed for the biomedical area, it is necessary for the implant to have mechanical properties that are like those of human bone, including the elastic modulus [8]. One of the most used heat treatments to modify the structure of the titanium alloys is solution heat treatment [9], where the material is heated until the precipitation dissolves, followed by rapid cooling of the material. A characteristic of this type of treatment is a reduction in ductility and increase in the mechanical and wear resistance of the material [10]. In titanium alloys, this type of treatment can retain the metastable phases α", ω, and β [11].

In the Ti-Ta-Zr system, the Ti-45Zr-10Ta, Ti40Zr-14Ta, Ti-35Zr-18Ta, and Ti-30Zr-22Ta alloys are known to have good biocompatibility, β-phase predominance, and a compressive Young's modulus ranging from 109–130 GPa across the four alloys, which is greater than that of cp-Ti [12]. The literature does not have much information about the structure, microstructure, and mechanical properties of Ti-Ta-Zr system alloys, but binary systems are well known. Zhou et al. [13; 14; 15] hardly studied Ti-Ta alloys and indicate that the most promising alloys of this binary system, for biomaterial use, is Ti-25Ta [16]. Some authors assert that zirconium is a neutral element in titanium alloys; that is, its addition does not modify the structure of the material [17; 18]. Recently new research has shown that zirconium helps the β-phase stabilization when another stabilizer element is present [19; 20; 21; 22].

The objective of this work was analyses the influence of solution heat treatments in the crystalline structure, microstructure, microhardness, and elastic modulus of ternary alloys of the Ti-25Ta-Zr system, with zirconium contents varying between 0 and 40 % in weight.

Experimental Procedure

In this study, the alloys were melted in an arc-melting furnace [23; 24], and then the ingots were submitted to a mechanical hot-rolling process at 1,273 K with air cooling. After the hot-rolling process, a solution heat treatment was made to reduces the internal stresses

caused by the thermomechanical treatment. The purpose of the treatment is eliminating residual internal stresses, removing most of the dislocations present in the material, and promoting the grains growth. The solution heat treatment consisted of raising the temperature to 1,273 K at a heating rate of 10 K/min, keeping it at this level for 0, 3, and 6 h and cooling by water [10].

The x-ray diffraction (XRD) measurements were performed on a Panalytical X'Pert-Pro model. The following parameters were used: Cu-Kα radiation (λ = 1.544 Å), 40 mA current, 45 kV potential, and continuous time mode.

To obtain the images via the microscopy technique, an Olympus optical microscope (OM), BX51M model was used. The images were obtained with magnifications of 1000x. The scanning electron microscopy (SEM) measurements were performed on a Carl Zeiss microscope, EVO-015 model, with a magnification of 2000x, and transmission electron microscopy (TEM) analysis were performed on a FEI Tecnai G^2 F20 200 kV equipped with a field emission gun (FEG), coupled to energy dispersive spectroscopy (EDS) microanalysis detector EDAX DX-4.

The used microdurometer in the hardness measurements was a Shimadzu (HMV-2 model). In the sample, five indentations were performed, with a force of 0.245 N, load of 25 g, and duration of 60 s. The measurements were based on ASTM E92 standard [25].

For the elastic modulus measurements, Sonelastic® equipment was used based on the impulse excitation technique. In this approach, the sample is held by its nodal points, and a magnetic pointer excites the sample with a slight mechanical impulse. A microphone captures the emitted sound and measures the attenuation frequencies of the acoustic response. Thus, it is possible to calculate the material's elastic modulus, based on ASTM E1876 standard [26].

Results and Discussion

The x-ray diffractograms for the samples of the Ti-25Ta-Zr system alloys are shown in Figure 10.1. It can be observed that, in some alloys, the crystalline structure is sensitive to thermomechanical processes.

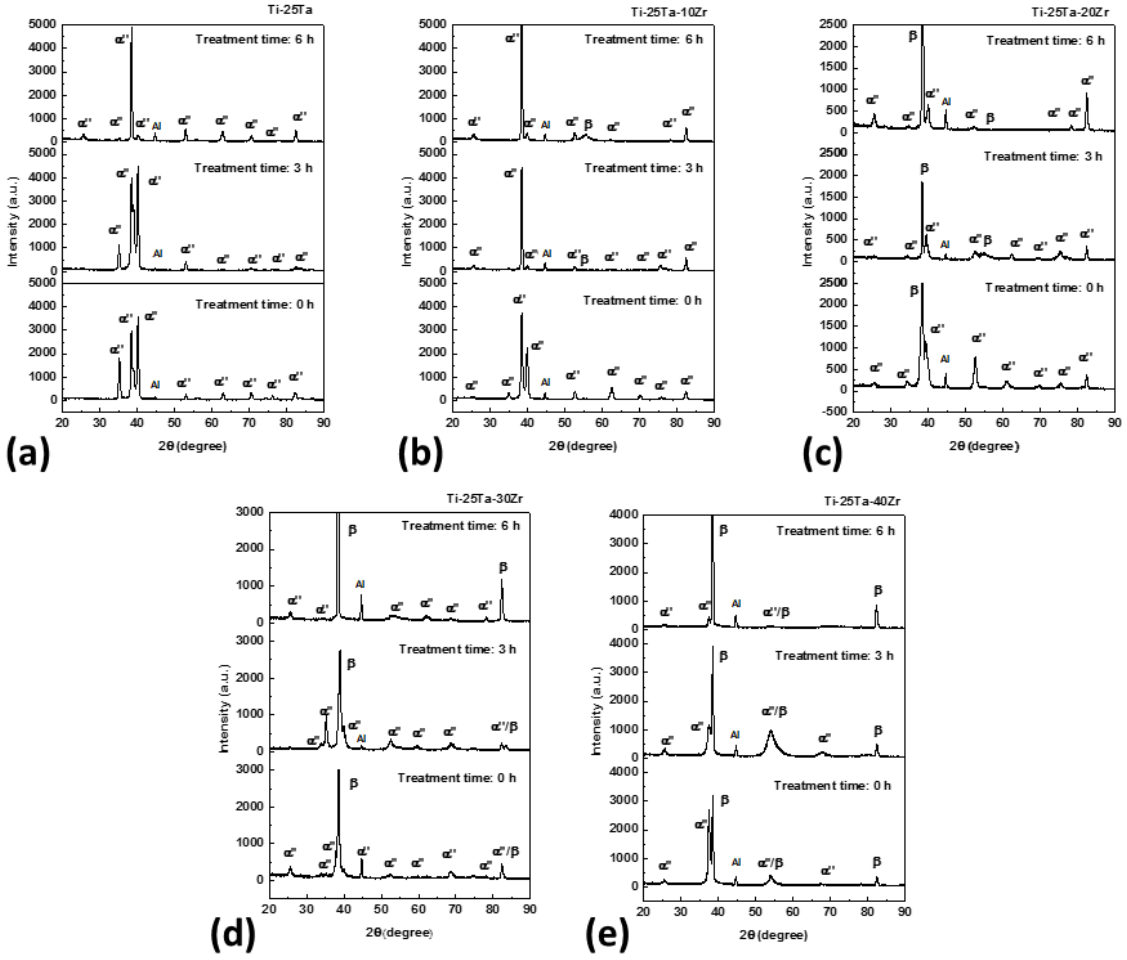


Figure 10.1: X-ray diffractograms for Ti-25Ta (a), Ti-25Ta-10Zr (b), Ti-25Ta-20Zr (c), Ti-25Ta-30Zr (d) and, Ti-25Ta-40Zr (e) alloys.

Analysis of the Ti-25Ta alloy shows that only α" phase peaks were identified. It is also possible to observe that the increase in solution heat treatment time promoted some modifications in the structure and microstructure of the alloy. These could be analyzed through the change in position and differences of intensities in the diffraction peaks, which are related to changes in the lattice parameters and crystallite size of the samples [11; 27].

Combining the results of XRD with OM and SEM, a typical martensitic α" structure can be seen in the micrographs for the Ti-25Ta alloy (Figure 10.2). After the solution heat treatment with rapid cooling, the micrographs showed an α" structure, with needles coming out of the grain boundary. The increase in solution heat treatment time promoted an increase in grain size and widening of the needles [6].

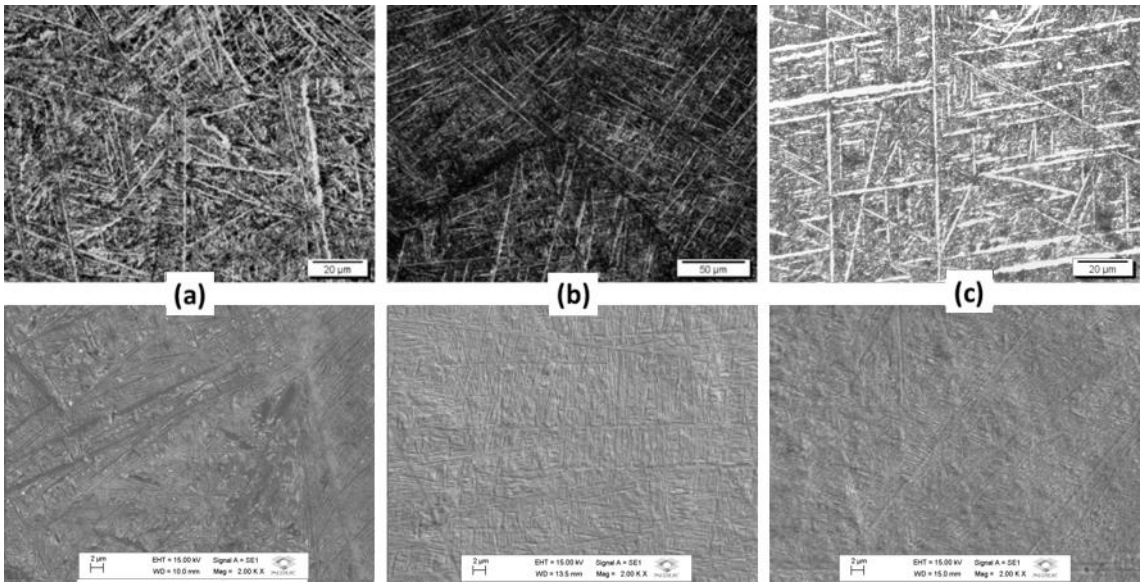


Figure 10.2: Micrographs of Ti-25Ta alloy after solution heat tretament with 0 h (a), 3 h (b) and, 6 h (c).

For the Ti-25Ta-10Zr alloy (Fig.10.1b), α" phase peaks were identified. It is again observed that the temperature could change the alloys' diffraction patterns. In the sample submitted to solution heat treatment for 6 h, it was observed that the intensity of the peaks, referring to the α" phase, increased the number of counts, and there was a decrease of the width of the same peaks. A small β peak could be observed, indicating that the increase in the time of the treatment induced the formation of the β phase in the alloy in question. In the micrographs showed in Figure 10.3, a typical martensitic α" structure and grain boundaries can be seen, corroborating the XRD results.

The α" and β phases were identified in the results for Ti-25Ta-20Zr alloy. The x-ray patterns were modified with the heat treatment, and the percentages of phases, lattice parameters, and crystallite size were likely modified in the different solution heat treatment conditions employed in the alloy. From the microscopy images (Figure 10.4), a typical martensitic α" structure, grain boundaries, and β matrix could be seen.

The α" and β phases were identified in Ti-25Ta-30Zr and Ti-25Ta-40Zr alloys. It is possible to observe that the peaks referring to the β phase become more refined and intense in the alloys subjected to a longer treatment, so the alloys submitted to the solution heat treatment for 6 h have a larger volumetric fraction of the β phase compared with the other conditions. The microscopy images showed only grain boundaries of the β matrix

for the alloy with 40% of zirconium, but in the alloy with 30%, some intra-grain needles could be observed in the time conditions of 0 and 3 h (Figures 10.5 and 10.6).

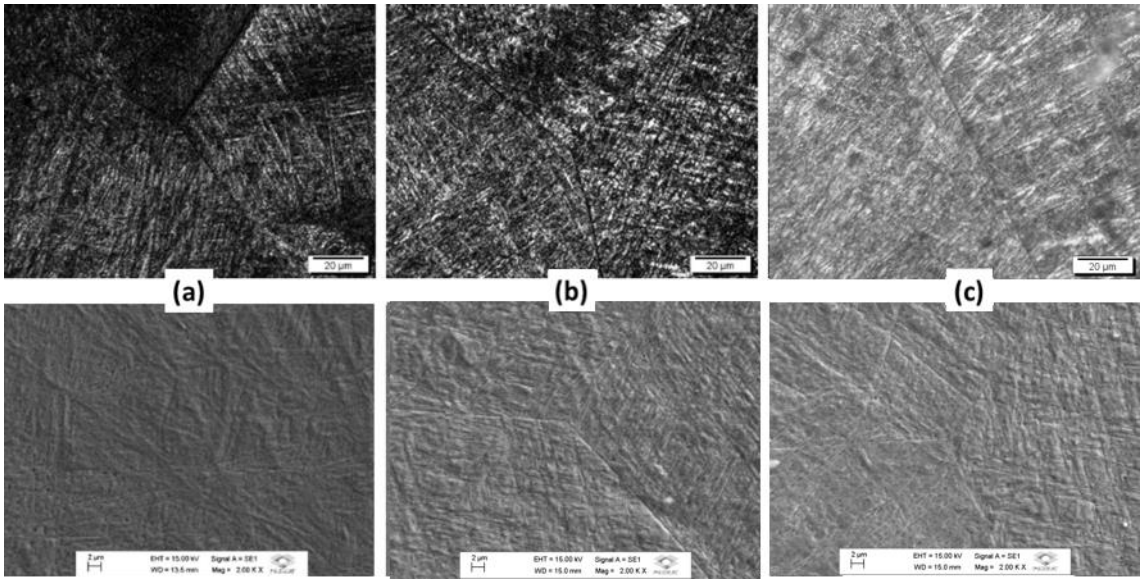


Figure 10.3: Micrographs of Ti-25Ta-10Zr alloy after solution heat tretament with 0 h (a), 3 h (b) and, 6 h (c).

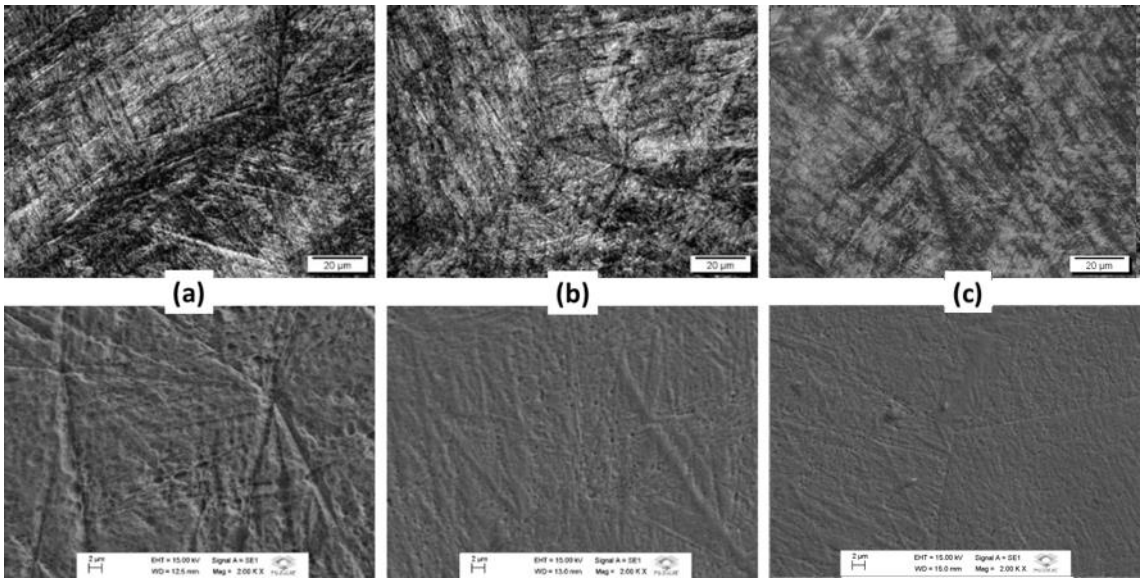


Figure 10.4: Micrographs of Ti-25Ta-20Zr alloy after solution heat tretament with 0 h (a), 3 h (b) and, 6 h (c).

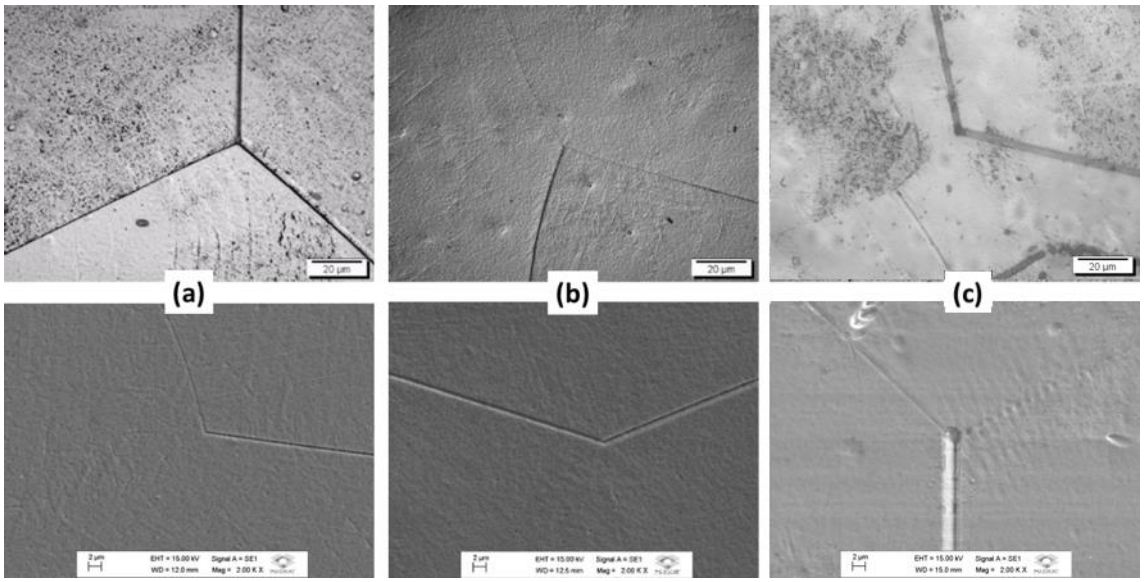


Figure 10.5: Micrographs of Ti-25Ta-30Zr alloy after solution heat tretament with 0 h (a), 3 h (b) and, 6 h (c).

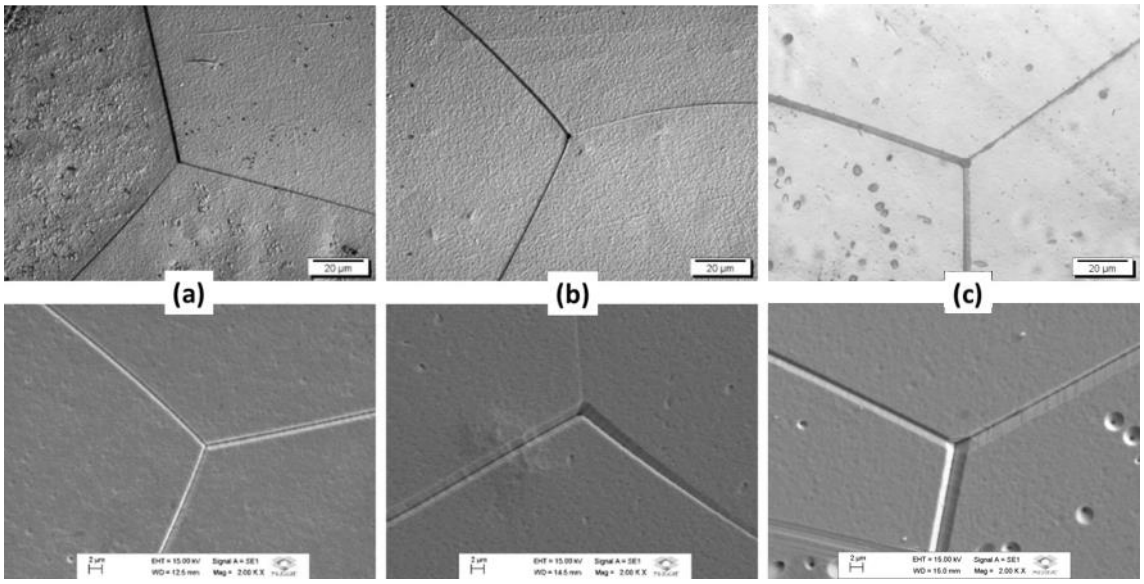


Figure 10.6: Micrographs of Ti-25Ta-40Zr alloy after solution heat tretament with 0 h (a), 3 h (b) and, 6 h (c).

Figure 10.7 shows the hardness values for each processing performed in the samples of each alloy used in this study. According to the literature, among the phases formed in titanium alloys, the ω phase presents the highest hardness value, followed by α, α', α", and β [15; 28]. It was observed that, after the solution heat treatment process, the Ti-25Ta alloy had the lowest hardness value of the studied Ti-25Ta-Zr system alloys. This alloy only had the α" phase in its volume, the other alloys were biphasic. The distinct

phases can be barriers for the movements of the dislocations, so the alloy with only one phase tends to have a lower hardness [29].

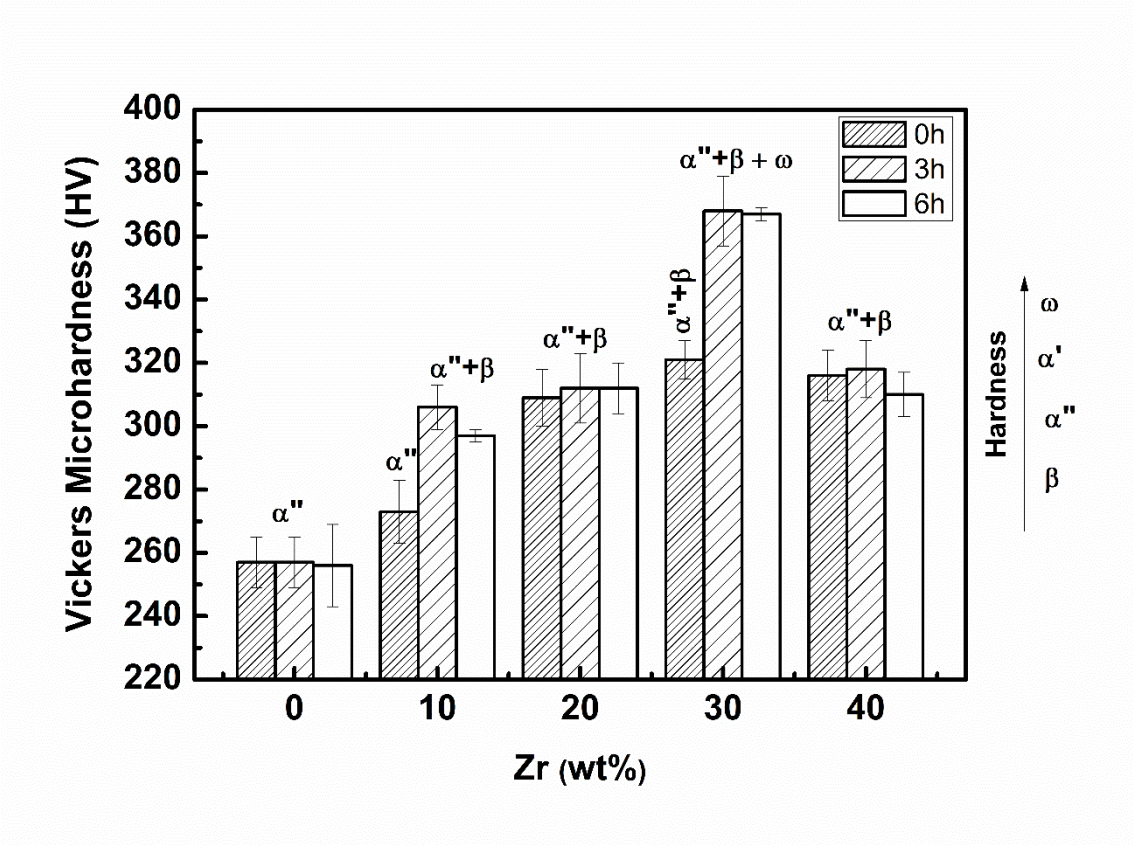


Figure 10.7: Ti-25Ta-Zr alloys hardness values after solution heat treatments.

In Ti-25Ta-10Zr alloy, there was an increase in the hardness value with the solution heat treatment time. It was observed that a longer treatment time induced β-phase precipitation. In the treatment for 0 h, the alloy only had the α" phase, and for the treatments with 3 h and 6 h of plateau, a small fraction of the β phase was observed in the XRD patterns. This increase can be explained by the presence of the α" and β phases, which may be an obstacle to the movement of the dislocations. This increase can be noted up to the alloy with 30% by weight from zirconium (Ti-25Ta-30Zr), but high hardness values were observed in the treatments with 3 h and 6 h; this hardness can be associated with the appearance of the nanophase ω, which has the characteristic of hardening the material and leaving it fragile [30; 31]. Finally, at 40 % in weight of zirconium, the hardness value fell under all conditions, indicating that the alloy did not have the ω phase. The hardness values of the alloys that had the same crystalline structure were similar (α" and

β). Due to this phase equality, the mechanical characteristics of the materials tended to be similar. Only in the Ti-25Ta-30Zr alloy (α" and β phases) was there an "anomaly" with reference to the hardness value; this represented the indication of the formation of the ω phase in this alloy.

Due to the high hardness of the Ti-25Ta-30Zr alloy subjected to 3 and 6 h of solution heat treatment, a more detailed analysis of the microstructure of the material was performed to see if the alloy had the ω phase as the enhancer. Figure 10.8 shows the bright and dark field TEM images with identification of the α"-phase needles in the β-phase matrix and the diffraction pattern of the selected area. Fine α"-phase needles with a width of approximately 50 nm in a β matrix can be observed in the images. Various sizes of ω-phase precipitates are visualized in the images, explaining why the alloy has high hardness [31].

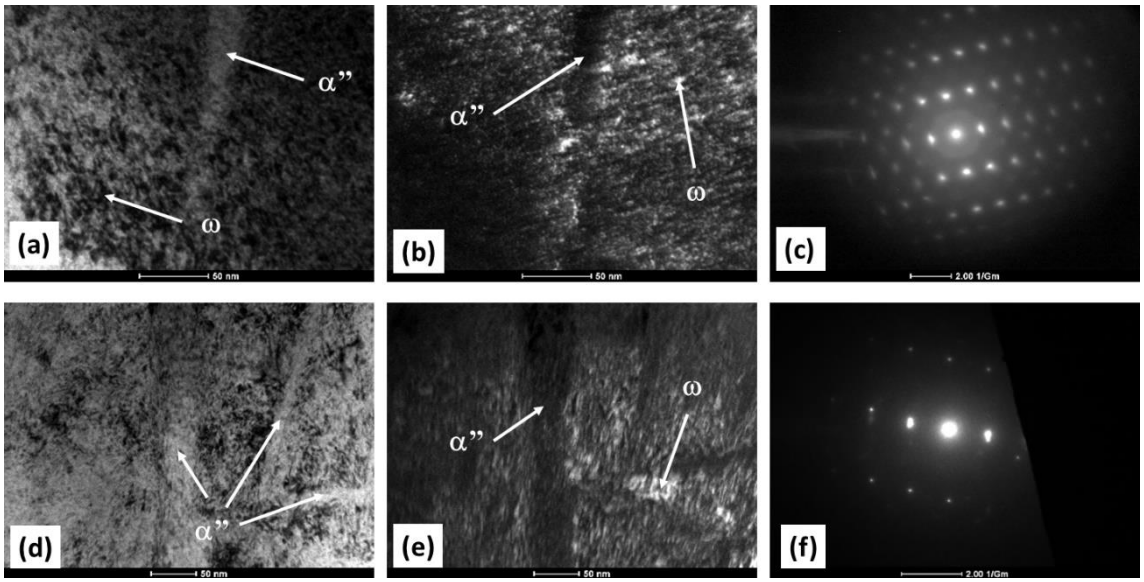


Figure 10.8: Transmission electron microscopy TEM images: bright field (a), dark field (b) and, diffraction pattern (c) for Ti-25Ta-30Zr after 3 h of solution heat treatment; and bright field (d), dark field (e) and, diffraction pattern (f) for Ti-25Ta-30Zr alloy after 6 h of solution heat treatment.

Figure 10.9 shows the values of the dynamic elastic modulus for the samples of all the alloys used in this paper, under the studied conditions. From the figure, it can be observed that the elastic modulus of the studied alloys was approximately 80 GPa for the non-zirconium alloy, while it reached a minimum value of 57 GPa for the alloy with the

highest zirconium content (40 % in weight; 6 h of solution heat treatment). It was not possible to observe a relationship between the values of the elastic modulus and the solution heat treatment time. It should be observed that the elastic modulus decreases with increasing zirconium content because zirconium acts as a β-stabilizer element and β-type alloys have lower elastic modulus values [19; 32]. In the Ti-25Ta-30Zr alloys subjected to the treatment for 3 and 6 h, it was possible to observe high elastic modulus values. Under the conditions presented, this alloy had high mechanical property values due to the precipitation of the ω phase [33].

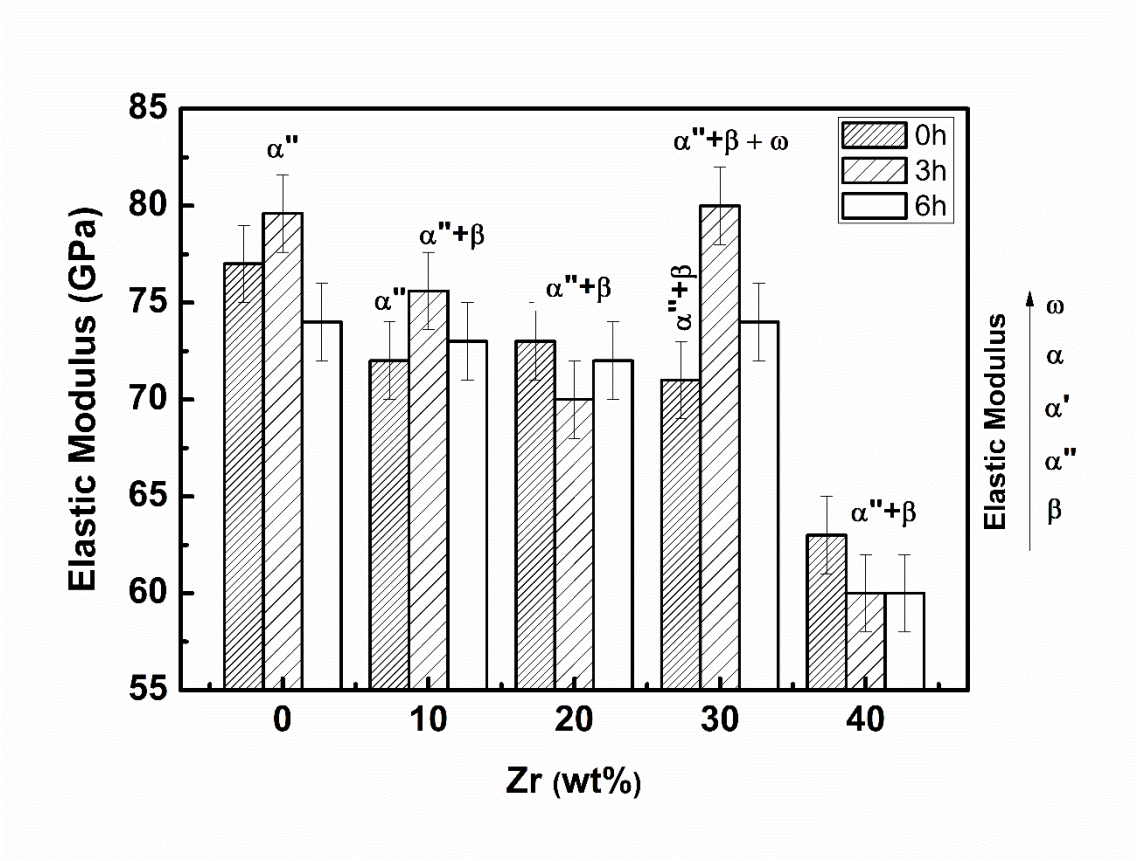


Figure 10.9: Ti-25Ta-Zr alloys elastic modulus values after solution heat treatments.

Conclusions

From the presented results, it is possible to conclude the following:

- The XRD and microscopy showed that the crystalline structure of the alloys was sensitive to the addition of zirconium and solution heat treatments;

- In the α-type alloys, the presence of fine needles inside the grains and their grain boundaries were related to the α-phase structures; with increased time, there was a decrease of these structures, indicating a greater stability of the β phase;
- Longer solution heat treatment time induced the formation of the β phase in the studied alloys;
- The microhardness of the alloys did not indicate great changes with the solution heat time; it was only possible to observe an increase in hardness with the addition of zirconium due to the hardening by solid solution heat treatment and phase precipitation;
- The elastic modulus decreased with high levels of zirconium due to the stabilization of the β phase;
- The results of hardness and elastic modulus indicated that there should be a small percentage of the ω phase in the Ti-25Ta-30Zr alloy submitted to solution heat treatment for 3 and 6 h; transmission electron microscopy images confirmed the existence of this phase;
- Ti-25Ta-40Zr alloy presented better mechanical compatibility to be used as biomaterial.

References

1 HANAWA, T. 1 - Overview of metals and applications. In: NIINOMI, M. (Ed.). **Metals for Biomedical Devices**: Woodhead Publishing, 2010. p.3-24.
2 NIINOMI, M. Mechanical properties of biomedical titanium alloys. **Materials Science and Engineering A,** v. 243, n. 1-2, p. 231-236, 1998.
3 LI, J. P.; VAN BLITTERSWIJK, C. A.; DE GROOT, K. Factors having influence on the rheological properties of Ti6A14V slurry. **Journal of Materials Science: Materials in Medicine,** v. 15, n. 9, p. 951-958, 2004.
4 LEI, Z. et al. Development of advanced materials via entropy engineering. **Scripta Materialia,** v. 165, p. 164-169, 2019.
5 KAUR, M.; SINGH, K. Review on titanium and titanium based alloys as biomaterials for orthopaedic applications. **Materials Science and Engineering: C,** v. 102, p. 844-862, 2019.
6 COLLINGS, E. W. **The Physical Metallurgy of Titanium Alloys**. Ohio: ASM International, 1989.
7 WELSCH, G.; BOYER, R.; COLLINGS, E. W. **Materials Properties Handbook: Titanium Alloys**. ASM International, 1993.

8 NIINOMI, M. Mechanical biocompatibilities of titanium alloys for biomedical applications. **Journal of the Mechanical Behavior of Biomedical Materials,** v. 1, n. 1, p. 30-42, 2008.
9 LEYENS, C.; PETERS, M. **Titanium and Titanium Alloys: Fundamentals and Applications**. New York: Wiley-VCH, 2005.
10 XAVIER, C. C. et al. Low temperature heat treatments on Ti-15Zr-xMo alloys. **Journal of Alloys and Compounds,** v. 727, n. Supplement C, p. 246-253, 2017
11 PETERS, M. et al. Structure and Properties of Titanium and Titanium Alloys. In: (Ed.). **Titanium and Titanium Alloys**: Wiley-VCH Verlag GmbH & Co. KGaA, 2005. p.1-36. ISBN 9783527602117.
12 BIESIEKIERSKI, A. et al. Extraordinary high strength Ti-Zr-Ta alloys through nanoscaled, dual-cubic spinodal reinforcement. **Acta Biomaterialia,** v. 53, p. 549-558, 2017.
13 ZHOU, Y. L. et al. Corrosion resistance and biocompatibility of Ti-Ta alloys for biomedical applications. **Materials Science and Engineering A,** v. 398, n. 1-2, p. 28-36, 2005.
14 ZHOU, Y. L.; NIINOMI, M.; AKAHORI, T. Effects of Ta content on Young's modulus and tensile properties of binary Ti–Ta alloys for biomedical applications. **Materials Science and Engineering: A,** v. 371, n. 1, p. 283-290, 2004.
15 ZHOU, Y.-L.; NIINOMI, M. Microstructures and mechanical properties of Ti–50 mass% Ta alloy for biomedical applications. **Journal of Alloys and Compounds,** v. 466, n. 1–2, p. 535-542, 2008.
16 _____. Ti–25Ta alloy with the best mechanical compatibility in Ti–Ta alloys for biomedical applications. **Materials Science and Engineering: C,** v. 29, n. 3, p. 1061-1065, 2009.
17 LONG, M.; RACK, H. J. Titanium alloys in total joint replacement--a materials science perspective. **Biomaterials,** v. 19, n. 18, p. 1621-1639, 1998.
18 GEETHA, M. et al. Ti based biomaterials, the ultimate choice for orthopaedic implants - A review. **Progress in Materials Science,** v. 54, n. 3, p. 397-425, 2009.
19 CORREA, D. R. N. et al. Effect of the substitutional elements on the microstructure of the Ti-15Mo-Zr and Ti-15Zr-Mo systems alloys. **Journal of Materials Research and Technology,** v. 4, n. 2, p. 180-185, 2015.
20 CORREA, D. R. N.; KURODA, P. A. B.; GRANDINI, C. R. Structure, Microstructure, and Selected Mechanical Properties of Ti-Zr-Mo Alloys for Biomedical Applications. **Advanced Materials Research,** v. 922, p. 75-80, 2014.
21 CORREA, D. R. N. et al. Microstructure and selected mechanical properties of aged Ti-15Zr-based alloys for biomedical applications. **Materials Science and Engineering: C,** v. 91, p. 762-771, 2018.
22 CORREA, D. R. N. et al. Development of Ti-15Zr-Mo alloys for applying as implantable biomedical devices. **Journal of Alloys and Compounds,** v. 749, p. 163--171, 2018.
23 KURODA, P. A. B. et al. Preparation, Structural, Microstructural, Mechanical and Cytotoxic Characterization of As-Cast Ti-25Ta-Zr Alloys. **Journal of Materials Science: Materials in Medicine**, v. 31, article 19, 2020.
24 QUADROS, F. D. F. et al. Preparation, structural and microstructural characterization of Ti-25Ta-10Zr alloy for biomedical applications. **Journal of Materials Research and Technology,** v. 8, n. 5, p. 4108-4114, 2019.
25 ASTM. **E92-82 - Standard Test Method for Vickers Hardness of Metallic Materials**. E92-82 - Standard Test Method for Vickers Hardness of Metallic Materials. West Conshohocken, PA: ASTM International. E92-82 2003.

26 _____. **E1876–01 - Standard Test Method for Dynamic Young's Modulus, Shear Modulus, and Poisson's Ratio by Impulse Excitation of Vibration**. E1876–01 - Standard Test Method for Dynamic Young's Modulus, Shear Modulus, and Poisson's Ratio by Impulse Excitation of Vibration. Philadelphia (USA): ASTM International. E1876–01 2002.

27 MARTINS JR, J. R. S.; GRANDINI, C. R. Structural characterization of Ti-15Mo alloy used as biomaterial by Rietveld method. **Journal of Applied Physics,** v. 111, n. 8, p. 083535-8, 2012.

28 GABRIEL, S. B. et al. Maximisation of the ratio of microhardness to the Young's modulus of Ti–12Mo–13Nb alloy through microstructure changes. **Materials Science and Engineering: C,** v. 33, n. 6, p. 3319-3324, 2013.

29 MANDA, P.; CHAKKINGAL, U.; SINGH, A. K. Hardness characteristic and shear band formation in metastable β-titanium alloys. **Materials Characterization,** v. 96, p. 151-157, 2014.

30 GRAY, G. T.; MORRIS, C. E.; LAWSON, A. C. **Omega Phase Formation in Titanium and Titanium Alloys**. Los Alamos National Laboratory, p.1-9. 1992

31 GLORIANT, T. et al. Characterization of nanophase precipitation in a metastable β titanium-based alloy by electrical resistivity, dilatometry and neutron diffraction. **Scripta Materialia,** v. 58, n. 4, p. 271-274, 2008.

32 NIINOMI, M. Recent research and development in titanium alloys for biomedical applications and healthcare goods. **Science and Technology of Advanced Materials,** v. 4, n. 5, p. 445-454, 2003.

33 TANE, M. et al. ω Transformation in cold-worked Ti–Nb–Ta–Zr–O alloys with low body-centered cubic phase stability and its correlation with their elastic properties. **Acta Materialia,** v. 61, n. 1, p. 139-150, 2013.

Capítulo 11

First draft (uncorrected) version for publication in Materials Science and Engineering C.

The Effect of Titanium on the Structure, Microstructure and Select Mechanical Properties of Zr-25Ta-Ti Alloys

Pedro Akira Bazaglia Kuroda[1,2] and Carlos Roberto Grandini[1,2]

[1] UNESP – Univ. Estadual Paulista, Lab de Anelasticidade e Biomateriais, 17.033.360, Bauru, SP, Brazil.

[2] IBTN – Institute of Biomaterials, Tribocorrosion and Nanomedicine.

Abstract:

This work aims to produce alloys of the Zr-25Ta-Ti system in order to analyze the influence of an increase in titanium on the structure, microstructure, microhardness and modulus of elasticity in the alloys. The elements zirconium, tantalum and titanium were used because they are elements that have a good resistance to corrosion in body fluids and good biocompatibility. Zr-25Ta-Ti alloys (Ti = 0, 15, 25 and 35 wt%) were prepared using an arc-melting furnace. To analyze the chemical composition, the elements were mapped by the EDX technique, gas analysis, spectroscopy chemical composition and density measurements. All chemical composition analyses show that the alloys produced are of good quality, with good chemical homogeneity and good stoichiometry. To analyze the structure and microstructure of the materials, X-ray diffraction measurements and microscopy techniques were performed. From the characterizations, it was observed that titanium acted as an α-stabilizing element since its increase in the alloys precipitated the formation of the orthorhombic α" phase, an intermediate phase from β to α. Regarding microhardness measurements, the alloys have a higher hardness compared to pure zirconium due to solid solution hardening that detaches the Zr-25Ta, which has a high hardness value due to the precipitation of the ω phase. Among the studied alloys, the Ti-25Ta-25Ti alloy stands out, demonstrating the lowest result of modulus of elasticity,

approximately two smaller than the human cortical bone, but many alloys used in the biomedical field, such as pure titanium, have a modulus of elasticity value three times higher than that of human bone.

Keywords: Zr Alloys; Biomaterials; Microstructure Mechanical Properties

Introduction

As technology advances and quality of life increases, the demand for metal biomaterials for use as orthopedic and dental implants increases. In the search for new materials, zirconium gained prominence when used as biomaterial, several studies in the literature show good results of mechanical properties, corrosion resistance and biocompatibility of zirconium alloys or titanium alloys that have zirconium in their chemical composition [1; 2; 3; 4; 5; 6; 7; 8; 9; 10; 11; 12].

Zirconium and titanium belong to the IVB group in the periodic table and are known to have similar structure and chemical properties, which enables the study of zirconium alloys for biomedical applications. In addition to having good mechanical property results compared to stainless steel and Co-Cr alloys [13], zirconium alloys have good corrosion resistance, good biocompatibility in body fluids and their implantation in bone tissue induces the formation of a small bone apatite layer on their surfaces [14].

. Zirconium is an element that has an allotropic transformation at a temperature of 862 °C, where below this temperature its crystalline structure is compact hexagonal (α phase) and above this temperature its crystalline structure is body-centered cubic (phase β) [15]. Titanium undergoes an allotropic transformation similar to that of zirconium at a temperature of 883 °C [15; 16]. Tantalum has a body-centered cubic crystal structure, is a weak β-stabilizer element, and is often used to control the structure and microstructure of the titanium alloys [17; 18; 19].

Tsuno et al. [20] produced binary Zr-Ta alloys (Ta = 10, 20, 25, 30, 40 and 50 wt%). The analysis of their structures and microstructures showed that, in the concentrations of 10 and 18Ta, the alloys are of type α. With tantalum fractions in the range between 30 and 50Ta, phases α and β coexist. Tantalum was found to act as a β-stabilizing element in zirconium alloys and produced similar results in titanium alloys.

Hsu et al. [21] studied Zr-Ti system alloys in which the weight percentage of titanium ranged from 10, 20, 30 and 40% by weight. In this study, the authors highlight that the Zr-10Ti alloy has only the α phase as microstructure and that, with titanium contents above 20 wt, it is already possible to visualize β phase precipitates. Moreover, the Zr-

40Ti alloy has only the β phase as its crystal structure. The results showed that the crystalline structure of alloys of the Zr-Ti system is dependent on the amount of titanium in solid solution.

Ternary alloys of the Zr-25Ta-Ti system have never been studied and produced. Knowing the qualities and potential of zirconium, titanium and tantalum alloys in the biomedical branch, it is expected that the system will have good structural, microstructural and mechanical properties for use as a biomaterial. The objective of this project is to produce alloys of the Zr-25Ta-Ti system, in which the weight of titanium varies from 0, 15, 25 and 35% in weight, and to analyze the effect of substitutional titanium on structure, microstructure and some mechanical properties.

Materials and Methods

Leaf-shaped zirconium elements, tantalum blades and titanium bars were separated into the nominal compositions for fusion. Ingot melting was performed using an arc furnace with a water-cooled copper crucible, non-consumable tungsten electrode and argon-controlled atmosphere. Recent literature uses this technique to produce high quality titanium alloys [15; 22; 23; 24; 25; 26; 27; 28; 29; 30; 31; 32; 33].

To verify the quality and stoichiometry of the samples produced, the chemical composition of the samples was verified using the acid solubilization technique, followed by the detection of the elements in an induced plasma optical emission spectrometer using dispersive and energy spectroscopy. For these measurements, a Carl Zeiss scanning electron microscope, model EVO-015, with an INCA probe was used. For gas analysis and density measurements, a Leco model TC400 gas analyzer and an Ohaus analytical balance for density determination by the Archimedes principle were employed.

The structure of the samples was analyzed using the X-ray diffraction technique. X-ray diffraction measurements were performed using a Rigaku MiniFlex 600 diffractometer with Cu-Kα radiation ($\lambda = 1.54056$ Å), 20 mA current and 40 kV potential. Measurements were made in fixed time mode, with 0.02º of step, in the range of 20º and 80º, and a rate of 10º per minute. To analyze the microstructure of the samples, the optical and scanning electron microscopy technique was used. An Olympus model BX51M microscope and a Carl Zeiss model EVO-015 electron microscope were used to obtain the images.

The mechanical properties were obtained by Vickers microhardness measurements using a Shimadzu HMV-2 microdurometer, with a load of 200g and a time

of 60s [34]. To measure the modulus of elasticity, Sonelastic® equipment based on the Impulse Excitation Technique was used [35].

Results and Discussion

Table 11.1 shows the chemical composition results of the samples produced. It is observed that the alloys have small metallic impurities, especially hafnium, an element found in nature together with zirconium, which makes it difficult to separate the elements; hence, materials with high levels of zirconium have a higher concentration of hafnium in their chemistry composition. After hafnium, nickel is the second most commonly detected metallic impurity; nickel is derived from precursor materials. The other impurity concentrations are not significant. From the table it can be concluded that the alloys are of good quality. The tantalum and zirconium concentrations were slightly below the nominal values established in the work, the expected results because the impurities decrease the detection of tantalum and zirconium elements.

Regarding the gas analysis results, the alloys have a low concentration of oxygen and nitrogen gas impurities. The fusion technique with the inert argon-controlled atmosphere has been satisfactorily performed since zirconium and titanium are highly reactive with oxygen.

Table 11.3 is the analysis of element detection by X-ray spectroscopy. The results show that the alloys have amounts of the zirconium and tantalum elements similar to the nominal values. These results corroborate the results obtained by the prior art (ICP). In addition to the quantification of the elements, mapping of the elements on the alloy surface was performed. Fig. 11.1 shows the mapping of the alloys produced in this work; the points in blue represent the zirconium, green represents the tantalum element and titanium is highlighted in red. From the image, it is not possible to observe segregated tantalum, zirconium and titanium. If the fusion was not performed satisfactorily, tantalum precipitates could be observed due to their high melting point.

Finalizing the chemical characterization, Fig. 11.2 shows the density results of the alloys compared to the theoretical values. It is observed that the density of the alloys are close to the theoretical values, indicating a good stoichiometry. The values differ slightly from the theoretical values due to the presence of metallic impurities that modify the density. Regarding the titanium concentration, it was observed that the density decreases with the addition of titanium. This happens because the titanium has a lower density value

compared to zirconium; therefore, its increase in alloy decreases the concentration of zirconium, thus decreasing the density.

Table 11.1. Chemistry analysis results for Zr-25Ta-Ti alloys

Element (wt%)	**Zr-25Ta**	**Zr-25Ta-15Ti**	**Zr-25Ta-25Ti**	**Zr-25Ta-35Ti**
Al	0.34	0.27	0.01	0.16
Cr	0.01	0.01	0.01	0.01
Cu	0.01	0.01	0.01	0.66
Fe	0.41	0.05	0.09	0.05
Hf	1.00	0.77	1.10	0.20
Mo	0.01	0.11	0.09	0.01
Ni	0.18	0.18	0.01	0.08
Si	0.01	0.01	0.01	0.07
Ta	21.7	21.64	23.5	23.5
Zr	72.2	59.3	45.1	37.2
Ti	0.02	14.8	Balance	Balance

Table 11.2. Gas analysis results for Zr-25Ta-Ti alloys

Alloy	**Oxygen (wt%)**	**Nitrogen (wt%)**
Zr-25Ta	0.132 ± 0.004	0.004 ± 0.001
Zr-25Ta-15Ti	0.131 ± 0.005	0.003 ± 0.001
Zr-25Ta-25Ti	0.178 ± 0.039	0.010 ± 0.001
Zr-25Ta-35Ti	0.144 ± 0.003	0.012 ± 0.001

Table 11.3. Quantitative chemical analysis by EDS for Zr-25Ta-Ti alloys

Alloy	**Ta (wt%)**	**Ti (wt%)**
Zr-25Ta	28.6 ± 0.2	-
Zr-25Ta-15Ti	27.6 ± 0.2	14.7 ± 0.2
Zr-25Ta-25Ti	25.4 ± 0.2	23.4 ± 0.2
Zr-25Ta-35Ti	25.2 ± 0.2	31.0 ± 0.2

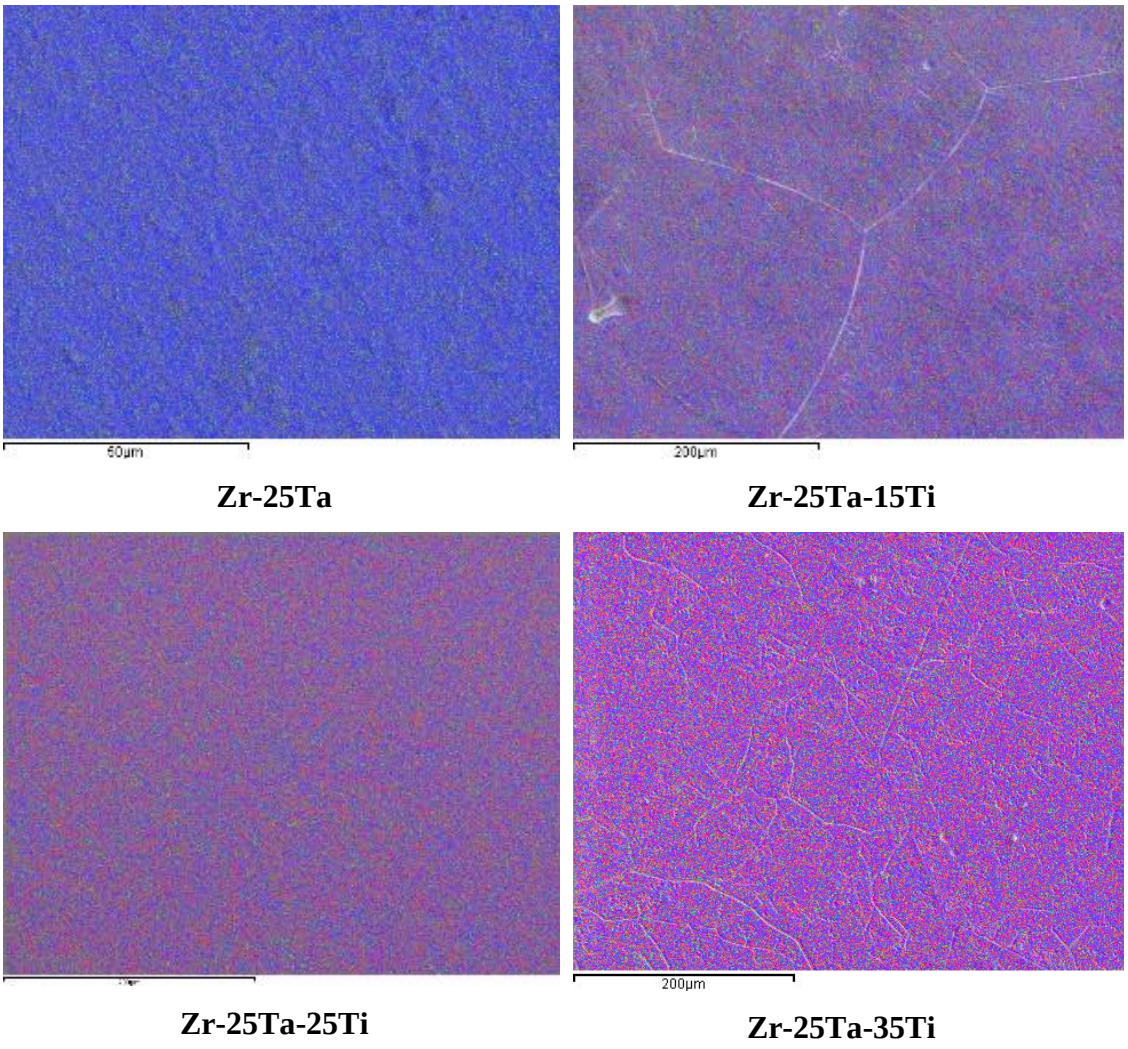


Figure 11.1. Chemical mapping for Zr-25Ta-Ti alloys, showing Ti, Ta and Zr together.

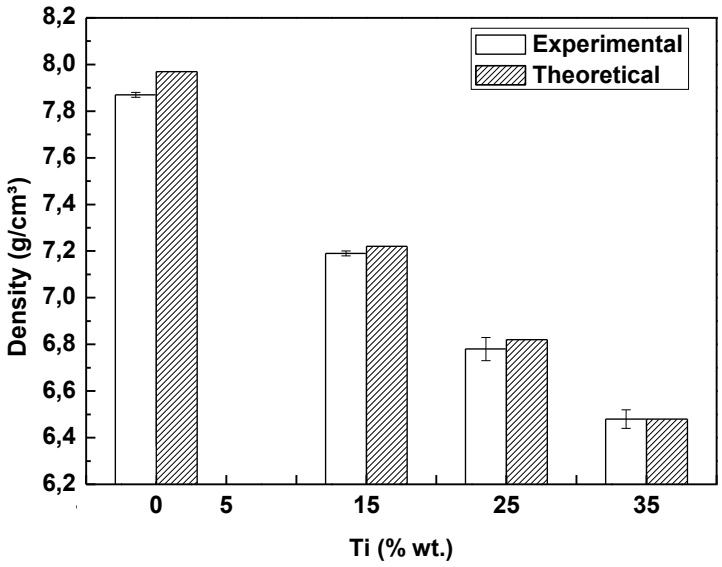


Figure 11.2. Density as a function of Ti concentration, for Zr-25Ta-Ti alloys.

Fig. 11.3 is an image of the results obtained by the x-ray diffraction technique. The results indicate that the Zr-25Ta alloy has the body-centered cubic, β, and tetragonal phase ω. Due to the presence of the ω phase, this alloy must have high hardness values and modulus of elasticity, making it difficult to use it after melting for biomedical applications. For Zr-25Ta-15Ti and Zr-25Ta-25Ti alloys, only β phase peaks can be observed. With the addition of 35% by weight of titanium, a small peak of the orthorhombic phase α" is observed at approximately 42°. In general, titanium acted as an α-stabilizer element in the Zr-25Ta-Ti system since its addition resulted in the nucleation of phase α", which is intermediate from β to α. With these results, it is expected that alloys with higher titanium contents will have martensitic phases in their structures and microstructures.

This work differs from the results found by Hsu [21]. In his work, the addition of titanium in the Zr-Ti system induces precipitation of the β phase. In this work, the addition of titanium induces the formation of martensitic phases. This characteristic difference must be related to the presence of tantalum, which acts as a β stabilizer. From the literature, we know that the titanium alloy Ti-25Ta (Zr-25Ta-75Ti, without the presence of zirconium) is a single-phase alloy, like the orthorhombic structure α" [17]; thus, titanium in the Zr-25Ta system suppresses the β phase.

Regarding the microscopy images, shown in Figs. 11.4 to 11.7, it is possible to observe and visualize a grain controller on the surface of the alloys and a matrix β for all alloys in the system. However, in Fig. 11.7, which shows the micrograph of the Zr-25Ta-35Ti alloy, it is possible to observe small α-orthorhombic phase precipitates. These precipitates are needles in localized intra-grain.

Comparing the results obtained to analyze the structure and microstructure, both techniques corroborate them. The alloy Zr-25Ta is of type β and ω, remembering that the phase ω is only detected via the technique of nanoscale microscopy. Zr-25Ta-15Ti and Zr-25Ta-25Ti alloys are β-type alloys, and the Zr-25Ta-35Ti alloy is a metastable β alloy with α" phase.

Regarding mechanical property measurements, Fig. 11.8 shows the results obtained from the Vickers microhardness of alloys with respect to titanium concentration. The results show that the alloy without the presence of titanium had a high hardness, 500 HV. This high hardness value is related to the presence of the ω phase, which is undesirable in biomedical alloys as it makes the material hard and brittle. With the addition of 15% by weight of titanium, there was a suppression of the ω phase, reducing the hardness of

the alloy. For alloys with 25% and 35% by weight of titanium, there was a decrease in the microhardness value. This decay is related to the loss of β phase stabilization due to titanium acting as α-stabilizer element.

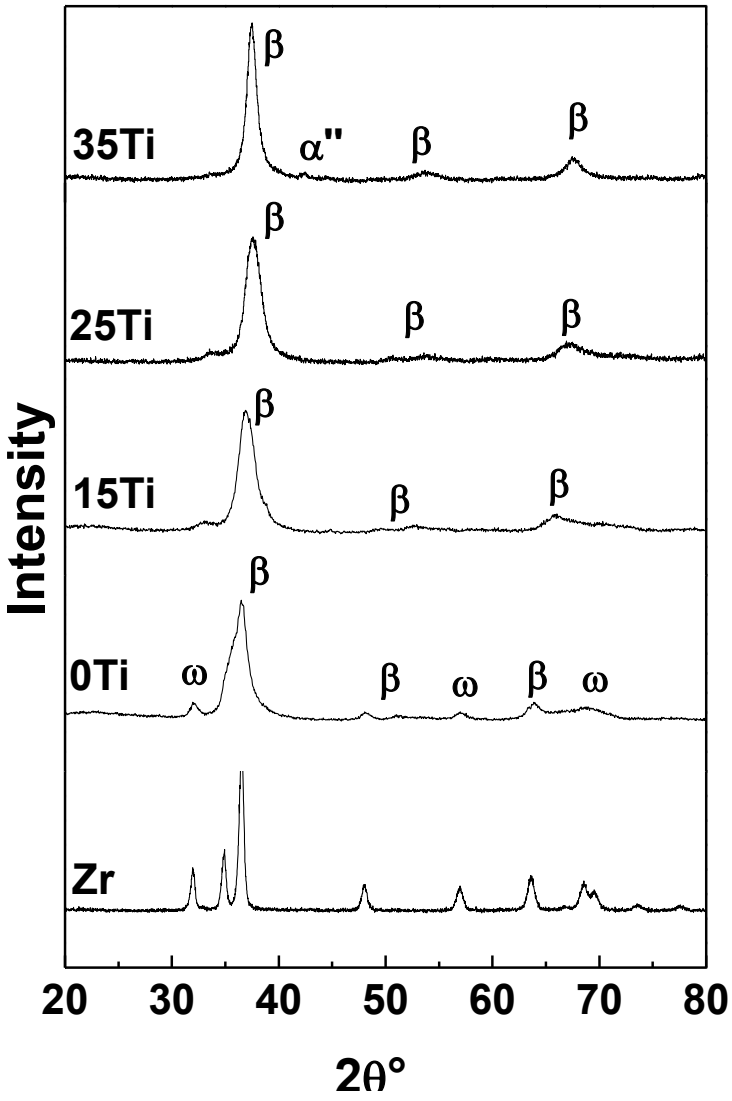


Figure 11.3. X-ray diffractograms for Zr-25Ta-Ti alloys.

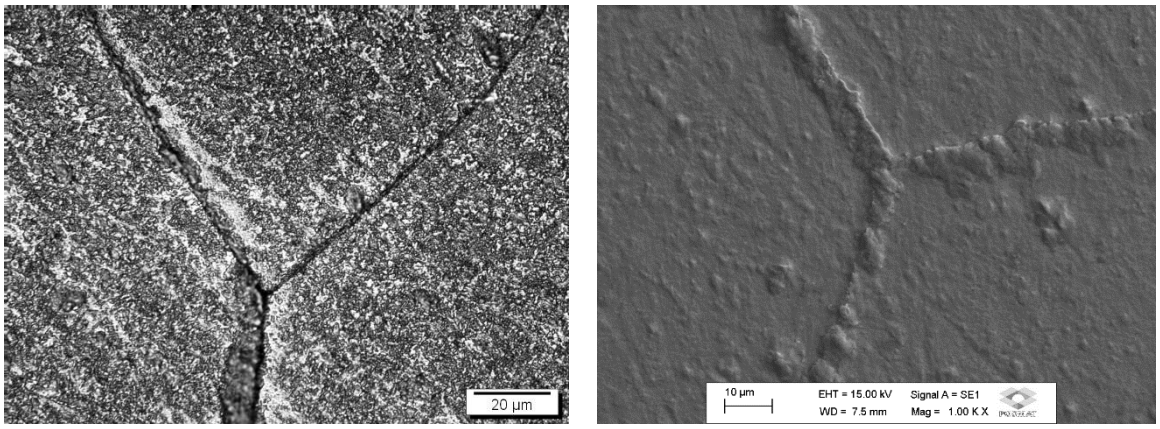


Figure 11.4. Micrographs for a sample of the Zr-25Ta alloy.

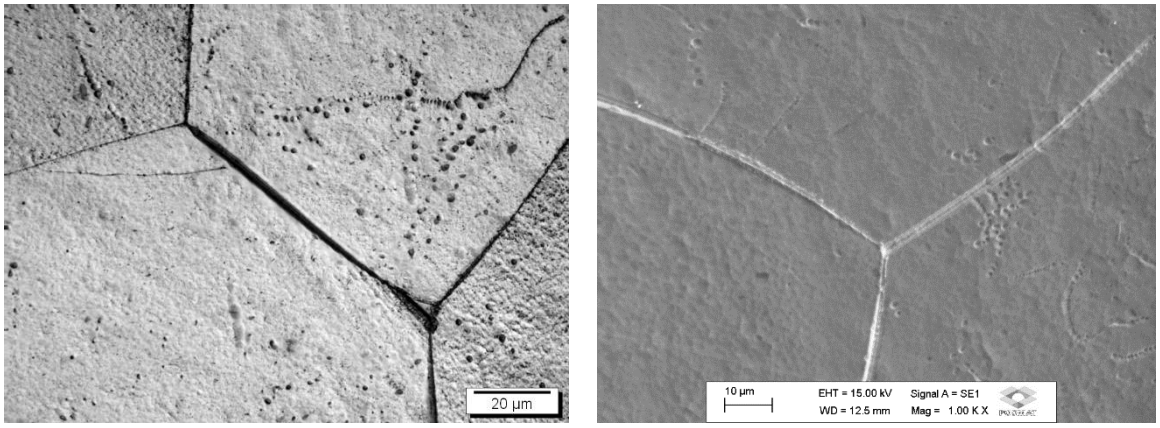


Figure 11.5. Micrographs for a sample of the Zr-25Ta-15Ti alloy.

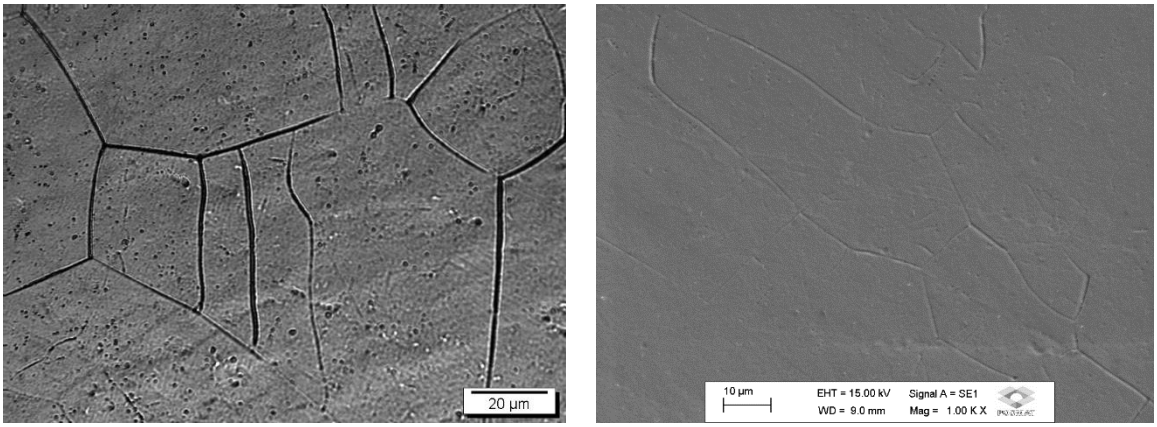


Figure 11.6. Micrographs for a sample of the Zr-25Ta-25Ti alloy.

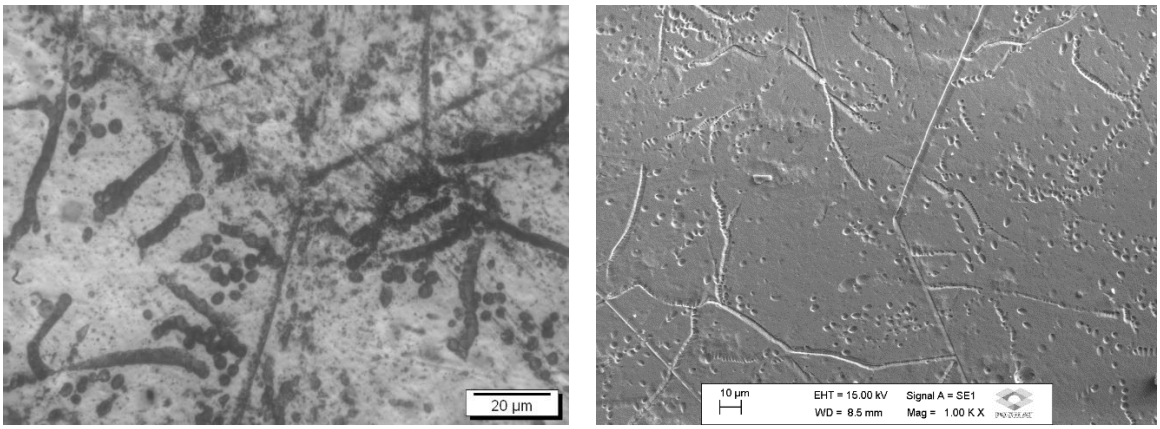


Figure 11.7. Micrographs for a sample of the Zr-25Ta-35Ti alloy.

The results for the modulus of elasticity are shown in Fig. 11.9. It is noted that the addition of titanium changed the modulus of elasticity of the alloys in a way similar to the hardness. The Zr-25Ta alloy has a high elastic modulus value due to the presence of the ω phase, but smaller than the ti-cp and the Ti-6Al-4V alloy. In the Zr-25Ta-15Ti alloy, there was a decrease in the modulus of elasticity value since the alloy has only the β phase as a crystalline structure. With the addition of 25% by weight of titanium, the Zr-25Ta-25Ti alloy has an excellent modulus value, 60 GPa, the lowest value of the system. This alloy has only β in its microstructure, as titanium is an α-stabilizing element. The increase modifies the atomic interaction forces of the β phase, which become weak due to lower β phase stability, decreasing the modulus of elasticity. For the Zr-25Ta-35Ti alloy, there is an increase in the modulus value because the alloys are biphasic, and distinct phases are barriers that hinder the movement of disagreements, causing an increase in mechanical property values.

The studied alloys have excellent mechanical properties, especially in relation to the modulus of elasticity. The alloys have better results than many orthopedic and dental implant alloys, such as cp-Ti, Ti-6Al-4V, Ti-15Mo, cp-Ta, Co-Cr alloys and stainless steel, among others [13].

Conclusions

From the results presented in this paper it is possible to conclude:

- Chemical composition and mapping measurements indicate that the alloys produced are homogeneous and preserve the proposed stoichiometry;

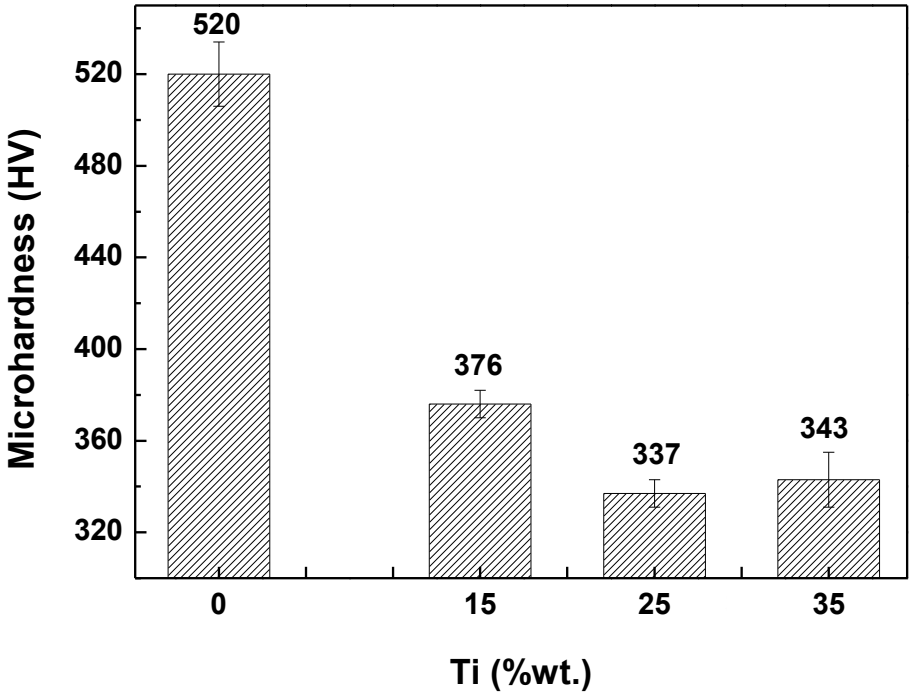
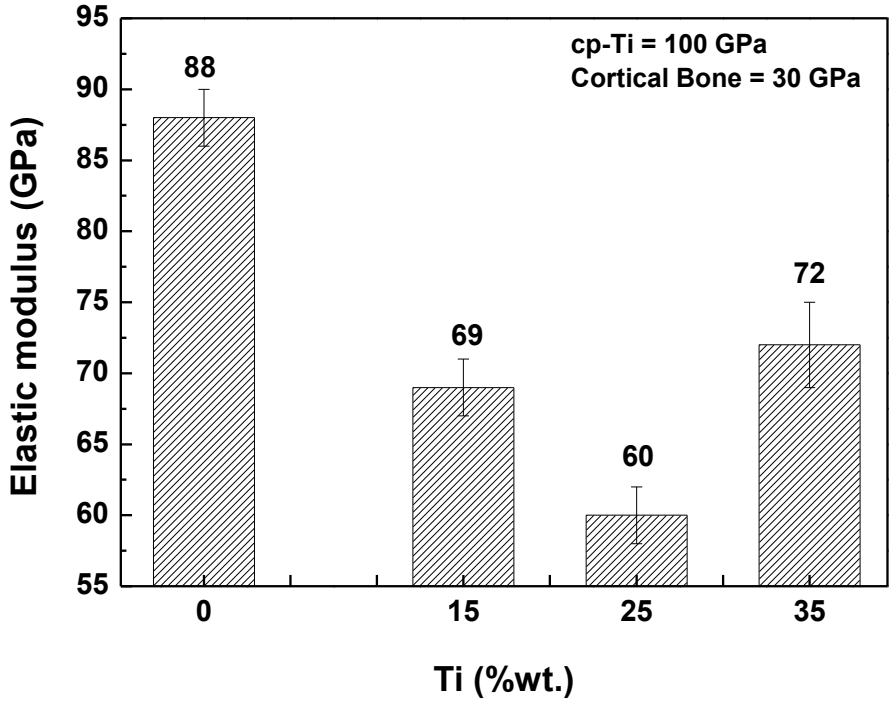


Figure 11.8. Vickers microhardness versus titanium concentration, for Zr-25Ta-Ti alloys.



.

Figure 11.9. Elastic modulus for Zr-25Ta-Ti alloys, as a function of titanium concentration.

- Structural and microstructural analyzes show that titanium acted as a α-stabilizing element because its addition to the alloys of the Zr-25Ta -Ti system precipitates the formation of phase α" in β-type alloys;
- The Zr-25Ta alloy has the ω phase in its structure, which makes it difficult to use as a biomaterial, as the alloy has a high hardness and elastic modulus value compared to the other alloys in the system. Even demonstrating the worst results of the system, this alloy still has better results than many alloys used as biomaterials, such as cp-Ti, Ti-6Al-4V, Co-Cr alloys and stainless steel, among others;
- The values of the microhardness and modulus of elasticity tend to fall with the addition of titanium; this is due to the lower stabilization of the β phase with the addition of titanium. Only for Zr-25Ta-35Ti alloys was there a small increase in modulus value because the alloy has two phases as microstructure, which makes the disagreement movement difficult and thus increases the alloy's modulus of elasticity;
- The Zr-25Ta-25Ti alloy is the best alloy. It has low hardness and the lowest elasticity value (60 GPa), only twice as high as cortical bone.

References

1 OKABE, F.; KIM, H. Y.; MIYAZAKI, S. Stress induced martensitic transformation and shape memory effect in Zr-Nb-Sn alloys. **Scripta Materialia,** v. 162, p. 412-415, 2019.
2 GUO, S. et al. A metastable β-type Zr-4Mo-4Sn alloy with low cost, low Young's modulus and low magnetic susceptibility for biomedical applications. **Journal of Alloys and Compounds,** v. 754, p. 232-237, 2018.
3 GUO, S. et al. A novel metastable β-type Zr-12Nb-4Sn alloy with low Young's modulus and low magnetic susceptibility. **Journal of Alloys and Compounds,** v. 745, p. 234-239, 2018.
4 HUA, N. et al. Mechanical properties and bio-tribological behaviors of novel beta-Zr-type Zr-Al-Fe-Nb alloys for biomedical applications. **Materials Science and Engineering: C,** v. 76, p. 1154-1165, 2017.
5 NIE, L. et al. Novel β-type Zr–Mo–Ti alloys for biological hard tissue replacements. **Materials & Design,** v. 53, p. 8-12, 2014.
6 MAYA, A. E. A. et al. Zr–Ti–Nb porous alloys for biomedical application. **Materials Science and Engineering: C,** v. 32, n. 2, p. 321-329, 2012.
7 MENDES, M. W. D. et al. A new titanium based alloy Ti–27Nb–13Zr produced by powder metallurgy with biomimetic coating for use as a biomaterial. **Materials Science and Engineering: C,** v. 63, p. 671-677, 2016.
8 JIANG, X. J. et al. Effect of rolling temperature on microstructure and mechanical properties of a TiZrAl alloy. **Materials Science and Engineering: A,** v. 635, p. 36-42, 2015.
9 KONDO, R. et al. Microstructure and mechanical properties of as-cast Zr–Nb alloys. **Acta Biomaterialia,** v. 7, n. 12, p. 4278-4284, 2011.

10 MEDVEDEV, A. E. et al. Microstructure and mechanical properties of Ti–15Zr alloy used as dental implant material. **Journal of the mechanical behavior of biomedical materials,** v. 62, p. 384-398, 2016.
11 VICENTE, F. et al. The Influence of Small Quantities of Oxygen in the Structure, Microstructure, Hardness, Elasticity Modulus and Cytocompatibility of Ti-Zr Alloys for Dental Applications. **Materials,** v. 7, n. 1, p. 542, 2014.
12 HAN, M.-K. et al. Effect of zirconium content on the microstructure, physical properties and corrosion behavior of Ti alloys. **Materials Science and Engineering: A,** v. 616, p. 268-274, 2014.
13 GEETHA, M. et al. Ti based biomaterials, the ultimate choice for orthopaedic implants – A review. **Progress in Materials Science,** v. 54, n. 3, p. 397-425, 5// 2009.
14 MEHJABEEN, A. et al. Zirconium Alloys for Orthopaedic and Dental Applications. **Advanced Engineering Materials,** v. 20, n. 9, p. 1800207, 2018.
15 KURODA, P. A. B.; BUZALAF, M. A. R.; GRANDINI, C. R. Effect of molybdenum on structure, microstructure and mechanical properties of biomedical Ti-20Zr-Mo alloys. **Materials Science and Engineering: C,** v. 67, p. 511-515, 2016.
16 DE ARAÚJO, R. O.; BUZALAF, M. A. R.; GRANDINI, C. R. Preparation and Characterization of Ti-10Mo-xZr Alloys for Biomedical Applications. **Materials Science Forum,** v. 869, p. 940-945, 2016.
17 ZHOU, Y.-L.; NIINOMI, M. Ti–25Ta alloy with the best mechanical compatibility in Ti–Ta alloys for biomedical applications. **Materials Science and Engineering: C,** v. 29, n. 3, p. 1061-1065, 2009.
18 _____. Microstructures and mechanical properties of Ti–50mass% Ta alloy for biomedical applications. **Journal of Alloys and Compounds,** v. 466, n. 1, p. 535-542, 2008.
19 ZHOU, Y. L.; NIINOMI, M.; AKAHORI, T. Effects of Ta content on Young's modulus and tensile properties of binary Ti–Ta alloys for biomedical applications. **Materials Science and Engineering: A,** v. 371, n. 1, p. 283-290, 2004.
20 TSUNO, A. T. et al. Effect of Ta content on the magnetic susceptibility of Zr–Ta binary alloys preventing artefacts for MRI. **Advances in Materials and Processing Technologies,** v. 2, n. 4, p. 606-614, 2016.
21 HSU, H.-C. et al. The structure and mechanical properties of as-cast Zr–Ti alloys. **Journal of Alloys and Compounds,** v. 488, n. 1, p. 279-283, 2009.
22 CORREA, D. R. N.; KURODA, P. A. B.; GRANDINI, C. R. Structure, Microstructure, and Selected Mechanical Properties of Ti-Zr-Mo Alloys for Biomedical Applications. **Advanced Materials Research,** v. 922, p. 75-80, 2014.
23 CORREA, D. R. N. et al. Adjustment of the microstructure and selected mechanical properties of biomedical Ti-15Zr-Mo alloys through oxygen doping. **Journal of Alloys and Compounds,** v. 775, p. 158-167, 2019.
24 CORREA, D. R. N. et al. Microstructure and selected mechanical properties of aged Ti-15Zr-based alloys for biomedical applications. **Materials Science and Engineering: C,** v. 91, p. 762-771, 2018.
25 CORREA, D. R. N. et al. Development of Ti-15Zr-Mo alloys for applying as implantable biomedical devices. **Journal of Alloys and Compounds,** v. 749, p. 163-171, 2018.
26 KURODA, P. A. B. Preparation, Microstructural Characterization, and Selected Mechanical Properties of Ti-20Zr-2.5Mo and Ti-20Zr-7.5Mo Used as Biomaterial. v. 869, p. 946-951, 2016.

27 QUADROS, F. D. F. et al. Preparation, structural and microstructural characterization of Ti-25Ta-10Zr alloy for biomedical applications. **Journal of Materials Research and Technology**, v. 8, p. 4108-4114, 2019.
28 KURODA, P. A. B. et al. Thermomechanical treatments influence on the phase composition, microstructure, and selected mechanical properties of Ti–20Zr–Mo alloys system for biomedical applications. **Journal of Alloys and Compounds**, p. 152108, 2019.
29 CORREA, D. R. N. et al. Effect of Some Heat Treatments on Anelastic Properties of Ti-15Zr-xMo Alloys. **Materials Science Forum,** v. 869, p. 907-912, 2016.
30 CORREA, D. R. N. et al. Tribocorrosion behavior of β-type Ti-15Zr-based alloys. **Materials Letters,** v. 179, p. 118-121, 2016.
31 CORREA, D. R. N. et al. Effect of the substitutional elements on the microstructure of the Ti-15Mo-Zr and Ti-15Zr-Mo systems alloys. **Journal of Materials Research and Technology,** v. 4, n. 2, p. 180-185, 2015.
32 CORREA, D. R. N. et al. Effect of Heat Treatment in the Structure and Microstructure of Ti-15Zr-XMo Alloys. **Defect and Diffusion Forum,** v. 365, p. 305-310, 2015.
33 LUZ, A. R. et al. Characterization of the morphology, structure and wettability of phase dependent lamellar and nanotube oxides on anodized Ti-10Nb alloy. **Applied Surface Science,** v. 448, p. 30-40, 2018.
34 E92−16, A. D. **Standard Test Methods for Vickers Hardness and Knoop Hardness of Metallic Materials**: ASTM International 2016.
35 E1876-15, A. D. **Standard Test Method for Dynamic Young's Modulus, Shear Modulus, and Poisson's Ratio by Impulse Excitation of Vibration**: ASTM International 2015.

Capítulo 12

Considerações Finais

Este estudo teve como objetivo principal desenvolver uma nova classe de ligas de titânio contendo tântalo e zircônio (Ti-25Ta-Zr) visando aplicações biomédicas.

Foram preparadas ligas do sistema Ti-25Ta-Zr (Zr = 0, 5, 10, 20, 30, 40 e 50 % em peso) pela técnica de fusão a arco-voltaico, que se mostrou satisfatória para a produção de ligas de titânio com alto ponto de fusão, pois as ligas possuem ótimos resultados de composição química, mostrando que a estequiometria proposta inicialmente fora satisfatoriamente atingida. Foi possível observar que as ligas com baixos teores de zircônio são do tipo α" e com o acréscimo do zircônio para valores acima de 40%, as ligas possuem apenas a fase β. Foi observada claramente a ação β-estabilizadora do zircônio em ligas ternárias, na presença de outro elemento β-estabilizador. Não foi observado nenhum efeito citotóxico nas ligas preparadas.

Após a preparação das amostras, as ligas com 0, 10, 20, 30 e 40% em peso de zircônio, passaram por um processo de conformação mecânica de laminação a quente e logo após foram submetidas a dois tratamentos de recozimento com resfriamento rápido e lento. As ligas foram submetidas a essas condições, visando homogeneizar a estrutura cristalina e diminuir as tensões internas oriundas do processo de laminação. Os resultados mostraram que o tratamento térmico realizado com o resfriamento lento enrijece e eleva o módulo de elasticidade das ligas. Assim, tal tratamento deve ser evitado para produzir ligas de titânio com baixo módulo de elasticidade.

Como a tendência é buscar ligas do tipo β, para buscar valores mais baixos de módulo de elasticidade, as ligas Ti-25Ta-Zr (Zr = 0, 10, 20, 30 e 40 % em peso) foram submetidas a diversos tratamentos térmicos de solubilização, para induzir a precipitação da fase β em ligas α", ou então, aumentar a fração volumétrica da fase β em ligas do tipo α"+β. Foram investigados tanto o efeito da temperatura do tratamento, quanto o tempo a que a amostra foi submetida ao tratamento térmico. Os resultados mostraram que os tratamentos térmicos de solubilização realizados a 1000 °C durante 6 horas induzem a formação da fase β e como consequência o módulo de elasticidade diminuiu.

Por fim, no sentido de investigar ligas possivelmente com módulo de elasticidade mais baixo, foram preparadas ligas do sistema Zr-25Ta-Ti. Estas ligas, com altos teores de zircônio foram fundidas e caracterizadas para analisar o efeito do titânio nas ligas de zircônio Zr-25Ta. Os resultados mostraram que o acréscimo de zircônio no sistema Ti-25Ta-Zr, para valores superiores a 50% em peso, eleva a dureza e módulo de elasticidade das ligas devido à maior estabilidade da fase β, além do surgimento da fase ω que possui como característica deixar o material quebradiço e frágil. Portanto ligas do sistema Ti-25Ta-Zr com teores de zircônio acima de 50% em peso, não são indicados para serem utilizados como um biomaterial devido a sua fragilidade.

Capítulo 13

Sugestões para Trabalhos Futuros

Após o desenvolvimento e caracterização inicial, como sucesso, de uma nova classe de ligas de titânio, visando aplicações biomédicas, algumas sugestões para trabalhos futuros no sentido de uma completa caracterização das ligas são propostas:

- Analisar o efeito do zircônio substitucional em outras propriedades mecânicas, como a fadiga e tração das ligas, obtendo o limite de escoamento elástico, resistência à tração, tensão e a deformação, e o módulo de cisalhamento. Estas informações são de fundamental importância para uma futura aplicação das ligas desenvolvidas na área ortopédica;
- Analisar a resistência à corrosão e tribo-corrosão das ligas, pois a superfície dos metais biomédicos em contato com fluidos corpóreos pode sofrer desgaste, diminuindo a longevidade do implante;
- Realizar testes de biocompatibilidade *in vivo* para propiciar uma garantia melhor no sentido da garantia da aplicação biomédica das ligas desenvolvidas;
- Modificar a superfície das ligas pela técnica de "*micro-arc oxidation"* com o objetivo de incorporar elementos que induzem o crescimento do tecido ósseo como o cálcio e fosforo, além da possibilidade de incorporar, na superfície dos materiais, elementos que são considerados anti-alergicos e antibactericidas.

Formação e Contribuição Científica

O autor, Pedro Akira Bazaglia Kuroda, iniciou suas atividades no Laboratório de Anelasticidade e Biomateriais, sob orientação do Prof. Dr. Carlos Roberto Grandini em agosto de 2010 com uma bolsa de Iniciação Científica (IC) do Programa Institucional de Bolsas de Iniciação Científica (PIBIC), do Conselho Nacional de Desenvolvimento Científico e Tecnológico (CNPq), na Universidade Estadual Paulista (UNESP), que foi renovada para o período 2011-2012 e 2012-2013. Neste período, desenvolveu atividades dentro do projeto "Efeito de Elementos Intersticiais nas Propriedades Anelásticas e Biocompatibilidade de Ligas Binárias de Ti usadas como Biomaterial", com o objetivo de dominar a preparação e caracterização de ligas de titânio contendo oxigênio intersticial. Na primeira fase, trabalhou com ligas binárias de titânio e depois com ligas ternárias, do sistema Ti-Zr-Mo. No ano de 2013, desenvolveu o projeto "Preparação e Caracterização de uma Liga de Titânio com a adição de Zircônio e Molibdênio para Aplicações Biomédicas", também IC, agora com bolsa da Fundação de Amparo à Pesquisa do Estado de São Paulo (FAPESP) (Proc. 2012/22.742-6), cujo objetivo foi estudar a influência do oxigênio intersticial na microestrutura e nas propriedades mecânicas da liga do sistema Ti-15Zr-7.5Mo. O desempenho acadêmico na graduação foi muito bom, concluindo o Curso de Licenciatura em Física sem reprovações e com o terceiro melhor coeficiente de rendimento acadêmico da turma, 8,24. Durante a graduação, participou eventos científicos no país, que culminou com a publicação resumos e trabalhos completos em anais de eventos.

Em março de 2014, iniciou seus estudos em nível de Mestrado, junto ao Programa de Pós-Graduação em Ciência e Tecnologia de Materiais (POSMAT) da UNESP, classificado como nível 6 pela Coordenadoria de Aperfeiçoamento de Pessoal de Nível Superior (CAPES), cursando e sendo aprovado em cinco disciplinas, todas elas com conceito A. Desenvolveu o projeto "Efeito do molibdênio substitucional na estrutura, microestrutura e algumas propriedades mecânicas de ligas do sistema Ti-20Zr-Mo", com bolsa concedida pela CAPES e defendeu sua Dissertação em 28/10/2015. Durante o mestrado, publicou três artigos em revista de circulação internacional; um capítulo de

livro, um artigo de divulgação. Participou de eventos no país, que culminou com a publicação resumos e trabalhos completos em anais de eventos. Participou de um trabalho considerado o melhor trabalho apresentado na VII Conferência sobre Temas de Tratamentos Térmicos.

Em agosto de 2015, iniciou seus estudos em nível de Doutorado, junto ao POSMAT da UNESP, sendo contemplado com uma bolsa da FAPESP (Proc. 2015/09.480-0), cursando e sendo aprovado em três disciplinas, todas elas com conceito A. Desenvolveu o projeto "Desenvolvimento e Caracterização de novas Ligas do Sistema Ti-25Ta-Zr para Aplicações Biomédicas", objeto deste trabalho. Durante o doutorado, além de seu trabalho, contribuiu para o desenvolvimento de outros projetos, preparando amostras em colaboração com outras instituições. Dentre eles, destacamos a participação no projeto "Desenvolvimento de Superfícies Hibridas Biofuncionalizadas Resistentes a Tribo-Corrosão em Ligas a Base de Ti" (FAPESP/M.ERA-NET Proc. 2015/50280-5) e colaboração na Tese de Doutorado de Aline R. Luz, da Universidade Federal do Paraná (UFPr). No laboratório colaborou, co-orientando três estudantes de IC orientadas pelo Prof. Carlos Roberto Grandini, Mycaela Vieira do Nascimento (bolsista FAPESP), Bárbara Letícia Tomaz Pedroso (bolsista PIBIC/CNPq) e Fernanda de Freitas Quadros (bolsista PIBIC/CNPq). É uma tradição do Laboratório de Anelasticidade e Biomateriais, incentivar os estudantes vinculados ao laboratório, atuar como Bolsista Didático em disciplinas oferecidas pelo Departamento de Física e durante seu doutorado, atuou como responsável pelas disciplinas Laboratório de Física 1 (4 Créditos com 44 alunos), Laboratório de Física 3 (2 créditos como 38 alunos), Fisica Geral (4 Créditos com 14 alunos) e Física 2 (4 créditos com 61 alunos em 2015, 55 alunos em 2017 e 34 alunos em 2019). Durante o doutorado, publicou quatorze artigos em revista de circulação internacional, além de ter mais três aceitos e cinco em análise. Participou de eventos no país e exterior, que culminou com a publicação resumos e trabalhos completos em anais de eventos. Participou de três trabalhos que receberam menção honrosa em congressos realizados no país.

Abaixo, pode ser vista a lista dos artigos publicados e dos prêmios recebidos durante a carreira:

PUBLICAÇÕES:

CAHA, I.; ALVES, A.P.; **KURODA, P.A.B.;** GRANDINI, C.R., PINTO, A.M.P.; ROCHA, L.A.; TOPTAN, F. Degradation behavior of Ti-Nb alloys: Corrosion behavior through 21 days of immersion and tribocorrosion behavior against alumina. *Accepted to Corrosion Science*, 2020.

KURODA, P.A.B.; SILVA, L.M.; SOUSA, K.S.J.; DONATO, T.A.G.; GRANDINI, C.R. Preparation, Structural, Microstructural, Mechanical, and Cytotoxic Characterization of Ti-15Nb Alloy for Biomedical Applications. *Accepted to Artificial Organs*, 2020.

KURODA, P.A.B.; NASCIMENTO, M.V.; GRANDINI, C.R. Preparação e caracterização de uma liga de titânio com a adição de tântalo e zircônio para aplicações biomédicas. *Aceito na Revista Matéria*, 2020.

KURODA, P.A.B.; QUADROS, F.F.; SOUSA, K.S.J.; DONATO, T.A.G.; ARAÚJO, R.O.; GRANDINI, C.R. Preparation, structural, microstructural, mechanical and cytotoxic characterization of as-cast Ti-25Ta-Zr alloys. *Journal of Materials Science: Materials in Medicine*, v. 31, p. 19, 2020.

KURODA, P.A.B.; LOURENÇO, M.L.; CORREA, D.R.N.; GRANDINI, C.R. Thermomechanical treatments influence on the phase composition, microstructure, and selected mechanical properties of Ti-20Zr-Mo alloys system for biomedical applications. *Journal of Alloys and Compounds*, v. 812, p. 152108, 2020.

KURODA, P.A.B.; QUADROS, F.F.; ARAÚJO, R.O.; AFONSO, C.R.M.; GRANDINI, C.R. Effect of Thermomechanical Treatments on the Phases, Microstructure, Microhardness and Young's Modulus of Ti-25Ta-Zr Alloys. *Materials*, v. 12, p. 3210, 2019.

QUADROS, F.F.; **KURODA, P.A.B**.; SOUSA, K.S.J.; DONATO, T.A.G.; GRANDINI, C.R. Preparation, structural and microstructural characterization of Ti-25Ta-10Zr alloy

for biomedical applications. *Journal of Materials Research and Technology*, v. 8, p. 4108-4114, 2019.

LUZ, A.R.; LEPIENSKI, C.M.; **KURODA, P.A.B.**; KUROMOTO, N.K. Characterization of the morphology, structure and wettability of phase dependent lamellar and nanotube oxides on anodized Ti-10Nb alloy. *Applied Surface Science*, v. 448, p. 30-40, 2018.

CORREA, D.R.N.; **KURODA, P.A.B.**; LOURENÇO, M.L.; BUZALAF, M.A.R.; GRANDINI, C.R. Adjustment of the microstructure and selected mechanical properties of biomedical Ti-15Zr-Mo alloys through oxygen doping. *Journal of Alloys and Compounds*, v. 775, p. 158-167, 2018.

CORREA, D.R.N.; **KURODA, P. A. B**.; LOURENÇO, M.L.; BUZALAF, M.A.R.; MENDOZA, M.E.; ARCHANJO, B.S.; ACHETE, C.A.; ROCHA, L.A.; GRANDINI, C.R. Microstructure and selected mechanical properties of aged Ti-15Zr-based alloys for biomedical applications. *Materials Science & Engineering C*, v. 91, p. 762-771, 2018.

CORREA, D.R.N.; **KURODA, P.A.B.**; LOURENÇO, M.L.; FERNANDES, C.J.C.; BUZALAF, M.A.R.; ZAMBUZZI, W.F.; GRANDINI, C.R. Development of Ti-15Zr-Mo alloys for applying as implantable biomedical devices. *Journal of Alloys and Compounds*, v. 749, p. 163, 2018.

CORREA, D.R.N.; LOURENCO, M.L.; **KURODA, P.A.B.**; BUZALAF, M.A.R.; GRANDINI, C.R. Effect of Some Heat Treatments on Anelastic Properties of Ti-15Zr-xMo Alloys. *Materials Science Forum*, v. 869, p. 907-912, 2016.

KURODA, P.A.B.; BUZALAF, M.A.R.; GRANDINI, C.R. Preparation, Microstructural Characterization, and Selected Mechanical Properties of Ti-20Zr-2.5Mo and Ti-20Zr-7.5Mo Used as Biomaterial. *Materials Science Forum*, v. 869, p. 946-951, 2016.

CORREA, D.R.N.; **KURODA, P.A.B.**; GRANDINI, C.R.; ROCHA, L.A.; OLIVEIRA, F.G.M.; ALVES, A.M.V.C.P.; TOPTAN, F. Tribocorrosion Behavior of β-Type Ti-15Zr-Based Alloys. *Materials Letters*, v. 179, p. 118-121, 2016.

KURODA, P.A.B.; BUZALAF, M.A.R.; GRANDINI, C.R. Effect of molybdenum on structure, microstructure and mechanical properties of biomedical Ti-20Zr-Mo alloys. *Materials Science & Engineering. C*, v. 67, p. 511-515, 2016.

CORREA, D.R.N.; **KURODA, P.A.B.**; LOURENCO, M.L.; GRANDINI, C.R. Effect of Heat Treatment in the Structure and Microstructure of Ti-15Zr-XMo Alloys. *Defect and Diffusion Forum*, v. 365, p. 305-310, 2015.

CORREA, D.R.N.; VICENTE, F.B.; ARAÚJO, R.O.; LOURENÇO, M.L.; **KURODA, P.A.B.**; BUZALAF, M.A.R.; GRANDINI, C.R. Effect of the substitutional elements on the microstructure of the Ti-15Mo-Zr and Ti-15Zr-Mo systems alloys. *Journal of Materials Research and Technology*, v. 4, p. 180-185, 2015.

CORREA, D.R.N.; **KURODA, P.A.B.**; GRANDINI, C.R. Structure, Microstructure, and Selected Mechanical Properties of Ti-Zr-Mo Alloys for Biomedical Applications. *Advanced Materials Research*, v. 922, p. 75-80, 2014.

PREMIAÇÕES ACADÊMICAS:

A Sociedade Latino Americana de Biomateriais e Órgãos Artificiais (SLABO) conferiu ao trabalho intitulado “Effect of zirconium on the structure and microstructure of Ti-25Ta-Zr alloys for biomedical aplications” menção honrosa, no 9° Congresso Latino-Americano de Orgãos Artificiais e Biomateriais, 2016.

A Sociedade Brasileira de Vácuo (SBV) conferiu ao trabalho intitulado “Preparation and microstructural characterization of Ti-25Ta-Zr alloys”, menção honrosa, no XXXVII Congresso Brasileiro de Aplicações de Vácuo na Indústria e na Ciência, 2016.

A Sociedade Brasileira de Vácuo (SBV) conferiu ao trabalho intitulado “Structure and Microstructural Characterization of Ti-25Ta-10Zr Alloys”, menção honrosa, no XXXVII Congresso Brasileiro de Aplicações de Vácuo na Indústria e na Ciência, 2016.

A Metallum Eventos e Congressos Ltda. conferiu ao trabalho intitulado “Efeito de tratamentos termomecânicos na microestrutura de ligas biomédicas de Ti-15Zr-Mo” a premiação como o melhor trabalho na Categoria Tratamento Térmico de Não Ferrosos na VII Conferência Brasileira sobre Temas de Tratamento Térmico, 2014.

Autorização dos Co-autores para incluir Artigos na Tese

Unesp

PROGRAMADEPÓS-GRADUAÇÃOEMCIÊNCIAETECNOLOGIADEMATERIAIS

POSMAT
PÓS-GRADUAÇÃO EM CIÊNCIA E TECNOLOGIA DE MATERIAIS

AUTORIZAÇÃO DOS CO-AUTORES PARA INCLUIR UM ARTIGO EM UMA DISSERTAÇÃO OU TESE

Para as dissertações e teses redigidas em formato de artigos, o aluno deve ter este formulário de autorização assinado por todos os co-autores do(s) artigo(s).

A - Identificação do Discente

NOME COMPLETO:Pedro Akira Bazaglia Kuroda	
CPF: 399728628-01	RG: 47092495-0
ENDEREÇO: Osório Volpato, 3-7. Jardim Olímpico, 17032-650, Bauru-SP	

B - Título da dissertação ou tese e do artigo inserido

Título da dissertação ou tese:DESENVOLVIMENTO E CARACTERIZAÇÃO DE NOVAS LIGAS DO SISTEMA Ti-25Ta-Zr PARA APLICAÇÕES BIOMÉDICAS

Título do artigo inserido (outros títulos de artigos podem ser indicados se estes foram escritos pelas mesmas pessoas):

- Preparation, Structural, Microstructural, Mechanical and Cytotoxic Characterization of as-cast Ti-25Ta-Zr Alloys.
- Preparação e caracterização de uma liga de titânio com a adição de tântalo e zircônio para aplicações biomédicas.
- Preparation, Structural and Microstructural Characterization of Ti-25Ta-10Zr Alloy for Biomedical Applications.
- Desenvolvimento da liga Ti-25Ta-50Zr para aplicações biomédicas.
- Effect of Thermomechanical Treatments on the Phases, Microstructure, Microhardness and Young's Modulus of Ti-25Ta-Zr Alloys.
- The effect of solution heat treatment on phase transformations, microstructure and properties of Ti-25Ta-xZr alloys used as a biomaterial.
- The effect of solubilization heat treatment time on the structure, microstructure, and selected mechanical properties of Ti-25Ta-Zr alloys used as biomaterials.
- The Effect of Titanium on the Structure, Microstructure and Select Mechanical Properties of Zr-25Ta-Ti Alloys.

Unesp

PROGRAMA DE PÓS-GRADUAÇÃO EM CIÊNCIA E TECNOLOGIA DE MATERIAIS

POSMAT
PÓS-GRADUAÇÃO EM CIÊNCIA E TECNOLOGIA DE MATERIAIS

C – Autorização dos co-autores

Por meio deste instrumento, autorizo a inserção do(s) artigo(s) referido(s) na alínea B e eventual distribuição na dissertação ou tese do discente, de acordo com as regras da Universidade Estadual Paulista "Júlio de Mesquita Filho" – – Faculdade de Ciências – Bauru-SP		
09/11/2019	Pedro Akira Bazaglia Kuroda	Pedro Kuroda
09/11/2019	Fernanda de Freiras Quadros	Fernanda de Freitas Quadros
09/11/2019	Karolyne dos Santos Jorge Sousa	Karolyne S. J. Sousa
09/11/2019	Tatiani Ayako Goto Donato	Tatiani A. G. Donato
09/11/2019	Raul Oliveira de Araújo	Raul Oliveira de Araújo
09/11/2019	Mycaela Viera do Nascimento	Mycaella V. Nascimento
09/11/2019	Barbara Letícia Tomaz Pedroso	Barbara Letícia
09/11/2019	Conrado Ramos Moreira Afonso	
09/11/2019	Carlos Roberto Grandini	

Pedro Kuroda

Pedro Akira Bazaglia Kuroda

Prof. Dr. Carlos Roberto Grandini